LOCALISED STRUCTURES IN SOME NON–STANDARD, SINGULARLY PERTURBED PARTIAL DIFFERENTIAL EQUATIONS

Paige N. Davis

Bachelor of Science (Advanced Mathematics) (Honours)

School of Mathematical Sciences

Science and Engineering Faculty

Queensland University of Technology

2020

Submitted in fulfilment of the requirement for the degree of

Doctor of Philosophy

Keywords

Stationary solutions

Travelling wave solutions

Linearised operators

Essential Spectrum

Absolute Spectrum

Point Spectrum

Geometric Singular Perturbation Theory

Heterogeneous equations

Jump-type defect

Evans Function

Abstract

This thesis addresses the existence and stability of localised solutions in some non-standard systems of partial differential equations (PDEs). Extending the analysis to these non-standard problems provides a foundation and insight for more general dynamical systems. Three different models were chosen to act as a vehicle for this analysis, a Keller-Segel model for bacterial chemotaxis, a Gatenby-Galenski model for tumour invasion with the acid-mediation hypothesis and stationary solutions to reaction-diffusion equations (RDEs) with a jump-type heterogeneity. The models are biologically and physically relevant RDEs which exhibit different non-standard structures and/or behaviours.

The Keller-Segel model chosen has a logarithmic chemotactic function, constant, sublinear or linear consumption and zero growth or decay of the bacterial population and attractant. This model supports travelling wave solutions which have been described in the literature as both linearly stable and unstable and in the case of linear consumption (conditionally) nonlinearly stable. We reconcile this apparent contradiction by locating the essential spectrum, absolute spectrum and point spectrum of the linear operators associated with the travelling wave solutions. We show that whilst all travelling wave solutions have essential spectrum in the right half plane, in the case of constant or sublinear consumption there exists a range of parameters such that the absolute spectrum is contained in the open left half plane and the essential spectrum can thus be weighted into the open left half plane implying a possible transient instability. For the constant and sublinear consumption rate models we also determine critical parameter values for which the absolute spectrum crosses into the right half plane, indicating the onset of an absolute instability of the travelling wave solution. We observe that this crossing always occurs off of the real axis which is atypical. Furthermore, we show that the absolute spectrum deforms as the consumption is changed illustrating a connection between the constant, sublinear and linear cases. We also show that there is an eigenvalue at zero which is order two for the constant and sublinear cases and embedded in the absolute spectrum in the linear case, proving spectral stability for the parameter range and weighted function space for which the absolute spectrum is contained in the left half plane.

The Gatenby-Galenski model is a slow-fast system which supports travelling waves with a range of speeds. For a high measure of tumour aggressivity travelling wave solutions exhibit an interstitial gap which has previously been observed experimentally. We prove the existence of the travelling wave solutions and give a geometric interpretation of the

formal asymptotic analysis of the interstitial gap utilising geometric singular perturbation theory to prove the persistence of the singular solution. It is shown that the width of the interstitial gap is determined by the distance between a layer transition of the tumour and a dynamical transcritical bifurcation of two components of the critical manifold.

Heterogeneous defects have been shown to have a profound impact on the existence of localised solutions, potentially pinning, rebounding or annihilating solutions. The jump-type defect is simple enough to make explicit analysis feasible while providing insight for future analysis of more complicated heterogeneities. We examine pinned stationary solutions located near the defect for which substantial existence analysis exists showing there are three main types of solution, trivial defect solutions, local defect solutions and global defect solutions. Through the use of an Evans function we locate the leading order spectrum of the general trivial defect solution which agrees with that of the associated homogeneous problem and derive the first order correction term, thus providing conditions for spectral stability to first order.

Statement of Original Authorship

I hereby declare that this submission is my own work and to the best of my knowledge it contains no material previously published or written by another person, nor material which to a substantial extent has been accepted for the award of any other degree or diploma at QUT or any other educational institution, except where due acknowledgement is made in the thesis. Any contribution made to the research by colleagues, with whom I have worked at QUT or elsewhere, during my candidature, is fully acknowledged.

I also declare that the intellectual content of this thesis is the product of my own work, except to the extent that assistance from others in the project's design and conception or in style, presentation and linguistic expression is acknowledged.

QUT Verified Signature

Paige N. Davis

2020

8 July 2020

Acknowledgements

This work was supported under the Australian Research Council's Discovery Early Career Researcher Award funding scheme DE140100741.

To my principal supervisor, Associate Professor Peter van Heijster, and my external supervisor, Doctor Robert Marangell, I would like to thank you for your support, understanding and guidance. Your help and advice were invaluable. You made my PhD a memorable, fun experience and I learned so much as I grew into a confident and competent mathematician. And thanks to Professor Graeme Pettet and Professor Scott McCue who acted as my associate supervisors.

To my friends and family, my wonderful and fierce mom, my awesome and eccentric dad, my goofy brothers, my lovely PhD cohort, thank you for supporting me and encouraging me. I love you all and am so grateful to have each of you in my life.

For Emma, who listened through all of my late-night phone calls, talked me through my worries, and made me laugh when no one else could. You are my sister, my confidante, and my partner in crime.

Finally, for Kiki, my beloved dog who lived the PhD life alongside me. You were my companion and the only reason I went outside some days. I will miss you forever.

List of publications

- P.N. Davis, P. van Heijster, and R. Marangell. Absolute instabilities of travelling wave solutions in a Keller–Segel model. *Nonlinearity*, 30:4029–4061, 2017. Presented in Chapter 2, sections §2.4 to §2.6.
- P.N. Davis, P. van Heijster, and R. Marangell. Spectral stability of travelling wave solutions in a Keller–Segel model. *Appl. Numer. Math.*, 141:54–61, 2018. Presented in Chapter 2, section §2.7.
- P.N. Davis, P. van Heijster, R. Marangell, and M.R. Rodrigo. Traveling wave solutions in a model for tumor invasion with the acid-mediation hypothesis. *Submitted*, 2018. Presented in Chapter 3.

The universe is vast.
You are also vast.
So is an ant.
There are different sizes of infinity.

Welcome to Night Vale

Contents

Keywords i

Abstract ii

Statement of Original Authorship iv

Acknowledgements v

List of publications vi

Chapter 1 Introduction 1
1.1 Research objectives . . . 1
1.2 Model equations . . . 2
1.2.1 A Keller-Segel model for bacterial chemotaxis with a logarithmic chemosensitivity function . . . 2
1.2.2 The Gatenby-Gawlinski model for tumour invasion with the acid-mediation hypothesis . . . 3
1.2.3 Reaction diffusion equations with a jump-type spatial defect . . . 5
1.3 Spectral stability . . . 6
1.3.1 Linearised operators . . . 7
1.3.2 Essential spectrum . . . 11
1.3.3 Weighted spaces . . . 13
1.3.4 Absolute spectrum . . . 14
1.3.5 Point spectrum . . . 16
1.3.6 The Evans function . . . 18
1.4 Geometric Singular Perturbation Theory . . . 19
1.4.1 Fenichel Theory and GSPT . . . 20
1.5 Outline and original contributions . . . 23

Chapter 2 The spectral stability of a Keller-Segel model with logarithmic chemosensitivity 27
2.1 Preface . . . 27
2.1.1 Abstract . . . 27
2.2 Introduction . . . 28
2.2.1 The Keller-Segel model . . . 28
2.3 Set-up, definitions, and main results . . . 30

2.3.1 Travelling wave solutions . . . 31
2.3.2 The spectral problem . . . 32
2.3.3 Spectral stability: Background and definitions . . . 33
2.3.4 Main results . . . 36
2.4 Constant consumption and zero diffusivity of the chemoattractant . . . 38
2.4.1 Set-up . . . 38
2.4.2 Essential spectrum . . . 38
2.4.3 The weighted essential spectrum and the absolute spectrum . . . 40
2.4.4 Proof of Theorem 2.3.3 for $\varepsilon = m = 0$ . . . 45
2.5 Sublinear and linear consumption and zero diffusivity of the chemoattractant 49
2.5.1 Set-up . . . 49
2.5.2 Essential spectrum . . . 51
2.5.3 The weighted essential spectrum and the absolute spectrum . . . 53
2.5.4 Proof of Theorem 2.3.3 for $0 < m < 1$ and $\varepsilon = 0$ . . . 53
2.5.5 Linear consumption . . . 55
2.6 Small diffusion . . . 56
2.6.1 Set-up . . . 56
2.6.2 Proof of Theorem 2.3.3 for $0 \leq m \leq 1$ and $0 < \varepsilon \ll 1$ . . . 59
2.7 Point Spectrum . . . 64
2.7.1 Locating the point spectrum . . . 67
2.7.2 The generalised eigenspace at $\lambda = 0$ . . . 68
2.7.3 Behaviour of eigenfunctions as $z \to \pm\infty$ . . . 69
2.7.4 The limit $m \to 1$ . . . 72
2.8 Summary and outlook . . . 73
2.8.1 Nonlinear (in)stability . . . 73
2.8.2 Dynamical implications of the spectral structure . . . 74

Chapter 3 Travelling wave solutions in a model for tumour invasion with the acid-mediation hypothesis 76
3.1 Preface . . . 76
3.2 Introduction . . . 76
3.2.1 Results and outline . . . 79
3.3 Setup of the slow-fast systems . . . 80
3.4 The existence of fast travelling wave solutions . . . 82
3.5 The existence of slow travelling wave solutions . . . 85
3.5.1 The properties of the critical manifold . . . 88
3.5.2 $0 < \alpha < 1$ . . . 89
3.5.3 $\alpha > 1$ . . . 93
3.6 Summary and outlook . . . 96
3.6.1 Spectral stability of the Gatenby-Galenski model . . . 97
3.6.2 Extensions and generalisations of the Gatenby-Galenski model . . . 97

Chapter 4 Stability of defect solutions 99
4.1 Introduction 99
4.2 Set-up, definitions, and main results 101
4.2.1 Types of defect solution 102
4.2.2 The stability of equilibrium solutions to the unperturbed PDE . . 104
4.2.3 The existence trivial defect solutions to the perturbed PDE 108
4.2.4 The perturbed spectral problem 109
4.2.5 The Evans function 109
4.3 A scalar example: The bistable equation with a generic defect 111
4.3.1 The essential and absolute spectrum of the unperturbed bistable equation 112
4.3.2 The solution profile of the trivial defect solution 113
4.3.3 The eigenvalue problem and the Evans function 114
4.4 Summary and outlook 118

Chapter 5 Summary and outlook 119
5.1 Summary 119
5.2 Future work for the Keller-Segel model with logarithmic chemosensitivity 120
5.3 Future work for the Gatenby-Gawlinski model with the acid-mediation hypothesis 121
5.3.1 Stability of solutions to the Gatenby-Gawlinski model 121
5.4 Future work on the stability of defect solutions 122
5.4.1 Local defect solutions to $n-$dimensional RDEs 122
5.4.2 The Fitzhugh-Nagumo model with a jump-type spatial defect . . . 122
5.4.3 The extended Fisher-Kolmogorov equation with a jump-type spatial defect 123

References 124

Appendix A Proof of Lemma 2.3.4 129

List of Figures

1.2.1 Chemotactic movement of E. coli 3

1.2.2 An interstitial gap present in a human squamous cell carcinoma and a slow TW solution of the GG model with an interstitial gap. 4

1.2.3 A depiction of three types of defect solutions. 6

1.3.1 Schematic depiction of convective and absolute instabilities 9

1.3.2 The essential spectrum of the FKPP in an unweighted function space . . 12

1.3.3 The essential spectrum of the FKPP equation with speed $c = 4$ in various weighted function spaces. 16

2.3.1 Travelling wave (TW) solutions to the Keller-Segel (KS) model for $m = 0$ and $m = 1$ 30

2.3.2 The spatial eigenvalues for different λ values. 35

2.4.1 The essential spectrum of the TW solutions to the KS model. 40

2.4.2 The absolute spectrum of TW solutions at the $z \to \infty$ end state. 42

2.4.3 The absolute spectrum and dispersion relations of TW solutions at the $z \to -\infty$ end state in various weighted function spaces. 43

2.4.4 The absolute spectrum and dispersion relations of TW solutions at the $z \to -\infty$ end state in the ideally weighted function spaces. 44

2.4.5 The essential and absolute spectrum of an absolutely unstable TW in an unweighted space and an ideally weighted space. 45

2.4.6 The essential and absolute spectrum of a transiently unstable TW in an unweighted space and an ideally weighted space. 46

2.4.7 The range of weighted spaces, against the chemotactic parameter, such that the TW is transiently unstable. 48

2.5.1 The essential and absolute spectrum under variation of the consumption parameter m. 52

2.5.2 The essential and absolute spectrum with a linear consumption parameter, $m = 1$. 56

2.5.3 The real component of the branch points, λ_{br}, against the magnitude of the imaginary component. 57

2.6.1 The essential and absolute spectrum of a transiently unstable TW in an unweighted space and an ideally weighted space with the inclusion of small diffusion of the attractant, *i.e.* $0 < \varepsilon \ll 0$. 60

2.7.1 A schematic of the general shape and typical location of essential and absolute spectrum of TW solutions to the KS model. 67

2.7.2 The $\mathbb{L}_2$ norm squared of the generalised eigenfunction associated with TWs for $\lambda = 0$, $\beta = 1.1$ and various m. 69

3.2.1 An interstitial gap present in a human squamous cell carcinoma and a slow TW solution of the GG model with an interstitial gap. 78

3.4.1 A fast TW solution obtained from numerically simulating the Gatenby–Gawlinsky (GG) model. 83

3.5.1 Three typical profiles of slow TW solutions of the GG model obtained numerically. 85

3.5.2 Schematic depiction of the four slow manifolds $S_{\text{S}}^{1,2,3,4}$ of the GG model with depictions of the three different types of slow TW solutions. 87

3.5.3 Schematic depiction of the slow flow on the different components of the critical manifold for the three different heteroclinic orbits associated to the three different types of slow TW solutions. 90

4.2.1 A depiction of three types of defect solutions. Image is taken from [21] and used with permission. 102

4.3.1 Trivial defect solution to scalar bistable equation 112

Chapter 1

Introduction

Reaction Diffusion Equations (RDEs) are partial differential equations (PDEs) which exhibit a wide range of complex behaviours and patterns, and they are used to model many different biological processes such as chemotaxis, population invasion, and wound healing (see for example [58]). The building blocks of pattern formation analysis are localised solutions; a solution that is arbitrarily close to a trivial background state except in a localised region. This thesis addresses the existence and stability of two types of localised solutions, stationary solutions and travelling waves (a solution that maintains a constant speed and shape), in some non-standard systems of RDEs from biology and physics.

In particular, we study the stability of travelling waves in a Keller-Segel model for bacterial chemotaxis with a logarithmic chemosensitivity function, the existence of travelling waves in the Gatenby-Gawlinski model for tumour invasion with the acid-mediation hypothesis, and the stability of a type of stationary solutions of a general RDE with a spatially dependent defect. Observe that these models are non–standard in various ways. The motivation behind using these real-world models to drive our research is both to tie our analysis to applications and to illustrate the insight that the rigorous and technical dynamical systems and functional analysis methods provide.

We will first provide the background of the three models, after which we outline the analysis of RDEs for two paradigmatic problems for which the existence and stability results are known in order to demonstrate the mathematical techniques that form the foundation from which we approach our non-standard problems. We start with the stability analysis for which we follow the framework outlined in [54, 88]. In order to perform stability analysis, we must first establish the existence of localised solutions. These include fronts or pulses which may be stationary solutions or travelling waves and which may evolve on different time scales, for example if one population diffuses orders of magnitude slower than the other. We use geometric singular perturbation theory (GSPT) [39, 51, 53] to prove the existence of solutions to these systems if there is a scale separation.

1.1 Research objectives

The objectives of this thesis are to

- to develop a deeper understanding of current stability techniques in the context of systems of equations in homogeneous media through the application to a specific example (the Keller-Segel model),
- to apply Geometric Singular Perturbation Theory to a non-standard fast-slow problem (the Gatenby-Gawlinski model) in order to answer open questions regarding the existence and characteristics of the solution profiles,
- to extend the current stability techniques to determine the stability of a trivial defect solution in systems with heterogeneous media, by tracking the potential point spectra that emerges from the absolute spectrum as a result of the inclusion of a heterogeneity.

1.2 Model equations

1.2.1 A Keller-Segel model for bacterial chemotaxis with a logarithmic chemosensitivity function

The Keller-Segel model was originally proposed to model a band of bacteria consuming a chemoattractant by E.F. Keller and L.A. Segel in [60, 61]. The model was based on the early experimental observations by J. Adler in Chemotaxis in Bacteria [1] where it was observed that E. coli would move towards a liquid solution in a travelling pulse of bacteria driven by chemotaxis, see Figure 1.2.1. The proposed model was given by

$$\begin{aligned} u_t &= \varepsilon u_{xx} - \alpha w u^m + \kappa u, \\ w_t &= \delta w_{xx} - \beta \left(\Phi_x(u) w\right)_x . \end{aligned} \tag{1.1}$$

Here, $x \in \mathbb{R}$ and $t \in \mathbb{R}^+$ are the spatial and temporal variables, respectively, $u(x,t)$, $w(x,t)$ represent nondimensionalised versions of the chemoattractant and bacterial cell population, with $\alpha,\ \kappa \geq 0, m \in \mathbb{R}$, and $\beta,\ \delta > 0$. It is assumed that the diffusion of the chemoattractant is taken to be much smaller than that of the bacteria, *i.e.* $0 \leq \varepsilon \ll \delta$. The movement of the bacterial cell species is governed by the gradient of the chemoattractant. The function $\Phi(u)$ is the so-called chemotactic function. The model (1.1) was shown to support travelling waves only when the chemotactic function is singular [94]. Furthermore, for a logarithmic chemosensitivity function $\Phi(u) = \log(u)$ the model supports travelling waves only if $\beta > 1-m, 0 \leq m \leq 1$. An overview of the model's development and analysis is given in [44].

The Keller-Segel model (1.1) is non–standard in two ways; the singularly perturbed nature of the problem due to the small parameter ε and the singularity of the chemotactic function as $u \to 0$. The singularly perturbed nature of the problem requires the analysis of the leading order ($\varepsilon = 0$ problem) and an argument of persistence of solutions and stability when $0 < \varepsilon \ll 1$. The singularity in the chemotactic function leads to an unusual shape of the spectrum. Specifically, the crossing of the absolute spectrum into the right half plane

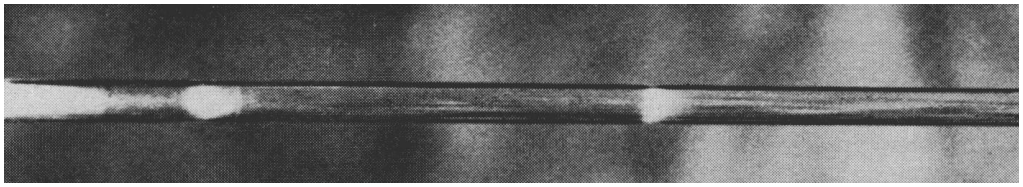

Figure 1.2.1: E. coli (white) consuming a liquid solution. Reprinted from J. Adler. Chemotaxis in bacteria. *Science*, 153(3737):708–716, 1966 with permission from AAAS. The E. coli population moves as a travelling pulse driven by the chemotactic function.

as the chemotactic parameter β is increased occurs away from the real axis. Furthermore, due to the second order derivative of the chemotactic function, when linearising about the travelling wave solutions a quasilinear (rather than semilinear) operator is obtained. Whilst the spectral stability of a parabolic, nonlinear operator implies the nonlinear stability [41], in the case of quasilinear operators this result has only been proven for certain cases [78]. The Keller-Segel model (1.1) for $0 \leq m < 1$ is not covered by [78] and certain subcases of the linear ($m = 1$) case are shown to be nonlinearly stable or unstable in [77].

The Keller-Segel model chosen supports travelling wave solutions which have been described in the literature as both linearly stable [87] and linearly unstable [80], and in the case of linear consumption (conditionally) nonlinearly stable [77]. We reconcile this apparent contradiction by locating the spectrum of the linear operators associated with the travelling wave solutions. We derive conditions for the spectral (in)stability of the travelling wave solutions and the critical parameters that indicate a transition from a transient to absolute instability. Furthermore, we show that the absolute spectrum deforms as the consumption parameter β is changed, illustrating a connection between the constant ($m = 0$), sublinear ($0 < m < 1$) and linear ($m = 1$) cases. In addition, we prove that the origin is a temporal eigenvalue of order 2 for $0 \leq m < 1$ and is embedded in the absolute spectrum for $m = 1$.

1.2.2 The Gatenby-Gawlinski model for tumour invasion with the acid-mediation hypothesis

The Gatenby–Gawlinski model was originally presented in [32] to model the invasion of healthy cells by tumour cells under the acid-mediation hypothesis. The hypothesis is that the tumour induces a change in the surrounding PH levels which is advantageous to tumour growth and invasion. The acid-mediation hypothesis is supported by mathematical analysis, clinical data and experimental observations in [32]. A nondimensionalised version of the Gatenby–Gawlinski model is given by the following system of singularly perturbed PDEs with nonlinear diffusion in the V-component,

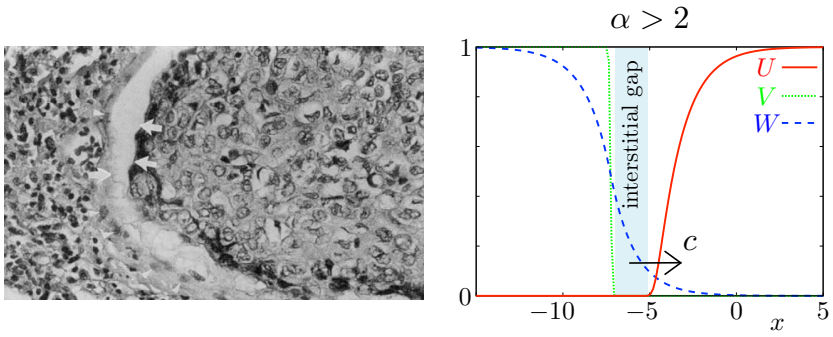

Figure 1.2.2: Left panel: an interstitial gap present in a human squamous cell carcinoma. Reprinted from R. A. Gatenby and E. T. Gawlinski. A reaction-diffusion model for cancer invasion. *Cancer Res.*, 56:5745–5753, 1996 with permission from AACR. Right panel: a slow travelling wave solution with an interstitial gap supported by (1.2).

$$\begin{cases} \dfrac{\partial U}{\partial \tau} = U(1 - U - \alpha W), \\ \dfrac{\partial V}{\partial \tau} = \beta V(1 - V) + \varepsilon \dfrac{\partial}{\partial x}\left[(1 - U)\dfrac{\partial V}{\partial x}\right], \\ \dfrac{\partial W}{\partial \tau} = \gamma(V - W) + \dfrac{\partial^2 W}{\partial x^2}. \end{cases} \tag{1.2}$$

Here, $x \in \mathbb{R}$ and $\tau \geq 0$ are the spatial and temporal variables, respectively, $U(x, \tau)$, $V(x, \tau)$, and $W(x, \tau)$ represent nondimensionalised versions of the normal cell density, tumour cell density, and excess acid concentration, respectively. As in [32], ε is assumed to be a small nonnegative parameter, *i.e.* $0 \leq \varepsilon \ll 1$, and the constants α, β, and γ are all positive and strictly $\mathcal{O}(1)$ with respect to ε. Numerical experiments in [32] indicated the presence of a region almost devoid of cells ahead of the travelling wave solution referred to as the *interstitial gap*. This gap has also been observed experimentally, see Figure 1.2.2.

The Gatenby-Gawlinski model (1.2) is a slow-fast system which supports travelling waves of various speeds. It was shown in [27] that the travelling waves supported by (1.2) fall into two categories; *fast travelling wave solutions* with speed of $\mathcal{O}(1)$ which are stationary solutions in the frame $(z, t) = (x - c\tau, \tau)$ and *slow travelling wave solutions* with speed of $\mathcal{O}(\varepsilon^p)$, $0 < p \leq \frac{1}{2}$ which are stationary solutions in the $(z, t) = (x - \varepsilon^p c\tau, \tau)$. The parameter c is $\mathcal{O}(1)$ in both cases. It was shown in [27] that travelling waves are not supported when $p > \frac{1}{2}$.

In Chapter 3 we focus on the two critical cases, examining the fast travelling wave solutions (*i.e.* $p = 0$) and a slow travelling wave solution with $p = \frac{1}{2}$. We were motivated by the findings of [27] where it was shown that the slow travelling wave solutions possess an interstitial gap when $\alpha > 2$ which ceases to exist for $0 < \alpha \leq 2$. We prove the existence of both the fast and slow travelling wave solutions and give a geometric interpretation of the formal asymptotic analysis of the interstitial gap utilising geometric singular perturbation theory to prove the persistence of the singular solution. We show that the width of the

interstitial gap is determined by the distance between a layer transition of the tumour and a dynamical transcritical bifurcation of two components of the critical manifold.

1.2.3 Reaction diffusion equations with a jump-type spatial defect

Heterogeneities can have an impact on the type of solutions, patterns formed and stability conditions. For example, travelling waves may be pinned, reflected, annihilated or split upon meeting the heterogeneity. See for example [100] where pinned solutions are shown to exist for a three component FitzHugh-Nagumo type system. There has been activity in the area of scalar equations, such as [14] which analyses the stability of pinned solutions to the sine-Gordon equation with a jump inhomogeneity, [105] which considers scalar reaction-advection-diffusion in periodic media, and [13, 64] which analyse the stability of inhomogeneous wave equations. In contrast, there has been less work done on systems of heterogeneous RDEs (see, however, [21, 46, 98]).

In Chapter 4, we consider a general, heterogeneous, PDE of the form

$$u_t = Du_{xx} + f(u) + \begin{cases} 0 & x < 0 \\ \varepsilon g(u) & x \geq 0 \end{cases} \tag{1.3}$$

with $u \in \mathbb{R}^n$, $(x,t) \in (\mathbb{R}, \mathbb{R}^+)$, D is a non-negative diagonal matrix, and f and g are sufficiently smooth functions. In order to analyse the stability of stationary solutions of heterogeneous PDEs we must first establish the existence and any assumptions or conditions that arise from the existence problem must be taken into account in the stability analysis. The existence equation for stationary solutions to (1.3) (*i.e.* $u_t = 0$) can be transformed into a first order system of ODEs which fits the more general form from [21]

$$\dot{u} = \begin{cases} h(u) & x \leq 0, \\ h(u) + \varepsilon j(u) & x > 0, \end{cases} \tag{1.4}$$

where $\dot{} = d/dx$ and $h(u), j(u) : \mathbb{R}^n \to \mathbb{R}^n$ are sufficiently smooth functions. The existence of a heteroclinic orbit to (1.4), referred to as a defect solution, has been shown in [21] under generic assumptions on h and j and under the assumption that the unperturbed system $\dot{u} = h(u)$ possesses a heteroclinic orbit. Homoclinic orbits may be considered simply as a heteroclinic orbit with the same end points as $x \to \pm\infty$.

The heteroclinic orbit in the homogeneous case is assumed to connect two hyperbolic fixed points P^- as $x \to -\infty$ and P^+ as $x \to \infty$. When $\varepsilon \neq 0$ there exist perturbed fixed points $P_\varepsilon^\pm$ which are $O(\varepsilon)$ close to $P^\pm$ and have $\lim_{\varepsilon\to 0} P_\varepsilon^\pm = P^\pm$ and $x = 0$. Without loss of generality, it is assumed that the heteroclinic orbit in (1.4), if it exists, connects the fixed point P^- as $x \to -\infty$ to the perturbed fixed point P_ε^+ as $x \to \infty$. In Chapter 4

we further summarise these conditions, the existence results of [21] and begin to develop the general theory for establishing the spectral stability of defect solutions to (1.3).

There are three types of defect solutions outlined in [21]. The first of these are *trivial defect solutions*, see the leftmost image of Figure 1.2.3, which are, to leading order, constant solutions $P^- = P^+$ in the unperturbed system with the defect occurring asymptotically close to both end points. The heteroclinic orbit in the perturbed system connects P^- to P_ε^+ which is $O(\varepsilon)$ away and the profile makes, at most, an $O(\varepsilon)$ excursion from these fixed points [21]. There exists a unique trivial defect solution and we can consider this as a perturbation of the trivial solution in the homogenous case. Chapter 4 establishes the conditions for stability of these trivial defect solutions.

Another type of solution, and the focus of both [21] and §5.4 as part of the ongoing work, are *local defect solutions*, see the middle image of Figure 1.2.3. In these types of solutions the defect occurs near either P^+ or P^-. The persistence or non-persistence of the heteroclinic orbit from the unperturbed system is established in [21]. It is found that the dimension of the problem and the nature of the linearised system near the end points are key in the conditions for the existence of defect solutions. There may be a unique local defect solution, a well-defined finite number of local defect solutions or a countably infinite number [21]. The final type of defect solution, which are not considered in this thesis are *global defect solutions* [21], see the rightmost image of Figure 1.2.3.

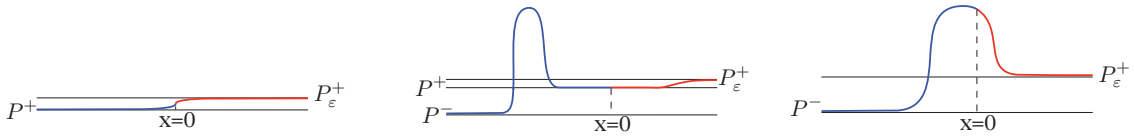

Figure 1.2.3: A depiction of three types of defect solutions. The defect occurs at the point $x = 0$. Left: a trivial defect solution. Middle: a local defect solution. The defect has occurred near P_ε^+. Right: a global defect solution. Image is from A. Doelman, P. van Heijster, and F. Xie. A geometric approach to stationary defect solutions in one space dimension. *SIAM Journal on Applied Dynamical Systems*, 15:655–712, 2016 copyright

1.3 Spectral stability

We review some of the existing stability techniques in the context of second order systems of equations in homogeneous media. These techniques are readily extendible to higher order systems. The following overview is mainly based on [54] and [88] which contain more detailed reviews of stability analysis techniques.

1.3.1 Linearised operators

Consider a generic second order RDE

$$u_t = Du_{xx} + f(u),\ u \in \mathbb{R}^N, \tag{1.5}$$

where D is an $N \times N$ diagonal matrix with non-negative entries and $f : \mathbb{R}^N \to \mathbb{R}^N$ is a sufficiently smooth function.

As we wish to focus on stability rather than existence, we make the assumption a solution exists.

Hypothesis 1.1. *The system* (1.5) *supports stationary solutions or travelling waves, i.e. solutions that travel with a constant or zero speed and maintain their shape with respect to time.*

In the case of travelling wave solutions we pass to a moving frame via the change of variables $z = x - ct$ where c is the constant speed of the wave. Travelling wave solutions to (1.5) are stationary solutions in this moving frame. We label the stationary solution to (1.5) as $\hat{u}$. In homogeneous media there will be a one parameter family of solutions to (1.5) due to the translation invariance of solutions, *i.e.* if $\hat{u}(x)$ is a solution to (1.5) then $\tilde{u} := \hat{u}(x + \kappa)$ is also a solution.

We now linearise (1.5) about $\hat{u}$ via the substitution $u(x,t) = \hat{u}(x) + p(x,t)$ where $p(x,t) \in \mathbb{R}^n$ is a perturbation. Considering only first order perturbation terms we obtain the linearised operator $\mathcal{L} : H^1(\mathbb{R}^N) \to H^1(\mathbb{R}^N)$;

$$p_t = \mathcal{L}p := \left(D\partial_{xx} + J_f(\hat{u})\right) p, \tag{1.6}$$

where J_f denotes the Jacobian of $f(u)$ with respect to u and the Sobolev space $H^1(\mathbb{R}^N)$ is the subset of once (weakly) differentiable functions such that both the function and its weak derivative are in $L^2(\mathbb{R}^N)$, i.e. square integrable. The eigenvalue problem associated with (1.6) is

$$\mathcal{L}p = \lambda p$$

with $\lambda \in \mathbb{C}$.

Remark 1.3.1. *The operator* $\mathcal{L}$ *in* (1.6) *is second order. However, we only require* $p \in H^1(\mathbb{R}^N)$ *implying a second order derivative need not exist necessarily. This is because we consider weak solutions* p *to* (1.6).

In particular, let ϕ *be a test function, that is a smooth function with compact support. If we multiply* (1.6) *by* ϕ *and integrate over the domain;*

$$\int_0^\infty \int_{-\infty}^\infty p_t\phi - Dp_{xx}\phi - J_f(\hat{u})p\phi \; dxdt = 0.$$

We integrate the first term by parts in t (exchanging the order of integration), the second by parts in x and leave the third term to obtain

$$\int_0^\infty \int_{-\infty}^\infty -p\phi_t + Dp_x\phi_x - J_f(\hat{u})p\phi \; dxdt = 0. \tag{1.7}$$

A solution to (1.6) *will also be a solution to* (1.7) *but there may be solutions p which satisfy* (1.7) *for all test functions that are not twice differentiable. These are referred to as weak solutions to* (1.6)*. We refer to [9] for more details.*

Definition 1.3.1. *([88] Definition 3.2) We say $\lambda \in \mathbb{C}$ is in the spectrum of the operator $\mathcal{L}$, denoted $\sigma(\mathcal{L})$, if the operator $\mathcal{L} - \lambda I$, where I is the identity matrix, is not invertible, i.e. the inverse does not exist or is not bounded.*

We call the solution $\hat{u}$ *spectrally stable* if all $\lambda \in \sigma(\mathcal{L})$ are contained in the left half plane, i.e. the real part $\Re(\lambda) < 0$ with the exception of $\lambda = 0$ which is the eigenvalue associated with the translational invariance of the solution. The spectrum of an operator falls naturally into two parts; the *essential spectrum*, denoted $\sigma_{ess}(\mathcal{L})$ and the *point spectrum*, denoted $\sigma_{pt}(\mathcal{L})$ [41]. There are a few different ways in which an instability will manifest. These instabilities are classified based on the manner in which a perturbation about a steady state spreads in space and grows/decays in time. We follow the classifications from [96]. An *absolute instability* is one where the norm of a perturbation, in a particular (unweighted) function space, grows at every point where it is applied while a *convective instability* is one where the perturbation moves as it grows, so the norm of the perturbation decays at each spatial point with respect to time but grows in norm overall, see Figure 1.3.1. If there are values of the spectrum in the right half plane in the unweighted function space that are shifted into the open left half plane in a weighted space then the steady state is referred to as *transiently unstable* with perturbations transmitted towards spatial infinity, see §1.3.3 for details on weighted spaces. If there is no way to resolve spectrum that has positive real part the steady state is referred to as *remnant instabilities*. Note that the perturbed solution may decay to a translate of the original solution due to the translation invariance of the solution. That is the solution $\hat{u}$ is still considered stable if, when perturbed, it evolves to $\hat{u}(x + \kappa)$ rather than $\hat{u}(x)$. These solutions are referred to as *orbitally stable*.

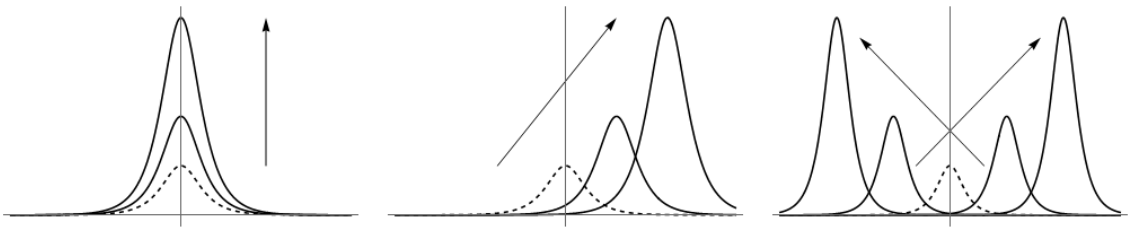

Figure 1.3.1: Types of instabilities. The dotted curve represents a small perturbation of a steady state of (1.5) and the arrows represent the direction of growth of the solid black curves with respect to time. The leftmost graph depicts an absolute instability. An absolute instability grows in norm with time at every spatial point where it is applied. The middle graph depicts a convective instability that grows in one direction but decays in norm with time at any specific spatial point. The right most graph depicts a convective instability that grows in both directions but decays in norm with time at any specific spatial point. This image was adapted from Figure 1. of [90] and Figure 2. of [96].

Much of the stability analysis we apply requires that the operator $\mathcal{L}$ is *exponentially asymptotic*.

Definition 1.3.2. *([54] Definition 3.1.1) An nth order operator $\mathcal{L}$ of the form*

$$\mathcal{L}p := \partial_x^n p + a_{n-1}(x)\partial_x^{n-1} p + \cdots + a_1(x)\partial_x p + a_0(x)p \tag{1.8}$$

is called exponentially asymptotic if all of the coefficients a_j are asymptotically constant, i.e. if there exists $r > 0$ such that

$$\lim_{x\to\pm\infty} e^{r|x|}|a_j(x) - a_j^{\pm}| = 0,$$

where $a_j^{\pm} := \lim_{x\to\pm\infty} a_j(x)$ for $j = 0, 1, ..., n-1$.

Definition 1.3.3. *([54] Definition 3.1.4) We define the* asymptotic operator *of* (1.8)

$$\mathcal{L}_\infty p := \partial_x^n p + a_{n-1}^\infty(x)\partial_x^{n-1} p + \cdots + a_1^\infty(x)\partial_x p + a_0^\infty(x)p$$

where
$$a_j^\infty = \begin{cases} a_j^- & x < 0, \\ a_j^+ & x \geq 0. \end{cases}$$

For simplicity, we assume we have a second order operator ($n = 2$) as is the case for our generic RDE (1.6). It is more convenient to work with an equivalent first order system of ODEs. To this end we take the eigenvalue problem $\mathcal{L}p = \lambda p$ and define the operator $\mathcal{T}(\lambda)$, which is equivalent to $\mathcal{L} - \lambda I$, by expressing the eigenvalue problem as a system of first order equations. This is done by introducing the variables $q_i = (p_i)_x$ for $i = 1, \ldots, N$.

We define the operator $\mathcal{T}(\lambda) : H^1(\mathbb{R}^N) \times L^2(\mathbb{R}^N) \to H^1(\mathbb{R}^N) \times L^2(\mathbb{R}^N)$ by

$$\mathcal{T}(\lambda) \begin{pmatrix} p_1 \\ \vdots \\ p_N \\ q_1 \\ \vdots \\ q_N \end{pmatrix} := \left(\frac{d}{dx} - A(x, \lambda) \right) \begin{pmatrix} p_1 \\ \vdots \\ p_N \\ q_1 \\ \vdots \\ q_N \end{pmatrix} = 0, \tag{1.9}$$

where $A(x, \lambda)$ is a $2N \times 2N$ matrix and we use the notation $\mathbf{p} := (p_1, \ldots, p_N, q_1, \ldots, q_N)^T$ where convenient.

As in Definition 1.3.3, we define the asymptotic operator associated with $\mathcal{T}(\lambda)$ as

$$\mathcal{T}_\infty(\lambda) := \begin{cases} d/dz - A_-(\lambda) & \text{if } z < 0, \\ d/dz - A_+(\lambda) & \text{if } z \geq 0, \end{cases} \tag{1.10}$$

where $A_\pm(\lambda) := \lim_{z \to \pm\infty} A(z, \lambda)$.

Example 1. ***Fisher-Kolmogorov-Petrovsky-Piscounov (FKPP) example***
Throughout this section we will use the prototypical FKPP equation as an illustrative example. This second order, scalar (i.e. $N = 1$) equation was developed in [31, 65] to model the invasion of a gene in a population. The existence and stability of travelling wave solutions for this problem has been well studied, see for example [35, 88] and references therein for an overview of known results. The non-dimensional FKPP equation is

$$u_t = u_{xx} + u(1 - u), \tag{1.11}$$

where $x \in \mathbb{R}$, $u \in \mathbb{R}$ and $t \in \mathbb{R}^+$.

We pass to a moving frame $z = x - ct$, $\tau = t$, where c is the speed of the travelling wave. In this frame (1.11) *becomes*

$$u_\tau = u_{zz} + cu_z + u(1 - u). \tag{1.12}$$

It is well known that a family of travelling wave front solutions $\hat{u}(z)$ exist for this problem for all non-negative wave speeds c with $\lim_{z \to -\infty} \hat{u}(z) = 1$ and $\lim_{z \to \infty} \hat{u}(z) = 0$. For $c \geq 2$ these wave fronts are non-negative, monotone and spectrally stable.

To derive this stability result we make the substitution $u(z, \tau) = \hat{u}(z) + p(z, \tau)$ into (1.12) *where $p(z, \tau)$ is a small perturbation and $\hat{u}(z)$ the travelling wave solution. By considering only leading order perturbation terms, we obtain the linearised operator*

$$p_\tau = (\partial_{zz} + c\partial_z + 1 - 2\hat{u})p,$$

and define the associated second order operator $\mathcal{L} : H^1(\mathbb{R}) \to H^1(\mathbb{R})$ *by*

$$\mathcal{L}p = (\partial_{zz} + c\partial_z + 1 - 2\hat{u})p. \tag{1.13}$$

For the eigenvalue problem $\mathcal{L}p = \lambda p$ *we set* $q := p_z$ *and define the operator* $\mathcal{T}(\lambda) : H^1(\mathbb{R}) \times L^2(\mathbb{R}) \to H^1(\mathbb{R}) \times L^2(\mathbb{R})$ *by*

$$\mathcal{T}(\lambda)\begin{pmatrix} p \\ q \end{pmatrix} := \left(\frac{d}{dz} - A(z,\lambda)\right)\begin{pmatrix} p \\ q \end{pmatrix} = 0, \text{ with } A(z,\lambda) := \begin{pmatrix} 0 & 1 \\ \lambda - 1 + 2\hat{u} & -c \end{pmatrix}. \tag{1.14}$$

For (1.14) *the asymptotic matrices are*

$$A_-(\lambda) = \begin{pmatrix} 0 & 1 \\ \lambda + 1 & -c \end{pmatrix} \text{ and } A_+(\lambda) = \begin{pmatrix} 0 & 1 \\ \lambda - 1 & -c \end{pmatrix}.$$

In the next sections we will introduce the essential spectrum and two related concepts; weighted spaces and the absolute spectrum. We will then introduce the point spectrum.

1.3.2 Essential spectrum

The essential spectrum provides information on the (in)stability of the asymptotic end states of the stationary solution (which may be a travelling wave solution in a moving frame). If part of the essential spectrum is in the right half plane, then the stationary solution is unstable and there is a continuum of unstable modes. The essential spectrum is found by analysing the dimensions of the unstable, stable and centre subspaces of $A_\pm(\lambda)$ (1.10). A convenient measure of the size of these subspaces is the Morse index, $i(A)$, which for a constant matrix A is defined as the dimension of its unstable subspace, see [54] Definition 3.1.9. So, for an asymptotic operator of the form of (1.10), we denote the Morse indices $i_\pm := i(A_\pm(\lambda)) := \dim(\mathbb{E}^u_\pm)$, where $\mathbb{E}^u_\pm$ denotes the unstable subspace of $A_\pm(\lambda)$ respectively. We have the following definition for the essential spectrum;

Definition 1.3.4. *([54] Definition 3.1.11) We say* $\lambda \in \sigma_{ess}(\mathcal{T}_\infty)$*, the essential spectrum of* $\mathcal{T}_\infty$*, if either*

i. $A_+(\lambda)$ *and* $A_-(\lambda)$ *are hyperbolic with a different number of unstable matrix eigenvalues, i.e.* $i_+ - i_- \neq 0$*; or*
ii. $A_+(\lambda)$ *or* $A_-(\lambda)$ *has at least one purely imaginary matrix eigenvalue.*

Due to the continuous dependence of the matrix eigenvalues on λ we have that the boundaries of the essential spectrum will consist of the values of λ that satisfy Definition 1.3.4 ii. These boundaries are the so-called *dispersion relations* which relate the temporal eigenvalues λ to the spatial eigenvalues μ (which are the matrix eigenvalues of $A_\pm(\lambda)$).

We have from [54] Section 2.2 that the asymptotic operator $\mathcal{T}_\infty$ is a relatively compact perturbation of $\mathcal{T}$ and thus by Weyl's theorem (see for example [54] Section 2.2) the essential spectrum of $\mathcal{T}_\infty$ and $\mathcal{T}$ coincide.

In general, we assume that the operator $\mathcal{L}$ (and therefore $\mathcal{T}$) is well-posed, *i.e.* there exists some $a_0 \in \mathbb{R}$ such that for all λ with $\Re(\lambda) > a_0$ we have $\lambda \notin \sigma(\mathcal{L})$. If there exist values $\Re(\lambda) \gg 1$ in the spectrum then the stationary solution would be unstable to high frequency perturbations [54].

Example 1. ***FKPP example continued***

We return to the operator $\mathcal{T}(\lambda)$ from (1.14) *and its associated asymptotic matrices. The matrix eigenvalues of $A_-(\lambda)$ and $A_+(\lambda)$ are respectively*

$$\mu^-_{1,2} = \frac{-c \pm \sqrt{c^2 + 4(\lambda+1)}}{2} \quad \textit{and} \quad \mu^+_{1,2} = \frac{-c \pm \sqrt{c^2 + 4(\lambda-1)}}{2}.$$

We take $\mu = ik$ where $k \in \mathbb{R}$ is a parameter, then the boundaries of the essential spectrum, also called the dispersion relations, (Part ii of Definition 2.4.) are

$$\lambda = -k^2 + ick - 1 \tag{1.15a}$$

$$\lambda = -k^2 + ick + 1 \tag{1.15b}$$

These parametric equations divide the complex plane into three regions, see Figure 1.3.2.

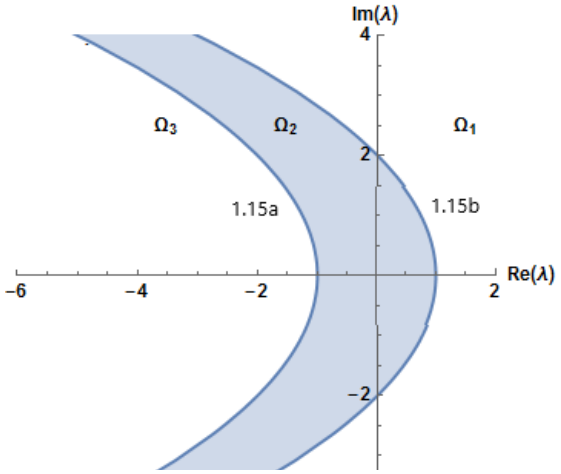

Figure 1.3.2: The essential spectrum of the FKPP equation in the unweighted space $H^1(\mathbb{R})$ for $c = 2$. In the region to the right of the parametric curves (1.15), labelled Ω_1, we have that $\Re(\mu_1^-) > 0 > \Re(\mu_2^-)$ and $\Re(\mu_1^+) > 0 > \Re(\mu_2^+)$. Thus, this region is not part of the essential spectrum. In the interior of the region labelled Ω_2 we have $\Re(\mu_1^-) > 0 > \Re(\mu_2^-)$ and $0 > \Re(\mu_1^+) \geq \Re(\mu_2^+)$. By Definition 1.3.4 i. Ω_2 is part of the essential spectrum. In Ω_3, we have $0 > \Re(\mu_1^-) \geq \Re(\mu_2^-)$ and $0 > \Re(\mu_1^+) \geq \Re(\mu_2^+)$ so this region is also not essential spectrum. The parabolic curves bounding Ω_2 are the dispersion relations (1.15a) and (1.15b) from left to right.

Note in (1.15b) $k = 0$ *gives* $\lambda = 1$ *for all values of* c. *This is the rightmost point of the essential spectrum and as it is in the right half plane every wave is unstable in the unweighted space* $H^1(\mathbb{R})$, *independent of the speed.*

1.3.3 Weighted spaces

In many cases, such as in Example 1, the essential spectrum associated with a solution contains purely imaginary values of λ and/or enters into the right half plane, implying instability. However, often solutions can be found through numerical simulations, implying some sort of stability. In [93] a cure proposed for this apparent contradiction is to work in an appropriately weighted space. If we weight the space, we are restricting the types of perturbations $p(x,t)$ we allow to apply to the travelling waves or stationary solutions. The weights shift the essential spectrum. If weights can be found that shift the essential spectrum into the open left half plane then the wave is stable to perturbations that decay at a rate faster than these weights (provided there are no values in the point spectrum with positive real part). In numerical simulations the perturbations typically used have compact support which is why the instability in the unweighted space is not observed; the essential spectrum indicates the (in)stability of perturbations at ∞.

Let $\tilde{p}(z,t) := e^{\nu z}p(z,t)$ in the weighted space $H^1_\nu(\mathbb{R})$ defined by the norm

$$\|p\|_{H^1_\nu} = \|e^{\nu z}p\|_{H^1} = \|\tilde{p}\|_{H^1}.$$

In particular, we have that $p \in H^1_\nu$ if $\tilde{p} \in H^1$ and $\tilde{q} \in L^2_\nu$ is defined similarly with respect to $q \in L^2$. If there exists ν that shifts the essential spectrum into the left half plane (provided there are no values in the point spectrum with positive real part) then we say the travelling wave solution is stable in $H^1_\nu(\mathbb{R})$. This substitution transforms (1.9) into

$$\mathcal{T}_\nu(\lambda)\begin{pmatrix} p \\ q \end{pmatrix} := \left(\frac{d}{dz} - (A(z,\lambda) + \nu I)\right)\begin{pmatrix} p \\ q \end{pmatrix} = 0,$$

where I is the $2N \times 2N$ identity matrix and $A(z,\lambda)$ is defined as before. We now calculate the *weighted essential spectrum*, denoted σ^ν_{ess}, defined as those values for which $(A_\pm(\lambda) + \nu I)$ have a different number of eigenvalues, Definition 1.3.4. The characteristic equation of $(A_+(\lambda) + \nu I)$ is given by

$$\det\left(A_+(\lambda) + \nu I - \mu^+ I\right) = 0,$$

where μ^+ is the spatial/matrix eigenvalue of $A_+(\lambda)$. The boundaries of the weighted essential spectrum are the values of λ such that $\mu^+ = ik + \nu$. That is, we are now comparing the magnitude of the real part of the spatial eigenvalue to the value ν rather than zero. This has the effect of shifting the essential spectrum.

By weighting the space, we are restricting our perturbations that grow and decay at a rate greater than ν as $z \to \pm\infty$. The sign of ν also indicate which asymptotic state of the wave is more sensitive to perturbations. For instance, if $\nu > 0$ then the weight penalises perturbations as $z \to \infty$, while allowing for perturbations that grow slower than $e^{-\nu z}$ as $z \to -\infty$. We note that we can also use a two-sided weight

$$\nu = \begin{cases} \nu_- \text{ if } & z < 0, \\ \nu_+ \text{ if } & z > 0, \end{cases}$$

which requires that the perturbation must decay exponentially in both directions.

Example 1. ***FKPP example continued***

If we make the substitution $\begin{pmatrix} \tilde{p} \\ \tilde{q} \end{pmatrix} := e^{\nu z} \begin{pmatrix} p \\ q \end{pmatrix}$ *then the asymptotic operator associated with* (1.14) *becomes*

$$\mathcal{T}_\nu(\lambda) \begin{pmatrix} p \\ q \end{pmatrix} = \left(\frac{d}{dz} - (A_\pm(\lambda) + \nu I) \right) \begin{pmatrix} p \\ q \end{pmatrix} = 0.$$

The characteristic equations $(A_\pm(\lambda) + \nu I)$ *are*

$$\begin{aligned} \text{from } A_-(\lambda) + \nu I: &\quad (\mu - \nu)^2 + c(\mu - \nu) - \lambda - 1 = 0 \\ \text{from } A_+(\lambda) + \nu I: &\quad (\mu - \nu)^2 + c(\mu - \nu) - \lambda + 1 = 0. \end{aligned}$$

If we once again set $\mu = ik$ *the boundaries of the weighted essential spectrum are*

$$\lambda = -k^2 - 2ik\nu + \nu^2 + ick - c\nu - 1 \text{ and } \lambda = -k^2 - 2ik\nu + \nu^2 + ick - c\nu + 1.$$

The rightmost points of these boundaries are found when $k = 0$ *and these points are* $\nu(\nu - c) \pm 1$. *These points are the most negative when* $\nu = \frac{c}{2}$. *For this value of* ν *the boundaries of the weighted essential spectrum are*

$$\lambda = -1 - \frac{c^2}{4} - k^2 \text{ and } \lambda = 1 - \frac{c^2}{4} - k^2.$$

These boundaries correspond to the optimally weighted essential spectrum and, in this case, coincide with the absolute spectrum. Furthermore, for $c > 2$, *these boundaries are real with* $\lambda < 0$, $\forall k \in \mathbb{R}$.

1.3.4 Absolute spectrum

Another important concept is that of the *absolute spectrum*, denoted σ_{abs}. For this we again follow the definitions from [54, 88]. The absolute spectrum is not spectrum in the usual sense as it does not arise from the definition that $\mathcal{L}$ is not invertible (Definition

1.3.1) but it provides important information about stability and gives an indication of how far the essential spectrum can be weighted. If the absolute spectrum moves into the right half plane when a parameter is changed then the essential spectrum cannot be weighted into the left half plane indicating the onset of an absolute instability.

For our generic operator $\mathcal{T}(\lambda) = d/dz - A(z,\lambda)$, whose asymptotic matrices $A_\pm(\lambda)$ are $2N \times 2N$, the well-posedness assumption states that $\lambda \in \mathbb{C}$ with $\Re(\lambda) \gg 1$ is not part of the spectrum, thus $dim(\mathbb{E}^u_-) = dim(\mathbb{E}^u_+) =: j$ where $\mathbb{E}^u_\pm$ are the unstable subspaces of $A_\pm(\lambda)$ respectively. We have the following definition for the absolute spectrum.

Definition 1.3.5. *For $\lambda \in \mathbb{C}$ we rank the $2N$ spatial eigenvalues of $A_\pm$, labelled $\mu^\pm_i$ for $i = 1, ..., 2N$, by the magnitude of their real parts, i.e.*

$$\Re(\mu^\pm_1(\lambda)) \geq \Re(\mu^\pm_2(\lambda)) \geq \ldots \geq \Re(\mu^\pm_j(\lambda)) \geq \Re(\mu^\pm_{j+1}(\lambda)) \geq \ldots \geq \Re(\mu^\pm_{2N}(\lambda)).$$

We say λ is in the absolute spectrum of $\mathcal{T}$, denoted $\sigma_{abs}(\mathcal{T})$ if either $\Re(\mu^+_j(\lambda)) = \Re(\mu^+_{j+1}(\lambda))$ or $\Re(\mu^-_j(\lambda)) = \Re(\mu^-_{j+1}(\lambda))$.

If $\lambda \notin \sigma_{abs}(\mathcal{T})$ then there exists $\nu_\pm \in \mathbb{R}$ such that $\Re(\mu^+_j(\lambda)) > \nu_+ > \Re(\mu^+_{j+1}(\lambda))$ and $\Re(\mu^-_j(\lambda)) > \nu_- > \Re(\mu^-_{j+1}(\lambda))$. This means that if $\lambda \notin \sigma_{abs}(\mathcal{T})$ then there exists a weight such that λ is not in the weighted essential spectrum. Values of λ such that $\Re(\mu^+_i) = \Re(\mu^+_{i+1})$ or $\Re(\mu^-_i) = \Re(\mu^-_{i+1})$ for $i \neq j$ are referred to as the *generalised absolute spectrum* [54,88]. We also note that the absolute spectrum is unaffected by weighting the space.

In the case $N = 1$, *i.e.* scalar 2nd order equations, the asymptotic matrices $A_\pm(\lambda)$ are 2×2 and the definition of the absolute spectrum simplifies immensely. Notably, for scalar equations, there is no generalised absolute spectrum. Nonetheless, it is worthwhile to consider the statement of Definition 1.3.5 in the scalar case. That is, 'For a 2×2 system (such as Example 1) the absolute spectrum is defined as the values of $\lambda \in \mathbb{C}$ where the real parts of the spatial eigenvalues, $\mu^-_{1,2}$ of $A_-(\lambda)$ are equal or the real parts of the spatial eigenvalues, $\mu^+_{1,2}$ of $A_+(\lambda)$ are equal.'

Example 1. ***FKPP example continued***

The absolute spectrum consists of $\lambda \in \mathbb{C}$ such that either $\mu^-_1 = \mu^-_2$ or $\mu^+_1 = \mu^+_2$. We have $\mu^-_1 = \mu^-_2$ when λ is on the real line with $\lambda \leq \frac{-c^2}{4} - 1$ and $\mu^+_1 = \mu^+_2$ when λ is on the real line with $\lambda \leq \frac{-c^2}{4} + 1$. Thus, we have

$$\sigma_{abs} = \left\{ \lambda : Im(\lambda) = 0 \text{ and } \lambda \leq \frac{-c^2}{4} + 1 \right\}. \tag{1.16}$$

Note that the minimum wave speed $c = 2$ corresponds to $\sigma_{abs} = (-\infty, 0]$. For $c < 2$ the absolute spectrum enters into the right half plane corresponding to the onset of absolute instability.

1.3.5 Point spectrum

The point spectrum consists of isolated eigenvalues with finite multiplicity [88]. For $\lambda \in \sigma_{pt}$ the null space of $\mathcal{L} - \lambda I$ (1.8) (equivalently of $\mathcal{T}(\lambda)$ (1.9)) is non-trivial and finite dimensional and as λ is isolated $\mathcal{L} - \lambda I$ is invertible in a δ-neighbourhood of λ, except at λ.

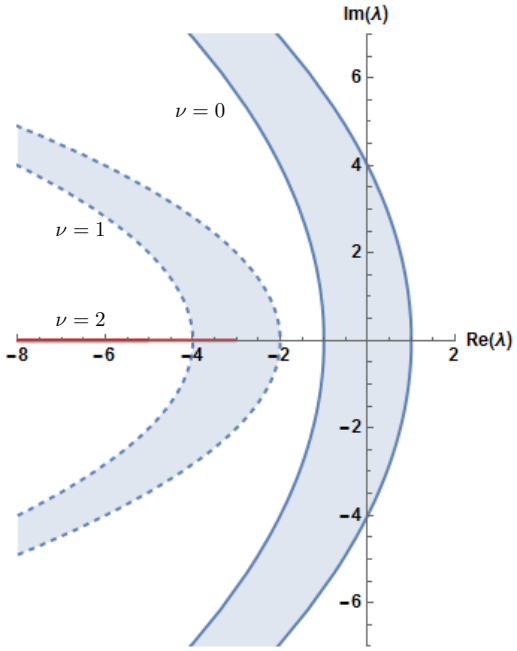

Figure 1.3.3: Weighted essential spectrum for the FKPP model with $c = 4$ and various weights. The unweighted essential spectrum ($\nu = 0$) is shown with blue solid boundary curves and a weighted essential spectrum with weight $\nu = 1$ is shown with dashed boundary curves. For these parameter values the absolute spectrum (red solid line) is $\lambda \in \mathbb{R}$ with $\lambda \in (-\infty, -3]$. The weighted essential spectrum with $\nu = 2$ coincides with the absolute spectrum. The associated travelling wave solution is potentially spectrally stable in $\mathcal{H}^1_1(\mathbb{R}^N) \times L^2_1(\mathbb{R}^N)$ and $\mathcal{H}^1_2(\mathbb{R}^N) \times L^2_2(\mathbb{R}^N)$ but is unstable in $\mathcal{H}^1(\mathbb{R}^N) \times L^2(\mathbb{R}^N)$ (the unweighted space). The lack of point spectrum in the right half plane must be established before spectral stability in the weighted spaces can be concluded for the FKPP travelling waves. We do not examine the point spectrum of the FKPP in this thesis.

To locate the point spectrum, we look for non-trivial solutions in the kernel of (1.9). That is, we look for $p \in H^1(\mathbb{R}^N) \times L^2(\mathbb{R}^N)$, or an appropriately weighted space, such that

$$p' = A(x; \lambda)p \tag{1.17}$$

where $p := (p_1, \ldots, p_N, q_1, \ldots, q_N)^T$ as before.

Definition 1.3.6. *A value $\lambda \in \mathbb{C} \backslash \sigma_{ess}(\mathcal{L})$ is a temporal eigenvalue of $\mathcal{L}$ if we can find a non-trivial solution to* (1.17) *in $H^1(\mathbb{R}^N) \times L^2(\mathbb{R}^N)$. The function p will be the temporal eigenfunction corresponding to λ.*

For p to be a solution to (1.17) it will necessarily decay to zero as $x \to \pm\infty$. For non-trivial solutions this can only happen in a specific way. For example, for $x \ll 0$ the system (1.17) behaves like

$$p' = A_-(\lambda)p$$

and for $\lambda \notin \sigma_{ess}$ we have that $A_-(\lambda)$ is hyperbolic. Thus, only solutions in the unstable subspace of $A_-(\lambda)$ can decay to zero as $x \to -\infty$.

From [35] we have the following proposition.

Proposition 1.3.2. *For $\lambda \in \mathbb{C}\backslash\sigma_{ess}(\mathcal{L})$, if p is a solution to (1.17) with $p \in H^1(\mathbb{R}^N) \times L^2(\mathbb{R}^N)$ then we have*

$$\lim_{z\to-\infty} p \to \mathbb{E}^u_- \quad \text{and} \quad \lim_{z\to\infty} p \to \mathbb{E}^s_+$$

where $\mathbb{E}^u_-$ is the unstable subspace of $A_-(\lambda)$ as $z \to -\infty$ and $\mathbb{E}^s_+$ is the stable subspace of $A_+(\lambda)$ as $z \to \infty$.

One important feature of the point spectrum is that it is unaffected by weights, *i.e.* the location of a temporal eigenvalue λ cannot be changed. If λ is an eigenvalue in the point spectrum with eigenvector p then $\tilde{p} = e^{\nu z}p$ is also an eigenfunction in the sense that it is a solution to the eigenvalue problem. However, this eigenfunction may not exist in the weighted space. We consider such values λ as temporal eigenvalues regardless of the weight used to shift the essential spectrum. Furthermore, if the essential spectrum is shifted so it encompasses λ, then λ is no longer isolated and so does not meet our definition of a temporal eigenvalue. We will refer to values λ that are encompassed by the essential spectrum in the unweighted space but isolated in a weighted space as a temporal eigenvalue of that weighted space.

The value $\lambda = 0$ is an eigenvalue in the point spectrum with eigenfunction $\partial_x\hat{u}$. If $\lambda = 0$ is not encompassed by the essential spectrum (in a weighted or unweighted space) and $\partial_x\hat{u}$ exists in the function space then $\lambda = 0$ is a value in the point spectrum. Taking a solution $\hat{u}$ to (1.5) we consider $p = \hat{u}_x$ in the eigenvalue problem $\mathcal{L}p = \lambda p$ associated with (1.6). As $\mathcal{L} = D\hat{u}_{xx} + J_f(\hat{u})$, this gives

$$D(\hat{u}_x)_{xx} + J_f(\hat{u})\hat{u}_x = \left(D\hat{u}_{xx} + f(\hat{u})\right)_x = 0. \tag{1.18}$$

So $\lambda = 0$ is an eigenvalue with eigenfunction $\partial_x\hat{u}$. This eigenfunction is associated with the translation invariance of the problem.

1.3.6 The Evans function

The Evans function is an analytic tool for locating the point spectrum and it was originally developed by Evans to study nerve impulses [23–26]. The Evans function was used and further developed in [50] to study the stability of travelling wave solutions to the Fitzhugh-Nagumo model. It was further extended in [2] where it was used to study the stability of travelling wave solutions to a singularly perturbed system of RDEs.

For (1.10) we denote the unstable eigenspace associated with $A_-(\lambda)$ as $\mathbb{E}^u_-$ and similarly the stable subspace of $A_+(\lambda)$ as $\mathbb{E}^s_+$. We define the largest connected component to the right of the essential spectrum as Ω_1. By the well-posedness assumption the region Ω_1 contains $\lambda \in \mathbb{C}$ with $\Re(\lambda) \gg 1$, see Figure 1.3.3 for an example. This region Ω_1 is the natural domain of the Evans function. On Ω_1 the matrices $A_\pm(\lambda)$ are hyperbolic with the same number of unstable eigenvalues. This means we must have $\dim(\mathbb{E}^u_-)+\dim(\mathbb{E}^s_+) = 2N$ on Ω_1. Let $\dim(\mathbb{E}^u_-) = j$ and $\dim(\mathbb{E}^s_+) = 2N - j$ with $0 \leq j \leq 2N$.

The Evans function is a Wronskian and for our generic second order system (1.6) it is defined as

$$E(\lambda) := \det\Big(\mathbf{W}_1, \dots \mathbf{W}_j, \mathbf{W}_{j+1}, \dots, \mathbf{W}_{2N}\Big) \tag{1.19}$$

where $\mathbf{W}_i$ for $i = 1, \dots, j$ are linearly independent solutions to (1.17) that decay to $\mathbb{E}^u_-$ as $x \to -\infty$ and $\mathbf{W}_i$ for $i = j+1, \dots, 2N$ are linearly independent solutions to (1.17) that decay to $\mathbb{E}^s_+$ as $x \to \infty$. The Evans function is analytic on Ω_1 [88] and for $\lambda \in \Omega_1$ the Evans function has the following properties

Theorem 1.3.3. *([88] Theorem 4.1):*

- *$E(\lambda)$ is real if λ is real,*
- *$E(\lambda) = 0$ if and only if λ is a point eigenvalue,*
- *The order of λ as a root of the Evans function corresponds to the algebraic multiplicity of λ as an eigenvalue.*

Thus, we locate the point spectrum in Ω_1 as the zeros of the Evans function. As the solutions $\mathbf{W}_i$ for $i = 1, ..., j$ are linearly independent they form a basis of $\mathbb{E}^u_-$, similarly the solutions $\mathbf{W}_i$ for $i = j+1, ..., 2N$ form a basis of $\mathbb{E}^s_+$. This choice of basis is not unique, however, the Evans function in two different bases will differ only by a non-zero function. This non-zero function corresponds to the determinant of a change of basis matrix. So, while the Evans function is dependent on the choice of basis, the zeros of the Evans function (*i.e.* the location of the point spectrum) are unaffected.

Remark 1.3.4. *The Evans function can be extended into the essential and absolute spectrum on an appropriate Riemann surface, see [54–56]. Zeroes of the Evans function on*

this extended domain give additional information about the transition from stable solutions to unstable ones by indicating where/whether new point spectrum will emerge under perturbations.

1.4 Geometric Singular Perturbation Theory

Many systems, especially those modelling natural processes, evolve according to time or length scales that differ on many orders of magnitude. A logical first step is to assume that the processes that evolve relatively slowly are constant or to assume the relatively fast processes are instantaneous. However, this leading order approach only works for regularly perturbed problems. In the case of a singularly perturbed problem a leading order approach results in a reduction of order of the problem and significant information is lost. Our aim is to construct the stationary solutions or travelling wave solutions to these singularly perturbed problems. The existence equation associated with singularly perturbed RDEs can often be written in the form

$$\varepsilon \dot{x} = f(x, y, \varepsilon), \quad \dot{y} = g(x, y, \varepsilon), \tag{1.20}$$

where $\dot{} = d/d\tau$, $x \in \mathbb{R}^n$, $y \in \mathbb{R}^m$ and $0 < \varepsilon \ll 1$. This formulation is referred to as the *slow problem*, the variable x is referred to as the *fast variable* and y is referred to as the *slow variable*. Taking the $\varepsilon \to 0$ limit is equivalent to assuming the change in the fast variable is instantaneous. However, in taking the $\varepsilon \to 0$ limit we lose the information pertaining to the fast transition and flow is restricted to the set $f(x, y, 0) = 0$. The singular ($\varepsilon \to 0$) limit of (1.20) is referred to as the *reduced problem* and is given by,

$$0 = f(x, y, 0), \quad \dot{y} = g(x, y, 0). \tag{1.21}$$

An alternative method is to rescale the area in which the fast transition occurs by setting $t = \frac{\tau}{\varepsilon}$, *i.e.*

$$x' = f(x, y, \varepsilon), \quad y' = \varepsilon g(x, y, \varepsilon), \tag{1.22}$$

where $' = d/dt$. This formulation is referred to as the *fast problem*. Taking the $\varepsilon \to 0$ limit of the fast problem is equivalent to assuming the slow variable y is constant. The singular limit of (1.22) is referred to as the *layer problem* and is given by,

$$x' = f(x, y, 0), \quad y' = 0. \tag{1.23}$$

The singular limits of (1.20) and of (1.22) contain crucial information and each describes a different aspect of the dynamics. GSPT is a useful tool for singularly perturbed problems, giving a geometric approach for obtaining an approximation to solutions that capture both the slow and fast dynamics utilising these singular limits. The fundamental tool used in

GSPT is the invariant manifold theory developed by Fenichel [29,30] which has been used extensively for problems with a clear time scale separation, see for instance [39, 51, 53] which provide in depth introductions to GSPT. In this section we will cover Fenichel's three main theorems and demonstrate the use of GSPT with an example.

1.4.1 Fenichel Theory and GSPT

We refer to $f(x, y, 0) = 0$ as the *critical manifold*, which we denote $\mathcal{M}_0$. The critical manifold is *normally hyperbolic* if the Jacobian of $f(x, y, 0)$ with respect to the fast variable x, restricted to $\mathcal{M}_0$, only has eigenvalues with non-zero real part. We denote the unstable and stable manifold associated with the manifold $\mathcal{M}_0$ as $\mathcal{W}_{u,s}(\mathcal{M}_0)$ respectively.

We include Fenichel's three theorems below. The theorems below can be found, with minor stylistic changes, in, for example, [39, 51, 53].

Theorem 1.4.1. ***Fenichel's First Theorem*** *Suppose the critical manifold $\mathcal{M}_0$ is compact and normally hyperbolic. Further, suppose f and g are smooth. Then, for $0 < \varepsilon \ll 1$ sufficiently small, there exists a manifold $\mathcal{M}_\varepsilon$ diffeomorphic to and given to leading order in ε by, $\mathcal{M}_0$, that is locally invariant under the flow of the full problem* (1.20).

Theorem 1.4.2. ***Fenichel's Second Theorem*** *Suppose the critical manifold $\mathcal{M}_0$ is compact, possibly with boundary, and normally hyperbolic, and suppose f and g are smooth. Then for ε sufficiently small, there exist manifolds $\mathcal{W}_s(\mathcal{M}_\varepsilon)$ and $\mathcal{W}_u(\mathcal{M}_\varepsilon)$, that are close and diffeomorphic to $\mathcal{W}_s(\mathcal{M}_0)$ and $\mathcal{W}_u(\mathcal{M}_0)$, respectively. The manifolds $\mathcal{W}_s(\mathcal{M}_\varepsilon)$ and $\mathcal{W}_u(\mathcal{M}_\varepsilon)$ are locally invariant under the flow of* (1.20).

Theorem 1.4.3. ***Fenichel's Third Theorem*** *Suppose $\mathcal{M}_0$ is compact, possibly with boundary, and normally hyperbolic, and suppose f and g are smooth. Then, for every $v_\varepsilon \in \mathcal{M}_\varepsilon$ with $\varepsilon > 0$ sufficiently small, there is an n-dimensional manifold $\mathcal{W}_s(v_\varepsilon) \subset \mathcal{W}_s(\mathcal{M}_\varepsilon)$, and an m-dimensional manifold $\mathcal{W}_u(v_\varepsilon) \subset \mathcal{W}_u(\mathcal{M}_\varepsilon)$, that are $\mathcal{O}(\varepsilon)$ close to, and diffeomorphic, to $\mathcal{W}_s(v_0)$ and $\mathcal{W}_u(v_0)$, respectively. The families $\{W_{u,s}(v_\varepsilon)|v_\varepsilon \in \mathcal{M}_\varepsilon\}$ are invariant in the sense that*

$$W_s(v_\varepsilon) \cdot t \subset W_s(v_\varepsilon \cdot t),$$

for all $t > 0$, and

$$W_u(v_\varepsilon) \cdot t \subset W_u(v_\varepsilon \cdot t)$$

for all $t < 0$, where t is an evolution parameter. That is, if $v_\varepsilon = v(0)$ then $v_\varepsilon \cdot t = v(t)$.

Often, the critical manifold $\mathcal{M}_0$ under consideration is not necessarily compact, but the compactification of the manifold is usually straightforward; we consider a compact subset of $\mathcal{M}_0$ with a boundary well outside of our domain of interest (*i.e.* a boundary well outside of the asymptotic limits of our singular solutions).

Example 2. *This example is a special case of the equation studied in [20, 99, 101]. While the existence and stability of this system is known, we use it throughout this section to demonstrate the use of GSPT. Consider*

$$u_t = \varepsilon^2 u_{xx} + u - u^3 + \varepsilon(\alpha v + \gamma), \qquad v_t = v_{xx} + u - v, \tag{1.24}$$

where $0 < \varepsilon \ll 1$. *We seek stationary solutions to* (1.24) *and so set* $u_t = v_t = 0$ *and express the equations as a system of first order ODEs using the substitutions* $u_x =: p$ *and* $v_x =: q$*:*

$$\begin{aligned} \varepsilon u' &= p, & v' &= q, \\ \varepsilon p' &= u^3 - u - \varepsilon(\alpha v + \gamma), & q' &= v - u, \end{aligned} \tag{1.25}$$

where $' = d/dx$. *This is the slow system and* x *the slow scale. Taking* $\varepsilon \to 0$ *gives*

$$p = 0, \qquad u^3 - u = 0. \tag{1.26}$$

Making the substitution $\xi = \frac{x}{\varepsilon}$ *in* (1.24) *gives*

$$\begin{aligned} \dot{u} &= p, & \dot{v} &= \varepsilon q, \\ \dot{p} &= u^3 - u - \varepsilon(\alpha v + \gamma), & \dot{q} &= \varepsilon(v - u), \end{aligned} \tag{1.27}$$

where $\dot{} = d/d\xi$. *This is the fast system and* ξ *the fast scale. Taking* $\varepsilon \to 0$ *gives*

$$\begin{aligned} \dot{u} &= p, & \dot{v} &= 0, \\ \dot{p} &= u^3 - u & ,\dot{q} &= 0. \end{aligned} \tag{1.28}$$

So $v = v_0$ *and* $q = q_0$ *are constant. The fast and slow systems (*(1.27) *and* (1.25)*, respectively) are equivalent for* $\varepsilon \neq 0$ *and solutions to* (1.26) *are the fixed points to* (1.28) *however, they are not equivalent in the* $\varepsilon \to 0$ *limit as* (1.25) *with* $\varepsilon = 0$ *is not defined away from these fixed points, i.e. the limit* $\varepsilon \to 0$ *is singular.*
We have three critical manifolds of fixed points for $\varepsilon = 0$*:*

$$M_0^{\pm} := \{p = 0, u = \pm 1, v, q \in \mathbb{R}\}, \qquad M_0^0 := \{p = 0, u = 0, v, q \in \mathbb{R}\}. \tag{1.29}$$

$M_0^{\pm}$ *are normally hyperbolic, i.e. if we take any point on either manifold the Jacobian of* (1.28) *has one positive and one negative eigenvalue. Points on* M_0^0 *are centres and as we are looking for heteroclinic or homoclinic solutions we do not consider this manifold. If we assume* v *and* q *are bounded we can take* $M_0^{\pm}$ *to be compact. We can thus use the theory of Fenichel [29], [30] which states there exists perturbed manifolds* $M_\varepsilon^{\pm}$ *with unstable and stable manifolds that are* $O(\varepsilon)$ *close and diffeomorphic to* $M_0^{\pm}$ *and its unstable and stable manifolds respectively.* $M_\varepsilon^{\pm}$ *is locally invariant under the flow of* (1.27) *(*$\varepsilon \neq 0$*). We*

expand $u(x) = u_0(x) + \varepsilon u_1(x) + O(\varepsilon^2)$ *and similarly for* $p(x)$ *and match order* ε *terms in* (1.25) *to find the perturbed manifolds*

$$M_\varepsilon^\pm := \left\{ p = O(\varepsilon^2), u = \pm 1 + \varepsilon \frac{(\alpha v + \gamma)}{2} + O(\varepsilon^2), v, q \in \mathbb{R} \right\}.$$

We now look for solutions that are $O(\varepsilon)$ *close to either* $M_\varepsilon^\pm$ *except in a localised region. As one example we look for a solution that approaches the unstable manifold of* M_ε^- *as* $x \to -\infty$ *and the stable manifold of* M_ε^+ *as* $x \to \infty$*. This solution will have a slow-fast-slow structure. We label these parts I, II and III respectively. To fulfil the asymptotic conditions* $u = -1$*, to leading order, on part I and* $u = 1$*, to leading order, on part III. The equation for* v*, to leading order, in the slow variable* x *is then*

$$v_{xx} = \begin{cases} v + 1 & \text{if } x < -\sqrt{\varepsilon} \\ v - 1 & \text{if } x > \sqrt{\varepsilon}. \end{cases}$$

We apply the boundary conditions that v *is finite as* $x \to \pm\infty$ *and by symmetry* $v \to 0$ *as* $x \to 0$*. The solution for* v *is then*

$$v = \begin{cases} e^x - 1 & \text{if } x < -\sqrt{\varepsilon} \\ e^{-x} + 1 & \text{if } x > \sqrt{\varepsilon}. \end{cases}$$

On part II we assume v *is a constant with respect to the fast variable* ξ *(this can be shown integrating* q *over all of* ξ *to show* $\Delta v = O(\varepsilon)$*). Thus, the equation for* u *becomes*

$$u_{\xi\xi} = u^3 - u \text{ and } u = \tanh\left(\frac{\xi}{\sqrt{2}}\right).$$

There is a Hamiltonian associated with (1.25) *for* $\varepsilon = 0$*;*

$$H = \frac{1}{2}(u^2 + p^2) - \frac{1}{4}(u^4 + 1).$$

Thus, the solutions to (1.25) *are level sets of the above Hamiltonian. Our problem with* $0 < \varepsilon \ll 1$ *is then a perturbed Hamiltonian problem and we can show a solution exists by showing the solution on the two manifolds (the Hamiltonian restricted to* $M_\varepsilon^\pm$*) on the*

same level set are equal to leading order of ε.

$$\Delta H = H|_{M_\varepsilon^+} - H|_{M_\varepsilon^-} = O(\varepsilon^2) \tag{1.30}$$

But we also have

$$\Delta H = \int_{-\frac{1}{\sqrt{\varepsilon}}}^{\frac{1}{\sqrt{\varepsilon}}} \frac{dH}{d\xi} d\xi = \int_{-\frac{1}{\sqrt{\varepsilon}}}^{\frac{1}{\sqrt{\varepsilon}}} \varepsilon p(\alpha v + \gamma) + O(\varepsilon^2) d\xi,$$

and since $v = 0$ *in the fast system, we have*

$$\Delta H = \varepsilon\gamma \int_{-\frac{1}{\sqrt{\varepsilon}}}^{\frac{1}{\sqrt{\varepsilon}}} p \, d\xi + O(\varepsilon\sqrt{(\varepsilon)}) = 2\varepsilon\gamma + O(\varepsilon\sqrt{(\varepsilon)}). \tag{1.31}$$

By equating powers of ε *in (1.30) and (1.31) we have* $\gamma = 0$ *as a condition for existence of a solution of this form to the* (1.24). *The expressions for* ΔH *are Melnikov type calculations (see [51]) for which* $v = 0$ *is a simple zero. Thus, the intersection of the unstable and stable manifolds of* M_ε^- *and* M_ε^+, *respectively, is transversal. This is sufficient to show the solution (which is in this intersection) persists under perturbation by* ε, *as long as* $\gamma = 0$.

We must establish the conditions for existence of solutions and perform our stability analysis under these conditions. Additionally, many of the ideas and procedures from GSPT are used in the Non-local eigenvalue problem (NLEP) approach [17–19]. The NLEP approach is covered in §3.6.1 as part of future work.

1.5 Outline and original contributions

This thesis is comprised of a combination of published and unpublished work. The main goal of this work was to develop the theory and techniques for the existence and stability analysis of some non–standard RDEs.

The contents of Chapter 2 concern the spectral stability of a Keller-Segel model for bacterial chemotaxis with no growth or decay of the chemoattractant or the bacterial population and a logarithmic chemotactic function. The majority of the contents of this chapter were published across two manuscripts, listed below.

- P.N. Davis, P. van Heijster, and R. Marangell. Absolute instabilities of travelling wave solutions in a Keller–Segel model. *Nonlinearity*, 30:4029–4061, 2017 ([10] in reference list).
- P.N. Davis, P. van Heijster, and R. Marangell. Spectral stability of travelling wave solutions in a Keller–Segel model. *Appl. Numer. Math.*, 141:54–61, 2018 ([11] in reference list).

The first manuscript was primarily concerned with the essential spectrum and the absolute spectrum. In this manuscript, we provide a full analysis and classification of the essential and absolute spectrum. The main result of the manuscript is that travelling wave solutions are transiently unstable for a small range of the chemotactic parameter before a bifurcation to an absolutely unstable regime. In the second manuscript we complete the spectral results by proving that the origin $\lambda = 0$ is an eigenvalue in the point spectrum with multiplicity two for all parameter values in the model with sublinear or constant consumption rate of the chemoattractant. This chapter clarifies the nature of the instabilities in the Keller-Segel model. Moreover, the spectrum of the linearised operator about the travelling waves is non–standard in that the leading edge of the absolute spectrum crosses into the right half plane away from the real axis. In many well studied problems the absolute spectrum consists of values that are purely real, for example, the FKPP equations shown in Example 1 above, or purely imaginary, for example, the nonlinear Schrödinger equation. The structure of the absolute spectrum of the Keller-Segel model is somewhat reminiscent of the example in [85] which was constructed to have such non–standard absolute spectrum.

Author contributions for [10, 11]

- All authors participated in useful discussions pertaining to the set-up of the problem, the interpretation and presentation of results.
- *P.N. Davis* (candidate) was primary author for both [10, 11], performed the calculations, interpretations and presentation in [10] and in collaboration performed the calculations, interpretations and presentation in [11]. The candidate also acted as corresponding author for [10].
- *P. van Heijster* guided and supervised the research, checked the analytic calculations, assisted with interpretation and presentation in [10] and in collaboration performed the calculations, interpretations and presentation in [11]. He also proofread and edited the manuscripts.
- *R. Marangell* guided and supervised the research, checked the analytic calculations, assisted with interpretation and presentation in [10, 11] and in collaboration performed the calculations, interpretations and presentation in [11]. He also proofread and edited the manuscripts and acted as corresponding author for [11].

The contents of Chapter 3 concern the proof of the existence of heteroclinic solutions in the Gatenby-Gawlinski model for tumour invasion with the acid-mediation hypothesis. The majority of the contents of this chapter was submitted as the following manuscript.

- P.N. Davis, P. van Heijster, R. Marangell, and M.R. Rodrigo. Traveling wave solutions in a model for tumor invasion with the acid-mediation hypothesis. *Submitted*, 2018 ([12] in reference list).

Numerical simulations by M.R. Rodrigo had shown the existence of both slow and fast (in terms of wave speed) travelling waves and, in certain parameter regimes, the existence of an 'interstitial gap'-a region mostly devoid of cells ahead of the invading population of tumour cells. The main goal of this project was to prove the existence of these travelling wave solutions from a dynamical systems perspective and to explain the existence and width of the interstitial gap. The differing timescales in the model allowed for a GSPT approach and we use this approach to prove the existence of the travelling wave solutions, give a leading-order approximation based on the singular limit of the slow and fast problems and prove the persistence of these approximations in the full system. It was through the use of GSPT that we were able to give a mathematical explanation of the interstitial gap: the width of the interstitial gap is determined by the distance between a layer transition of the tumour and a dynamical transcritical bifurcation of two components of the critical manifold. The existence of this dynamical transcritical bifurcation is non–standard as the loss of normal hyperbolicity means that Fenichel theory does not apply at the bifurcation. We prove the persistence of solutions as the trajectories cross the bifurcation and conclude the chapter with some open questions and suggestions for future work.

Author contributions for [12]

- All authors participated in useful discussions pertaining to the set-up of the problem, the interpretation and presentation of results.
- *P.N. Davis* (candidate) was primary author for the main section (and calculations therein) §3.5 The candidate also co-authored the set-up of the GSPT problem, §3.3, and participated in discussions of and analysis of all remaining sections. The candidate acted as corresponding author, checked the analytic calculations and updated the manuscript for consistency with her thesis. The candidate also wrote §3.1 extended §3.6 for inclusion in her thesis. She also proofread and edited the full manuscript.
- *P. van Heijster* was primary author for the sections §3.2 and §3.3 and co-authored sections §3.4 and §3.6 with the candidate. He participated in discussions of and analysis of the all sections. He also proofread and edited the manuscript.
- *R. Marangell* assisted with the set-up of the problem, participated in discussions of and analysis of the all sections, checked the analytic calculations. He also proofread and edited the manuscript.
- *M.R. Rodrigo* wrote the more biologically motivated components of the introduction §3.2 and conclusion §3.6, participated in discussions of and analysis of the all sections, performed the numerical simulations and generated the figures of travelling wave profiles. He also proofread and edited the manuscript.

Chapter 4 regards the stability of defect solutions, following on from the existence results of [21] by A. Doelman, P. van Heijster and F. Xie. In this chapter we formulate the Evans function for the model (1.3). For the trivial defect solution, we calculate the leading order Evans function as well as the first and second order correction terms for a scalar PDE example. From this we prove that the roots of the Evans function are given, to leading order, by the branch points of the absolute spectrum of the associated homogeneous problem. Furthermore, we show that any point spectrum that emerges as a result of the inclusion of the defect is within $\mathcal{O}(\varepsilon)$ of the branch points. The candidate (P.N. Davis) is the primary author for this chapter and this work has been done under the supervision and guidance of P. van Heijster and R. Marangell.

Author contributions for Chapter 4

- All authors participated in useful discussions pertaining to the set-up of the problem, the interpretation and presentation of results.
- *P.N. Davis* (candidate) was primary author for this chapter and performed the calculations therein.
- *P. van Heijster* guided and supervised the research, checked the analytic calculations, proofread and edited the Chapter.
- *R. Marangell* guided and supervised the research, checked the analytic calculations, proofread and edited the Chapter.

The thesis concludes with a discussion and summary of the results, open questions and the future directions of research. Specifically, we are interested in the dynamical implications of the Keller-Segel model's spectral instability, the nonlinear stability of solutions to the Keller-Segel model, extensions and generalisations of both the Keller-Segel model and the Gatenby-Gawlinski model and the stability of the travelling wave solutions to the Gatenby-Gawlinski model. Current and future work also includes generalising the Evans function approach to the stability of the trivial defect solution to encompass the $n-$dimensional trivial defect solution, local defect solution and the application to known problems with the addition of defects; the Fitzhugh-Nagumo model and the extended Fisher-Kolmogorov model.

Chapter 2

The spectral stability of a Keller-Segel model with logarithmic chemosensitivity

2.1 Preface

The contents of this chapter were published across two manuscripts, [10] and [11]. For the sake of presentation, the introduction, set-up and conclusion sections have been merged. Sections §2.4 to §2.6, in combination with parts of the introduction, set-up and conclusion sections, were published in [10] whilst §2.7, in combination with parts of the introduction, set-up and conclusion sections, was published in [11].

2.1.1 Abstract

We investigate the spectral stability of travelling wave solutions in a Keller-Segel model of bacterial chemotaxis with a logarithmic chemosensitivity function and a constant, sublinear, or linear consumption rate. Linearising around the travelling wave solutions, we first locate the essential and absolute spectrum of the associated linear operators and find that all travelling wave solutions have essential spectrum in the right half plane. However, we show that in the case of constant or sublinear consumption there exists a range of parameters such that the absolute spectrum is contained in the open left half plane and the essential spectrum can thus be weighted into the open left half plane. For the constant and sublinear consumption rate models we also determine critical parameter values for which the absolute spectrum crosses into the right half plane, indicating the onset of an absolute instability of the travelling wave solution. We observe that this crossing always occurs off of the real axis. We then investigate the point spectrum associated with the travelling wave solutions. We show that, for constant or sublinear consumption, there is an eigenvalue at the origin of order two. This is associated with the translation invariance of the model and the existence of a continuous family of solutions with varying wave speed. The full spectral analysis implies that the travelling wave solutions are absolutely unstable if the chemotactic coefficient is above the critical value, while they are transiently unstable otherwise.

2.2 Introduction

2.2.1 The Keller-Segel model

A general Keller-Segel model of chemotaxis is

$$\begin{aligned} u_t &= \varepsilon u_{xx} - \alpha w u^m + \kappa u, \\ w_t &= \delta w_{xx} - \beta \left(\Phi_x(u) w\right)_x, \end{aligned} \tag{2.1}$$

with $(x,t) \in (\mathbb{R}, \mathbb{R}^+)$. The model represents the directed movement of a cell species w, such as a bacterial population, governed by the gradient of a chemical u. The function $\Phi(u)$ is the so-called chemotactic function. We take $(x,t) \in \mathbb{R}\times\mathbb{R}^+$, with $\alpha,\ \kappa \geq 0, m \in \mathbb{R}$, and $\beta,\ \delta > 0$ and assume that the diffusion of the chemical is taken to be much smaller than that of the bacteria, *i.e.* $0 \leq \varepsilon \ll \delta$.

Originally proposed by Keller and Segel in the 1970's (see [60,61]) much of the focus in the literature has been on the so-called minimal Keller-Segel model (see, for example, [45, 52] and references therein, as well as the review paper [44]). This is (2.1) with a chemotactic function of the form $\Phi_x(u) = u$ and $\kappa = 0$ (representing no growth of the chemical in the absence of the bacteria). The minimal Keller-Segel model admits solutions that blow-up in finite or infinite time [44]. As blow-up solutions are not biologically feasible, efforts have been made to prevent, or bound, blow-up solutions in the minimal Keller-Segel model by appending the model; for instance by selecting an appropriate growth term [66], by bounding the chemotactic function [45], or by incorporating nonlinear diffusivity [103].

Alternatively, by moving away from the minimal Keller-Segel model, one can find travelling wave solutions by the choice of a singular chemotactic function [61,94]. The literature predominantly discusses the case when the growth term $\kappa = 0$, and when $\Phi(u) = \log(u)$ [22,28,49,59,61,94]. For instance, it was shown in [61,94] that, in the absence of a growth term for the bacterial population w, the chemosensitivity function must be singular for travelling wave solutions to exist. In this chapter, we consider such a Keller-Segel model:

$$\begin{aligned} u_t &= \varepsilon u_{xx} - \alpha w u^m, \\ w_t &= \delta w_{xx} - \beta \left(\frac{w u_x}{u}\right)_x. \end{aligned} \tag{2.2}$$

The condition $\beta/\delta + m > 1$ is necessary for finite solutions [61]. It has been shown that for $m > 1$ and $m < 0$, (2.2) admits no travelling wave solutions [94, 103], thus we take $0 \leq m \leq 1$. When $0 \leq m \leq 1$, there are two main cases; first, for $0 \leq m < 1$, the model supports a travelling front of the chemical attractant coupled with a travelling pulse for the bacterial population [80, 103]. This has been used to model travelling bands of bacteria [43, 82]. When $m = 1$, (2.2) supports a pair of travelling fronts and has been

used to model the boundary behaviours of populations of bacteria [81]. See Figure 2.3.1 for plots of travelling wave solutions in these two cases.

While the existence of travelling wave solutions to (2.2) has been studied since the model's inception, stability analysis of these travelling wave solutions has been comparatively limited. A typical first step in the stability analysis of travelling wave solutions is to linearise around the travelling wave solution and to compute the spectrum of the resulting linearised operator. For travelling wave solutions in (2.2), with $\varepsilon = m = 0$, the essential spectrum (see Definition 2.3.2) of the associated linear operator, dealing with instabilities at infinity, was located in [80]. It was shown that the essential spectrum always intersects the right half plane and so the waves are (spectrally) unstable. It is possible to shift the essential spectrum using weighted function spaces, see §2.3.3. In [80] a weighted function space was considered for a range of weights and it was shown that in this range the spectrum remains unstable. However, the reason for restricting weights to a small range is unclear. These results were generalised in [103] for $0 \leq m \leq 1$. In [35], (2.2) was studied with $m = 0 = \varepsilon$ and it was shown, via a numerical Evans function computation, that the point spectrum of $\mathcal{L}_0^0$ contains no eigenvalues with positive real part for complex values with norm up to $\mathcal{O}(10^9)$. In addition, it was shown that the origin is a second order root of the Evans function and hence is an eigenvalue with algebraic multiplicity two.

In this chapter, we locate the essential spectrum associated with travelling wave solutions in (2.2). By computing the absolute spectrum (see Definition 2.3.3), we show that for all $0 \leq m < 1$ there exists a range of the chemotactic parameter β, independent of the speed of the travelling wave solution, such that the essential spectrum can be weighted fully into the left half plane for an appropriate two-sided weight. We also prove that the origin is an eigenvalue with algebraic multiplicity two, confirming the numerical results of [35]. An early proof offered by [87] shows that there are no positive eigenvalues for $0 \leq \varepsilon \ll 1$ under the assumption that eigenvalues are real-valued. However, it is unclear that this assumption holds, since the linearised operator $\mathcal{L}$ (2.9) is not self-adjoint. The results of this chapter, that the origin is an eigenvalue of order 2, together with the numerical results of [35], confirm that there is a parameter range where the travelling wave solutions are transiently unstable. However, we do emphasize that as the linearised operator is quasilinear, the spectral stability results do not allow us to immediately conclude the nonlinear stability of solutions. See §2.3.4 for a more in depth explanation of the main results and §2.8 for a discussion of nonlinear stability.

In §2.3, we describe the linearised eigenvalue problem associated with a travelling wave solution to (2.2), outline the relevant spectral theory, and state our main results. In §2.4, we locate the essential and absolute spectrum and explain the procedure for calculating the so-called ideal weight (see Definition 2.3.4), in the case of constant consumption and zero diffusivity of the attractant, *i.e.* $\varepsilon = m = 0$. We also calculate the range of β values for which the essential spectrum can be weighted into the left half plane. Outside this

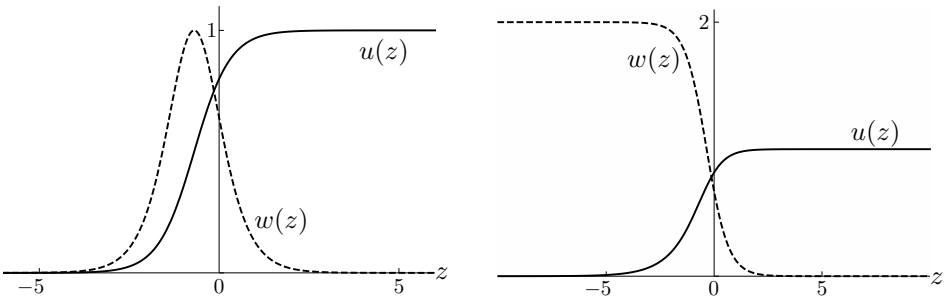

Figure 2.3.1: Travelling wave solutions to (2.5) for $\varepsilon = 0$, $\beta = c = 2$. Left panel: For $m = 0$ the travelling wave solutions are a front and a pulse. Right panel: For $m = 1$ the travelling wave solutions are a pair of travelling fronts.

range the travelling wave solutions are absolutely unstable. In §2.5, we extend the results of the constant consumption case ($m = 0$) to the case of sublinear ($0 < m < 1$) and linear consumption ($m = 1$), still in the absence of diffusion of the attractant. While the procedures of §2.5 are similar to the procedures of §2.4, the computations are algebraically more involved and therefore we split these two sections. In §2.6, we include a small, non-zero, diffusivity of the attractant in the model, *i.e.* $0 < \varepsilon \ll 1$, and show that (in)stability conditions are to leading order the same as before. In §2.7.1 we present the results from [11]. That is, we prove that the origin persists as an element of the point spectrum with algebraic multiplicity two for travelling wave solutions to (2.2) with $0 \leq m < 1$ and $0 \leq \varepsilon \ll 1$. We conclude the chapter with a summary and discussion of future work.

2.3 Set-up, definitions, and main results

We briefly discuss the existence of travelling wave solutions to (2.2) and define the stability problem. Following [80], we nondimensionalise (2.2) through the change of variables $\tilde{x} := \sqrt{\frac{\alpha}{\delta}}x$, $\tilde{t} := \alpha t$. Then, (2.2) becomes

$$\begin{aligned} u_{\tilde{t}} &= \tilde{\varepsilon} u_{\tilde{x}\tilde{x}} - w u^m, \\ w_{\tilde{t}} &= w_{\tilde{x}\tilde{x}} - \tilde{\beta}\left(\frac{w u_{\tilde{x}}}{u}\right)_{\tilde{x}}, \end{aligned} \tag{2.3}$$

where we have set $\tilde{\varepsilon} := \frac{\varepsilon}{\delta}$ and $\tilde{\beta} := \frac{\beta}{\delta}$. We drop the tildes for notational convenience

$$\begin{aligned} u_t &= \varepsilon u_{xx} - w u^m, \\ w_t &= w_{xx} - \beta\left(\frac{w u_x}{u}\right)_x, \end{aligned} \tag{2.4}$$

and the conditions on our parameters are now $0 \leq \varepsilon \ll 1$, $\beta + m > 1$ and $0 \leq m \leq 1$.

2.3.1 Travelling wave solutions

We make the change of variables $z = x - ct$, where $c > 0$ is a constant, finite wave speed. In this moving frame, we have

$$\begin{aligned} u_t &= \varepsilon u_{zz} + c u_z - w u^m, \\ w_t &= w_{zz} + c w_z - \beta \left(\frac{w u_z}{u} \right)_z . \end{aligned} \tag{2.5}$$

Travelling wave solutions exist as stationary solutions to (2.5), *i.e.* $(u(z,t), w(z,t)) = (u(z), w(z))$ and satisfy

$$\begin{aligned} 0 &= \varepsilon u_{zz} + c u_z - w u^m, \\ 0 &= w_{zz} + c w_z - \beta \left(\frac{w u_z}{u} \right)_z . \end{aligned} \tag{2.6}$$

When $0 \leq m < 1$, travelling wave solutions satisfy (2.6) with

$$\lim_{z \to -\infty} u(z) = \lim_{z \to -\infty} w(z) = 0, \quad \lim_{z \to \infty} u(z) = u_r, \quad \lim_{z \to \infty} w(z) = 0,$$

where $u(z)$ is a wavefront and $w(z)$ is a pulse [80,103] (see the left panel of Figure 2.3.1). When $m = 1$ travelling wave solutions satisfy (2.6) with

$$\lim_{z \to -\infty} u(z) = 0, \quad \lim_{z \to -\infty} w(z) = \frac{c^2}{\beta} + \varepsilon \frac{c^2}{\beta^2}, \quad \lim_{z \to \infty} u(z) = u_r, \quad \lim_{z \to \infty} w(z) = 0,$$

where both $u(z)$ and $w(z)$ are now wavefronts [103] (see the right panel of Figure 2.3.1).

Though explicit formulas for travelling wave solutions are known only for $\varepsilon = 0$ (*i.e.* zero-diffusivity of the chemoattractant), the existence of travelling wave solutions in (2.2) has been shown for $0 \leq m \leq 1$ and small enough values of the diffusivity of the chemoattractant (*i.e.* $0 \leq \varepsilon \ll 1$), see, for example, [38, 80, 103] and the references therein. To leading order in ε, the profiles of travelling wave solutions are given by

$$\begin{aligned} u(z) &= \left(u_r^{-1/\gamma} + \sigma e^{-c(z+z^*)} \right)^{-\gamma} , \\ w(z) &= e^{-c(z+z^*)} \left(u(z) \right)^{\beta} , \\ \gamma &= \frac{1}{\beta + m - 1}, \quad \sigma = \frac{\beta + m - 1}{c^2}, \end{aligned} \tag{2.7}$$

where z^* is a constant associated with the location of the centre of the travelling wave solution, and u_r is the end state of the chemoattractant [28,80,103]. Because of translation invariance, we set $z_* = 0$, and because of scaling invariance in the nondimensionalisation of (2.2) to (2.3), we take $u_r = 1$ [38], in the remainder of this chapter without loss of generality. Furthermore, from [80,103] we have the following limits for the travelling wave

solutions

$$\lim_{z\to-\infty}\frac{u_z}{u}=\frac{c}{\beta+m-1},\qquad \lim_{z\to-\infty}\frac{w}{u^{1-m}}=\frac{c}{\beta+m-1}\left(\frac{c\varepsilon}{\beta+m-1}+c\right), \tag{2.8}$$

which will be useful for the stability analysis in the upcoming sections.

2.3.2 The spectral problem

To determine the stability of the travelling wave solutions (u,w) of (2.4), we consider $U(z,t)=u(z)+p(z,t)$, and $W(z,t)=w(z)+q(z,t)$, where p,q are perturbations in some appropriately chosen Banach space $\mathcal{X}$. Substituting U and W into (2.5) and considering only leading order terms for p and q, we obtain the linear operator $\mathcal{L}_\varepsilon^m$ defined by,

$$\begin{pmatrix}p\\q\end{pmatrix}_t=\mathcal{L}_\varepsilon^m\begin{pmatrix}p\\q\end{pmatrix},\qquad \mathcal{L}_\varepsilon^m:=\begin{pmatrix}\varepsilon\partial_{zz}+c\frac{\partial}{\partial z}-mwu^{m-1} & -u^m\\ \mathcal{L}_{21} & \mathcal{L}_{22}\end{pmatrix} \tag{2.9}$$

where the entries of $\mathcal{L}_\varepsilon^m$ are

$$\begin{aligned}
\mathcal{L}_{11}&:=\varepsilon\frac{\partial^2}{\partial z^2}+c\frac{\partial}{\partial z}-mwu^{m-1},\\
\mathcal{L}_{12}&:=-u^m,\\
\mathcal{L}_{21}&:=\beta\left(\frac{w_zu_z}{u^2}+\frac{wu_{zz}}{u^2}-\frac{2wu_z^2}{u^3}\right)+\beta\left(\frac{2wu_z}{u^2}-\frac{w_z}{u}\right)\frac{\partial}{\partial z}-\frac{\beta w}{u}\frac{\partial^2}{\partial z^2},\\
\mathcal{L}_{22}&:=\beta\left(\frac{u_z^2}{u^2}-\frac{u_{zz}}{u}\right)+\left(c-\frac{\beta u_z}{u}\right)\frac{\partial}{\partial z}+\frac{\partial^2}{\partial z^2}.
\end{aligned} \tag{2.10}$$

Though the terms of (2.10) appear singular as $u_\varepsilon^m\to 0$ in the $z\to-\infty$ limit, they are in fact bounded [103].

The associated eigenvalue problem is obtained by taking perturbations of the form

$$\begin{pmatrix}p(z,t)\\q(z,t)\end{pmatrix}=e^{\lambda t}\begin{pmatrix}p(z)\\q(z)\end{pmatrix}$$

where we now make the choice that $p,q\in\mathbb{H}^1(\mathbb{R})$. Here, $\mathbb{H}^1(\mathbb{R})$ is the usual Sobolev space of once (weakly) differentiable functions such that both the function and its first (weak) derivative (in z) are in $\mathbb{L}^2(\mathbb{R})$, *i.e.* square integrable. Equation (2.9) becomes

$$\begin{aligned}
\mathcal{L}_\varepsilon^m&:\mathbb{H}^1(\mathbb{R})\times\mathbb{H}^1(\mathbb{R})\to\mathbb{H}^1(\mathbb{R})\times\mathbb{H}^1(\mathbb{R})\\
&\mathcal{L}_\varepsilon^m\begin{pmatrix}p\\q\end{pmatrix}=\lambda\begin{pmatrix}p\\q\end{pmatrix}.
\end{aligned} \tag{2.11}$$

2.3.3 Spectral stability: Background and definitions

A travelling wave solution is said to be spectrally stable if the spectrum of the associated linear operator $\sigma(\mathcal{L})$ is contained in the closed left half plane except for the origin. The spectrum $\sigma(\mathcal{L})$ is defined in the following definition.

Definition 2.3.1. *([88] Definition 3.2) We say $\lambda \in \mathbb{C}$ is in the spectrum of a linear operator $\mathcal{L}$, denoted $\sigma(\mathcal{L})$, if the operator $\mathcal{L} - \lambda I$, where I is the identity operator, is not invertible,* i.e. *the inverse does not exist or is not bounded.*

The spectrum of a linear operator $\mathcal{L}$ falls naturally into two parts, the essential spectrum, denoted $\sigma_{\text{ess}}(\mathcal{L})$, and the point spectrum, denoted $\sigma_{\text{pt}}(\mathcal{L})$ [91].

The essential spectrum

We define an operator $\mathcal{T}(\lambda)$, equivalent to $\mathcal{L}-\lambda I$, by transforming the eigenvalue problem into a system of first order order ordinary differential equations (ODEs);

$$\mathcal{T}(\lambda)\mathbf{p} := \left(\frac{d}{dz} - M(z,\lambda)\right)\mathbf{p} = 0. \tag{2.12}$$

The essential spectrum of an operator of the form in (2.12) is found by analysing the asymptotic behaviour of the operator $\mathcal{T}(\lambda)$. We set $M_{\pm}(\lambda) := \lim_{z\to\pm\infty} M(z,\lambda)$ and define the asymptotic operator associated with $\mathcal{T}(\lambda)$ as the piecewise constant operator

$$\mathcal{T}_{\infty}(\lambda) := \begin{cases} \dfrac{d}{dz} - M_{-}(\lambda) & \text{if } z < 0, \\ \dfrac{d}{dz} - M_{+}(\lambda) & \text{if } z \geq 0. \end{cases} \tag{2.13}$$

The essential spectrum is found by analysing the dimensions of the unstable, stable and centre subspaces of $M_{\pm}(\lambda)$. We define the Morse index $i(A)$ of a constant matrix A as the dimension of its unstable subspace, see [54] Definition 3.1.9. So, for an asymptotic operator of the form of (2.13), we denote the Morse indices $i_{\pm} := i(M_{\pm}(\lambda)) := \dim(\mathbb{E}^u_{\pm})$, where $\mathbb{E}^u_{\pm}$ denotes the unstable subspace of $M_{\pm}(\lambda)$ respectively.

Definition 2.3.2. *([54] Definition 3.1.11) We say $\lambda \in \sigma_{\text{ess}}(\mathcal{T}_{\infty})$, the essential spectrum of $\mathcal{T}_{\infty}$, if either*

1. *$M_{+}(\lambda)$ and $M_{-}(\lambda)$ are hyperbolic with a different number of unstable matrix eigenvalues,* i.e. *$i_{+} - i_{-} \neq 0$; or*
2. *$M_{+}(\lambda)$ or $M_{-}(\lambda)$ has at least one purely imaginary matrix eigenvalue.*

The essential spectrum is conserved under relatively compact perturbations of an operator. This follows from Weyl's essential spectrum theorem, see for example [54] Theorem

2.2.6 and [57] Theorem 5.35. In a variety of operators that arise from linearisation about travelling wave solutions, including the Keller-Segel model (2.5), the operator $\mathcal{T}_\infty$ is a relatively compact perturbation of $\mathcal{T}$ (see for example [54] Theorem 3.1.11 or [41]) and so their essential spectra coincide.

Due to the continuous dependence of $\mathcal{T}(\lambda)$ on λ we have that the essential spectrum is bounded by the values of λ where $M_+(\lambda)$ or $M_-(\lambda)$ has at least one purely imaginary matrix eigenvalue. These λ values form curves in the complex plane referred to as the dispersion relations of the respective matrices.

Generally, the region of the complex plane containing $\Re(\lambda) \gg 1$ is not contained in the essential spectrum, *i.e.* the region to the right of the essential spectrum has $i_+ = i_-$. This condition is related to well-posedness of the eigenvalue problem [54] (see also the left panel of Figure 2.3.2) and is satisfied for the Keller-Segel model discussed in this chapter.

Remark 2.3.1. *Following the terminology of [54, 91], we refer to the matrix eigenvalues μ of $M_\pm(\lambda)$ as the spatial eigenvalues and to λ as the temporal spectral parameter. Values λ for which there is a solution to* (2.11) *are referred to as temporal eigenvalues. We note that temporal eigenvalues as defined here can be either in σ_{ess} or in σ_{pt}.*

The absolute spectrum

The absolute spectrum, denoted σ_{abs}, is not spectrum in the usual sense as it does not arise from Definition 2.3.1, see, for instance, [54,88,90]. However, it provides important stability information as it gives an indication of how far the essential spectrum can be shifted by allowing for perturbations in weighted spaces (instead of $\mathbb{H}^1$), see also Figure 2.3.2. If the absolute spectrum contains values in the right half plane the solutions are said to be *absolutely unstable* [54, 90]. The absolute spectrum of $\mathcal{T}_\infty$ (equivalently of $\mathcal{T}$) is defined in the following definition

Definition 2.3.3. *([88] Definition 6.1) Take an N dimensional asymptotic operator, $\mathcal{T}_\infty$, in the form of* (2.13)*, that is well-posed in the sense that $i_+ = i_- = j$ for $\Re(\lambda) \gg 1$. For $\lambda \in \mathbb{C}$ we rank the N spatial eigenvalues $\mu_i^\pm$ of the asymptotic matrices $M_\pm$ by the magnitude of their real parts,* i.e.

$$\Re(\mu_1^\pm(\lambda)) \geq \Re(\mu_2^\pm(\lambda)) \geq \ldots \geq \Re(\mu_j^\pm(\lambda)) \geq \Re(\mu_{j+1}^\pm(\lambda)) \geq \ldots \geq \Re(\mu_N^\pm(\lambda)).$$

We define the sets

$$\sigma_{\text{abs}}^+ = \left\{ \lambda \in \mathbb{C} \,\middle|\, \Re(\mu_j^+) = \Re(\mu_{j+1}^+) \right\} \text{ and } \sigma_{\text{abs}}^- = \left\{ \lambda \in \mathbb{C} \,\middle|\, \Re(\mu_j^-) = \Re(\mu_{j+1}^-) \right\}, \quad (2.14)$$

and the absolute spectrum of $\mathcal{T}_\infty$ (and of $\mathcal{T}$) is $\sigma_{\text{abs}} := \sigma_{\text{abs}}^+ \cup \sigma_{\text{abs}}^-$.

Due to the continuous dependence of $\mathcal{T}$ on λ, the Morse indices will only change upon crossing one of the dispersion relations and so the absolute spectrum will always be to the

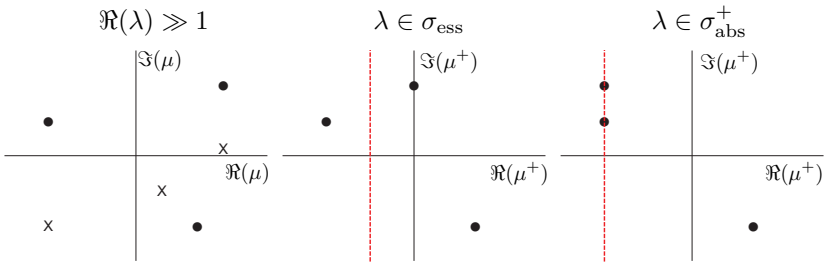

Figure 2.3.2: A schematic of the spatial eigenvalues of the asymptotic matrices $M_+(\lambda)$ (dots) and $M_-(\lambda)$ (crosses), with $M_\pm(\lambda)$ 3×3 matrices, for three distinct values $\lambda \in \mathbb{C}$. Left panel: for $\Re(\lambda) \gg 1$, $M_\pm(\lambda)$ are hyperbolic and $i_\pm = 2$. Middle panel: $\lambda \in \sigma_{\text{ess}}$ since $M_+(\lambda)$ has a purely imaginary spatial eigenvalue. However, there exists a weight, represented by the red line, such that $i_+ = 2$ in this weighted space. So, $\lambda \notin \sigma_{\text{ess}}$ in the weighted space (and $\lambda \notin \sigma^+_{\text{abs}}$). Right panel: $\Re(\mu^+_1) > \Re(\mu^+_2) = \Re(\mu^+_3)$, so $\lambda \in \sigma^+_{\text{abs}}$ (since $i_+ = 2$ for $\Re(\lambda) \gg 1$, see left panel). Observe that the order of the spatial eigenvalues persists under all weights, *i.e.* the absolute spectrum does not change under weighting the space. However, there exists a unique weight, represented by the red line, such that λ is in the boundary of the weighted essential spectrum. This image is adapted from Figure 3.6 of [54].

left of the rightmost boundary of the essential spectrum. That is, moving λ from right to left in the complex plane we will first encounter a dispersion relation of either $M_\pm(\lambda)$ before (potentially) encountering the absolute spectrum, see also Figure 2.3.2.

Remark 2.3.2. *For an operator $\mathcal{T}$, with Morse indices $i_+ = i_- = j$ in the region to the right of the essential spectrum, the set of $\lambda \in \mathbb{C}$ with $\Re(\mu^+_i(\lambda)) = \Re(\mu^+_{i+1}(\lambda))$ or $\Re(\mu^-_i(\lambda)) = \Re(\mu^-_{i+1}(\lambda))$ where $i \neq j$ is referred to as the generalised absolute spectrum.*

Weighted spaces

The presence of essential spectrum of a linear operator in the right half plane implies instability of the travelling wave solution in $\mathbb{H}^1$. However, for many travelling wave solutions that are widely considered 'stable', the linearised operator associated with them has essential spectrum in the right half plane; one such example is the well-known Fisher-Kolmogorov-Petrovsky-Piscounov (F-KPP) equation. A resolution proposed for this apparent contradiction is to work in an appropriately weighted space [93]. Weighting the space adjusts the types of perturbations allowed. Following [54], we define the weighted space $\mathbb{H}^1_\nu(\mathbb{R})$ by the norm

$$\|p\|_{\mathbb{H}^1_\nu} = \|e^{\nu z} p\|_{\mathbb{H}^1} = \|\tilde{p}\|_{\mathbb{H}^1}, \tag{2.15}$$

where $\tilde{p} := e^{\nu z} p$. So, $p \in \mathbb{H}^1_\nu$ if and only if $\tilde{p} \in \mathbb{H}^1$. We define $\mathbb{L}^2_\nu$ similarly. The weight provides information as to whether the travelling wave solutions are more sensitive to perturbations in front of the wavefront (*i.e.* as $z \to \infty$) or behind the wavefront (*i.e.* as $z \to -\infty$). In other words, if $\nu > 0$ then the perturbation $p(z,t)$ must decay at a rate

faster than $e^{-\nu z}$ as $z \to \infty$, while it is allowed to grow exponentially at any rate less than $e^{-\nu z}$ as $z \to -\infty$. We can also consider a two-sided weight

$$\nu = \begin{cases} \nu_- \text{ if } & z \leq 0, \\ \nu_+ \text{ if } & z > 0, \end{cases} \tag{2.16}$$

which forces the perturbation to decay exponentially in both directions. It turns out that we need to consider a two-sided weight (2.67) in the case of the Keller-Segel model (2.4).

A practical consequence of considering $\mathcal{L}$ on weighted function spaces is that the essential spectrum is moved. In particular, assume we have an operator $\mathcal{T}$ of the form of (2.12) coming from the linearisation around a travelling wave solution and with asymptotic operator (2.13). The operator $\mathcal{T}(\lambda)$ in the weighted space is given by

$$\mathcal{T}(\lambda)\tilde{\mathbf{p}} = \mathbf{p}' - (M(z,\lambda) + \nu I)\mathbf{p} = 0,$$

with asymptotic matrices $M_\pm(\lambda)+\nu I$ [54]. Hence, we need to consider the magnitude and sign of the real part of the spatial eigenvalues compared to the weight, *i.e.* we consider $\mu-\nu$, the spatial eigenvalues of $M_\pm(\lambda)+\nu I$, instead of μ, the spatial eigenvalues of $M_\pm(\lambda)$ (see Figure 2.3.2). If the operator $\mathcal{T}$ has its essential spectrum in the right half plane in the unweighted space, weights of interest are those that move this essential spectrum into the open left half plane. If such weights ν exist (and if there is no point spectrum in the right half plane), we say the travelling wave solution is spectrally stable in $\mathbb{H}^1_\nu(\mathbb{R})$ and it is referred to as being *transiently unstable* [90, 96].

Since the order of the spatial eigenvalues is not changed, the absolute spectrum is unaffected by weighting the function space and the presence of absolute spectrum in the right half plane indicates an *absolute instability*. In particular, in the case of an absolute instability no weights can be found that move the essential spectrum into the left half plane since the absolute spectrum is to the left of the rightmost boundary of the essential spectrum.

2.3.4 Main results

In this section, we state the main results of this chapter related to the location of the absolute spectrum of travelling wave solutions supported by (2.4).

Theorem 2.3.3. *Assume that $c > 0, 0 \leq m < 1$ and $\beta > 1 - m$. Let β_{crit} be the unique real root larger than one of*

$$\begin{aligned} f(\beta) = {} & 310\beta^{10} - 3234\beta^9 + 17112\beta^8 - 49101\beta^7 + 76180\beta^6 - 58398\beta^5 \\ & + 10056\beta^4 + 15040\beta^3 - 9680\beta^2 + 1716\beta - 4. \end{aligned} \tag{2.17}$$

Then, there exists an $\varepsilon_0 > 0$ such that for all $0 \leq \varepsilon < \varepsilon_0$ the absolute spectrum of $\mathcal{L}$ given in (2.9) is fully contained in the left half plane for all $1 - m < \beta < \beta^m_{\text{crit}}(\varepsilon)$, with $\beta^m_{\text{crit}}(\varepsilon)$ to leading order given by $\beta^m_{\text{crit}} := \beta_{\text{crit}}(1 - m)$. Crucially, at $\beta = \beta^m_{\text{crit}}(\varepsilon)$ the absolute spectrum crosses the imaginary axis into the right half plane away from the real axis with increasing β. For $\beta > \beta^m_{\text{crit}}(\varepsilon)$ the absolute spectrum of $\mathcal{L}$ (2.9) contains values in the right half plane and the travelling wave solutions of (2.4) are thus absolutely unstable.

For $m = 1$, the absolute spectrum of $\mathcal{L}$ (2.9) includes the origin for all parameter values.

The fact that the polynomial f (2.17) has only one real root larger than one follows directly from Sturm's Theorem, see, for instance, Theorem 6.3d in [40]. This result is summarised in the following lemma, the proof of which is contained in Appendix A.

Lemma 2.3.4. *The polynomial*

$$\begin{aligned} f(\beta) = 310\beta^{10} - 3234\beta^9 + 17112\beta^8 - 49101\beta^7 + 76180\beta^6 - 58398\beta^5 \\ + 10056\beta^4 + 15040\beta^3 - 9680\beta^2 + 1716\beta - 4. \end{aligned} \tag{2.18}$$

has only one real root for $\beta \in [1, \infty)$. Moreover, this root is irrational.

In particular, $\beta_{\text{crit}} \approx 1.6195$. Moreover, for every $0 \leq m < 1$ and $1 < \beta < \beta^m_{\text{crit}}(\varepsilon)$ there exists a range of two-sided weights ν (2.67) such that weighted essential spectrum is contained in the open left half plane, see Remark 2.4.2 and Remark 2.5.2. Also, observe that the above leading order results are independent of the wave speed c, see Remark 2.4.3.

Thus, we fully classify the (in)stabilities coming from the weighted essential spectrum of travelling wave solutions of (2.4) for the complete parameter range for which travelling wave solutions exist, *i.e.* for $0 \leq m \leq 1$ and $1 - m < \beta$ [94, 103]. In essence, we obtain the complete picture of the essential spectrum, extending the initial results obtained in [80, 103].

As we are primarily concerned with the absolute spectrum, we define the *ideal weight* as the weight such that the weighted dispersion relations intersect the rightmost points of the absolute spectrum.

Definition 2.3.4. *The ideal weight for the operator (2.9) is the unique two-sided weight such that the dispersion relations of $M_\pm(\lambda) + \nu_\pm I$ intersect the leading edges of the $\sigma^\pm_{\text{abs}}$ respectively.*

This definition is motivated by the fact that as β increases, the ideally weighted essential spectrum and the absolute spectrum cross into the right half plane simultaneously.

2.4 Constant consumption and zero diffusivity of the chemoattractant

For clarity of presentation, we first prove Theorem 2.3.3 in the case of constant consumption ($m = 0$) and zero diffusivity of the chemoattractant ($\varepsilon = 0$). We show that the absolute spectrum is contained in the left half plane when $1 < \beta < \beta_{\text{crit}}$ (with β_{crit} the root of (2.17)), while it contains values in the right half plane when $\beta > \beta_{\text{crit}}$. Consequently, when $1 < \beta < \beta_{\text{crit}}$, there exists a two-sided weight ν (2.67) such that the essential spectrum is contained in the open left half plane in the ideally weighted space, while all travelling wave solutions are absolutely unstable when $\beta \geq \beta_{\text{crit}}$.

2.4.1 Set-up

In the $\varepsilon = m = 0$ case, the eigenvalue problem (2.11) reduces to

$$\mathcal{L}_0^0 \begin{pmatrix} p \\ q \end{pmatrix} = \lambda \begin{pmatrix} p \\ q \end{pmatrix}, \quad \text{with} \quad \mathcal{L}_0^0 = \begin{pmatrix} c\frac{\partial}{\partial z} & -1 \\ \mathcal{L}_{21} & \mathcal{L}_{22} \end{pmatrix},$$

where $\mathcal{L}_{21}$ and $\mathcal{L}_{22}$ are given by (2.10), restated here for convenience,

$$\begin{aligned} \mathcal{L}_{21} &:= \beta \left(\frac{w_z u_z}{u^2} + \frac{w u_{zz}}{u^2} - \frac{2 w u_z^2}{u^3} \right) + \beta \left(\frac{2 w u_z}{u^2} - \frac{w_z}{u} \right) \frac{\partial}{\partial z} - \frac{\beta w}{u} \frac{\partial^2}{\partial z^2}, \\ \mathcal{L}_{22} &:= \beta \left(\frac{u_z^2}{u^2} - \frac{u_{zz}}{u} \right) + \left(c - \frac{\beta u_z}{u} \right) \frac{\partial}{\partial z} + \frac{\partial^2}{\partial z^2}. \end{aligned}$$

Here (u, w) are the (explicit) travelling wave solutions given in (2.7). We define the operator $\mathcal{T}_0(\lambda)$, equivalent to $\mathcal{L} - \lambda I$, by setting $s = q_z$. The operator $\mathcal{T}_0(\lambda)$, with $p, q \in \mathbb{H}^1(\mathbb{R})$ and $s \in \mathbb{L}^2(\mathbb{R})$, is given by

$$\mathcal{T}_0(\lambda) \begin{pmatrix} p \\ q \\ s \end{pmatrix} := \begin{pmatrix} p \\ q \\ s \end{pmatrix}' - M_0(z, \lambda) \begin{pmatrix} p \\ q \\ s \end{pmatrix} = 0, \qquad M_0(z, \lambda) := \begin{pmatrix} \frac{\lambda}{c} & \frac{1}{c} & 0 \\ 0 & 0 & 1 \\ \mathcal{A}_0 & \mathcal{B}_0 & \mathcal{C}_0 \end{pmatrix}, \tag{2.20}$$

with

$$\begin{aligned} \mathcal{A}_0 &= \beta \left(\frac{2 w u_z^2}{u^3} - \frac{w_z u_z}{u^2} - \frac{w u_{zz}}{u^2} \right) + \frac{\lambda \beta}{c} \left(\frac{w_z}{u} - \frac{2 w u_z}{u^2} \right) + \frac{\lambda^2 \beta w}{c^2 u}, \\ \mathcal{B}_0 &= \beta \left(\frac{u_{zz}}{u} - \frac{u_z^2}{u^2} \right) + \frac{\beta}{c} \left(\frac{w_z}{u} - \frac{2 w u_z}{u^2} \right) + \frac{\lambda \beta}{c^2} \left(\frac{w}{u} \right) + \lambda, \\ \mathcal{C}_0 &= \frac{\beta u_z}{u} - c + \frac{\beta}{c} \frac{w}{u}. \end{aligned}$$

2.4.2 Essential spectrum

We first locate the essential spectrum in the unweighted function space. We calculate the dispersion relations of the asymptotic matrices as these act as the boundaries of the

essential spectrum. From (2.6), with $\varepsilon = 0$, we have $u_z = w/c$ and by integrating the second equation we get $w_z = -cw + \beta\,(wu_z/u)$ (where the integration constant is zero [38, 61]). Thus, all terms of M_0 can be written in terms of w/u. From (2.8), or directly from the travelling wave profiles (2.7), we have,

$$\lim_{z\to\infty} \frac{w}{u} = 0, \quad \lim_{z\to-\infty} \frac{w}{u} = \frac{c^2}{\beta - 1}$$

Using these facts, the limits of $\mathcal{A}_0$, $\mathcal{B}_0$ and $\mathcal{C}_0$ as $z \to \pm\infty$, denoted $\mathcal{A}_0^{\pm}$, $\mathcal{B}_0^{\pm}$ and $\mathcal{C}_0^{\pm}$, are straightforward to compute and are, respectively, given by

$$\begin{aligned} \mathcal{A}_0^+ &= 0, & \mathcal{A}_0^- &= \frac{\beta\lambda\left((\beta-1)\lambda - c^2\right)}{(\beta-1)^2}, \\ \mathcal{B}_0^+ &= \lambda, & \mathcal{B}_0^- &= \frac{\left(2\beta^2 - 3\beta + 1\right)\lambda - c^2\beta}{(\beta-1)^2}, \\ \mathcal{C}_0^+ &= -c, & \mathcal{C}_0^- &= \frac{c(\beta+1)}{\beta-1}. \end{aligned}$$

We also define the asymptotic matrices,

$$M_0^{\pm}(\lambda) := \lim_{z\to\pm\infty} M_0(z,\lambda) = \begin{pmatrix} \frac{\lambda}{c} & \frac{1}{c} & 0 \\ 0 & 0 & 1 \\ \mathcal{A}_0^{\pm} & \mathcal{B}_0^{\pm} & \mathcal{C}_0^{\pm} \end{pmatrix}.$$

Setting the spatial eigenvalues to be purely imaginary, *i.e.* $\mu = ik$, $k \in \mathbb{R}$ in the characteristic polynomials of $M_0^{\pm}$ we obtain their dispersion relations. The dispersion relations of M_0^+ are

$$\lambda = -k^2 + ick, \quad \text{and} \quad \lambda = ick. \tag{2.21}$$

Note that the imaginary axis is one of the dispersion relations, while the other is a parabola opening to the left half plan with vertex at the origin, see Figure 2.4.2.

The dispersion relations of M_0^- are given by

$$\lambda^2 + \left(k^2 - \frac{i(\beta-2)ck}{\beta-1}\right)\lambda + \frac{(\beta+1)c^2k^2}{\beta-1} + ick\left(\frac{\beta c^2}{(\beta-1)^2} - k^2\right) = 0. \tag{2.22}$$

Equation (2.22) is quadratic in the temporal parameter λ and cubic in the parameter k (and thus in the spatial eigenvalue).

The boundary of the essential spectrum is traced out by the solutions $\lambda \in \mathbb{C}$, parametrised by k, from (2.21) and (2.22). We label the connected set containing $\Re(\lambda) \gg 1$ as Ω_1, see Figure 2.4.1. For $\lambda \in \Omega_1$, we have that the dimensions of the unstable subspaces of $M_0^{\pm}$ are both two, *i.e.* $i_{\pm} = 2$. There are two other regions in the complex plane where $i_+ = i_-$. We denote these regions Ω_2 and Ω_3, see Figure 2.4.1. The remaining part

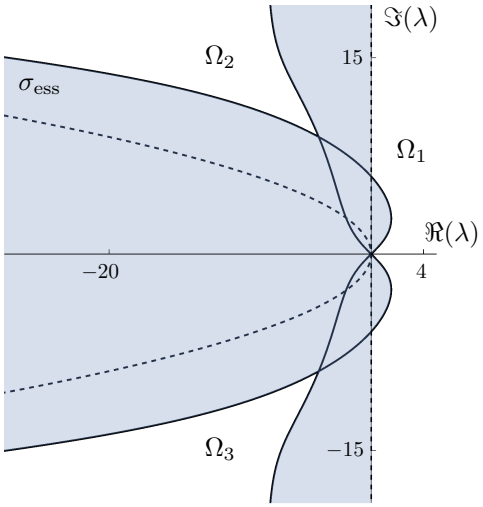

Figure 2.4.1: The essential spectrum σ_{ess} of the operator $\mathcal{L}$ about the travelling wave solutions (u, w) (2.7) for $\varepsilon = m = 0$ and $\beta = c = 2$. The solid curves are the dispersion relations of M_0^-, while the dashed curves are the dispersion relations of M_0^+. The shaded region is $\lambda \in \mathbb{C}$ such that $i_+ \neq i_-$ and the essential spectrum is the union of the shaded region and the dispersion relations. Observe that the entire imaginary axis is included in the essential spectrum. The general shape of the unweighted essential spectrum is qualitatively similar for all values $\beta > 1$, while changing the wave speed c only affects the scaling of the image, see Remark 2.4.3. Note this figure is a slight correction to Figure 6 from [35].

of the complex plane is the essential spectrum. It is clear from Figure 2.4.1 that part of the essential spectrum is in the right half plane. This agrees with previous results; by considering (2.22) for small $|k|$ values it was shown all travelling wave solutions for $\varepsilon = m = 0$ are unstable in the unweighted space [80].

2.4.3 The weighted essential spectrum and the absolute spectrum

To further investigate the stability properties of the travelling wave solutions, we consider the spectrum in various two-sided weighted spaces, locate the absolute spectrum and identify the ideal weight. We substitute $\tilde{\mathbf{p}} = e^{\nu z}\mathbf{p}$, where $\mathbf{p} = (p, q, s)^T$, into (2.20) and consider the weighted space $\mathbb{H}^1_\nu$ (2.66) with ν a two-sided weight (2.67). This substitution transforms (2.20) into

$$\mathcal{T}_0(\lambda)\tilde{\mathbf{p}} = \mathbf{p}' - (M_0(z, \lambda) + \nu I)\mathbf{p} = 0,$$

with $M_0(z, \lambda)$ as given in (2.20). The essential spectrum in the weighted space is bounded by the dispersion relations of the asymptotic matrices $M_0^\pm + \nu_\pm I$.

The weighted dispersion relations and absolute spectrum from M_0^+

First, we consider the dispersion relations of $M_0^+(\lambda) + \nu_+ I$;

$$\lambda = -c\nu_+ + ick, \quad \text{and} \quad \lambda = -k^2 - \nu_+(c - \nu_+) + i(ck - 2k\nu_+). \tag{2.23}$$

For $\nu_+ \in (0, c)$ the real part of the dispersion relations (2.23) have strictly negative real parts and the furthest left these relations can be shifted is for the ideal weight $\nu_+^* = c/2$. Under this weight, the dispersion relations (2.23) reduce to

$$\lambda = -\frac{c^2}{2} + ick, \quad \text{and} \quad \lambda = -\frac{c^2}{4} - k^2. \tag{2.24}$$

Next, we calculate σ_{abs}^+, the subset of the absolute spectrum arising from the spatial eigenvalues for $z \to \infty$. Since $i_+ = 2 = i_-$ for $\Re(\lambda) \gg 1$, we search for $\lambda \in \mathbb{C}$ such that the spatial eigenvalues with the second and third largest real part have the same real part (see Definition 2.3.3). The spatial eigenvalues of M_0^+ are

$$\mu_1^+ = \frac{\lambda}{c}, \quad \mu_2^+ = \frac{-c + \sqrt{c^2 + 4\lambda}}{2}, \quad \mu_3^+ = \frac{-c - \sqrt{c^2 + 4\lambda}}{2}. \tag{2.25}$$

For $\Re(\lambda) \geq -\frac{c^2}{2}$, we have that $\Re(\mu_1^+) \geq \Re(\mu_2^+) \geq \Re(\mu_3^+)$. Consequently, the absolute spectrum in this region is given by $\lambda \in \mathbb{C}$ such that $\Re(\mu_2^+) = \Re(\mu_3^+)$. That is, $\left\{\lambda \in \mathbb{R} \middle| -\frac{c^2}{2} \leq \lambda \leq \frac{-c^2}{4}\right\}$. For $\Re(\lambda) < -\frac{c^2}{2}$, we have that μ_2^+ has the largest real part and the absolute spectrum in this region is thus given by $\lambda \in \mathbb{C}$ such that $\Re(\mu_1) = \Re(\mu_3)$. That is, $\left\{\lambda = \lambda_1 + i\lambda_2,\ \lambda_1, \lambda_2 \in \mathbb{R} \middle| \lambda_1 < -\frac{c^2}{2};\ \lambda_2 = \pm\lambda_1\left(1 + \frac{2\lambda_1}{c^2}\right)\right\}$. So, σ_{abs}^+ is given by

$$\begin{aligned}\sigma_{\text{abs}}^+ = &\left\{\lambda \in \mathbb{R} \middle| -\frac{c^2}{2} \leq \lambda \leq \frac{-c^2}{4}\right\} \cup \\ &\left\{\lambda = \lambda_1 + i\lambda_2,\ \lambda_1, \lambda_2 \in \mathbb{R} \middle| \lambda_1 < -\frac{c^2}{2};\ \lambda_2 = \pm\lambda_1\left(1 + \frac{2\lambda_1}{c^2}\right)\right\}.\end{aligned} \tag{2.26}$$

Obviously, σ_{abs}^+ is fully contained in the left half plane for all $c > 0$. Consequently, no absolute instabilities arise from $z \to \infty$. See Figure 2.4.2 for a plot of σ_{abs}^+ (2.26) and the ideally weighted dispersion relations (2.24) and the unweighted dispersion relations (2.21) (or (2.23) with $\nu_+ = 0$).

The weighted dispersion relations and absolute spectrum from M_0^-

The characteristic equation of M_0^- is given by

$$\mu^3 - \mu^2\left(\frac{(\beta+1)c}{\beta - 1} + \frac{\lambda}{c}\right) + \mu\left(\frac{(2-\beta)\lambda}{\beta - 1} + \frac{\beta c^2}{(\beta-1)^2}\right) + \frac{\lambda^2}{c} = 0, \tag{2.27}$$

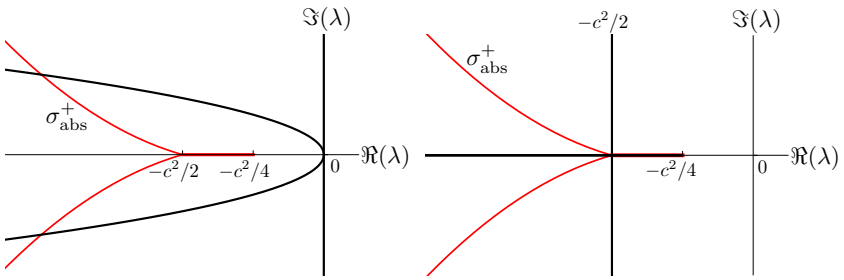

Figure 2.4.2: The subset of the absolute spectrum σ^+_{abs} (red) and the dispersion relations of $M_0^+ + \nu_+ I$ (black). Left panel: the dispersion relations (2.23) in the unweighted space, *i.e.* $\nu_+ = 0$. The imaginary axis is one of the dispersion relations. Right panel: the ideally weighted dispersion relations (2.24), *i.e.* $\nu_+^* = c/2$. Note that the parabola from the left panel collapses to the real line under the ideal weight.

and the dispersion relations of $M_0^- + \nu_- I$ are implicitly given by

$$\lambda^2 + \left(\frac{c(2-\beta)(ik-\nu_-)}{\beta - 1} - (ik-\nu_-)^2 \right) \lambda + \frac{\beta c^3 (ik-\nu_-)}{(\beta-1)^2} - \frac{(\beta+1)c^2(ik-\nu_-)^2}{\beta-1} + c(ik-\nu_-)^3 = 0. \tag{2.28}$$

For a fixed β and c and for various weights ν_-, we can plot the weighted dispersion relations (2.28), see, for example, Figure 2.4.3. Observe that the weighted dispersion relations (2.28) have self-intersections for some $\lambda \in \mathbb{C}$ over a large range of weights ν_-, including $\nu_- = 0$ (related to the unweighted space). This self-intersection corresponds to two complex roots of the characteristic polynomial (2.27) of the form $\mu^-_{1,2} = -\nu_- + ik_{1,2}$ with $k_{1,2} \in \mathbb{R}$. Thus, we have $\Re(\mu_1^-) = \Re(\mu_2^-)$, while the third spatial eigenvalue μ_3^- has a larger real part. Consequently, the λ value at the self-intersection is part of the absolute spectrum.

There exists some weight $\nu_-^* < 0$ such that the self-intersection vanishes for $\nu_- < \nu_-^*$, see, for instance, the right panel of Figure 2.4.3. For $\nu_- = \nu_-^*$, the self-intersection forms a cusp of the weighted dispersion relations (2.28) and is thus the ideal weight, see Figure 2.4.4. For $\nu_- > \nu_-^*$, the self-intersections trace out the subset of the absolute spectrum σ^-_{abs}. This allows us to directly locate σ^-_{abs} using a root-finding algorithm on the dispersion relations of $M_0^- + \nu_- I$. Values $\lambda \in \sigma^-_{\text{abs}}$ such that there is a second order root (in μ) of the characteristic polynomial (2.27) are referred to as *branch points* λ_{br}, see Remark 2.4.1 and Figure 2.4.4. For the Keller-Segel model, the cusp of the ideally weighted dispersion relations correspond to the second order root and so the branch points are the rightmost points of σ^-_{abs}, see Figure 2.4.4.

To locate the branch points λ_{br}, we treat the characteristic polynomial (2.27) as a cubic polynomial in μ and determine the second order roots. This requires finding $\lambda \in \mathbb{C}$ such

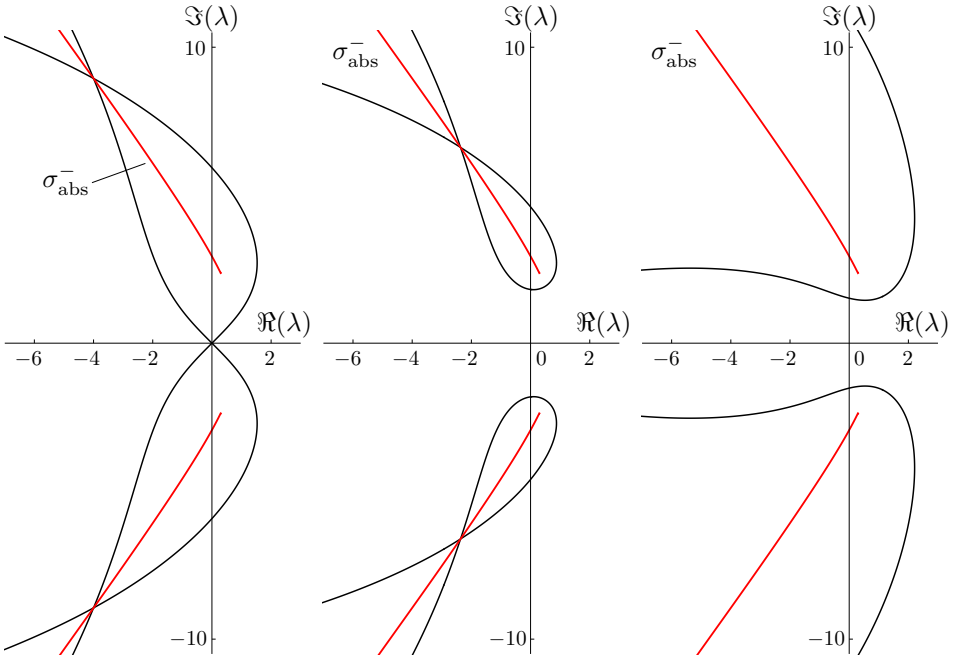

Figure 2.4.3: The subset of the absolute spectrum σ^-_{abs} (red) and the dispersion relations of $M_0^- + \nu_- I$ (black) for $\beta = c = 2$ and various weights ν_-. The dispersion relations (2.28) in the unweighted space (left panel), a weighted space with $\nu_- = -1/4$ (middle panel), and a weighted space with $\nu_- = -3/2$ (right panel). As ν_- is further decreased, the dispersion relations move further into the right half plane. For $\nu_- > 0$, the leading edge of the weighted dispersion relation also moves further into the right half plane.

that the discriminant of (2.27) is zero. That is, we solve

$$\lambda^5 + \frac{(2\beta-1)^2c^2\lambda^4}{4(\beta-1)^2} + \frac{\beta(18\beta^2-37\beta+20)c^4\lambda^3}{2(\beta-1)^3} + \frac{\beta(5\beta^3-28\beta^2+50\beta-26)c^6\lambda^2}{4(\beta-1)^4} - \frac{\beta(\beta^2-6\beta+2)c^8\lambda}{2(\beta-1)^4} + \frac{\beta^2c^{10}}{4(\beta-1)^4} = 0. \tag{2.29}$$

We look for roots of (2.29) that correspond to the two smallest spatial eigenvalues having the same real part, *i.e.* the values $\lambda \in \sigma^-_{\text{abs}}$ that solve (2.29). For given parameters, we find a pair of complex conjugate solutions to (2.29) that are in the absolute spectrum; these solutions are the branch points $\lambda^{\pm}_{br}$ that form the leading edge of σ^-_{abs}. Note that the other three roots of (2.29) are part of the generalised absolute spectrum, see Remark 2.3.2.

Locating the branch points $\lambda^{\pm}_{br}$ also allows us to compute the ideal weight ν^*_-, since ν^*_- corresponds to the negative of the real part of the second order root μ evaluated at the branch point $\lambda^{\pm}_{br}$. That is,

$$\nu^*_- := -\min\{\Re(\mu_i(\lambda_{br})),\ i = 1, 2, 3\}. \tag{2.30}$$

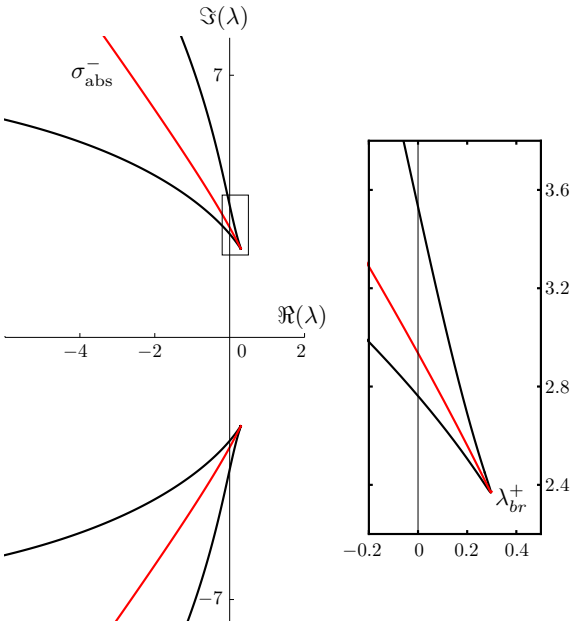

Figure 2.4.4: The subset of the absolute spectrum σ^-_{abs} (red) and the ideally weighted dispersion relations of $M_0^- + \nu_-^* I$ (black) for $\beta = c = 2$, where the ideal weight $\nu_-^* \approx -0.73$. The weighted dispersion relations form cusps whose tips coincide with the leading edge of the absolute spectrum, *i.e.* the branch points $\lambda^\pm_{br}$ (see Remark 2.4.1). Since the absolute spectrum, and thus the essential spectrum, enter into the right half plane, the travelling wave solution is absolutely unstable for this parameter set.

We have outlined how to locate the full essential and absolute spectrum, as well as how to compute the ideal weights, for a given parameter set. See, for example, Figures 2.4.5 and 2.4.6. For the parameter values used in Figure 2.4.5, the ideally weighted essential spectrum and absolute spectrum contain values in the right half plane and the travelling wave solution is thus absolutely unstable. In contrast, for the parameter values used in Figure 2.4.6, there exists a range of weights such that the essential spectrum (in the weighted space) is in the open left half plane and the travelling wave solution is potentially only transiently unstable. Observe that M_0^+ requires positive weights ν_+ to shift its dispersion relations into the open left half plane, while M_0^- requires negative weights ν_-, necessitating the two-sided weight (2.67).

Remark 2.4.1. *We refer to the value λ such that $\mu(\lambda)$ is a second order root of* (2.27) *and $\lambda \in \sigma_{\text{abs}}$ as a branch point because it is a branch point of the Evans function, an analytic tool used to locate the point spectrum. In general, not all spatial eigenvalues with algebraic multiplicity greater than one are contained in the absolute spectrum, they also occur in the generalised absolute spectrum. It is also not always the case that the leading edge of the absolute spectrum is a branch point, see for example [90]. However, for the Keller-Segel model the leading edge of the sets $\sigma^\pm_{\text{abs}}$ do coincide with branch points.*

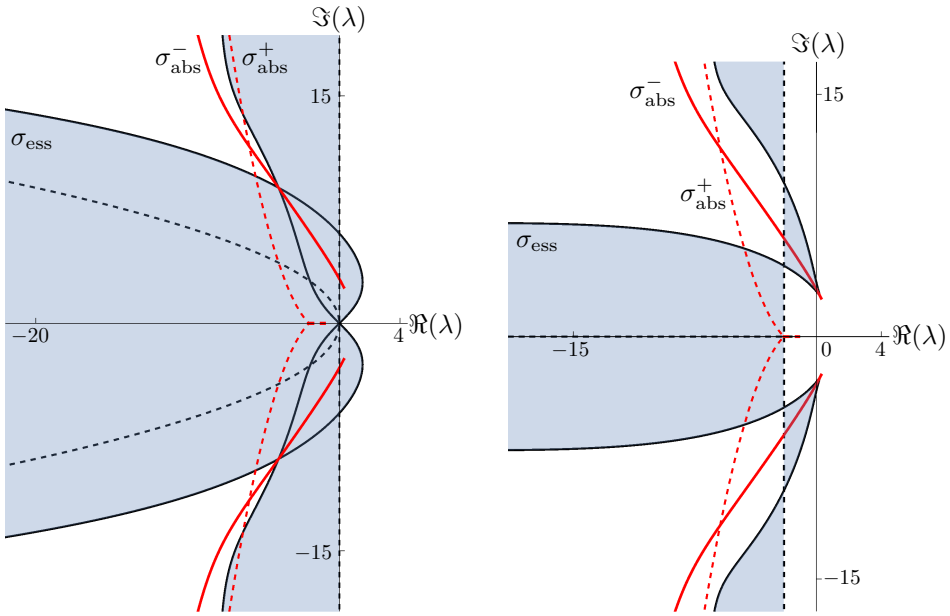

Figure 2.4.5: The essential and absolute spectrum in the unweighted space (left panel) and in the ideally weighted space (right panel) for $\beta = c = 2$, $\varepsilon = 0$ and $m = 0$, where the ideal weight is $\nu_-^* \approx -0.73$ and $\nu_+^* = c/2 = 1$. The dispersion relations of $M_0^+ + \nu_+ I$ (2.23) are shown as black dashed lines, while those of $M_0^- + \nu_- I$ (2.28) are shown as black solid lines, σ^+_{abs} is shown as red dashed lines and σ^-_{abs} as red solid lines. The shaded regions are the interior of the (weighted) essential spectrum. Note the ideally weighted essential spectrum still contains values in the right half plane and the travelling wave solutions are thus absolutely unstable.

2.4.4 Proof of Theorem 2.3.3 for $\varepsilon = m = 0$

From Figures 2.4.5 and 2.4.6 it is clear that there is a transition from absolute spectrum fully contained in the left half plane to absolute spectrum entering into the right half plane. Consequently, there must be a critical set of parameters such that the branch point λ_{br} solving (2.29) is purely imaginary. Thus, we set $\lambda_{br} := i\lambda$, $\lambda \in \mathbb{R}$, and equate the real and imaginary parts of (2.29) to zero. This gives

$$\lambda^4 - \frac{\beta\left(5\beta^3 - 28\beta^2 + 50\beta - 26\right)c^4\lambda^2}{(\beta-1)^2(2\beta-1)^2} + \frac{\beta^2 c^8}{(\beta-1)^2(2\beta-1)^2} = 0, \tag{2.31}$$

$$\lambda\left(\lambda^4 - \frac{\beta\left(18\beta^2 - 37\beta + 20\right)c^4\lambda^2}{2(\beta-1)^3} - \frac{\beta\left(\beta^2 - 6\beta + 2\right)c^8}{2(\beta-1)^4}\right) = 0. \tag{2.32}$$

Since $\lambda = 0$ is not a solution of (2.31), the transition occurs away from the real axis, *i.e.* the branch points form a complex conjugate pair. Moreover, we can divide out λ from (2.32) and the roots of (2.32) are given by $\lambda = \pm\sqrt{\Lambda_{1,2}}$ with

$$\Lambda_{1,2} = \frac{c^4\left(\beta\left(18\beta^2 - 37\beta + 20\right) \pm \sqrt{\Delta}\right)}{4(\beta-1)^3}, \tag{2.33}$$

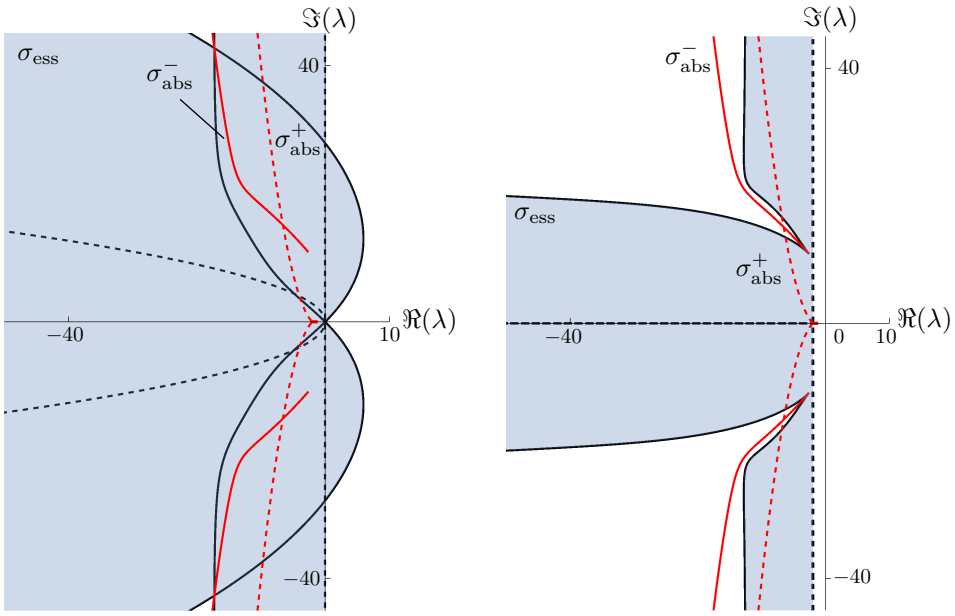

Figure 2.4.6: The essential and absolute spectrum in the unweighted space (left panel) and in the ideally weighted space (right panel) for $\beta = 1.3 < \beta_{\text{crit}}$ (2.17), $c = 2$, $\varepsilon = 0$ and $m = 0$, where the ideal weight is $\nu_-^* \approx -2.445$ and $\nu_+^* = c/2 = 1$. The dispersion relations of $M_0^+ + \nu_+ I$ (2.23) are shown as black dashed lines, while those of $M_0^- + \nu_- I$ (2.28) are shown as black solid lines, σ^+_{abs} is shown as red dashed lines and σ^-_{abs} as red solid lines. The shaded regions are the interior of the (weighted) essential spectrum. Note the ideally weighted essential spectrum is fully contained in the left half plane.

where

$$\Delta := \beta\left(324\beta^5 - 1324\beta^4 + 2025\beta^3 - 1360\beta^2 + 320\beta + 16\right).$$

It follows from Sturm's Theorem, see, for instance, Theorem 6.3d in [40], that $\Delta > 0$ for all $\beta > 1$, *i.e.* $\Lambda_{1,2}$ are real-valued for $\beta > 1$. Substituting these roots into (2.31) gives

$$\begin{aligned}&\frac{\beta c^8}{8(\beta-1)^4}\Big(1116\beta^7 - 5050\beta^6 + 8422\beta^5 - 5440\beta^4 - 455\beta^3\\ &+2104\beta^2 - 704\beta + 8 \pm \left(62\beta^4 - 154\beta^3 + 90\beta^2 + 35\beta - 32\right)\sqrt{\Delta}\Big) = 0.\end{aligned}$$

Since $\beta > 1$ and $c > 0$, this is equivalent to

$$\begin{aligned}&\left(1116\beta^7 - 5050\beta^6 + 8422\beta^5 - 5440\beta^4 - 455\beta^3 + 2104\beta^2 - 704\beta + 8\right)\\ &= \pm\left(-62\beta^4 + 154\beta^3 - 90\beta^2 - 35\beta + 32\right)\sqrt{\Delta},\end{aligned} \tag{2.34}$$

which is independent of c, see Remark 2.4.3. Squaring (2.34) gives

$$\begin{aligned}16(\beta-1)^3 f(\beta) &= 16(\beta-1)^3\left(310\beta^{10}-3234\beta^9+17112\beta^8-49101\beta^7+76180\beta^6\right.\\ &\quad\left.-58398\beta^5+10056\beta^4+15040\beta^3-9680\beta^2+1716\beta-4\right)\\ &= 0,\end{aligned}$$

where $f(\beta)$ is the same polynomial as the polynomial (2.17) of Theorem 2.3.3. The purely imaginary branch points indicating the transition to absolute instability are determined by the root β_{crit}. In particular, $\beta_{\text{crit}} \approx 1.6195$ solves (2.31) and (2.32) with $\lambda_{br}^{\pm} = \pm i\sqrt{\Lambda_1(\beta_{\text{crit}})} \approx \pm 1.0883\, c^2\, i$.

As there is only one root of (2.17) satisfying the condition $\beta > 1$, the absolute spectrum is fully contained in the open left half plane for $1 < \beta < \beta_{\text{crit}}$, *i.e.* the transition into the right half plane only happens for $\beta = \beta_{\text{crit}}$. Since the absolute spectrum always contains values in the right half plane for $\beta > \beta_{\text{crit}}$, all travelling wave solutions with $\beta > \beta_{\text{crit}}$ are absolutely unstable. This concludes the proof of Theorem 2.3.3 for $\varepsilon = m = 0$.

Remark 2.4.2. *It is possible for the absolute spectrum of an operator to be contained in the open left half plane, yet the weighted essential spectrum contains values in the right half plane for all weights. This is referred to as an essential instability, see [90] for examples of essential instabilities. We now show that for a range of weights, the weighted dispersion relations, and thus the weighted essential spectrum, do not cross into the right half plane for* $1 < \beta < \beta_{\text{crit}}$, i.e. *travelling wave solutions in the Keller-Segel model do not exhibit essential instabilities. The ideally weighted dispersion relations* (2.24) *and absolute spectrum* σ_{abs}^{+} (2.26) *associated with* M_0^+ *are contained in the open left half plane for* $1 < \beta < \beta_{\text{crit}}$. *What remains to prove is that there exists a range of weights such that the weighted dispersion relations of* M_0^- (2.28) *are fully contained in the open left half plane for* $1 < \beta < \beta_{\text{crit}}$.

The characteristic polynomial of $M_0^- + \nu_- I$ (2.28) *is quadratic in* $\lambda \in \mathbb{C}$. *So, we can explicitly solve for* $\lambda_{1,2}$ *and extract the real parts of the solutions. It follows that*

$$\lim_{|k|\to\infty} \Re(\lambda_1) = -c\left(\frac{c\beta}{\beta-1} + \nu_-\right), \qquad \lim_{|k|\to\infty} \Re(\lambda_2) = -\infty. \tag{2.35}$$

That is, the dispersion relations of $M_0^- + \nu_- I$ *approach vertical lines in the complex plane. Requiring that* $\Re(\lambda_1) < 0$ *as* $|k| \to \infty$ *gives a lower bound on admissible weights* $\nu_- > -\frac{c\beta}{\beta-1}$ *(note that it turns out that this lower bound is not sharp, see Figure 2.4.7).*

Next, we compute the values λ where the dispersion relations of $M_0^- + \nu_- I$ (2.28) cross the imaginary axis. Therefore, we assume that λ is purely imaginary and solve (2.28). This way, we eliminate the parameter k and obtain a cubic polynomial equation in $\Lambda := \Im(\lambda)^2$ (with unknowns β, c and ν_-). Non-negative real roots of this polynomial in Λ correspond to the intersections of the dispersion relations of $M_0^- + \nu_- I$ with the imaginary axis. In the

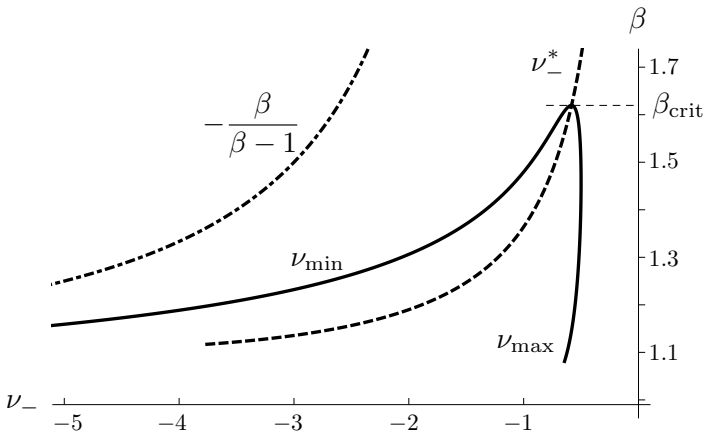

Figure 2.4.7: The area in between the curves $\nu_{\min}$ and $\nu_{\max}$ indicates the range of weights ν_- such that the absolute spectrum and weighted essential spectrum are contained in the open left half plane for $c = 1,\ m = 0,\ \varepsilon = 0$ (and $\nu_+^* = c/2 = 1/2$). For $\beta = \beta_{\text{crit}}$ the values $\nu_{\min},\ \nu_{\max}$ and the ideal weight ν_-^* coincide and so the essential spectrum cannot be weighted into the open left half plane for $\beta \geq \beta_{\text{crit}}$. The dot-dashed curve represents the asymptotic condition $\nu_- > -\frac{\beta}{\beta-1}$ coming from (2.35).

unweighted case $\nu_- = 0$ it has one positive root and a root at the origin, see also the left panels of Figure 2.4.5 and 2.4.6. For decreasing ν_-, these two roots approach each other and collide at $\nu_{\max} = \nu_{\max}(\beta, c)$ (while the third root stays negative). The polynomial has no non-negative real roots if we further decrease ν_-. These weights correspond to the case where the weighted dispersion relations do not intersect the imaginary axis and are thus fully contained in the open left half plane. At $\nu_{\min} = \nu_{\min}(\beta, c)$ two positive roots reappear (while the third root is still negative) and these positive roots persist upon further decreasing ν_-. In other words, for weights $\nu_- \in (\nu_{\min}, \nu_{\max})$ the dispersion relations of $M_0^- + \nu_- I$ (2.28) never intersect the imaginary axis and are fully contained in the open left half plane. The values $\nu_{\min}$ and $\nu_{\max}$ are given as the roots of an 11^{th} order polynomial in ν_- and the range of admissible weights shrinks to a point as $\beta \uparrow \beta_{\text{crit}}$, see Figure 2.4.7. In particular, one rediscovers $f(\beta)$ (2.17) by equating the derivative of this 11^{th} order polynomial to zero. This is equivalent to finding β such that $\nu_{\min} = \nu_{\max}$. Obtaining the range of admissible weights is straightforward for given values of β and c, but complicated to determine for general $1 < \beta < \beta_{\text{crit}}$ and c. See Figure 2.4.7 for a plot of $\nu_{\max}$ and $\nu_{\min}$ (and the ideal weight ν_-^* obtained from (2.30)) versus β.

Remark 2.4.3. *The results on the existence of a range of weights to move the essential spectrum into the open left half plane and the (in)stability of the absolute spectrum are independent of the wave speed c. This is not a coincidence as the dispersion relations can be rescaled to be independent of c. In particular, the substitutions* $\lambda = c^2\tilde{\lambda},\ \nu = c\tilde{\nu},\ k = c\tilde{k}$ *transform the dispersion relations of* $M_0^+ + \nu_+ I$ (2.23) *into*

$$c^2\tilde{\lambda} = c^2\left(-\tilde{\nu}_+ + i\tilde{k}\right), \quad \textit{and} \quad c^2\tilde{\lambda} = c^2\left(-\tilde{k}^2 - \tilde{\nu}_+(1-\tilde{\nu}) + i(\tilde{k} - 2\tilde{k}\tilde{\nu}_+\right),$$

which is equivalent to the dispersion relations of $M_0^+ + \nu_+ I$ (2.23) *for* $c = 1$. *Similarly, the dispersion relations of* $M_0^- + \nu_- I$ (2.28) *become*

$$c^4\left(\tilde{\lambda}^2 + \left(\frac{(2-\beta)(i\tilde{k}-\tilde{\nu}_-)}{\beta-1} - (i\tilde{k}-\tilde{\nu}_-)^2\right)\tilde{\lambda} + \frac{\beta(i\tilde{k}-\tilde{\nu}_-)}{(\beta-1)^2} - \frac{(\beta+1)(i\tilde{k}-\tilde{\nu}_-)^2}{\beta-1} + (i\tilde{k}-\tilde{\nu}_-)^3\right) = 0,$$

which is equivalent to the dispersion relations of $M_0^- + \nu_- I$ (2.28) *for* $c = 1$. *In other words, the magnitude of* c *does not affect the (in)stability results and only affects the multiplicative scaling of the spectrum. As a consequence, all the figures presented in this chapter are generic in* c *up to the above scaling of* λ, ν *and* k.

2.5 Sublinear and linear consumption and zero diffusivity of the chemoattractant

In this section, we examine the effect of the parameter m on the location of the weighted essential spectrum and absolute spectrum associated with a travelling wave solution. Since travelling wave solutions only exist for $0 \leq m \leq 1$, *e.g.* [103], we take $0 < m \leq 1$. We prove Theorem 2.3.3 for $0 < m \leq 1$ and $\varepsilon = 0$. It turns out that the analysis for $0 < m < 1$ is similar, at least qualitatively, to the analysis of the previous section for $m = 0$. The analysis simplifies significantly for $m = 1$ and we note that the results of this case can be in part deduced from [77] where a version of the Keller-Segel model with nonzero growth rate is studied.

In particular, we show that for sublinear consumption, *i.e.* $0 < m < 1$, there exists a critical value $\beta^m_{\text{crit}} = \beta_{\text{crit}}(1-m)$ (with β_{crit} the root of (2.17)) such that for $1 - m < \beta < \beta^m_{\text{crit}}$ the absolute spectrum is fully contained in the open left half plane. The absolute spectrum enters the right half plane for $\beta > \beta^m_{\text{crit}}$ and all travelling wave solutions are thus absolutely unstable for $\beta > \beta^m_{\text{crit}}$. For linear consumption, *i.e.* $m = 1$, we show that the absolute spectrum always contains the origin. Consequently, the essential spectrum cannot be weighted into the open left half plane.

2.5.1 Set-up

For $0 < m \leq 1$ and $\varepsilon = 0$, the eigenvalue problem is given by (2.11), which we restate for convenience

$$\mathcal{L}_0^m \begin{pmatrix} p \\ q \end{pmatrix} = \lambda \begin{pmatrix} p \\ q \end{pmatrix}, \qquad \mathcal{L}_0^m := \begin{pmatrix} c\frac{\partial}{\partial z} - mwu^{m-1} & -u^m \\ \mathcal{L}_{21} & \mathcal{L}_{22} \end{pmatrix} \tag{2.36}$$

with

$$\begin{aligned}\mathcal{L}_{21} &:= \beta\left(\frac{w_z u_z}{u^2} + \frac{w u_{zz}}{u^2} - \frac{2w u_z^2}{u^3}\right) + \beta\left(\frac{2w u_z}{u^2} - \frac{w_z}{u}\right)\frac{\partial}{\partial z} - \frac{\beta w}{u}\frac{\partial^2}{\partial z^2},\\ \mathcal{L}_{22} &:= \beta\left(\frac{u_z^2}{u^2} - \frac{u_{zz}}{u}\right) + \left(c - \frac{\beta u_z}{u}\right)\frac{\partial}{\partial z} + \frac{\partial^2}{\partial z^2},\end{aligned} \tag{2.37}$$

where u and w are the travelling wave solutions given in (2.7). Observe that the first row of $\mathcal{L}$ simplifies significantly in the cases $m = 0$ and $m = 1$. We take a slightly different approach as in §2.4 and first write (2.36) as a third order equation in p, see Remark 2.5.1. From the first row of (2.36) we have

$$q = cu^{-m}p_z - (mwu^{-1} + \lambda u^{-m})p\,, \tag{2.38}$$

and we differentiate this to obtain

$$\begin{aligned}q_z &= cu^{-m}p_{zz} + ((cu^{-m})_z - (mwu^{-1} + \lambda u^{-m}))p_z\\ &\quad - \left(mwu^{-1} + \lambda u^{-m}\right)_z p,\\ q_{zz} &= cu^{-m}p_{zzz} + \left(2(cu^{-m})_z - (mwu^{-1} + \lambda u^{-m})\right)p_{zz}\\ &\quad + \left((cmu^{-m})_{zz} - 2(mwu^{-1} + \lambda u^{-m})_z\right)p_z - (mwu^{-1} + \lambda u^{-m})_{zz}p.\end{aligned} \tag{2.39}$$

We substitute (2.38) and (2.39) into the second row of (2.36), that is into $\mathcal{L}_p p + \mathcal{L}_q q = \lambda q$, and we eliminate w using $w = cu_z u^{-m}$ ((2.6) with $\varepsilon = 0$). The resulting third order operator is

$$p_{zzz} - \mathcal{C}_m p_{zz} - \mathcal{B}_m p_z - \mathcal{A}_m p = 0 \tag{2.40}$$

where

$$\begin{aligned}\mathcal{A}_m =\ & \left(\lambda(m+1)(\beta+m) - c^2 m\right)\frac{u_z^2}{cu^2} + 2(m+1)(\beta+m)\frac{u_z^3}{u^3} - 2\lambda m\frac{u_z}{u}\\ & - (2\beta+3m)\frac{u_z u_{zz}}{u^2} - \lambda(\beta+m)\frac{u_{zz}}{cu} - \frac{\lambda^2}{c},\\ \mathcal{B}_m =\ & \left(2c^2 m - \lambda(\beta+2m)\right)\frac{u_z}{cu} - 3(m+1)(\beta+m)\frac{u_z^2}{u^2} + (2\beta+3m)\frac{u_{zz}}{u} + 2\lambda,\\ \mathcal{C}_m =\ & \frac{\lambda}{c} - c + (2\beta+3m)\frac{u_z}{u}.\end{aligned} \tag{2.41}$$

Next, we define $p_1 := p_z$ and $p_2 := p_{zz}$ to obtain the operator $\mathcal{T}_m(\lambda)$

$$\mathcal{T}_m(\lambda)\begin{pmatrix} p \\ p_1 \\ p_2 \end{pmatrix} := \begin{pmatrix} p \\ p_1 \\ p_2 \end{pmatrix}' - M_m(z,\lambda)\begin{pmatrix} p \\ p_1 \\ p_2 \end{pmatrix} = 0, \tag{2.42}$$

$$M_m(z,\lambda) := \begin{pmatrix} 0 & 1 & 0 \\ 0 & 0 & 1 \\ \mathcal{A}_m & \mathcal{B}_m & \mathcal{C}_m \end{pmatrix}.$$

While we have used a slightly different approach compared to §2.4, the spectrum of $\mathcal{T}_0(\lambda)$ in (2.20) and the spectrum of $\mathcal{T}_m(\lambda)$ (2.42) agree in the limit $m \to 0$.

Remark 2.5.1. *The substitutions* (2.38) *and* (2.39) *are necessary due to the appearance of the term* w/u *appearing in* $\mathcal{L}_p$ (2.37). *While the term* w/u *is bounded for* $m = 0$, *the term is unbounded as* $z \to -\infty$ *for* $0 < m \leq 1$. *However, by making the substitutions* (2.38) *and* (2.39) *in* (2.36), *we obtain* (2.40), *which is asymptotically constant and equivalent to* $\mathcal{L}$ (2.36). *The equivalence of* (2.40) *and* $\mathcal{L}$ (2.36) *becomes clearer when we see that* (2.40) *is actually the linearised eigenvalue problem obtained from eliminating* $w(z,t) = u^{-m}(z,t)\left(cu_z(z,t) - u_t(z,t)\right)$ *from* (2.5) *first.*

2.5.2 Essential spectrum

We use the limits given in (2.8) (with $\varepsilon = 0$) and the fact that $u_{zz} = (wu^m)_z/c$ (2.6), to obtain

$$\lim_{z\to-\infty}\frac{u_z}{u} = \frac{c}{\beta+m-1}, \quad \lim_{z\to-\infty}\frac{u_{zz}}{u} = \frac{c^2}{(\beta+m-1)^2}, \quad \lim_{z\to\infty}(u,u_z,u_{zz}) = (1,0,0).$$

Using these limits, the asymptotic values of $\mathcal{A}_m$, $\mathcal{B}_m$ and $\mathcal{C}_m$ as $z \to \pm\infty$, denoted $\mathcal{A}_m^{\pm}$, $\mathcal{B}_m^{\pm}$ and $\mathcal{C}_m^{\pm}$ respectively, are

$$\mathcal{A}_m^+ = -\frac{\lambda^2}{c}, \quad \mathcal{B}_m^+ = 2\lambda, \quad \mathcal{C}_m^+ = \frac{\lambda}{c} - c, \tag{2.43}$$

and

$$\begin{aligned} \mathcal{A}_m^- &= -\frac{\lambda^2}{c} - \frac{cm(\beta+m-2)}{(\beta+m-1)^2}\lambda + \frac{c^3 m(\beta+m)}{(\beta+m-1)^3}, \\ \mathcal{B}_m^- &= \frac{(\beta-2)}{\beta+m-1}\lambda - \frac{c^2\left(\beta+m(\beta+m+2)\right)}{(\beta+m-1)^2}, \\ \mathcal{C}_m^- &= \frac{\lambda}{c} + \frac{c(\beta+2m+1)}{\beta+m-1}. \end{aligned} \tag{2.44}$$

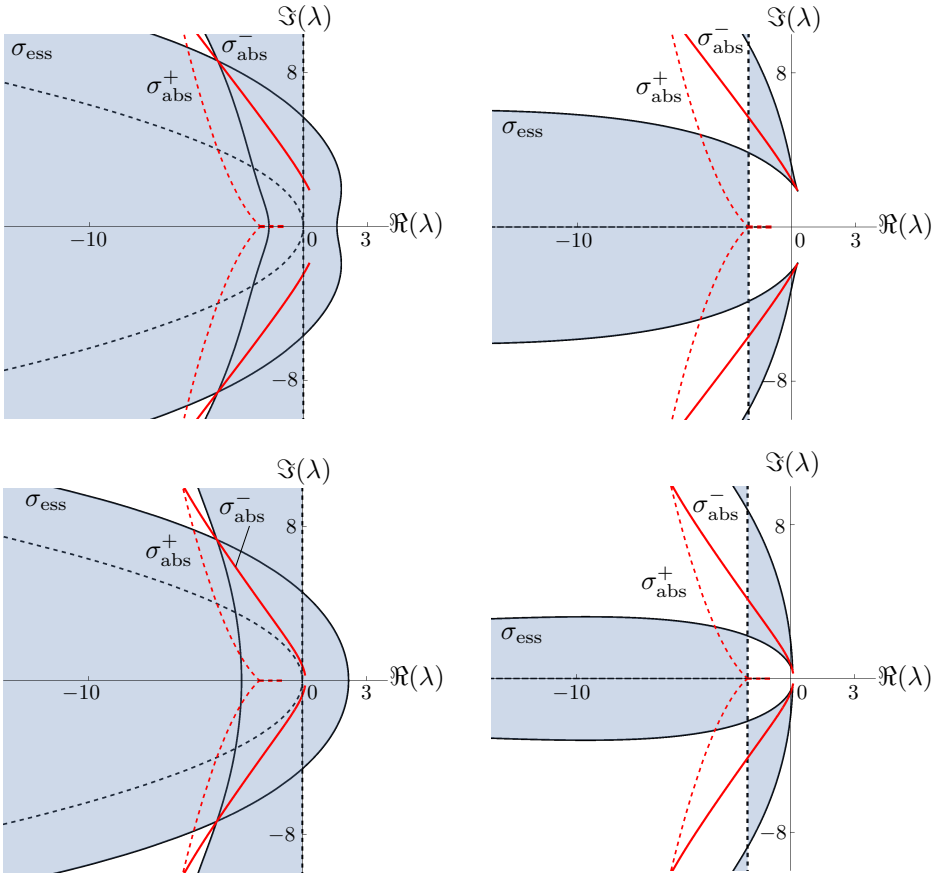

Figure 2.5.1: The essential and absolute spectrum for $m = 0.1$ (upper panels) and $m = 0.7$ (lower panels) with $\beta = c = 2$ and $\varepsilon = 0$. The dispersion relations of $M_m^+ + \nu_+ I$ (dashed black) and $\sigma_{\rm abs}^{m,+}$ (dashed red) are the same in all four panels and the ideal weight for $z \to \infty$ is still given by $\nu_+^* = c/2 = 1$. The dispersion relations of $M_m^- + \nu_- I$ are shown as solid black lines and $\sigma_{\rm abs}^{m,-}$ as solid red. Upper left panel: the spectrum in the unweighted space for $m = 0.1$. Upper right panel: the ideally weighted space for $m = 0.1$, where the ideal weight is $\nu_-^* \approx -0.778$. Lower left panel: the spectrum in the unweighted space for $m = 0.7$. Lower right panel: the ideally weighted space for $m = 0.7$, where $\nu_-^* \approx -0.959$. As m increases to one, the real and imaginary components of the branch points $\lambda_{br}^{\pm}$ decrease and approach the origin, see §2.5.5.

We define the asymptotic matrices

$$M_m^{\pm}(\lambda) := \lim_{z \to \pm\infty} M_m(z, \lambda) = \begin{pmatrix} 0 & 1 & 0 \\ 0 & 0 & 1 \\ \mathcal{A}_m^{\pm} & \mathcal{B}_m^{\pm} & \mathcal{C}_m^{\pm} \end{pmatrix}, \tag{2.45}$$

related to the asymptotic operator associated with $\mathcal{T}_m$ (2.42). The dispersion relations of M_m^+ are independent of m and β, and the same as for $m = 0$ (2.21). The dispersion

relations of M_m^- depend on m and are implicitly given by

$$\begin{aligned}\lambda^2 + \left(k^2 + \frac{c^2 m(\beta+m-2)}{(\beta+m-1)^2} - \frac{ick(\beta-2)}{\beta+m-1}\right)\lambda + \frac{c^2k^2(\beta+2m+1)}{\beta+m-1} \\ - \frac{c^4 m(\beta+m)}{(\beta+m-1)^3} + \frac{ic^3k\,(\beta+m(m+\beta+2))}{(\beta+m-1)^2} - ick^3 = 0.\end{aligned} \tag{2.46}$$

In the limit $m \to 0$, (2.46) coincides with the dispersion relations of M_0^- (2.22). The dispersion relations M_m^+ (2.21) and M_m^- (2.46) form the boundaries of the essential spectrum and $\lambda \in \mathbb{C}$ such that *i.e.* $i_+ \neq i_-$ (see Definition 2.3.2) forms the interior of the (unweighted) essential spectrum. See the two left panels of Figure 2.5.1 for the unweighted essential spectrum for two different values of m.

2.5.3 The weighted essential spectrum and the absolute spectrum

As for $m = 0$, we consider a two-sided weight of the form (2.67). Since the dispersion relations of M_m^+ and M_0^+ are the same, the ideal weight for $z \to \infty$ are unchanged for $0 < m \leq 1$. That is, $\nu_+^* = c/2$. Consequently, $\sigma_{\text{abs}}^{m,+} = \sigma_{\text{abs}}^+$ (2.26). See also Figure 2.4.2.

The dispersion relations of $M_m^- + \nu_- I$ are implicitly given by

$$\begin{aligned}\lambda^2 + \lambda\left(-(ik-\nu_-)^2 + \frac{c^2 m(\beta+m-2)}{(\beta+m-1)^2} - \frac{c(ik-\nu_-)(\beta-2)}{\beta+m-1}\right) \\ - \frac{c^2(ik-\nu_-)^2(\beta+2m+1)}{\beta+m-1} - \frac{c^4 m(\beta+m)}{(\beta+m-1)^3} \\ + \frac{c^3(ik-\nu_-)(\beta+m(\beta+m+2))}{(\beta+m-1)^2} + c(ik-\nu_-)^3 = 0.\end{aligned} \tag{2.47}$$

The shift in the essential spectrum due to weighting in the $0 < m \leq 1$ case is qualitatively similar to the behaviour shown in Figure 2.4.3. That is, under a large range of weights the dispersion relations have self-intersections and these self-intersections form part of the absolute spectrum $\sigma_{\text{abs}}^{m,-}$. Thus, we can once again use a find root procedure on the weighted dispersion relations (2.47) to locate $\sigma_{\text{abs}}^{m,-}$. See Figure 2.5.1 for the unweighted essential spectrum, the ideally weighted essential spectrum, and the absolute spectrum for two different values of m.

2.5.4 Proof of Theorem 2.3.3 for $0 < m < 1$ and $\varepsilon = 0$

For $0 < m < 1$ and $\varepsilon = 0$, a polynomial $f_m(\beta)$, similar to the polynomial $f(\beta)$ (2.17) for $m = 0$, can be derived. Its root $\beta_{\text{crit}}^m = \beta_{\text{crit}}(1-m) > 1 - m$ predicts the transition of the absolute spectrum into the right half plane (for increasing β). For $1 - m < \beta < \beta_{\text{crit}}^m$, the absolute spectrum is fully contained in the open left half plane. For $\beta > \beta_{\text{crit}}^m$, the absolute spectrum enters the right half plane and the travelling wave solutions are thus absolutely unstable.

To determine the transition of the absolute spectrum into the right half plane we follow the same procedure as in §2.4.4 and we treat the characteristic polynomial of M_m^- as a cubic polynomial in μ and equate the discriminant to zero. This gives

$$\begin{aligned}&\lambda^5 + \frac{c^2(2\beta+m-1)^2}{4(\beta+m-1)^2}\lambda^4 + \frac{\beta c^4\left(18\beta^2+37\beta(m-1)+20(m-1)^2\right)}{2(\beta+m-1)^3}\lambda^3\\&+\frac{\beta c^6\left(5\beta^3+28\beta^2(m-1)+50\beta(m-1)^2+26(m-1)^3\right)}{4(\beta+m-1)^4}\lambda^2\\&+\frac{\beta c^8(m-1)\left(\beta^2+6\beta(m-1)+2(m-1)^2\right)}{2(\beta+m-1)^4}\lambda+\frac{\beta^2c^{10}(m-1)^2}{4(\beta+m-1)^4}=0.\end{aligned}\tag{2.48}$$

This discriminant has a purely imaginary root under the condition

$$0=\frac{\beta^2c^{20}(m-1)}{64(\beta+m-1)^{13}}f_m(\beta)\tag{2.49}$$

where

$$\begin{aligned}f_m(\beta) :=& \left(310\beta^{10}+3234\beta^9(m-1)+17112\beta^8(m-1)^2+49101\beta^7(m-1)^3\right.\\&+76180\beta^6(m-1)^4+58398\beta^5(m-1)^5+10056\beta^4(m-1)^6\\&\left.-15040\beta^3(m-1)^7-9680\beta^2(m-1)^8-1716\beta(m-1)^9-4(m-1)^{10}\right).\end{aligned}\tag{2.50}$$

For $m=1$, (2.49) is trivially satisfied. Therefore, we treat the $m=1$ case separately, see §2.5.5. Upon introducing the variable $B=\frac{\beta}{(1-m)}$ (and setting $0<m<1$), (2.49) becomes,

$$\begin{aligned}0&=\frac{-B^2c^{20}}{64(B-1)^{13}}\left(310B^{10}-3234B^9+17112B^8-49101B^7+76180B^6\right.\\&\quad\left.-58398B^5+10056B^4+15040B^3-9680B^2+1716B-4\right)\\&=\frac{-B^2c^{20}}{64(B-1)^{13}}f(B),\end{aligned}\tag{2.51}$$

where f is given by (2.17). The roots of f_m and f are related by $\beta_{\text{crit}}^m=\beta_{\text{crit}}(1-m)$, and β_{crit}^m is the only root of (2.49) that satisfies the condition $\beta+m>1$. In conclusion, we have that the absolute spectrum is fully contained in the open left half plane for $0\leq m<1, \varepsilon=0$ and $1-m<\beta<\beta_{\text{crit}}^m$, while the absolute spectrum enters into the right half plane for $0\leq m<1, \varepsilon=0$ and $\beta>\beta_{\text{crit}}^m$. This concludes the proof of Theorem 2.3.3 for $0<m<1$ and $\varepsilon=0$.

Remark 2.5.2. *Similar to the $m=0$ case, there also exist a range of weights $\nu_{\min}^m<\nu_-<\nu_{\max}^m$ for $0<m<1$ and $\varepsilon=0$, such that the weighted essential spectrum is contained in the open left half plane for $1-m<\beta<\beta_{\text{crit}}^m$. In other words, there are no essential instabilities in this case. See also Remark 2.4.2.*

2.5.5 Linear consumption

In the case of linear consumption, *i.e.* $m = 1$, the travelling wave solutions (u, w) (2.7) are a pair of wavefronts, rather than a pulse and a wavefront, see, for example, the right panel of Figure 2.3.1. In this case, the absolute spectrum and the ideally weighted essential spectrum contain the origin for all β and as a result the essential spectrum cannot be weighted into the open left half plane.

The dispersion relations of M_1^+ are independent of m and β, see §2.5.2, and therefore $\sigma_{\text{abs}}^{1,+} = \sigma_{\text{abs}}^{+}$ (2.26) is fully contained in the open left half plane. Consequently, we only need to examine $\sigma_{\text{abs}}^{1,-}$. The characteristic polynomial of M_1^- is

$$\begin{aligned}&\mu^3 - \mu^2\left(\frac{\beta\left(\beta+3\right)c}{\beta^2} + \frac{\lambda}{c}\right) + \mu\left(\frac{(2-\beta)\lambda}{\beta} + \frac{\beta\left(\beta^2+(\beta-1)+4\beta\right)c^2}{\beta^3}\right)\\ &- \frac{(\beta+1)c^3}{\beta^3} + \frac{(\beta-1)c\lambda}{\beta^2} + \frac{\lambda^2}{c} = 0.\end{aligned} \tag{2.52}$$

To locate $\sigma_{\text{abs}}^{1,-}$, we follow the same process as for $0 \leq m < 1$. In particular, we locate $\lambda \in \sigma_{\text{abs}}^{1,-}$ such that the characteristic polynomial (2.52) has a second order root in μ. That is, we locate the branch points $\lambda_{br}^{\pm}$. We equate the discriminant of (2.52) to zero to obtain

$$\lambda^2\left(4\lambda^3 + 4c^2\lambda^2 + 36c^4\lambda + 5c^6\right) = 0, \tag{2.53}$$

which has a second order root $\lambda = 0$. For $\lambda = 0$, (2.52) becomes

$$(\beta\mu - c(\beta+1))(c-\beta\mu)^2 = 0 \quad \Longrightarrow \quad \mu_1 = \frac{(\beta+1)c}{\beta}, \quad \mu_{2,3} = \frac{c}{\beta}. \tag{2.54}$$

Since $\Re(\mu_1) > \Re(\mu_2) = \Re(\mu_3)$, $0 \in \sigma_{\text{abs}}^{1,-}$ and the ideal weight is $\nu_-^* = -\Re(\mu_{2,3}) = -\frac{c}{\beta}$ (2.30). Furthermore, the ideally weighted essential spectrum and the absolute spectrum contain the origin for all β. That is, there are no parameter values such that the essential spectrum can be weighted fully into the open left half plane, see, for example, Figure 2.5.2. Note that the other three roots of (2.53) are part of the generalised absolute spectrum. This concludes the proof of Theorem 2.3.3 for $m = 1$ and $\varepsilon = 0$.

Remark 2.5.3. *For $0 \leq m < 1, \varepsilon = 0$ and $\beta > \beta_{\text{crit}}^m$, the absolute spectrum contains values in the right half plane. However, for a large chemotactic parameter,* i.e. *$\beta \gg 1$, the end points of the absolute spectrum $\lambda_{br}^{\pm}$ approach zero, see Figure 2.5.3. Actually, in the limit $\beta \to \infty$, the discriminant of the characteristic polynomial of M_m^- (2.48) reduces to the discriminant of the characteristic polynomial of M_1^- (2.53). That is, the branch points $\lambda_{br}^{\pm}$ of the absolute spectrum approach the origin from the right. Furthermore, the ideally weighted essential spectrum for $0 \leq m < 1, \varepsilon = 0$ and β large is qualitatively similar to*

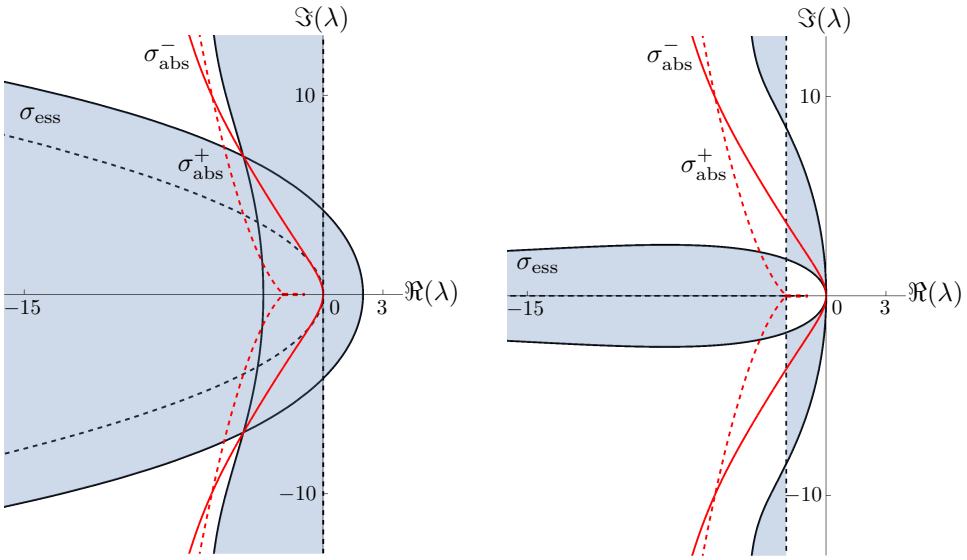

Figure 2.5.2: The essential and absolute spectrum in the unweighted space (left panel) and in the ideally weighted space (right panel) for $\beta = c = 2$, $\varepsilon = 0$ and $m = 1$, where the ideal weight is $\nu_-^* = -c/\beta = -1$ and $\nu_+^* = c/2 = 1$. The dispersion relations of $M_1^+ + \nu_+ I$ (2.23) are shown as black dashed lines, while those of $M_1^- + \nu_- I$ (2.47) are shown as black solid lines, $\sigma_{\text{abs}}^{1,+}$ is shown as red dashed lines and $\sigma_{\text{abs}}^{1,-}$ as red solid lines. The shaded regions are the interior of the (weighted) essential spectrum. The absolute spectrum contains the origin (for all parameter values β and c) and the essential spectrum thus cannot be weighted into the open left half plane.

the ideally weighted essential spectrum shown in the right panel of Figure 2.5.2 for $m = 1$ *and* $\varepsilon = 0$.

2.6 Small diffusion

In this section, we finish the proof of Theorem 2.3.3 and show that the results obtained for $\varepsilon = 0$ persist to leading order when we allow for small diffusion of the attractant u in (2.4) (*i.e.* for $0 < \varepsilon \ll 1$). In particular, we show that for $|\lambda| = \mathcal{O}(1)$ the weighted essential spectrum and absolute spectrum correspond, in leading order, to the spectra in the $\varepsilon = 0$ case. For $|\lambda|$ large, the spectra differ significantly, however, the differences do not alter the explicit stability results since they occur in the open left half plane.

2.6.1 Set-up

We treat the various consumption rates $0 \leq m \leq 1$ simultaneously. First, we eliminate the perturbation q, and its derivatives, from (2.9). From the first row of (2.9) we have

$$q = \varepsilon u^{-m} p_{zz} + c u^{-m} p_z - (mwu^{-1} + \lambda u^{-m}) p. \tag{2.55}$$

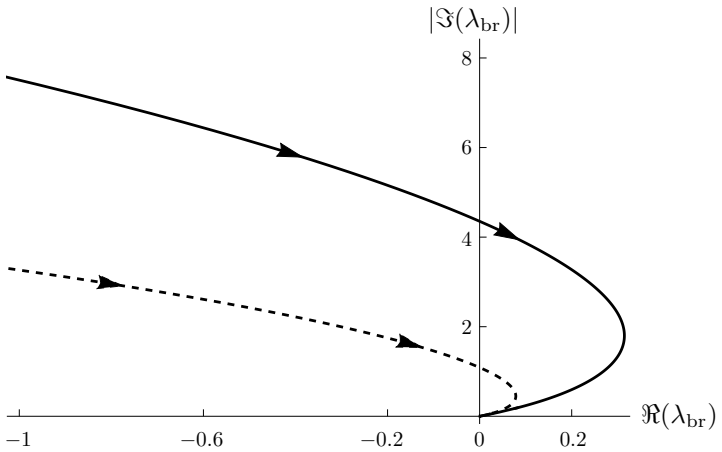

Figure 2.5.3: Plot of the real component of the branch points versus the magnitude of the imaginary component of the branch points parametrised by $\beta > 1$ for $m = 0, \varepsilon = 0$ and $c = 1$ (dashed line) and $c = 2$ (solid line). For both curves the intersections with the imaginary axis away from the origin correspond to $\beta = \beta_{\rm crit}$ and $\lim_{\beta\to\infty} |\lambda_{br}| = 0$. Note that the figure is qualitatively similar for $0 < m < 1$.

Differentiating (2.55) gives

$$\begin{aligned} q_z &= \varepsilon u^{-m} p^{(3)} + \left((\varepsilon u^{-m})_z + c u^{-m}\right) p_{zz} \\ &\qquad + ((c u^{-m})_z - (m w u^{-1} + \lambda u^{-m})) p_z q + (m w u^{-1} + \lambda u^{-m})_z p, \\ q_{zz} &= \varepsilon u^{-m} p^{(4)} + \left(2(\varepsilon u^{-m})_z + c u^{-m}\right) p^{(3)} \\ &\quad + \left((\varepsilon u^{-m})_{zz} + 2(c u^{-m})_z - (m w u^{-1} + \lambda u^{-m})\right) p_{zz} \\ &\quad + \left((c m u^{-m})_{zz} - 2(m w u^{-1} + \lambda u^{-m})_z\right) p_z + (m w u^{-1} + \lambda u^{-m})_{zz} p. \end{aligned} \tag{2.56}$$

We substitute (2.55) and (2.56) into the second row of (2.9) $\mathcal{L}_p p + \mathcal{L}_q q = \lambda q$. The resulting singular fourth ODE is

$$\varepsilon p_{zzzz} - \mathcal{D}_{m,\varepsilon} p_{zzz} - \mathcal{C}_{m,\varepsilon} p_{zz} - \mathcal{B}_{m,\varepsilon} p_z - \mathcal{A}_{m,\varepsilon} p = 0 \tag{2.57}$$

where

$$\begin{aligned}
\mathcal{A}_{m,\varepsilon} :=&(\beta+m)\left(c^2+\lambda+\lambda m\right)\frac{u_z^2}{u^2}-2c\lambda m\frac{u_z}{u}-c(\beta+m)\frac{u_zu_{zz}}{u^2}-\lambda^2\\
&-\lambda(\beta+m)\frac{u_{zz}}{u}-c(\beta-2)(\beta+m)\frac{u_z^3}{u^3}\\
&+\varepsilon\bigg(c(\beta+m)\frac{u_zu_{zz}}{u^2}-(\beta-2)(\beta+m)\frac{u_z^2u_{zz}}{u^3}-(\beta+m)\frac{u_{zz}^2}{u^2}-\lambda m\frac{u_{zz}}{u}\bigg),\\
\mathcal{B}_{m,\varepsilon} :=&2c\lambda-\left(\beta c^2+\lambda(\beta+2m)\right)\frac{u_z}{u}+c(\beta-m-3)(\beta+m)\frac{u_z^2}{u^2}+c(\beta+m)\frac{u_{zz}}{u}\\
&+\varepsilon\left((\beta-2)(\beta+m)\frac{u_zu_{zz}}{u^2}-c(\beta+m)\frac{u_{zz}}{u}\right),\\
\mathcal{C}_{m,\varepsilon} :=&-c^2+c(2(\beta+m)+m)\frac{u_z}{u}+\lambda+\varepsilon\bigg(\lambda-(m+1)(\beta+m)\frac{u_z^2}{u^2}+cm\frac{u_z}{u}\\
&+2(\beta+m)\frac{u_{zz}}{u}\bigg),\\
\mathcal{D}_{m,\varepsilon} :=&-c+\varepsilon\left((\beta+2m)\frac{u_z}{u}-c\right),
\end{aligned}$$

with (u,w) the travelling wave solutions given, to leading order, by (2.7). We set $p_1 := p_z$, $p_2 := p_{zz}$ and $p_3 := p_{zzz}$ and define the operator $\mathcal{T}_\varepsilon$ by

$$\mathcal{T}_{m,\varepsilon}(\lambda)\begin{pmatrix}p\\p_1\\p_2\\p_3\end{pmatrix} := \begin{pmatrix}p\\p_1\\p_2\\p_3\end{pmatrix}' - M_{m,\varepsilon}(z,\lambda)\begin{pmatrix}p\\p_1\\p_2\\p_3\end{pmatrix} = 0,$$

where

$$M_{m,\varepsilon}(z,\lambda) := \begin{pmatrix}0 & 1 & 0 & 0\\ 0 & 0 & 1 & 0\\ 0 & 0 & 0 & 1\\ \mathcal{A}_{m,\varepsilon}/\varepsilon & \mathcal{B}_{m,\varepsilon}/\varepsilon & \mathcal{C}_{m,\varepsilon}/\varepsilon & \mathcal{D}_{m,\varepsilon}/\varepsilon\end{pmatrix}. \tag{2.58}$$

All terms in $\mathcal{T}_{m,\varepsilon}$ can be expressed in terms of either u_z/u or w/u, since $u_{zz} = (cu_z - w)/\varepsilon$ and $w_z = -cw + \beta\left(\frac{wu_z}{u}\right)$ (2.6). Using (2.8), the limits of $\mathcal{A}_{m,\varepsilon}$, $\mathcal{B}_{m,\varepsilon}$, $\mathcal{C}_{m,\varepsilon}$ and $\mathcal{D}_{m,\varepsilon}$ as $z \to \pm\infty$ are

$$\mathcal{A}^+_{m,\varepsilon} := -\lambda^2, \qquad \mathcal{B}^+_{m,\varepsilon} := 2c\lambda, \qquad \mathcal{C}^+_{m,\varepsilon} := -c^2+\lambda(1+\varepsilon), \qquad \mathcal{D}^+_{m,\varepsilon} := -c(1+\varepsilon),$$

and

$$\begin{aligned}
\mathcal{A}^-_{m,\varepsilon} &= \frac{c^4 m(\beta+m)}{(\beta+m-1)^3} - \lambda^2 - \frac{c^2\lambda m(\beta+m-2)}{(\beta+m-1)^2} - \varepsilon\left(\frac{\lambda c^2 m}{(\beta+m-1)^2} - \frac{c^4 m(\beta+m)}{(\beta+m-1)^4}\right)\\
\mathcal{B}^-_{m,\varepsilon} &= \frac{c\lambda(\beta-2)}{(\beta+m-1)} - \frac{c^3(\beta+m(\beta+m+2))}{(\beta+m-1)^2} + \varepsilon\frac{c^3(m+1)(\beta+m)}{(\beta+m-1)^3},\\
\mathcal{C}^-_{m,\varepsilon} &= \left(\frac{c^2(\beta+2m+1)}{\beta+m-1} + \lambda\right) + \varepsilon\left(\frac{\beta c^2}{(\beta+m-1)^2} + \lambda\right),\\
\mathcal{D}^-_{m,\varepsilon} &= -c + \varepsilon\frac{c(m+1)}{\beta+m-1}\,.
\end{aligned} \tag{2.59}$$

We define the asymptotic matrices $M^{\pm}_{m,\varepsilon}(\lambda) := \lim_{z\to\pm\infty} M^m_\varepsilon(z,\lambda)$. That is,

$$M^{\pm}_{m,\varepsilon}(\lambda) = \begin{pmatrix} 0 & 1 & 0 & 0\\ 0 & 0 & 1 & 0\\ 0 & 0 & 0 & 1\\ \mathcal{A}^{\pm}_{m,\varepsilon}/\varepsilon & \mathcal{B}^{\pm}_{m,\varepsilon}/\varepsilon & \mathcal{C}^{\pm}_{m,\varepsilon}/\varepsilon & \mathcal{D}^{\pm}_{m,\varepsilon}/\varepsilon \end{pmatrix}. \tag{2.60}$$

2.6.2 Proof of Theorem 2.3.3 for $0 \le m \le 1$ and $0 < \varepsilon \ll 1$

The matrices $M^{\pm}_{m,\varepsilon}$ have four spatial eigenvalues, while $M^{\pm}_m$ have only three. We show that the fourth spatial eigenvalue is far into the left half plane for both asymptotic matrices $M^{\pm}_{m,\varepsilon}$ (and for $|\lambda| = \mathcal{O}(1)$), while the other three spatial eigenvalues are, to leading order, given by the spatial eigenvalues of $M^{\pm}_m$.

The characteristic polynomial of $M^+_{m,\varepsilon}$ is

$$\varepsilon\left(\mu^4 + c\mu^3 - \lambda\mu^2\right) + (\mu^2 + c\mu - \lambda)(c\mu - \lambda) = 0, \tag{2.61}$$

which is regular in λ, but singularly perturbed in μ. In the limit $\varepsilon \to 0$, we recover the characteristic polynomial of M^+_m. The dispersion relations of $M^+_{m,\varepsilon} + \nu_+ I$ are

$$\lambda = -k^2 - \nu_+(c-\nu_+) + i(ck - 2k\nu_+)\,, \quad \lambda = -\varepsilon k^2 - \nu_+(c-\nu_+\varepsilon) + i(ck - 2\varepsilon k\nu_+). \tag{2.62}$$

For $\nu_+ \in (0,c)$, (2.62) is fully contained in the open left half plane and the ideal weight is still $\nu^*_+ = c/2$. Observe that, unlike the $\varepsilon = 0$ case, both dispersion relations of $M^{m,+}_\varepsilon + \nu_+ I$ are parabolas in k and consequently they no longer approach a vertical line in the limit $|k| \to \infty$.

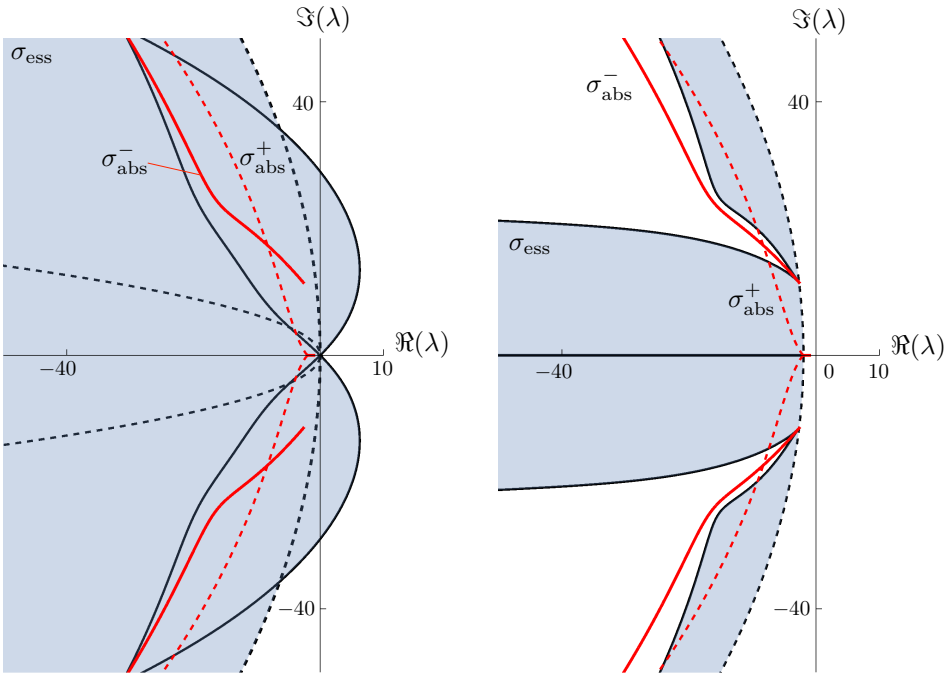

Figure 2.6.1: The essential and absolute spectrum in the unweighted space (left panel) and in the ideally weighted space (right panel) for $\beta = 1.3 < \beta_{\text{crit}}$ (2.17), $c = 2$, $\varepsilon = 0.02$ and $m = 0$, where the ideal weight is $\nu_-^* \approx -2.447$ and $\nu_+^* = c/2 = 1$. The dispersion relations of $M^+_{m,\varepsilon} + \nu_+ I$ (2.62) are shown as black dashed lines, while those of $M^-_{m,\varepsilon} + \nu_- I$ are shown as black solid lines, σ^+_{abs} is shown as red dashed lines and σ^-_{abs} as red solid lines. The shaded regions are the interior of the (weighted) essential spectrum. Observe that the (weighted) essential spectra and absolute spectra agree, to leading order, for $|\lambda| = \mathcal{O}(1)$, but not for $|\lambda|$ large, to the spectra for the same parameter set but with $\varepsilon = 0$, see Figure 2.4.6. Also note that the ideal weights are similar.

The spatial eigenvalues of (2.61) are

$$\begin{aligned}
\mu_1^+ &= \frac{-c + \sqrt{c^2 + 4\varepsilon\lambda}}{2\varepsilon} = \frac{\lambda}{c} - \frac{\lambda^2\varepsilon}{c^3} + \mathcal{O}(\varepsilon^2), \\
\mu_{2,3}^+ &= \frac{-c \pm \sqrt{c^2 + 4\lambda}}{2}, \\
\mu_4^+ &= \frac{-c - \sqrt{c^2 + 4\varepsilon\lambda}}{2\varepsilon} = -\frac{c}{\varepsilon} - \frac{\lambda}{c} + \frac{\lambda^2\varepsilon}{c^3} + \mathcal{O}(\varepsilon^2),
\end{aligned}$$

where the asymptotic expansions only hold for $|\lambda| = \mathcal{O}(1)$. The spatial eigenvalues $\mu^+_{1,2,3}$ are, to leading order, the same as those in the $\varepsilon = 0$ case (2.25). The singular spatial eigenvalue μ_4^+ approaches $-\infty$ as $\varepsilon \to 0$ (for $|\lambda| = \mathcal{O}(1)$).

The characteristic polynomial of $M^-_{m,\varepsilon}$ is

$$\mu^2\left(-\frac{c^2(\beta+2m+1)}{\beta+m-1}-\lambda\right)+\frac{\mu\left(c^3(\beta+m(\beta+m+2))-(\beta-2)c\lambda(\beta+m-1)\right)}{(\beta+m-1)^2}$$
$$+\frac{c^2\lambda m(\beta+m-2)}{(\beta+m-1)^2}-\frac{c^4m(\beta+m)}{(\beta+m-1)^3}+c\mu^3+\lambda^2+\varepsilon\Bigg(\frac{c^3\mu(m+1)(\beta+m)}{(\beta+m-1)^3}$$
$$+\mu^2\left(-\frac{\beta c^2}{(\beta+m-1)^2}-\lambda\right)+\frac{c^2m\left(\lambda(\beta+m-1)^2-c^2(\beta+m)\right)}{(\beta+m-1)^4}$$
$$-\frac{c\mu^3(m+1)}{\beta+m-1}+\mu^4\Bigg). \tag{2.63}$$

which is still regular in λ, but singularly perturbed in μ. In the limit $\varepsilon\to 0$, we recover the characteristic polynomial of M^-_m

$$c\mu^3-\mu^2\left(\frac{c^2(\beta+2m+1)}{\beta+m-1}+\lambda\right)+\mu\left(\frac{c^3(\beta+m(r+2))}{(\beta+m-1)^2}-\frac{(\beta-2)c\lambda}{(\beta+m-1)}\right)$$
$$-\frac{c^4m(\beta+m)}{(\beta+m-1)^3}+\frac{c^2\lambda m(\beta+m-2)}{(\beta+m-1)^2}+\lambda^2=0,$$

and three of the spatial eigenvalues of $M^-_{m,\varepsilon}$ are, to leading order, thus given by the spatial eigenvalues of M^-_m for $|\lambda|=\mathcal{O}(1)$. We use the expansion $\mu=\eta_{-1}/\varepsilon+\eta_0+\mathcal{O}(\varepsilon)$ to determine the leading order contribution of the singular spatial eigenvalue of $M^-_{m,\varepsilon}$. Substituting this expansion into (2.63) gives, to leading order, $\eta_{-1}^3(\eta_{-1}+c)=0$. The singular spatial eigenvalue of $M^-_{m,\varepsilon}$ is $\mu_4^-=-c/\varepsilon+\mathcal{O}(1)$ (for $|\lambda|=\mathcal{O}(1)$). In particular, both singular spatial eigenvalues are to leading order the same and approach $-\infty$ as $\varepsilon\to 0$.

For $|\lambda|=\mathcal{O}(1)$, the (weighted) dispersion relations of $M^\pm_{m,\varepsilon}$ are $\mathcal{O}(\varepsilon)$ perturbations of those from $M^\pm_m$, since $\mu^\pm_{1,2,3}$ are, to leading order, the same as those in the $\varepsilon=0$ case. Furthermore, the singular spatial eigenvalues $\mu_4^\pm$ have asymptotically large negative real parts (for $|\lambda|=\mathcal{O}(1)$) and thus do not affect the dispersion relations or Morse indices. Moreover, the characteristic polynomials of $M^\pm_{m,\varepsilon}$ are regularly perturbed in λ. Consequently, the Morse indices $i_\pm$ and the interior of the essential spectrum are unaffected by the singular spatial eigenvalues $\mu_4^\pm$. Similarly, since $\mu_4^\pm$ also does not affect the ranking of $\mu^\pm_{1,2,3}$, the absolute spectrum is, to leading order, the same as for the $\varepsilon=0$ case. In particular, the branch points $\lambda^\pm_{br}$ are, to leading order, the same as those for the $\varepsilon=0$ case and there is some parameter $\beta^m_{\text{crit}}(\varepsilon)$, given to leading order by β^m_{crit}, such that the branch points, and therefore the absolute spectrum, are contained in the open left half plane for $1-m<\beta<\beta^m_{\text{crit}}(\varepsilon)$.

The above asymptotic analysis is only valid for $|\lambda|=\mathcal{O}(1)$, since the singular spatial eigenvalues $\mu_4^\pm$ become $\mathcal{O}(1)$ for $|\lambda|$ large. However, we show, using asymptotic analysis

that, to leading order, there are no additional intersections between the dispersion relations of $M^{\pm}_{m,\varepsilon} + \nu_{\pm} I$ and the imaginary axis for $|\lambda|$ large as long as $\nu_- > -\frac{c(\beta+m)}{\beta+m-1}$. This condition arises from the asymptotic limits of the weighted dispersion relations $M^-_m + \nu_- I$ (see (2.35) for the analogous condition for $m = 0$).

Lemma 2.6.1. *Let $\nu_- > -\frac{c(\beta+m)}{\beta+m-1}$ and $|\lambda| = \Theta(\varepsilon^{-\zeta})$ with[1] $\zeta > 0$. There are no intersections between the dispersion relations of $M^-_m + \nu_- I$ and the imaginary axis.*[2]

Proof. We show that there are no intersections between $M^-_m + \nu_- I$ and the imaginary axis by considering all possible rescalings of λ and k larger than $\Theta(1)$. That is, we take the dispersion relations of $M^-_m + \nu_- I$ and set $\lambda = \varepsilon^{-\zeta}\tilde{\lambda}$ and $k = \varepsilon^{-\theta}\tilde{k}$ where $|\tilde{\lambda}| = \Theta(1)$, $\tilde{k} = \Theta(1)$, $\tilde{k} \neq 0$ and $\zeta, \theta > 0$. This results in the rescaled weighted dispersion relations,

$$
\begin{aligned}
&\frac{c\left(-\nu + ik\varepsilon^{-\theta}\right)\left(c^2\left(\beta + m^2 + (\beta+2)m\right) - (\beta-2)\lambda\varepsilon^{-\zeta}(\beta+m-1)\right)}{(\beta+m-1)^2} \\
&- \frac{\left(-\nu + ik\varepsilon^{-\theta}\right)^2\left(c^2(\beta+2m+1) + \lambda\varepsilon^{-\zeta}(\beta+m-1)\right)}{\beta+m-1} \\
&+ \frac{-c^4 m(\beta+m) + c^2\lambda m\varepsilon^{-\zeta}\left(\beta^2 - 3\beta + m^2 + (2\beta-3)m + 2\right) + \lambda^2\varepsilon^{-2\zeta}(\beta+m-1)^3}{(\beta+m-1)^3} \\
&+ \varepsilon\left(\frac{c^3(m+1)(\beta+m)\left(-\nu + ik\varepsilon^{-\theta}\right)}{(\beta+m-1)^3} - \frac{\left(-\nu + ik\varepsilon^{-\theta}\right)^2\left(\beta c^2 + \lambda\varepsilon^{-\zeta}(\beta+m-1)^2\right)}{(\beta+m-1)^2}\right. \\
&\left.+ \frac{c^2\lambda m\varepsilon^{-\zeta}(\beta+m-1)^2 - c^4 m(\beta+m)}{(\beta+m-1)^4} - \frac{c(m+1)\left(-\nu + ik\varepsilon^{-\theta}\right)^3}{\beta+m-1} + \left(-\nu + ik\varepsilon^{-\theta}\right)^4\right) \\
&+ c\left(-\nu + ik\varepsilon^{-\theta}\right)^3 = 0
\end{aligned}
\tag{2.64}
$$

We now consider the leading order terms of the rescaled weighted dispersion relations. To determine viable values of ζ and θ we use the method of dominant balance, see for example [6]. We find that there are three different cases, (i) $0 < \theta < 1$, (ii) $\theta = 1$ and (iii) $\theta > 1$, that lead to three different dominant balances. Depending on the values of ζ, θ the leading order term is $\mathcal{O}(\varepsilon^{1-4\theta})$, $\mathcal{O}(\varepsilon^{-3\theta})$, and/or $\mathcal{O}(\varepsilon^{-\zeta-2\theta})$. We consider the dominant balance between the leading order terms in each of the three cases and show that for these balances that the leading order terms of the rescaled weighted dispersion relations are never purely imaginary.

(i) For $0 < \theta < 1$ the leading order terms of (2.64) are $\mathcal{O}(\varepsilon^{-3\theta})$ and $\mathcal{O}(\varepsilon^{-\zeta-2\theta})$ with the dominant balance $-3\theta = -\zeta - 2\theta$. This balance implies $\zeta = \theta$ and that this dominant balance is valid for $0 < \zeta, \theta < 1$. The leading order term of (2.64) gives $\tilde{\lambda}$ as purely imaginary and thus to find the leading order term of the real component

[1] The expression $|\lambda| = \Theta(\varepsilon^{-\zeta})$ is also often written as $|\lambda| = \mathcal{O}_s(\varepsilon^{-\zeta})$ and denotes 'strict order', *i.e.* $|\lambda| = \mathcal{O}(\varepsilon^{-\zeta})$ and $\varepsilon^{-\zeta} = \mathcal{O}(|\lambda|)$.

[2] The technical details of the proof of this lemma were omitted from [10].

of $\tilde{\lambda}$ we must consider the next order term. This in turn leads us to three subcases, $0 < \theta < \frac{1}{2}$, $\theta = \frac{1}{2}$, $\frac{1}{2} < \theta < 1$.
When $0 < \theta < 1/2$ (and $\zeta = \theta$), the next order term is $\mathcal{O}(\varepsilon^{-2\theta})$. The weighted dispersion relations (2.64), with $\theta = \zeta$, to $\mathcal{O}(\varepsilon^{-2\theta})$, are then

$$\varepsilon^{-3\theta}(\tilde{\lambda}\tilde{k}^2 - ic\tilde{k}^3) + \varepsilon^{-2\theta}\left(\frac{c^2\tilde{k}^2(\beta+2m+1) + c\tilde{k}(3\tilde{k}\nu(\beta+m-1)}{\beta+m-1}\right.$$
$$\left. - \frac{i(\beta-2)\tilde{\lambda}) + \tilde{\lambda}(\beta+m-1)(\tilde{\lambda}+2i\tilde{k}\nu)}{\beta+m-1}\right) + \mathcal{O}(\varepsilon^{-2\theta}) = 0,$$

which, after solving explicitly for $\tilde{\lambda}$ gives, to $\mathcal{O}(\varepsilon^{\theta})$,

$$\lambda = -k^2\varepsilon^{-\theta} - \frac{ik(c(m+1)+2\nu(\beta+m-1))}{\beta+m-1} + \mathcal{O}(\varepsilon^{\theta}),$$
$$\lambda = ick - \frac{c(c(\beta+m)+\nu(\beta+m-1))}{\beta+m-1}\varepsilon^{\theta} + \mathcal{O}(\varepsilon^{2\theta}),$$

which, have negative real part, to leading order, when $\nu_- > -\frac{c(\beta+m)}{\beta+m-1}$.
When $\theta = \zeta = \frac{1}{2}$, the leading order terms $\mathcal{O}(\varepsilon^{-3\theta})$ and $\mathcal{O}(\varepsilon^{-\zeta-2\theta})$ are of $\mathcal{O}(\varepsilon^{-3/2})$ and the next order terms are those of order $\mathcal{O}(\varepsilon^{1-4\theta})$, $\mathcal{O}(\varepsilon^{-2\theta})$, $\mathcal{O}(\varepsilon^{-\zeta-2\theta})$ and $\mathcal{O}(\varepsilon^{-2\zeta})$, which are all of $\mathcal{O}(\varepsilon^{-1})$. The dispersion relations (2.64) to $\mathcal{O}(\varepsilon^{-1})$ are

$$\varepsilon^{-3/2}(\tilde{\lambda}\tilde{k}^2 - ic\tilde{k}^3) + \left(\frac{c^2k^2(\beta+2m+1) - ick(\beta-2)\tilde{\lambda}}{\beta+m-1} + \tilde{\lambda}^2 + k^4\right.$$
$$\left. +3ck^2\nu + 2i\tilde{\lambda}k\nu\right)\varepsilon^{-1} + \mathcal{O}(\varepsilon^{-1/2}) = 0$$

which, after solving explicitly for $\tilde{\lambda}$ gives, to $\mathcal{O}(\varepsilon^{\theta})$,

$$\lambda = -\tilde{k}^2\varepsilon^{-\frac{1}{2}} - \frac{i\tilde{k}(c(m+1)+2\nu(\beta+m-1))}{\beta+m-1} + \mathcal{O}(\varepsilon^{\frac{1}{2}}),$$
$$\lambda = ic\tilde{k} - \sqrt{\varepsilon}\left(\frac{c^2(\beta+m)}{\beta+m-1} + \left(c\nu + \tilde{k}^2\right)\right) + \mathcal{O}(\varepsilon)$$

which, have negative real part, to leading order, when $\nu_- > -\frac{c(\beta+m)}{\beta+m-1}$.
When $\frac{1}{2} < \theta < 1$, the next order terms are those of $\mathcal{O}(\varepsilon^{1-4\theta})$, however, to this order the dispersion relations (2.64) gives $\varepsilon^{-3\theta}(\tilde{\lambda}\tilde{k}^2 - ic\tilde{k}^3) + \varepsilon^{1-4\theta}\tilde{k}^4 = 0$ which implies the second dispersion relation is $\tilde{k} = 0$. Thus, we take (2.64) to $\mathcal{O}(\varepsilon^{-2\theta})$,

$$\varepsilon^{-3\theta}(\tilde{\lambda}\tilde{k}^2 - ic\tilde{k}^3) + \varepsilon^{1-4\theta}\tilde{k}^4 + \varepsilon^{-2\theta}\left(\frac{c^2\tilde{k}^2(\beta+2m+1) - i(\beta-2)c\tilde{k}\tilde{\lambda}}{\beta+m-1}\right.$$
$$\left. +3c\tilde{k}^2\nu + 2i\tilde{k}\tilde{\lambda}\nu + \tilde{\lambda}^2\right) + \mathcal{O}(\varepsilon^{1-3\theta}) = 0,$$

which, after solving explicitly for $\tilde{\lambda}$ gives, to $\mathcal{O}(\varepsilon^{1-\theta})$,

$$\lambda = -\tilde{k}^2\varepsilon^{-\theta} - \frac{i\tilde{k}(c(m+1)+2\nu(\beta+m-1))}{\beta+m-1} + \mathcal{O}(\varepsilon^{1-\theta}),$$
$$\lambda = ic\tilde{k} - \tilde{k}^2\varepsilon^{\theta} + \mathcal{O}(\varepsilon^{1-\theta}),$$

which, have negative real part, to leading order, when $\nu_- > -\frac{c(\beta+m)}{\beta+m-1}$.

(ii) For $\theta = 1$ the leading order terms are of $\mathcal{O}(\varepsilon^{1-4\theta})$ and $\mathcal{O}(\varepsilon^{-3\theta})$ with the dominant balance $1-4\theta = -3\theta$. This dominant balance holds for $\zeta \leq 1$. However, if $\zeta < 1$ the leading order term of (2.64) is $\tilde{k}^4 - ic\tilde{k}^3 = 0$ implying $\tilde{k} = 0$ to leading order, independent of $\tilde{\lambda}$. Therefore, if $\theta = 1$ we must also have $\zeta = 1$. For $\theta = \zeta = 1$, the leading order term of (2.64) is $-ic\tilde{k}^3 + \tilde{k}^4 + \tilde{\lambda}\tilde{k}^2 = 0$ which implies $\tilde{\lambda} = -\tilde{k^2} + ic\tilde{k}$ which is always in the left half plane, independent of the weight.

(iii) For $\theta > 1$ the leading order terms are of $\mathcal{O}(\varepsilon^{1-4\theta})$ and $\mathcal{O}(\varepsilon^{-\zeta-2\theta})$ with the dominant balance $-\zeta-2\theta$. This implies $\zeta = 2\theta-1$ and the dominant balance holds for $\zeta, \theta > 1$. The leading order term of (2.64) is then $\tilde{k}^2\left(\tilde{k}^2 + \tilde{\lambda}\right) = 0$ and $\tilde{\lambda} = -\tilde{k}^2$, to leading order, and is thus contained in the open left half plane independent of ν_-.

□

As the dispersion relations do not intersect the imaginary axis for large $|\lambda|$, the essential spectrum, and therefore the absolute spectrum, does not enter into the right half plane, except in the region $|\lambda| = \mathcal{O}(1)$. See Figure 2.6.1 for an example of the spectral picture in the case $\varepsilon \neq 0$. This concludes the complete proof of Theorem 2.3.3.

2.7 Point Spectrum

In this section we prove that the origin persists as an element of the point spectrum with algebraic multiplicity two for travelling wave solutions to (2.2) with $0 \leq m < 1$ and $0 \leq \varepsilon \ll 1$. This is done by explicitly solving the associated (generalised) eigenvalue problem and analysing the asymptotic behaviour of the (generalised) eigenfunctions. In §2.7.1, we study the eigenvalue problem by first computing the eigenfunction of the origin associated with the translation invariance of (2.2). Next, we compute a generalised eigenfunction, which is due to the existence of a family of travelling wave solutions under varying the wave speed c. By analysing the asymptotic behaviour of the (generalised) eigenfunctions we prove that they are contained in the range of exponentially weighted function spaces for which the essential spectrum is stable. This concludes the spectral stability of travelling wave solutions to (2.2) in these weighted function spaces. In §2.7.4 we extend the analysis to the $m = 1$ case. In this case, we cannot conclude spectral stability as there is no spectral gap in any exponentially weighted function space. However, nonlinear (in)stability results have been obtained in certain cases for Keller-Segel models with linear consumption rate

[70, 71, 77]. We include the $m = 1$ case for completeness and to highlight how and why the spectral gap vanishes in the $m \to 1$ limit. We begin this section with a brief summary of the relevant results regarding the essential and absolute spectrum.

Throughout this section we refer to the travelling wave solutions $(u(z), w(z))$ to (2.6) as $(u_\varepsilon^m, w_\varepsilon^m)$ with subscripts and superscripts explicitly denoting the dependence on ε and m respectively. Furthermore, observe that the relationship between w_0^m and u_0^m shown in (2.7) also holds for $\varepsilon \neq 0$. That is, $w_\varepsilon^m(z) = e^{-cz}\left(u_\varepsilon^m(z)\right)^\beta$ [28].

We again consider the linear operator $\mathcal{L}_\varepsilon^m : \mathbb{H}^1(\mathbb{R}) \times \mathbb{H}^1(\mathbb{R}) \to \mathbb{H}^1(\mathbb{R}) \times \mathbb{H}^1(\mathbb{R})$ and the associated eigenvalue problem (2.11), restated here for convenience

$$\mathcal{L}_\varepsilon^m \begin{pmatrix} p \\ q \end{pmatrix} = \lambda \begin{pmatrix} p \\ q \end{pmatrix}, \qquad \mathcal{L}_\varepsilon^m := \begin{pmatrix} \mathcal{L}_{11} & \mathcal{L}_{12} \\ \mathcal{L}_{21} & \mathcal{L}_{22}. \end{pmatrix}.$$

The entries of $\mathcal{L}_\varepsilon^m$ are

$$\begin{aligned}
\mathcal{L}_{11} &:= \varepsilon\frac{\partial^2}{\partial z^2} + c\frac{\partial}{\partial z} - mwu^{m-1}, \\
\mathcal{L}_{12} &:= -u^m, \\
\mathcal{L}_{21} &:= \beta\left(\frac{w_z u_z}{u^2} + \frac{wu_{zz}}{u^2} - \frac{2wu_z^2}{u^3}\right) + \beta\left(\frac{2wu_z}{u^2} - \frac{w_z}{u}\right)\frac{\partial}{\partial z} - \frac{\beta w}{u}\frac{\partial^2}{\partial z^2}, \\
\mathcal{L}_{22} &:= \beta\left(\frac{u_z^2}{u^2} - \frac{u_{zz}}{u}\right) + \left(c - \frac{\beta u_z}{u}\right)\frac{\partial}{\partial z} + \frac{\partial^2}{\partial z^2},
\end{aligned}$$

where we have dropped the ε subscripts and m superscripts from $(u_\varepsilon^m, w_\varepsilon^m)$ for convenience.

The spectrum of an operator consists of values of $\lambda \in \mathbb{C}$ such that the inverse of the eigenvalue operator $\mathcal{L} - \lambda I$ does not exist or is unbounded. Recall Definition 2.7.1,

Definition 2.7.1. *([54] Definition 2.2.3) For a closed linear operator $\mathcal{L} : \mathcal{D}(\mathcal{L}) \subset X \to X$, where X is a Banach space and $\mathcal{D}(\mathcal{L})$ is dense in X, the spectrum is decomposed into two sets:*

(a) The essential spectrum σ_{ess} of the operator $\mathcal{L}$ is the set of all $\lambda \in \mathbb{C}$ such that
- *$\mathcal{L} - \lambda I$ is not Fredholm or,*
- *$\mathcal{L} - \lambda I$ is Fredholm with a non zero Fredholm index,*

where the Fredholm index of $\mathcal{L}$ is

$$ind(\mathcal{L}) = dim(ker(\mathcal{L})) - codim(range(\mathcal{L})).$$

(b) The point spectrum of the operator $\mathcal{L}$ is the set of all $\lambda \in \mathbb{C}$ such that the operator $\mathcal{L} - \lambda I$ is Fredholm with index zero, but the operator is not invertible. That is,

$$\sigma_{\text{pt}} = \left\{\lambda \in \mathbb{C} : ind(\mathcal{L} - \lambda I) = 0,\ but\ (\mathcal{L} - \lambda I)^{-1}\ does\ not\ exist\right\}.$$

As in [54], we use the term *eigenvalue* to refer to all values λ in the spectrum of the operator whereas *point spectrum* refers to isolated eigenvalues of finite multiplicity. Eigenvalues which have eigenfunctions that decay to zero as $z \to \pm\infty$ may be embedded in the essential spectrum and are thus not considered point spectra.

Throughout this section we will also consider the fourth order ODE associated with the eigenvalue problem, (2.57),

$$\varepsilon p_{zzzz} - \mathcal{D}_{m,\varepsilon} p_{zzz} - \mathcal{C}_{m,\varepsilon} p_{zz} - \mathcal{B}_{m,\varepsilon} p_z - \mathcal{A}_{m,\varepsilon} p = 0.$$

The essential spectrum of the operator $\mathcal{L}$ in (2.36) depends on the asymptotic behaviour of the operator. In particular, it depends on the magnitude and signs of the spatial eigenvalues of the asymptotic states as $z \to \pm\infty$. These spatial eigenvalues are found as the roots of the following equations

$$\begin{aligned} \varepsilon(\mu^+)^4 - \mathcal{D}^+_{m,\varepsilon}(\mu^+)^3 - \mathcal{C}^+_{m,\varepsilon}(\mu^+)^2 - \mathcal{B}^+_{m,\varepsilon}(\mu^+) - \mathcal{A}^+_{m,\varepsilon} = 0, \\ \varepsilon(\mu^-)^4 - \mathcal{D}^-_{m,\varepsilon}(\mu^-)^3 - \mathcal{C}^-_{m,\varepsilon}(\mu^-)^2 - \mathcal{B}^-_{m,\varepsilon}(\mu^-) - \mathcal{A}^-_{m,\varepsilon} = 0, \end{aligned} \tag{2.65}$$

where $\mathcal{A}^\pm_{m,\varepsilon}$, $\mathcal{B}^\pm_{m,\varepsilon}$, $\mathcal{C}^\pm_{m,\varepsilon}$ and $\mathcal{D}^\pm_{m,\varepsilon}$ respectively denote the limits of $\mathcal{A}_{m,\varepsilon}$, $\mathcal{B}_{m,\varepsilon}$, $\mathcal{C}_{m,\varepsilon}$ and $\mathcal{D}_{m,\varepsilon}$ as $z \to \pm\infty$. Observe that the expressions (2.65) are exactly the characteristic equations of (2.57) in the limit $z \to \pm\infty$. The essential spectrum consists of values $\lambda \in \mathbb{C}$ such that any of the spatial eigenvalues $\mu^\pm$ are purely imaginary or the number of unstable spatial eigenvalues at $\pm\infty$ differ. This is equivalent to Definition 2.7.1 [54].

All travelling wave solutions to (2.5) have essential spectra in the right half plane for perturbations in $\mathbb{H}^1(\mathbb{R})$ [10, 80]. Thus, we follow the usual procedure outlined in [54] and introduce the weighted function space $\mathbb{H}^1_\nu(\mathbb{R})$ defined by the norm

$$\|p\|_{\mathbb{H}^1_\nu} = \|e^{\nu z} p\|_{\mathbb{H}^1} = \|\tilde{p}\|_{\mathbb{H}^1}, \tag{2.66}$$

where $\tilde{p} := e^{\nu z} p$. So, $p \in \mathbb{H}^1_\nu$ if and only if $\tilde{p} \in \mathbb{H}^1$. We define $\mathbb{L}^2_\nu$ similarly. It was shown in previous sections that a two-sided weight is required for the current problem. That is,

$$\nu = \begin{cases} \nu_- \text{ if } & z \leq 0, \\ \nu_+ \text{ if } & z > 0, \end{cases} \tag{2.67}$$

which forces the perturbation to decay exponentially in both directions. Using a weighted function space has the effect of shifting the essential spectrum. In particular, in the weighted function space we consider the spatial eigenvalues are $\mu^+ + \nu_+$ and $\mu^- + \nu_-$ as $z \to \pm\infty$ respectively. In other words, the weighted essential spectrum consists of values $\lambda \in \mathbb{C}$ such that any of the spatial eigenvalues $\mu^\pm + \nu_\pm$ are purely imaginary or the number of weighted unstable spatial eigenvalues at $\pm\infty$ differ.

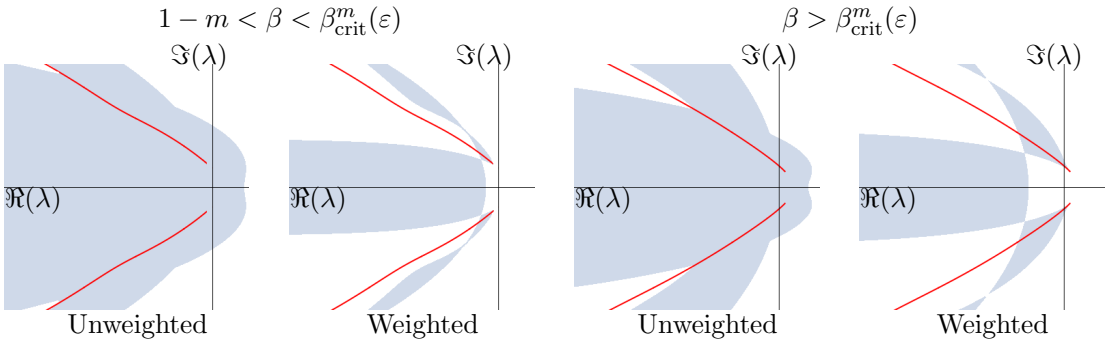

Figure 2.7.1: A schematic of the typical weighted and unweighted essential spectra (blue regions) associated with travelling wave solutions $(u_\varepsilon^m, w_\varepsilon^m)$ of (2.2). The red curves indicate the subset of the absolute spectrum that determines how far the essential spectrum can be shifted by weighting the function space. For $1-m<\beta<\beta^m_{\text{crit}}(\varepsilon)$ the absolute spectrum is contained in the left half plant and a two-sided weight exists such that the weighted essential spectrum is contained in the open left half plane.

Recall the result from Theorem 2.3.3; all travelling wave solutions $(u_\varepsilon^m(z), w_\varepsilon^m(z))$ are absolutely unstable for $\beta>\beta^m_{\text{crit}}(\varepsilon)$, precluding the possibility of spectral stability. Thus, we focus on the parameter regime that is potentially transiently unstable, *i.e.* $1-m<\beta<\beta^m_{\text{crit}}(\varepsilon)$ in the remainder of this chapter. To be able to conclude transient instability, *i.e.* spectral stability in an exponentially weighted function space [88], we must show that for the weights that shift the essential spectrum into the left half plane, there are no values λ in the point spectrum with $\Re(\lambda)\geq 0$ other than for $\lambda=0$. The location of the point spectrum does not change upon moving to a weighted space [54], however, it is necessary to show that the eigenfunctions associated with the point spectrum are contained in these weighted function spaces. See Figure 2.7.1.

2.7.1 Locating the point spectrum

Locating the point spectrum amounts to finding nontrivial solutions $(p,q)^T$ to (2.36) that decay to zero as $z\to\pm\infty$ for some $\lambda\in\mathbb{C}\backslash\sigma_{\text{ess}}$. While $\lambda=0$ is in the essential spectrum in the unweighted space for all m it is not in the weighted function space for a range of weights when $0\leq m<1$ [10, 35], see also Figure 2.7.1. It was shown in [35] that $\lambda=0$ is a root of order two of the Evans function for travelling solutions to (2.2) with $\varepsilon=m=0$. Thus, in these appropriately weighted function spaces $\lambda=0$ is an isolated eigenvalue associated to the invariances of the problem. Hence, $\lambda=0$ is part of the point spectrum. We show that the eigenvalue $\lambda=0$ persists with multiplicity two for $0\leq m<1$ by determining two linearly independent eigenfunctions that form the generalised eigenspace. In the singular limit $\varepsilon\to 0$, these functions and their norms are

explicitly computed. We also show these eigenfunctions persist for sufficiently small $\varepsilon > 0$ and are contained in the weighted function spaces that have stable essential spectrum.[3]

2.7.2 The generalised eigenspace at $\lambda = 0$

In order to obtain the eigenfunction, we first differentiate (2.6) with respect to z and obtain

$$\begin{aligned}
0 &= \varepsilon u_{zzz} + c u_{zz} - w_z u^m - m w u^{m-1} u_z = \mathcal{L}_{11} u_z + \mathcal{L}_{12} w_z, \\
0 &= w_{zzz} + c w_{zz} - \beta(\frac{w_z u_z}{u})_z - \beta(\frac{w u_{zz}}{u})_z + (\beta \frac{w u_z^2}{u^2})_z = \mathcal{L}_{21} u_z + \mathcal{L}_{22} w_z,
\end{aligned}$$

which is equivalent to

$$0 = \mathcal{L} \begin{pmatrix} u_z(z) \\ w_z(z), \end{pmatrix}$$

where we have omitted the ε subscripts and m superscripts. Hence $((u_\varepsilon^m)_z, (w_\varepsilon^m)_z)$ solves the linearised eigenvalue problem (2.36) for $\lambda = 0$, and $\lambda = 0$ is thus an eigenvalue with associated eigenfunction $((u_\varepsilon^m)_z, (w_\varepsilon^m)_z)$. This is typical for travelling wave solutions and arises from the translation invariance of solutions in the moving frame z.

If we instead differentiate (2.6) with respect to the wave speed c, we obtain

$$\begin{aligned}
0 &= \varepsilon u_{zzc} + u_z + c u_{zc} - w_c u^m - m w u^{m-1} u_c \\
&= \mathcal{L}_{11} u_c + \mathcal{L}_{12} w_c + u_z, \\
0 &= w_{zzc} + w_z + c w_{zc} - \beta \left(\frac{w_z u_z}{u} \right)_c - \beta \left(\frac{w u_{zz}}{u} \right)_c + \beta \left(\frac{w u_z^2}{u^2} \right)_c \\
&= \mathcal{L}_{21} u_c + \mathcal{L}_{22} w_c + w_z,
\end{aligned}$$

which is equivalent to

$$\mathcal{L} \begin{pmatrix} u_c(z) \\ w_c(z) \end{pmatrix} = - \begin{pmatrix} u_z(z) \\ w_z(z) \end{pmatrix}.$$

Hence $((u_\varepsilon^m)_c, (w_\varepsilon^m)_c)$ is a generalised eigenfunction of (2.36) for $\lambda = 0$ and $\lambda = 0$ has algebraic multiplicity at least two and a geometric multiplicity of at least two. It was shown in [35] that $\lambda = 0$ is a second order root of the Evans function and thus the algebraic and geometric multiplicity are each precisely two.

[3] The formulation of the (generalised) eigenfunctions, eigenspace and analysis of the asymptotic behaviour of these functions remains valid when $\beta > \beta_{\text{crit}}^m(\varepsilon)$.

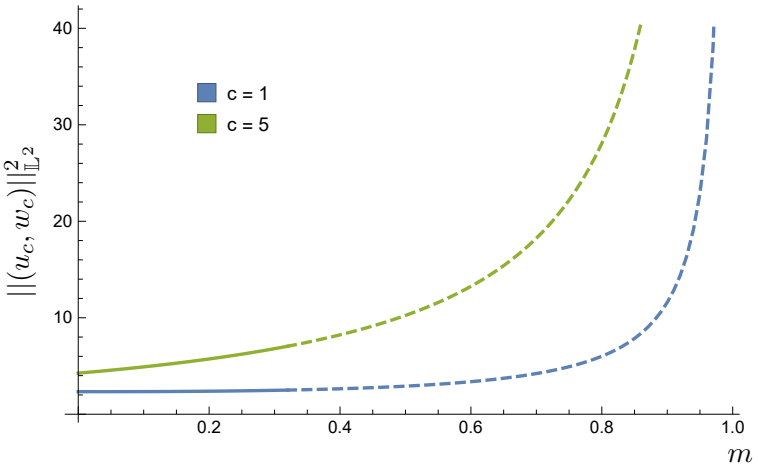

Figure 2.7.2: The $\mathbb{L}_2$ norm squared of the generalised eigenfunction for $\varepsilon = 0$, *i.e.* $||((u_m^0)_c, (w_m^0)_c||^2_{\mathbb{L}^2}$, is shown for $\beta = 1.1$ over varying values of m and two different wave speeds c. The solid curves represent m values such that $1 - m < \beta < \beta^m_{\text{crit}}(0)$ and the dashed line represent values such that $\beta > \beta^m_{\text{crit}}(0)$. Observe that both squared norms have an asymptote at $m = 1$.

For ε small we can explicitly compute the leading order (generalised) eigenfunctions from (2.7). In particular,

$$\begin{aligned}
(u_0^m)_z(z) &= \frac{1}{c} e^{-cz} (u_0^m)^{\beta+m}, \\
(w_0^m)_z(z) &= -ce^{-cz} (u_0^m)^{\beta} + \beta e^{-cz} (u_0^m)^{\beta-1} (u_0^m)_z, \\
(u_0^m)_c(z) &= \frac{(cz+2)u_0^m}{c\,(c^2 e^{cz} + \beta + m - 1)}, \\
(w_0^m)_c(z) &= -ze^{-cz} (u_0^m)^{\beta} + \beta e^{-cz} (u_0^m)^{\beta-1} (u_0^m)_c.
\end{aligned} \tag{2.68}$$

We have $((u_0^m)_z, (w_0^m)_z) \in \mathbb{L}^2 \times \mathbb{L}^2$ and $((u_0^m)_c, (w_0^m)_c) \in \mathbb{L}^2 \times \mathbb{L}^2$ with

$$||((u_0^m)_z, (w_0^m)_z)||^2_{\mathbb{L}^2} = \frac{c}{4 + 2(\beta + m - 1)} + \frac{c^5}{\beta^2 - 2(\beta + m - 1)^2}. \tag{2.69}$$

The exact expression for $||(u_c, w_c)||_{\mathbb{L}^2}$ is not informative; instead see Figure 2.7.2 for computations of $||(u_c, w_c)||_{\mathbb{L}^2}$ specific values of β, m, c.

2.7.3 Behaviour of eigenfunctions as $z \to \pm\infty$

As we have shown the existence and boundedness of the (generalised) eigenfunctions, what remains is to show that the functions are contained in the weighted spaces $\mathbb{H}^1_\nu(\mathbb{R})$ where the essential spectrum is weighted into the left half plane. We do this through examining the asymptotic behaviour of the eigenfunctions. The exponential decay rate of the eigenfunctions as $z \to \pm\infty$ are greater than the weighted spatial eigenvalues at $z \to \pm\infty$. Hence, we conclude that $\lambda = 0$ is in fact point spectrum for all $0 \leq m < 1$ in

the space $\mathbb{H}^1_\nu(\mathbb{R})$. Since the eigenvalue problem can be expressed as an equivalent ODE (2.57) in p, u and their derivatives, it is sufficient to show u_z and u_c are contained in $\mathbb{H}^1_\nu(\mathbb{R})$. It was shown in [103] that solutions to (2.6) can be related to solutions of a Fisher equation by first eliminating $w(z)$ using $w^m_\varepsilon(z) = e^{-cz}\,(u^m_\varepsilon(z))^\beta$. Then, by introducing the change of variable $u^m_\varepsilon(z) = v(z)\exp\left(\frac{c}{\beta+m-1}z\right)$ the following ODE in $v(z)$ is obtained

$$\varepsilon v'' + sv' + \eta v - v^{\beta+m} = 0, \tag{2.70}$$

where $s = c\left(1 + \frac{2\varepsilon}{\beta+m-1}\right)$ and $\eta = \frac{c^2(\varepsilon+\beta+m-1)}{(\beta+m-1)^2}$. We have the following result for $v(z)$ adapted from Lemma 3.1 ii a of [103]

Lemma 2.7.1. *([103]) There exists a nonnegative travelling wave solution $v(z)$ of (2.70) if and only if $\beta \geq 1-m$. For $\beta > 1-m$ the travelling wave solution $v(z)$ is a wavefront with $v'(z) < 0$ and satisfies the asymptotic conditions*

$$\lim_{z\to-\infty} v(z) = \eta^{\frac{1}{\beta+m-1}}, \ \lim_{z\to\infty} v(z) = 0.$$

The wavefront $v(z)$ has the following asymptotic behaviours:

$$v(z) \sim \eta^{\frac{1}{\beta+m-1}} - C_1 e^{\kappa_1 z}, \ \text{as } z \to -\infty \text{ and } v(z) \sim C_2 e^{\kappa_2 z}, \ \text{as } z \to \infty \tag{2.71}$$

where

$$\kappa_1 = \kappa_2 - \frac{c}{2\varepsilon} + \frac{c}{2\varepsilon}\sqrt{1 + \frac{4\varepsilon(\beta+m)(\varepsilon+\beta+m-1)}{(\beta+m-1)^2}} \text{ and } \kappa_2 = -\frac{c}{\beta+m-1}.$$

From (2.65) the unweighted spatial eigenvalues μ^- for $\lambda = 0$ are given by

$$\mu^-_1 = \frac{c}{\beta+m-1}, \ \mu^-_2 = \mu^-_1 m,$$
$$\mu^-_{3,4} = -\frac{c}{2\varepsilon} \mp \frac{c}{2\varepsilon}\sqrt{1 + \frac{4\varepsilon(\beta+m)(\beta+m+\varepsilon-1)}{(\beta+m-1)^2}}.$$

Using (2.71) and $u^m_\varepsilon(z) = v(z)e^{\frac{c}{\beta+m-1}z}$ we have the following asymptotic behaviour as $z \to -\infty$

$$
\begin{aligned}
(u_\varepsilon^m)_z(z) &\sim \frac{c\eta^{\frac{1}{\beta+m-1}}}{\beta+m-1}e^{\frac{c}{\beta+m-1}z} - C_1\left(\kappa_1 + \frac{c}{\beta+m-1}\right)e^{\left(\kappa_1+\frac{c}{\beta+m-1}\right)z} \\
&\sim \frac{c\eta^{\frac{1}{\beta+m-1}}}{\beta+m-1}e^{\mu_1^- z} - C_1\left(\kappa_1 + \frac{c}{\beta+m-1}\right)e^{\mu_4^- z}, \\
(u_\varepsilon^m)_c(z) &\sim \left(\frac{\eta^{\frac{1}{\beta+m-1}} + \eta_c\eta^{\frac{2-\beta-m}{\beta+m-1}}}{\beta+m-1}\right)e^{\frac{c}{\beta+m-1}z} - C_1\left(\frac{1}{\beta+m-1} + (\kappa_1)_c\right)ze^{\left(\kappa_1+\frac{c}{\beta+m-1}\right)z} \\
&\sim \left(\frac{\eta^{\frac{1}{\beta+m-1}} + \eta_c\eta^{\frac{2-\beta-m}{\beta+m-1}}}{\beta+m-1}\right)e^{\mu_1^- z} - C_1\left(\frac{1}{\beta+m-1} + (\kappa_1)_c\right)ze^{\mu_4^- z}.
\end{aligned}
$$

The asymptotic decay rates of u_z, u_c as $z \to -\infty$ are precisely the two largest unstable unweighted spatial eigenvalues. In the weighted space $\mathbb{H}^1_\nu(\mathbb{R})$ the spatial eigenvalues are $\mu_-^i + \nu_-$ for $i = 1, 2, 3, 4$. It was shown in §2.4.3 that the range of weights for $z \to -\infty$ are negative. Thus, the eigenfunctions decay faster than the weighted spatial eigenvalues as $z \to -\infty$.

From (2.65) we have the unweighted spatial eigenvalues as $z \to \infty$ for $\lambda = 0$,

$$
\mu_+^1 = -c, \qquad \mu_+^2 = -\frac{c}{\varepsilon}, \qquad \mu_+^{3,4} = 0.
$$

From (2.71) we have $u_\varepsilon^m(z) \sim C_2$, as $z \to \infty$ and so we cannot compare the exact asymptotic exponential decay rates of the derivatives of $u_\varepsilon^m(z)$ to the spatial eigenvalues. It was shown in §2.4.3 that positive weights $\nu_+ \in (0, c)$ can be used to weight the essential spectrum into the open left half plane. Thus, as $(u_\varepsilon^m)_z$ and $(u_\varepsilon^m)_c$ are solutions to the eigenvalue problem both (generalised) eigenfunctions will decay to zero exponentially in the stable subspace spanned by the eigenvectors associated with $\mu_+^{1,2}$. Thus as $\nu_+ > 0$ we can conclude that there is some weighted space such that the (generalised) eigenfunctions decay faster than the weighted spatial eigenvalues as $z \to \infty$.

Hence, as the (generalised) eigenfunctions decay faster than the weighted spatial eigenvalues as $z \to \pm\infty$ we can conclude that $(u_c, w_c), (u_z, w_z) \in \mathbb{H}^1_\nu(\mathbb{R})$ for the range of weights that shift the essential spectrum into the open left half plane. Thus, the eigenvalue $\lambda = 0$ is isolated and in the point spectrum in these weighted spaces.

The inclusion of a small diffusion parameter amounts to a perturbation of the operator and there are only a few possible ways new point eigenvalues can appear. These point eigenvalues emerge as perturbations of the eigenvalues in the $\varepsilon = 0$ case or as new eigenvalues emerging from, and to leading order given by, the branch points of the absolute spectrum. From [54] it follows that eigenvalues in the point spectrum are, to leading order, given by those in the $\varepsilon = 0$ case. It has been shown via a numerical Evans function computation that there are no point eigenvalues in the open right half plane (excluding

$\lambda = 0$) when $\varepsilon = 0$ up to $|\lambda| \sim \mathcal{O}(10^9)$ [35]. As a result, there can be no point spectra in this region for $0 < \varepsilon \ll 1$. The ODE (2.57) varies smoothly in λ as $m \to 0$ and so the results of [35] hold for $0 < m < 1$. Thus, the only eigenvalues that can potentially destabilise the $\varepsilon = 0$ spectrum are those that emerge from the branch points of the absolute spectrum. As the operator $\mathcal{L} - \lambda I$ (2.36) varies smoothly in λ near $\varepsilon = 0$ any eigenvalues that emerge from the branch points will be of the form

$$\lambda = \lambda_{\text{br}} + C\varepsilon^2 + \mathcal{O}(\varepsilon^3),$$

for some $C \in \mathbb{C}$ [54]. Therefore, choosing $\beta < \beta^m_{\text{crit}}(\varepsilon)$ such that $|\Re(\lambda_{\text{br}})|$ is not $\mathcal{O}(\varepsilon^2)$ will prevent any emerging point spectrum from destabilising the spectrum.

2.7.4 The limit $m \to 1$

In the case of linear consumption, the travelling wave solutions are a pair of travelling wavefronts given, to leading order, by (2.7) with $m = 1$. These wavefronts satisfy (2.6) and asymptote to

$$\lim_{z\to-\infty}(u^1_\varepsilon(z), w^1_\varepsilon(z)) = \left(0, \frac{c^2}{\beta} + \varepsilon\frac{c^2}{\beta^2}\right), \quad \lim_{z\to\infty}(u^1_\varepsilon(z), w^1_\varepsilon(z)) = (u_r, 0), \tag{2.72}$$

with u_r scaled to one without loss of generality. Furthermore, the essential spectrum of $\mathcal{L}^1_\varepsilon$ (2.36) includes the origin for all parameter values and all possible weights (2.67), see Theorem 2.3.3. Therefore, this case is markedly different from $0 \leq m < 1$ and must be treated separately.

Similar to the previous analysis in §2.7.1, we compute the functions $((u^1_\varepsilon)_z, (w^1_\varepsilon)_z)$ and $((u^1_\varepsilon)_c, (w^1_\varepsilon)_c)$. These functions are given, to leading order, by (2.68) with $m = 1$. While the function $((u^1_\varepsilon)_z, (w^1_\varepsilon)_z)$ persists as a solution to the eigenvalue problem (2.36) with a finite norm $||((u^1_\varepsilon)_z, (w^1_\varepsilon)_z)||_{\mathbb{L}^2}$ given, to leading order, by (2.69), the leading order function $((u^1_0)_c, (w^1_0)_c)$ is unbounded and hence $((u^1_\varepsilon)_c, (w^1_\varepsilon)_c)$ is not a solution to the generalised eigenvalue problem, see Figure 2.7.2. The eigenvalue $\lambda = 0$ is order one, in the sense that one of the eigenfunctions associated with $\lambda = 0$ persists when $m \to 1$. As there is no exponentially weighted function space such that $\lambda = 0$ is isolated, it is not considered point spectrum.

The intuitive reason for the reduction of order as $m \to 1$ is that there is no longer a family of solutions in c, since, when $m = 1$, the end state of w^1_ε as $z \to -\infty$ depends on c, see (2.72). Thus, for fixed end states a travelling wave solution exists with a unique wave speed c, whereas for $0 \leq m < 1$ travelling wave solutions exist for any wave speed c. Alternatively, the reduction of order can be seen by examining the deformation of the absolute spectrum as $m \to 1$. The absolute spectrum does not contain $\lambda = 0$ for

$0 \leq m < 1$ but, as $m \to 1$ the branches of absolute spectrum approach $\lambda = 0$. Thus the order is reduced as $m \to 1$ due to an eigenvalue disappearing into the absolute spectrum.

2.8 Summary and outlook

In this chapter, we located the weighted essential spectrum and absolute spectrum associated with travelling wave solutions to the Keller-Segel model (2.4) for $0 \leq m \leq 1$, $\beta > 1 - m$ and $0 \leq \varepsilon \ll 1$. By locating the branch points, that form the leading edge of the absolute spectrum, we proved that the absolute spectrum and ideally weighted essential spectrum are contained in the open left half plane for $1 - m < \beta < \beta^m_{\text{crit}}(\varepsilon)$ and we derived leading order expressions determining $\beta^m_{\text{crit}}(\varepsilon)$. We also developed a procedure for locating the range of weighted spaces for which the weighted essential spectrum is in the open left half plane. For $\beta > \beta^m_{\text{crit}}(\varepsilon)$, all travelling wave solutions have absolute spectrum in the right half plane and the travelling wave solutions are thus absolutely unstable. These results provide a complete picture of the absolute spectrum and weighted essential spectrum associated with all possible travelling wave solutions to the Keller-Segel model (2.4) and they expand on the previous results for the essential spectrum known in the literature [80, 103]. Furthermore, it is now clear how the absolute spectrum and weighted essential spectrum deform between the limit cases $m = 0$ and $m = 1$. Moreover, we showed that the transition to the absolutely unstable parameter regime is characterised by the absolute spectrum crossing into the right half plane away from the real axis (similar to the example in [85]).

In [35], the Evans function associated with travelling wave solutions to (2.4) with $m = 0$ and $\varepsilon = 0$ was calculated numerically using a Riccati transformation. It was shown that there is a second order temporal eigenvalue at the origin and that there are no other eigenvalues in the right half plane with $|\lambda| < 10^7$. Due to the translation invariance, $\lambda = 0$ was expected to persist as an eigenvalue (with order at least one) for $0 < \varepsilon \ll 1$. We have now proved, barring the existence of extremely large values of $|\lambda|$ in the right half plane, that the travelling wave solutions to (2.2) are spectrally stable in an appropriately weighted function space for $1 - m < \beta < \beta^m_{\text{crit}}(\varepsilon)$ for $0 \leq m < 1$ and $0 \leq \varepsilon \ll 1$, *i.e.* transiently unstable. In particular, the point eigenvalue $\lambda = 0$, proven to be of order two when $\varepsilon = m = 0$ in [35], does not perturb in the $\varepsilon \neq 0$ case. This is because the existence of a continuous family of solutions in c and the existence of a family of solutions due to translation invariance is preserved when $\varepsilon \neq 0$.

2.8.1 Nonlinear (in)stability

Ideally, one would like to use the spectral stability results presented in this chapter to conclude nonlinear (in)stability of the travelling wave solutions. For a sectorial semilinear operator with a spectral gap (*i.e.* the spectrum is contained in the open left half plane

except for the translation invariance eigenvalue at the origin), spectral stability implies nonlinear (orbital) stability of the associated travelling wave solution [41, 91]. However, while the operator $\mathcal{L}$ (2.9) appears to be sectorial for $0 < \varepsilon \ll 1$, see, for instance, Figure 2.6.1, it is quasilinear rather than semilinear. In [78], it was shown that for a large class of quasilinear parabolic reaction-diffusion systems one can still deduce nonlinear stability results from the spectral stability results, as long as the linearised operator fulfils certain conditions. Unfortunately, the Keller-Segel model studied in this chapter does not fall into the class of quasilinear parabolic reaction-diffusion systems considered in [78], though potentially the analysis of [78] could be extended to encompass this model. For the Keller-Segel model (2.1) with nonlinear diffusion and with logarithmic chemosensitivity (*i.e.* $\Phi(u) = \log(u)$), linear consumption (*i.e.* $m = 1$) and nonzero growth (*i.e.* $\kappa > 0$), the general theory for semilinear operators was extended in [77] to prove nonlinear instability results in certain cases of the model.

In the case that $m = 1$ one can use a Hopf-Cole transformation in conjunction with energy estimates in order to prove the nonlinear (orbital) stability of travelling waves for $0 \leq \varepsilon \ll 1$ [49,70,71,77,103]. These energy estimates have the potential to provide a bound on large λ. However, these energy estimates are notoriously difficult for specific linearised operators and the computation is further complicated by both the non-self-adjointness of the operator $\mathcal{L}_\varepsilon^m$ given in (2.36) and the fact that the Hopf-Cole transformation is not applicable when $0 \leq m < 1$. Alternatively, in order to apply the general theory for semilinear systems, [41] proposes to transform a quasilinear system to a semilinear system. Observe that this approach is akin to the method used in §2.5. It is a challenge to see if any of these methods can be used to obtain nonlinear stability results for the travelling wave solutions of (2.4) studied in this chapter.

2.8.2 Dynamical implications of the spectral structure

The dynamical implications of the absolute spectrum in the right half plane for travelling wave solutions of the Keller-Segel model (2.4) are not known. In typical examples, such as the F-KPP equation, the transition to an absolutely unstable regime is associated with the so-called linear spreading speed, *i.e.* the speed 'generic' initial conditions will eventually travel at. Note that in the F-KPP equation this is known as the minimal wave speed. In other words, the linear spreading speed is the speed of a travelling wave solution 'selected' by the model. However, in the Keller-Segel model (2.4) the transition to the absolutely unstable regime is, to leading order, independent of the wave speed and it thus does not seem to have an influence on the asymptotic speed of a generic initial condition (that evolves to a travelling wave solution). Rather, the initial condition of the bacteria population w determines the wave speed [80]. Note that in the case of a Keller-Segel model (2.1) with a growth term, the absolute spectrum does appear to have an influence on the wave speed selection [8, 77]. Moreover, as the transition of the absolute spectrum

into the right half plane is complex valued, one expects oscillatory instabilities to manifest themselves near this critical parameter. These type of bifurcations have been studied in [89, 92]. As there are no instabilities arising from the point spectrum (barring extremely large values of $|\lambda|$) it is of interest to examine the dynamical implications and nature of this bifurcation as it is atypical for the absolute spectrum to cross into the right half plane away from the real line. Future work will examine this bifurcation, both analytically and numerically, to determine the impact, if any, on the wave speed, wavefront selection and whether oscillatory behaviour is observed.

Chapter 3

Travelling wave solutions in a model for tumour invasion with the acid-mediation hypothesis

3.1 Preface

The contents of this chapter were submitted for publication under the title "Traveling wave solutions in a model for tumor invasion with the acid-mediation hypothesis" [12]. The manuscript is presented here with minor stylistic changes, expanded discussion and outlook given in §3.6.

Abstract

In this chapter, we prove the existence of slow and fast travelling wave solutions in the original Gatenby–Gawlinski model. We prove the existence of a slow travelling wave solution with an interstitial gap. This interstitial gap has previously been observed experimentally, and here we derive its origin from a mathematical perspective. We give a geometric interpretation of the formal asymptotic analysis of the interstitial gap and show that it is determined by the distance between a layer transition of the tumour and a dynamical transcritical bifurcation of two components of the critical manifold. This distance depends, in a nonlinear fashion, on the destructive influence of the acid and the rate at which the acid is being pumped.

3.2 Introduction

Altered energy metabolism is a characteristic feature of many solid cancer tumours and it has been recognised as a possible phenotypic hallmark [34]. The discovery of this altered metabolism feature dates back to the seminal work of Warburg [104], who observed that certain carcinomas undergo glucose metabolism by glycolysis and not by mitochondrial oxidative phosphorylation (MOP), as normal cells do. MOP produces lactic acid as a toxic by-product and is usually reserved for conditions of hypoxia. Paradoxically, cancer cells maintain the glycolytic phenotype even in the presence of sufficient oxygen to undergo MOP. This phenomenon is known as *aerobic glycolysis* or the *Warburg effect*. The underlying causes of the Warburg effect still remain largely unknown. One explanation for this phenomenon is the so-called *acid-mediation hypothesis*, that is, the hypothesis that tumour progression is facilitated by the acidification of the region around the tumour-host interface. This leads to a comparative advantage for tumour cells since they are more

adapted to low pH environmental conditions than healthy cells. The resulting tissue degradation facilitates tumour invasion of the tissue microenvironment [33].

Gatenby and Gawlinski [32] formulated the acid-mediation hypothesis in a reaction-diffusion framework. They proposed a reaction-diffusion system in which tumour cells produce an excess of H^+ ions due to aerobic glycolysis, which results in local acidification and thus destruction of the surrounding healthy tissue. After a suitable nondimensionalisation [32], the Gatenby–Gawlinski model can be written as the following system of singularly perturbed partial differential equations (PDEs) with nonlinear diffusion (in the V-component):

$$\begin{cases} \dfrac{\partial U}{\partial \tau} = U(1-U-\alpha W), \\ \dfrac{\partial V}{\partial \tau} = \beta V(1-V) + \varepsilon \dfrac{\partial}{\partial x}\left[(1-U)\dfrac{\partial V}{\partial x}\right], \\ \dfrac{\partial W}{\partial \tau} = \gamma(V-W) + \dfrac{\partial^2 W}{\partial x^2}. \end{cases} \tag{3.1}$$

Here, $x \in \mathbb{R}$ and $\tau \geq 0$ are the spatial and temporal variables, respectively. The quantities $U(x,\tau)$, $V(x,\tau)$, and $W(x,\tau)$ represent nondimensionalised versions of the normal cell density, tumour cell density, and excess acid concentration, respectively. As in the quantitative discussions presented in [32], ε is assumed to be a small nonnegative parameter, i.e. $0 \leq \varepsilon \ll 1$. In addition, the constants α, β, and γ are all positive and strictly $\mathcal{O}(1)$ with respect to ε. The parameter α measures the destructive influence of H^+ ions on the normal tissue and therefore its value can be taken as an indicator of tumour aggressivity. For $\alpha \geq 1$, solutions of (3.1) model the situation in which total destruction of normal tissue occurs after the invasion of tumour tissue. On the other hand, for $0 < \alpha < 1$, solutions of (3.1) correspond to the case where a residual concentration with value $1-\alpha$ of healthy tissue remains behind the spreading benign wave.

Gatenby and Gawlinski [32] investigated the travelling wave (TW) solutions that are compatible with (3.1) and a number of interesting results were obtained. For instance, numerical simulations hinted at the existence of an *interstitial gap* (i.e. a region practically devoid of cells and located ahead of the invading tumour front) for large values of the parameter α. Subsequently, the existence of such a gap was verified experimentally [32, Fig. 4]. In addition, arguments pointing toward comparatively faster invasive processes when $\alpha > 1$ were provided in [32]. Fasano, Herrero, and Rodrigo [27] further investigated the TW solutions that are compatible with (3.1). Using a nonstandard matched asymptotic analysis they showed that (3.1) supports TW solutions that travel with speed $\mathcal{O}(1)$ and TW solutions that travel with speed $\mathcal{O}(\varepsilon^p)$ for $0 < p \leq 1/2$. They called the former TWs *fast TW solutions* and the latter TWs *slow TW solutions*, and the authors also obtained bounds for the wave speed in terms of the model parameters. Most notably, the authors

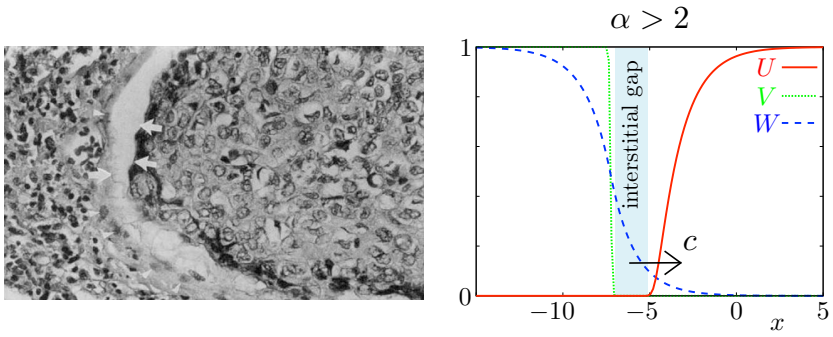

Figure 3.2.1: Left panel: an interstitial gap present in a human squamous cell carcinoma. Reprinted from R. A. Gatenby and E. T. Gawlinski. A reaction-diffusion model for cancer invasion. *Cancer Res.*, 56:5745–5753, 1996 with permission from AACR. Right panel: a slow TW solution with an interstitial gap supported by (3.1).

identified slow TWs with an interstitial gap when $\alpha > 2$ and the leading order width of this gap was estimated as

$$z_+ = \frac{1}{\sqrt{\gamma}} \log \frac{\alpha}{2} > 0. \tag{3.2}$$

This interstitial gap ceases to exist when $0 < \alpha \leq 2$. Finally, the authors of [27] showed that TW solutions cannot be found when $p > 1/2$. See Fig. 3.2.1 for a slow TW solution with an interstitial gap obtained by a numerical simulation of (3.1).

Different generalizations of the original Gatenby–Gawlinski model have also been proposed in the literature. For instance, Holder, Rodrigo, and Herrero [42] included a cellular competition term in the U-equation and replaced the acid production term in the W-equation by a logistic-type reaction term. After nondimensionalisation, this generalised Gatenby–Gawlinski model becomes

$$\begin{cases} \dfrac{\partial U}{\partial \tau} = U(1 - U - \alpha(V + W)), \\ \dfrac{\partial V}{\partial \tau} = \beta V(1 - V) + \varepsilon \dfrac{\partial}{\partial x}\left[(1 - U)\dfrac{\partial V}{\partial x}\right], \\ \dfrac{\partial W}{\partial \tau} = \delta V(1 - V) - \gamma W + \dfrac{\partial^2 W}{\partial x^2}. \end{cases} \tag{3.3}$$

This generalization was motivated by the fact that tumours tend to present with very heterogeneous acid profiles and there is some experimental evidence of higher acid concentrations near the region of the interstitial gap. As a consequence of the addition of the nonlinear acid production term to the model, the profile of the excess acid concentration became pulse-like (instead of front-like in the original Gatenby–Gawlinski model; see, for instance, Fig. 3.2.1). The authors obtained results with regards to fast and slow TW solutions via matched asymptotic analysis similar to those in [27] and they also obtained estimates for the interstitial gap.

A different generalization of the Gatenby–Gawlinski model (3.1) was given by McGillen et al. [75]. Here, the authors added cellular competition terms for both the U- and V-equations, as well as a term in the V-equation that incorporates acid-mediated tumour cell death. After nondimensionalisation, this generalised Gatenby–Gawlinski model becomes

$$\begin{cases} \dfrac{\partial U}{\partial \tau} = U(1 - U - \alpha_1 V - \alpha_2 W), \\ \dfrac{\partial V}{\partial \tau} = \beta V(1 - V) - \delta_1 UV - \delta_2 VW + \varepsilon \dfrac{\partial}{\partial x}\left[(1 - U)\dfrac{\partial V}{\partial x}\right], \\ \dfrac{\partial W}{\partial \tau} = \gamma(V - W) + \dfrac{\partial^2 W}{\partial x^2}, \end{cases} \tag{3.4}$$

and results analogous to those in [27, 42] were derived.

3.2.1 Results and outline

In this chapter, we study the original nondimensionalised Gatenby–Gawlinski model (3.1) and prove the formal results of [27] regarding the existence of fast and slow TW solutions[1]. Moreover, we explain – from a mathematical perspective – the origin of the interstitial gap. We focus on the two critical cases $p = 0$ (fast TW solutions) and $p = 1/2$ (slow TW solutions). To prove the asymptotic results from [27], we rewrite the PDE model (3.1) in its travelling wave framework upon introducing $(z, t) := (x - \varepsilon^p c\tau, \tau)$ with $p = 0$ or $p = 1/2$ and with $\mathcal{O}(1)$ wave speed c. TW solutions to (3.1) now correspond to stationary solutions in this new framework and the problem reduces to studying heteroclinic orbits in an ordinary differential equation (ODE). Next, we use the multi-scale structure of (3.1) to write this resulting ODE problem in a five-dimensional *slow-fast* system of first order ODEs [68][2]. For the fast TW solutions there will be one *fast component* and four *slow components*, while the slow-fast splitting for the slow TW solutions is three fast components and two slow components. The details regarding the formulation of the slow-fast systems are given in §3.3.

We study these slow-fast systems for the fast TW solutions (see §3.4) and the slow TW solutions (see §3.5) using geometric singular perturbation theory (GSPT) [39, 51, 53]. In particular, we study the dynamics of the associated lower dimensional *fast layer problems* and *slow reduced problems* in the singular limits as $\varepsilon \to 0$. Next, we appropriately concatenate the dynamics of these lower dimensional systems to obtain information regarding the heteroclinic orbit – and thus fast and slow TW solutions to (3.1) – in the singular limit as $\varepsilon \to 0$. Finally, we use Fenichel theory [30] to show that these solutions persist for positive but small ε. It turns out that for the fast TW solutions, independent of the value

[1] See the discussion in §3.6 regarding using the techniques of this chapter to analyse TW solutions found in (3.3) and (3.4).

[2] Note that the *slow* and *fast* in *slow-fast system* is not related to the *slow* and *fast* in *slow TW solution* and *fast TW solution*. This terminology is standard in the GSPT literature and we decided not to change it.

of α, all the dynamics take place on the attracting *critical manifold* of the slow reduced problem and the application of GSPT and Fenichel theory is straightforward. In essence, the model is a regularly perturbed problem for the fast TW solutions, and we will show that the asymptotic results of [27] are correct and persist for $0 < \varepsilon \ll 1$. See §3.4 for the details.

In §3.5 we study the slow TW solutions and now the tumour aggressivity parameter α becomes important. In particular, we have to distinguish between three cases: $0 < \alpha < 1$, $1 < \alpha < 2$, and $\alpha > 2$. In the first case, a slow TW solution in the singular limit $\varepsilon \to 0$ starts on one branch of the critical manifold (at $z = -\infty$) and transitions through the fast layer problem (which we assume, without loss of generality, to happen at $z = 0$) to a second branch of the critical manifold, and the layer dynamics will have a Fisher–KPP imprint [69, 79, 102, e.g]. Again, we will show that such a slow TW solution persists for $0 < \varepsilon \ll 1$ by applying GSPT and Fenichel Theory. In the latter two cases ($1 < \alpha < 2$ and $\alpha > 2$) there is an additional complication related to a dynamical transcritical bifurcation of the two connected components on each branch of the critical manifold [67,68, e.g]. For $1 < \alpha < 2$, the transcritical bifurcation happens before the fast transition through the layer problem (at $z = 0$), while the bifurcation happens after the transition for $\alpha > 2$, see Fig. 3.5.2. For $1 < \alpha < 2$ the transcritical bifurcation happens (to leading order in ε) at

$$z_- = \frac{1}{\sqrt{\gamma}} \log \frac{2(\alpha - 1)}{\alpha} < 0\,, \tag{3.5}$$

while the transcritical bifurcation happens (to leading order in ε) at z_+ (3.2) for $\alpha > 2$, see also [27]. In other words, for $\alpha > 2$ the length of the interstitial gap is to leading order determined by the distance between the fast transition through the layer problem and the dynamical transcritical bifurcation. We conclude the chapter with a summary and outlook regarding future projects.

3.3 Setup of the slow-fast systems

Since we are looking for TW solutions supported by (3.1), we introduce the travelling frame coordinates $(z, t) := (x - \varepsilon^p c\tau, \tau)$ for $0 \leq p$. Here, the speed c of the TW solution is assumed to be strictly $\mathcal{O}(1)$ with respect to ε. Moreover, as we are interested in waves of invasion, we assume, without loss of generality, that $c > 0$. A TW solution is stationary in this co-moving frame and will therefore satisfy the following system of ODEs:

$$\begin{cases} -\varepsilon^p c \dfrac{\mathrm{d}u}{\mathrm{d}z} = u(1 - u - \alpha w), \\ -\varepsilon^p c \dfrac{\mathrm{d}v}{\mathrm{d}z} = \beta v(1 - v) + \varepsilon \dfrac{\mathrm{d}}{\mathrm{d}z}\left[(1 - u)\dfrac{\mathrm{d}v}{\mathrm{d}z}\right], \\ -\varepsilon^p c \dfrac{\mathrm{d}w}{\mathrm{d}z} = \gamma(v - w) + \dfrac{\mathrm{d}^2 w}{\mathrm{d}z^2}. \end{cases} \tag{3.6}$$

The fixed points of (3.6) are $(u,v,w) = (0,0,0), (1,0,0), (0,1,1)$ and $(1-\alpha,1,1)$. We examine TW solutions with asymptotic boundary conditions $(u,v,w) \to ((1-\alpha)_+,1,1)$ as $z \to -\infty$ and $(u,v,w) \to (1,0,0)$ as $z \to \infty$ as these solutions represent tumour invasion into healthy tissue. Here,

$$(1-\alpha)_+ = \max\{1-\alpha, 0\},$$

which represents the residual concentration of healthy tissue that remains behind the TW solution. Upon introducing the two new variables $r := \varepsilon^{1-p}(1-u)v_z + cv$ (see Remark 3.3.1) and $s := w_z$, we can rewrite (3.6) as an equivalent slow-fast system of five first order ODEs

$$\begin{cases} \varepsilon^p \dfrac{\mathrm{d}u}{\mathrm{d}z} = -\dfrac{1}{c}u(1-u-\alpha w), \\ \varepsilon^{1-p}\dfrac{\mathrm{d}v}{\mathrm{d}z} = \dfrac{r-cv}{1-u}, \\ \varepsilon^p \dfrac{\mathrm{d}r}{\mathrm{d}z} = -\beta v(1-v), \\ \dfrac{\mathrm{d}w}{\mathrm{d}z} = s, \\ \dfrac{\mathrm{d}s}{\mathrm{d}z} = -\varepsilon^p cs - \gamma(v-w). \end{cases} \tag{3.7}$$

TW solutions of (3.1) now correspond to heteroclinic orbits of (3.7) connecting its two equilibrium points. That is,

$$\begin{aligned} \lim_{z\to-\infty}(u,v,r,w,s) &= ((1-\alpha)_+,1,c,1,0) =: Z^-, \\ \lim_{z\to\infty}(u,v,r,w,s) &= (1,0,0,0,0) =: Z^+. \end{aligned} \tag{3.8}$$

There are three critical p-values that balance the asymptotic scalings of (3.7), namely, $p = 0$, $p = 1/2$, and $p = 1$. In [27] it was shown that the case $p = 1$ does not lead to TW solutions and we therefore do not consider this case in this chapter (actually it was shown in [27] that there are no TWs for $p > 1/2$). In addition, (3.7) has three asymptotic scalings for $0 \le p \le 1/2$. In this chapter we consider only the cases $p = 0$ – corresponding to fast TW solutions – and $p = 1/2$ – corresponding to slow TW solutions. We refer the reader to [27] for the procedure to apply when $0 < p < 1/2$.

Equation (3.7) is in its *slow formulation*[3] [51, 53, 68]. Upon introducing the fast variable $y := \varepsilon^{p-1} z$, the ODEs can be written in their *fast formulation*

$$\begin{cases} \dfrac{\mathrm{d}u}{\mathrm{d}y} = -\dfrac{\varepsilon^{1-2p}}{c} u(1-u-\alpha w), \\ \dfrac{\mathrm{d}v}{\mathrm{d}y} = \dfrac{r-cv}{1-u}, \\ \dfrac{\mathrm{d}r}{\mathrm{d}y} = -\varepsilon^{1-2p}\beta v(1-v), \\ \dfrac{\mathrm{d}w}{\mathrm{d}y} = \varepsilon^{1-p} s, \\ \dfrac{\mathrm{d}s}{\mathrm{d}y} = -\varepsilon c s - \varepsilon^{1-p}\gamma(v-w). \end{cases} \tag{3.9}$$

The slow problem (3.7) and fast problem (3.9) are equivalent for $\varepsilon \neq 0$. However, they differ in the singular limit $\varepsilon \to 0$. In particular, for the fast TW solutions, i.e. when $p = 0$, the (u, r, w, s)-variables are *slow variables* and the v-variable is a *fast variable*. That is, for $p = 0$ the slow problem (3.7) in the singular limit $\varepsilon \to 0$ is a four-dimensional system of ODEs (in the slow variables) with one algebraic constraint (determined by the original equation for the fast variable). In contrast, the fast problem (3.9) for $p = 0$ in the singular limit $\varepsilon \to 0$ is a one-dimensional ODE (in the fast variable) with (up to) four additional parameters (coming from the slow equations). For the slow TW solutions, i.e. when $p = 1/2$, only the (w, s)-variables are slow variables and the (u, v, r)-variables are fast variables.

Remark 3.3.1. *The scaling of the new variable r as $r := \varepsilon^{1-p}(1-u)v_z + cv$ is chosen such that $-\varepsilon^p r_z$ is equal to the reaction term of the v-component in the original ODE model* (3.6)*. That is, $-\varepsilon^p r_z = \beta v(1-v)$* (3.7)*. This particular scaling of r is inspired by a series of manuscripts [3,36,37,84] on TW solutions for chemotaxis-driven and haptotaxis-driven cell migration problems and it arises naturally when writing an extended version of* (3.6) *as a singularly perturbed system of coupled balance laws.*

3.4 The existence of fast travelling wave solutions

We start with studying the fast TW solutions supported by (3.1) and prove that the asymptotic results of [27] persist for $0 < \varepsilon \ll 1$. In particular, we show that, for sufficiently small ε, (3.1) supports fast TW solutions $(U_{\mathrm{F}}, V_{\mathrm{F}}, W_{\mathrm{F}})(x, \tau)$ (see Fig. 3.4.1 for a fast TW

[3]Recall that the *slow* in *slow formulation* is not related to the *slow* in *slow TW solution*, that is, (3.7) is the slow formulation of the ODEs associated to both the slow TW solutions with $p = 1/2$ and the fast TW solutions with $p = 0$.

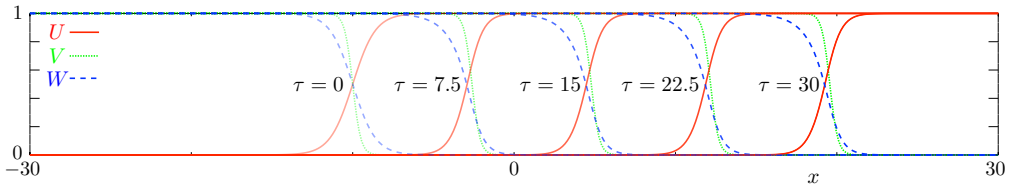

Figure 3.4.1: A fast TW solution obtained from numerically simulating the Gatenby–Gawlinsky model (3.1) on a domain of size 60 with $(\alpha, \beta, \gamma, \varepsilon) = (3, 4, 2, 4 \times 10^{-5})$. The observed wave speed is $c \approx 0.985$, which is, as expected, $\mathcal{O}(1)$.

solution obtained by directly simulating (3.1)). These fast TW solution are, to leading order in ε, given by $(U_{\mathrm{F}}, V_{\mathrm{F}}, W_{\mathrm{F}})(x, \tau) = (u_0, v_0, w_0)(z)$, with

$$\begin{aligned} v_0(z) &= \frac{1}{1 + e^{\beta z / c}}\,, \\ w_0(z) &= \frac{\gamma}{\rho_+ - \rho_-} \left(\int_z^\infty e^{\rho_+ (z-\xi)} v_0(\xi)\, \mathrm{d}\xi + \int_{-\infty}^z e^{\rho_- (z-\xi)} v_0(\xi)\, \mathrm{d}\xi \right)\,, \\ u_0(z) &= \frac{c \Phi_0(z)}{\int_z^\infty \Phi_0(\xi)\, \mathrm{d}\xi}, \quad \Phi_0(z) = e^{-(1/c) \int_0^z (1 - \alpha w_0(\xi))\, \mathrm{d}\xi}\,, \end{aligned} \tag{3.10}$$

where $\rho_\pm = (-c \pm \sqrt{c^2 + 4\gamma})/2$.

Taking $p = 0$ in the fast system of ODEs (3.9) and considering the singular limit $\varepsilon \to 0$ leads to the fast layer problem for the fast TW solutions[4]

$$\begin{cases} \dfrac{\mathrm{d}v}{\mathrm{d}y} = \dfrac{r - cv}{1 - u}, \\ \dfrac{\mathrm{d}u}{\mathrm{d}y} = 0, \\ \dfrac{\mathrm{d}r}{\mathrm{d}y} = 0, \\ \dfrac{\mathrm{d}w}{\mathrm{d}y} = 0, \\ \dfrac{\mathrm{d}s}{\mathrm{d}y} = 0. \end{cases} \tag{3.11}$$

All of the variables except v are constant in (3.11) and it can thus be seen as a single first order ODE with four additional parameters. It follows directly from (3.11) that $v = r/c$ is an equilibrium point. Therefore, we define the four-dimensional critical manifold

$$S_{\mathrm{F}}^0 := \left\{ (u, v, r, w, s) \;\middle|\; v = \frac{r}{c} \right\}\,. \tag{3.12}$$

[4] We rearranged the order of the equations in (3.11) to emphasise the slow-fast structure of the problem.

Since $c > 0$ by assumption, we have that the critical manifold S_{F}^0 is an attracting, normally hyperbolic manifold [51, 53, e.g] for $u < 1$. The critical manifold S_{F}^0 loses normal hyperbolicity for $u = 1$ and is repelling for $u > 1$. As we will show, the u-component is always between 0 and 1 and only approaches 1 as $z \to \infty$; see (3.8), (3.10) and, in particular, Remark 3.4.1. Moreover, both asymptotic boundary conditions $Z^{\pm}$ (3.8) lie on the critical manifold S_{F}^0.

Taking $p = 0$ in the slow system of ODEs (3.7) and considering the singular limit $\varepsilon \to 0$ leads to the slow reduced problem for the fast TW solutions

$$\begin{cases} 0 = \dfrac{r - cv}{1 - u}, \\ \dfrac{\mathrm{d}u}{\mathrm{d}z} = -\dfrac{1}{c} u(1 - u - \alpha w), \\ \dfrac{\mathrm{d}r}{\mathrm{d}z} = -\beta v(1 - v), \\ \dfrac{\mathrm{d}w}{\mathrm{d}z} = s, \\ \dfrac{\mathrm{d}s}{\mathrm{d}z} = -cs - \gamma(v - w). \end{cases} \tag{3.13}$$

Hence, the reduced problem is a system of four first order ODEs restricted to the critical manifold S_{F}^0 (3.12). Upon imposing the algebraic constraint $v = r/c$, the system of four first order ODEs of (3.13) can be written as

$$\begin{cases} \dfrac{\mathrm{d}u}{\mathrm{d}z} = -\dfrac{1}{c} u(1 - u - \alpha w), \\ \dfrac{\mathrm{d}v}{\mathrm{d}z} = -\dfrac{\beta}{c} v(1 - v), \\ \dfrac{\mathrm{d}^2 w}{\mathrm{d}z^2} + c\dfrac{\mathrm{d}w}{\mathrm{d}z} - \gamma w = -\gamma v\,. \end{cases}$$

It was shown in [27] that this system, with boundary conditions as in (3.8), is solved by (3.10). Hence, the u-component is strictly increasing and approaching one in the limit $z \to \infty$ [27].

In the singular limit $\varepsilon \to 0$, the critical manifold S_{F}^0 (3.12) is normally hyperbolic and attracting in the fast direction for $u < 1$, the asymptotic boundary conditions (3.8) lie on S_{F}^0, and the reduced problem (3.13) restricted to the critical manifold supports the appropriate heteroclinic orbit (for which $u(z) < 1$ for all $z \in \mathbb{R}$). Therefore, by applying standard GSPT and Fenichel theory [30,39,51,53,68] (see Remark 3.4.1), we can conclude that this heteroclinic orbit persists in (3.7)-(3.9), with $p = 0$, for $0 < \varepsilon \ll 1$. Moreover, the persisting heteroclinic orbit is to leading order in ε given by its singular limit. This heteroclinic orbit corresponds to the fast TWs of (3.1) and the fast TWs are thus to leading order given by (3.10).

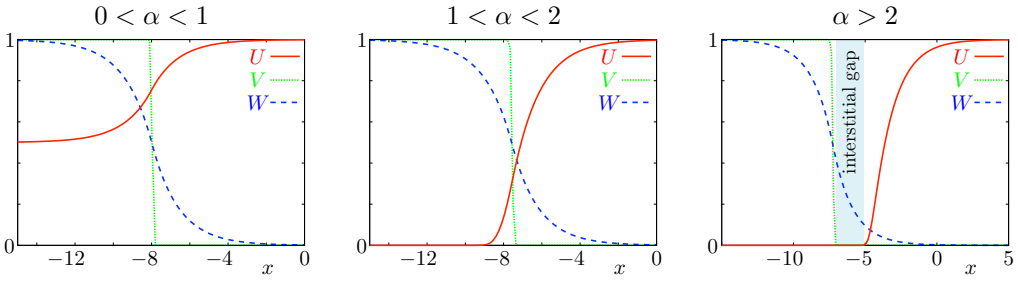

Figure 3.5.1: Three typical profiles of slow TW solutions obtained from numerically simulating the Gatenby–Gawlinsky model (3.1) on a domain of size 60 for three different α values and with $(\beta, \gamma, \varepsilon) = (1, 0.5, 4 \times 10^{-5})$. In the left panel, $\alpha = 0.5$ and the observed wave speed is $c \approx 0.0188 = 2.97 \times \sqrt{\varepsilon}$. In the middle panel, $\alpha = 1.5$ and the observed wave speed is $c \approx 0.0375 = 5.93 \times \sqrt{\varepsilon}$. In the right panel, $\alpha = 15$ and the observed wave speed is $c \approx 0.0375 = 5.93 \times \sqrt{\varepsilon}$. The interstitial gap is only observed in the right panel where $\alpha = 15 > 2$.

Remark 3.4.1. *The slow problem* (3.7) *and fast problem* (3.9) *are – both for* $p = 0$ *and* $p = 1/2$ *– singular along* $\{u = 1\}$. *However,* u *is always smaller than one, and it only approaches one in the limit* $z \to \infty$, *see, for instance,* (3.8) *and* (3.10). *A similar type of singularity is encountered in, for instance, a version of the generalised Gierer–Meinhardt model [18] and the Keller–Segel model [38]. We refer to [18] for details on how GSPT and Fenichel theory can be extended to deal with this type of singularity at an asymptotic boundary condition.*

3.5 The existence of slow travelling wave solutions

Next, we study the slow TW solutions (U_S, V_S, W_S) supported by the Gatenby–Gawlinsky model (3.1) and prove the formal asymptotic results of [27] and show their persistence for sufficiently small ε. Depending on the magnitude of α, there are three different types of slow TW solutions [27], see Fig. 3.5.1.

Taking $p = 1/2$ in the fast system of ODEs (3.9) and considering the singular limit $\varepsilon \to 0$ leads to the fast layer problem for the slow TW solutions

$$\begin{cases} \dfrac{\mathrm{d}u}{\mathrm{d}y} = -\dfrac{1}{c}u(1-u-\alpha w), \\ \dfrac{\mathrm{d}v}{\mathrm{d}y} = \dfrac{r-cv}{1-u}, \\ \dfrac{\mathrm{d}r}{\mathrm{d}y} = -\beta v(1-v), \\ \dfrac{\mathrm{d}w}{\mathrm{d}y} = 0, \\ \dfrac{\mathrm{d}s}{\mathrm{d}y} = 0. \end{cases} \tag{3.14}$$

The fast layer problem (3.14) is again singular for $u = 1$. However, as in the fast TW case, we will show that the u-components associated to the heteroclinic orbits of interest stay smaller than one and only approach one in the limit $z \to \infty$. Therefore, this singularity does not lead to any significant complications, see Remark 3.4.1. Analysis of the equilibrium points of the layer problem (3.14) yields a two-dimensional critical manifold S_{S}^0 in $\mathbb{R}^5$. This critical manifold consists of two disjoint branches $S_{\mathrm{S}}^{A,B}$. In turn, each of these branches consists of two connected components. In other words, the critical manifold S_{S}^0 is the union of the four two-dimensional manifolds $S_{\mathrm{S}}^{1,2,3,4}$. These four manifolds are parameterised by the slow variables (w, s) and are given by

$$\begin{aligned} S_{\mathrm{S}}^A: \quad & \begin{cases} S_{\mathrm{S}}^1 := \left\{(u,v,r,w,s) \;\middle|\; u = 0, v = 0, r = 0\right\}, \\ S_{\mathrm{S}}^2 := \left\{(u,v,r,w,s) \;\middle|\; u = 1 - \alpha w, v = 0, r = 0\right\}, \end{cases} \\ S_{\mathrm{S}}^B: \quad & \begin{cases} S_{\mathrm{S}}^3 := \left\{(u,v,r,w,s) \;\middle|\; u = 0, v = 1, r = c\right\}, \\ S_{\mathrm{S}}^4 := \left\{(u,v,r,w,s) \;\middle|\; u = 1 - \alpha w, v = 1, r = c\right\}. \end{cases} \end{aligned} \tag{3.15}$$

The manifolds S_{S}^1 and S_{S}^2 intersect on S_{S}^A along the line $\alpha w = 1$. Similarly, S_{S}^3 and S_{S}^4 intersect on S_{S}^B (which is disjoint from S_{S}^A) along the line $\alpha w = 1$. These intersections are nondegenerate in nature since $\alpha \neq 0$, see Fig. 3.5.2.

The three different types of slow TW solutions, see Fig. 3.5.1, can now be understood from the different pathways these TW solutions take through phase space along the four manifolds $S_{\mathrm{S}}^{1,2,3,4}$ in the singular limit:

- For $0 < \alpha < 1$, the right asymptotic boundary condition Z^+ (3.8) is located on S_{S}^2 (as is the case for $\alpha > 1$), while the left[5] asymptotic boundary condition Z^- (3.8) is located on S_{S}^4. Since both α and w are positive but less than 1, $\alpha w \neq 1$. As a result, the heteroclinic orbit associated to a slow TW solution starts at Z^- on S_{S}^4 and transitions, via the layer dynamics, to S_{S}^2. Subsequently, it asymptotes to Z^+.
- For $1 < \alpha < 2$, the right asymptotic boundary condition Z^+ (3.8) is located on S_{S}^2, while the left asymptotic boundary condition Z^- (3.8) is located on S_{S}^3. The heteroclinic orbit associated to a slow TW solution thus starts at Z^- on S_{S}^3, switches – via a dynamical transcritical bifurcation [67] – to S_{S}^4 at $z = z^-$ (3.5) (i.e. when $w(z^-) = 1/\alpha$), before transitioning, via the layer dynamics, to S_{S}^2. Subsequently, it asymptotes to Z^+.
- For $\alpha > 2$, the right asymptotic boundary condition Z^+ (3.8) is located on S_{S}^2, while the left asymptotic boundary condition Z^- (3.8) is again located on S_{S}^3. The heteroclinic orbit associated to a slow TW solution now starts at Z^- on S_{S}^3, transitions, via the layer dynamics, to S_{S}^1 and switches – via a dynamical transcritical bifurcation – to S_{S}^2 at $z = z_+$ (3.2) (i.e. when $w(z_+) = 1/\alpha$). Subsequently, it

[5]Throughout this chapter 'left' and 'right' refer to position relative to the layer transition for a solution plotted against z. Thus, $z < 0$ is 'left' and $z > 0$ is 'right'

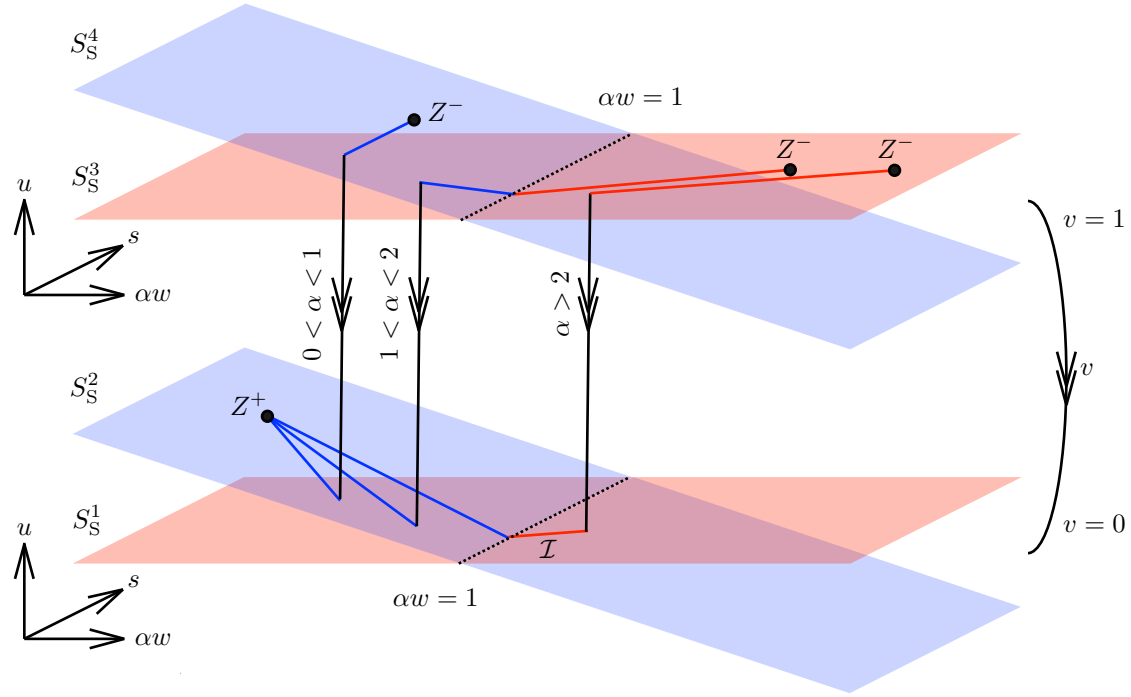

Figure 3.5.2: Schematic depiction of the four manifolds $S_S^{1,2,3,4}$ (3.15) and the three different heteroclinic orbits associated to the three different types of slow TW solutions, see also Fig. 3.5.1 and Fig. 3.5.3. The dots indicate the equilibrium points $Z^{\pm}$ that determine the asymptotic boundary conditions (3.8). (Recall that Z^- depends on α for $\alpha < 1$ and note that the horizontal axis represents αw. Consequently, the location of Z^- changes for different α values). The black dotted line at $\alpha w = 1$ indicates the location where the manifolds coincide and where the critical manifold S_S^0 loses normal hyperbolicity. The interstitial gap is related to the part of the heteroclinic orbit on S_S^1 (*i.e.* the red curve labelled $\mathcal{I}$) since here both u (normal cell density) and v (tumour cell density) are zero. This only happens for $\alpha > 2$.

asymptotes to Z^+. In this case we expect to see an interstitial gap since both u and v are (to leading order) zero on S_S^1.

See also Fig. 3.5.2 for a schematic depiction of the four manifolds $S_S^{1,2,3,4}$ (3.15) and the three different heteroclinic orbits associated to the three different types of slow TW solutions. Finally, note that Z^- lies on the intersection of S_S^3 and S_S^4 for the boundary case $\alpha = 1$. Similarly, for $\alpha = 2$ the transition through the fast field occurs, in the singular limit, at the intersection of S_S^3 and S_S^4.

3.5.1 The properties of the critical manifold

To understand the hyperbolic properties of the critical manifold S_{S}^0, we compute Jacobian J of the fast equations of (3.14)

$$J = \begin{pmatrix} -\frac{1}{c}(1-2u-\alpha w) & 0 & 0 \\ \frac{r-cv}{(1-u)^2} & -\frac{c}{1-u} & \frac{1}{1-u} \\ 0 & \beta(2v-1) & 0 \end{pmatrix}.$$

The eigenvalues of the Jacobian J are given by

$$\lambda_1 = -\frac{1}{c}(1-2u-\alpha w)\,,\ \lambda_{2,3} = \frac{1}{2(1-u)}\left(-c \pm \sqrt{c^2+4\beta(2v-1)(1-u)}\right), \tag{3.16}$$

with the associated eigenvectors

$$\begin{aligned} \vec{v}_1 &= \left(f(u,r,v;\alpha,c,w), \lambda_1(r-cv), \beta(2v-1)(r-cv)\right)^T, \\ \vec{v}_{2,3} &= \left(0, \lambda_{2,3}, \beta(2v-1)\right)^T, \end{aligned} \tag{3.17}$$

where

$$f(u,r,v;\alpha,c,w) = (1-u)\left(\lambda_1\left(\lambda_1(1-u)+c\right) - \beta(2v-1)\right).$$

The eigenvalues (3.16) on the four manifolds $S_{\mathrm{S}}^{1,2,3,4}$ (3.15) reduce to

$$\begin{aligned} S_{\mathrm{S}}^1: &\quad \lambda_1^1 = -\frac{1}{c}(1-\alpha w)\,, &\quad \lambda_{2,3}^1 &= \frac{1}{2}\left(-c \pm \sqrt{c^2-4\beta}\right), \\ S_{\mathrm{S}}^2: &\quad \lambda_1^2 = \frac{1}{c}(1-\alpha w)\,, &\quad \lambda_{2,3}^2 &= \frac{1}{2\alpha w}\left(-c \pm \sqrt{c^2-4\alpha\beta w}\right), \\ S_{\mathrm{S}}^3: &\quad \lambda_1^3 = -\frac{1}{c}(1-\alpha w)\,, &\quad \lambda_{2,3}^3 &= \frac{1}{2}\left(-c \pm \sqrt{c^2+4\beta}\right), \\ S_{\mathrm{S}}^4: &\quad \lambda_1^4 = \frac{1}{c}(1-\alpha w)\,, &\quad \lambda_{2,3}^4 &= \frac{1}{2\alpha w}\left(-c \pm \sqrt{c^2+4\alpha\beta w}\right). \end{aligned} \tag{3.18}$$

So, since the system parameters and the speed c are assumed to be positive, $\Re(\lambda_3^{1,2,3,4}) < 0$ on the associated manifolds. In addition, $\Re(\lambda_2^{1,2}) < 0$, while $\lambda_2^{3,4} > 0$ (since β and $\alpha\beta w$ are positive). The signs of the eigenvalues indicate that the fast transition, which is either from S_{S}^4 to S_{S}^2 or from S_{S}^3 to S_{S}^1, is always from a component of the manifold with two unstable eigenvalues to a component with only one unstable eigenvalue (since, as will follow from the upcoming analysis, $\lambda_1^{1,2,3,4} > 0$ during the fast transition). Crucially, this latter unstable eigenvalue remains unchanged by the fast transition, i.e. $\lambda_1^1 = \lambda_1^3$ and $\lambda_1^2 = \lambda_1^4$. Furthermore, $\lambda_1^{1,2,3,4}$ have real part zero if, and only if, $\alpha w = 1$. Consequently, the critical manifold S_{S}^0 loses normal hyperbolicity at $w = 1/\alpha$ (i.e. where S_{S}^1 coincides with S_{S}^2 and S_{S}^3 coincides with S_{S}^4) and this loss happens through the first eigenvalue. This loss of normal hyperbolicity is nondegenerate and transcritical in nature since $\alpha \neq 0$, see Fig. 3.5.2. In other words, we have an *exchange of stability* between the two components

on each of the two branches $S_{\mathrm{S}}^{A,B}$ at $w = 1/\alpha$ and the critical manifold S_{S}^{0} undergoes a dynamical transcritical bifurcation [67]. For $\alpha > 2$, this point ($w = 1/\alpha$) determines the rightmost point of the interstitial gap.

We next study the slow reduced dynamics on the critical manifold S_{S}^{0}. Taking $p = 1/2$ in the slow system of ODEs (3.7) and considering the singular limit $\varepsilon \to 0$ leads to the slow reduced problem for the slow TW solutions

$$\begin{cases} 0 = -\dfrac{1}{c}u(1-u-\alpha w), \\ 0 = \dfrac{r-cv}{1-u}, \\ 0 = -\beta v(1-v), \\ \dfrac{\mathrm{d}w}{\mathrm{d}z} = s, \\ \dfrac{\mathrm{d}s}{\mathrm{d}z} = -\gamma(v-w). \end{cases}$$

So, the slow reduced dynamics on the four manifolds $S_{\mathrm{S}}^{1,2,3,4}$ is given by the linear equations

$$\frac{\mathrm{d}w}{\mathrm{d}z} = s, \quad \frac{\mathrm{d}s}{\mathrm{d}z} = -\gamma(v^* - w),$$

where $v^* = 0$ on $S_{\mathrm{S}}^{1,2}$ and $v^* = 1$ on $S_{\mathrm{S}}^{3,4}$. These are solved by

$$w(z) = C_1^{1,2}e^{\sqrt{\gamma}z} + C_2^{1,2}e^{-\sqrt{\gamma}z},\ s(z) = C_1^{1,2}\sqrt{\gamma}e^{\sqrt{\gamma}z} - C_2^{1,2}\sqrt{\gamma}e^{-\sqrt{\gamma}z} \tag{3.19}$$

on $S_{\mathrm{S}}^{1,2}$, and

$$w(z) = 1 + C_1^{3,4}e^{\sqrt{\gamma}z} + C_2^{3,4}e^{-\sqrt{\gamma}z},\ s(z) = C_1^{3,4}\sqrt{\gamma}e^{\sqrt{\gamma}z} - C_2^{3,4}\sqrt{\gamma}e^{-\sqrt{\gamma}z} \tag{3.20}$$

on $S_{\mathrm{S}}^{3,4}$, for arbitrary constants $C_{1,2}^{1,2,3,4} \in \mathbb{R}$. These constants are determined by the asymptotic boundary conditions (3.8) and by the dynamics of the layer problem (3.14). Consequently, the constants are dependent on the specific α-value, see Fig. 3.5.3. We now must distinguish between the three different α-cases, $0 < \alpha < 1,\ 1 < \alpha < 2,\ \alpha > 2$, in order to analyse the specific dynamics in each case.

3.5.2 $0 < \alpha < 1$

To further study the slow TW solutions for $0 < \alpha < 1$, we divide our spatial domain (in the slow variable z) into two slow fields $I_{\mathrm{s}}^{\pm}$ – away from the layer dynamics – and one fast field I_{f} – near the layer dynamics. In particular,

$$I_{\mathrm{s}}^{-} := (-\infty, -\varepsilon^{3/8}),\ I_{\mathrm{f}} := [-\varepsilon^{3/8}, \varepsilon^{3/8}],\ I_{\mathrm{s}}^{+} := (\varepsilon^{3/8}, \infty), \tag{3.21}$$

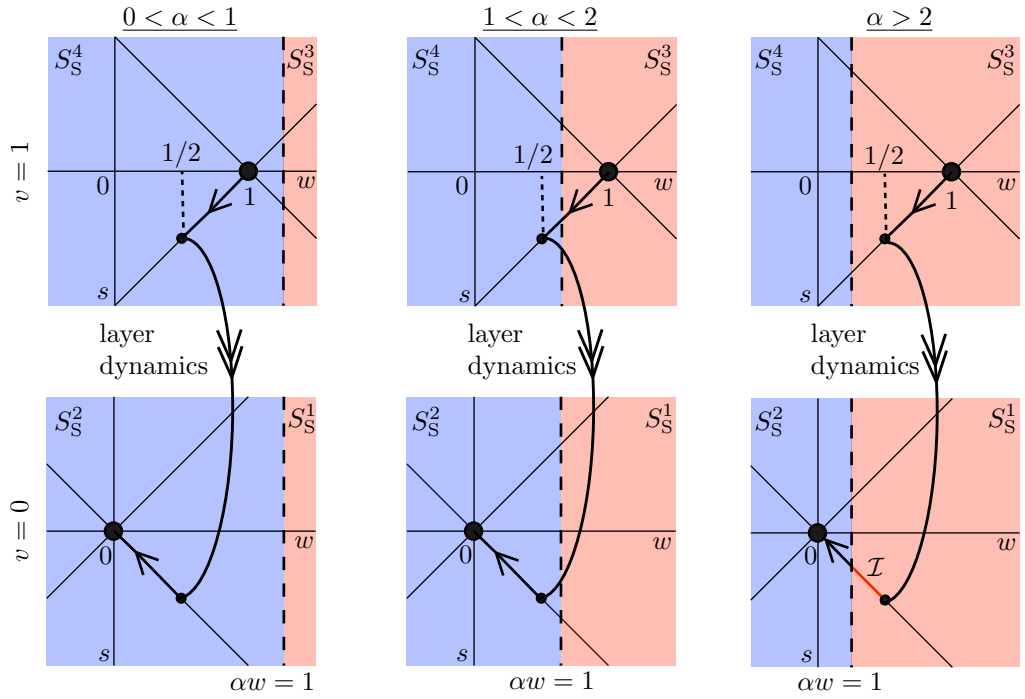

Figure 3.5.3: Schematic depiction of the slow flow on the different components of the critical manifold for the three different heteroclinic orbits associated to the three different types of slow TW solutions, see also Fig. 3.5.1 and Fig. 3.5.2. The jump between the branches of the slow manifold, i.e. the fast transition, occurs at $w = 1/2$ in each of the three cases. The black dashed lines at $\alpha w = 1$ indicate the locations where the manifolds coincide on the respective branches and where the heteroclinic orbits change manifolds. We only observe an interstitial gap in the latter case where $\alpha > 2$ (*i.e.* red curve labelled $\mathcal{I}$ on S_S^1 in the bottom right frame).

where we, without loss of generality, assumed that the layer dynamics is centred around zero. The asymptotic scaling $\varepsilon^{3/8}$ of the boundaries of these fast and slow fields is chosen such that it is asymptotically small with respect to the slow variable z and asymptotically large with respect to the fast variable $y := \varepsilon^{-1/2} z$. In particular, $\varepsilon^{3/8} \ll 1$, while $\varepsilon^{3/8-1/2} \gg 1$.

As $z \to -\infty$ the heteroclinic orbit associated to the slow TW solution should approach Z^- (3.8) and, hence, the critical manifold of interest is S_S^4 for $z \in I_s^-$ (see the top left frame of Fig. 3.5.3). Consequently, the slow w and s components are given by (3.20). To ensure that the solution has the correct asymptotic behaviour as $z \to -\infty$ we must set $C_2^4 = 0$. Similarly, for $z \in I_s^+$ the critical manifold of interest is S_S^2 (see the bottom left frame of Fig. 3.5.3) and the slow w and s components are given by (3.19) with $C_1^2 = 0$.

During the transition through the fast field I_f, the ε-dependent slow equations (w, s) are given by

$$\frac{\mathrm{d}w}{\mathrm{d}y} = \sqrt{\varepsilon} s, \quad \frac{\mathrm{d}s}{\mathrm{d}y} = -\varepsilon c s - \sqrt{\varepsilon}\gamma(v - w). \tag{3.22}$$

Therefore, and by the asymptotic scale of the fast field, the change of both w and s are, to leading order, constant during this transition. In other words, both w and s should match to leading order at zero. This determines the two remaining integration constants C_1^4 and C_2^2 and gives

$$w(z) = \begin{cases} 1 - \dfrac{1}{2}e^{\sqrt{\gamma}z}\,, & z \in I_{\mathrm{s}}^-\,, \\ \dfrac{1}{2}e^{-\sqrt{\gamma}z}\,, & z \in I_{\mathrm{s}}^+\,, \end{cases} \qquad s(z) = \begin{cases} -\dfrac{1}{2}\sqrt{\gamma}e^{\sqrt{\gamma}z}\,, & z \in I_{\mathrm{s}}^-\,, \\ -\dfrac{1}{2}\sqrt{\gamma}e^{-\sqrt{\gamma}z}\,, & z \in I_{\mathrm{s}}^+\,. \end{cases} \tag{3.23}$$

Hence, the fast transition always occurs at $w = 1/2$ and the leading order profiles in the slow fields are now known (by combining (3.15) and (3.23)) for the five different components. In particular,

$$u(z) = \begin{cases} (1-\alpha) + \dfrac{\alpha}{2}e^{\sqrt{\gamma}z}\,, & z \in I_{\mathrm{s}}^-\,, \\ 1 - \dfrac{\alpha}{2}e^{-\sqrt{\gamma}z}\,, & z \in I_{\mathrm{s}}^+\,. \end{cases} \tag{3.24}$$

What remains is understanding the layer dynamics in the fast field I_{f}. In this fast field the dynamics of the heteroclinic orbit is, to leading order, determined by (3.14), and the orbit has to transition from S_{S}^4 (where $\Re(\lambda_{1,2}^4) > 0$ and $\Re(\lambda_3^4) < 0$) to S_{S}^2 (where $\Re(\lambda_1^2) > 0$ and $\Re(\lambda_{2,3}^2) < 0$). Since w is to leading order constant in the fast field, the u-equation of (3.14) is of logistic-type and, by (3.15), $u = 1 - \alpha w$ on both $S_{\mathrm{S}}^{2,4}$. Consequently, and since the logistic equation does not support pulse-type solutions, u is also constant during the fast transition. In particular, $u = 1 - \alpha w = 1 - \alpha/2$ in I_{f}, see (3.24). The resulting (v, r)-equations (3.14), with $u = 1 - \alpha/2$, can be written as

$$\frac{\alpha}{2}\frac{\mathrm{d}^2 v}{\mathrm{d}y^2} + c\frac{\mathrm{d}v}{\mathrm{d}y} + \beta v(1-v) = 0\,, \tag{3.25}$$

which is exactly the TW ODE associated to TWs in the classical Fisher–KPP equation[6]. Hence, there exists a heteroclinic connection between $(v, r) = (1, 0)$ and $(v, r) = (0, 0)$ in the fast field. In addition, the (v, r)-components are nonnegative during this transition if, and only if, $c \geq c_{min} := \sqrt{2\alpha\beta}$ [7] – the so-called *minimum wave speed* of the associated Fisher-KPP equation – see, for instance, [79] and references therein. The last observation also follows directly from the fact that $\lambda_{2,3}^2$ (3.18) – with $w = 1/2$ – are complex-valued for $c < c_{min}$. Moreover, observe that the first components of the eigenvectors $\vec{v}_{2,3}$ (3.17) associated to $\lambda_{2,3}$ are zero, that is, the u-component indeed does not change during the fast transition. This completes the analysis of the layer problem, and hence the analysis of the heteroclinic orbits for $0 < \alpha < 1$, in the singular limit $\varepsilon \to 0$.

[6] This does not come as a surprise since the V-component of the original PDE (3.1), in the fast variable y and for $U = 1 - \frac{1}{2}\alpha$, is the Fisher–KPP equation $V_\tau = \beta V(1-V) + \frac{\alpha}{2}V_{yy}$.

[7] The expression for c_{min} also arose from the formal analysis of [27].

Persistence for $0 < \varepsilon \ll 1$

For $0 < \alpha < 1$, we show the persistence of the singular heteroclinic orbits for sufficiently small ε in (3.7)-(3.9) (with $p = 1/2$) and thus the existence of slow TW solutions in (3.1). By (3.24), a singular orbit only approaches $u = 1$ in the limit $z \to \infty$ (see also Remark 3.4.1). Furthermore, as $0 < \alpha < 1$ and as w is given by (3.23), we have that $\alpha w \neq 1$ along the singular orbit. Therefore, the critical manifold S_{S}^0 does not lose normal hyperbolicity along the singulars orbit and each singular orbit is a heteroclinic connection between two normally hyperbolic components of the critical manifold. Fenichel's First Persistence Theorem [30] states that, for ε small enough (and after appropriately compactifying S_{S}^2 and S_{S}^4), there exist locally invariant slow manifolds $S_{\mathrm{S},\varepsilon}^2$ and $S_{\mathrm{S},\varepsilon}^4$ in the full ε-dependent system (i.e. (3.7)-(3.9) with $p = 1/2$) that are $\mathcal{O}(\sqrt{\varepsilon})$-close to S_{S}^2 and S_{S}^4, respectively. Observe that $Z^{\pm}$ (3.8) are independent of ε and, hence, $S_{\mathrm{S},\varepsilon}^{2,4}$ coincide with $S_{\mathrm{S}}^{2,4}$ in the asymptotic limits $z \to \pm\infty$. Fenichel's Second Persistence Theorem [30] states that the full ε-dependent system also possesses locally invariant stable and unstable manifolds $\mathcal{W}^u(S_{\mathrm{S},\varepsilon}^4)$ and $\mathcal{W}^s(S_{\mathrm{S},\varepsilon}^2)$ which are $\mathcal{O}(\sqrt{\varepsilon})$-close to the stable and unstable manifolds $\mathcal{W}^u(S_{\mathrm{S}}^4)$ and $\mathcal{W}^s(S_{\mathrm{S}}^2)$, respectively. We also have the necessary property of the singular problem that the heteroclinic connections (singular orbits) are contained in the intersection $\mathcal{W}^u(S_{\mathrm{S}}^4) \cap \mathcal{W}^s(S_{\mathrm{S}}^2)$ and it follows that the orbit persists (in the intersection of $\mathcal{W}^u(S_{\mathrm{S},\varepsilon}^4) \cap \mathcal{W}^s(S_{\mathrm{S},\varepsilon}^2)$) for $0 < \varepsilon \ll 1$ if the intersection $\mathcal{W}^u(S_{\mathrm{S}}^4) \cap \mathcal{W}^s(S_{\mathrm{S}}^2)$ is transversal, see [39, 51, 53, e.g.].

The slow TW problem has three fast variables (u, v, r) and two slow variables (w, s). Moreover, for $0 < \alpha < 1$, $\Re(\lambda_1^2) > 0$ and $\Re(\lambda_{2,3}^2) < 0$, see (3.18). Therefore, $\dim(\mathcal{W}^s(S_{\mathrm{S},\varepsilon}^2)) = \dim(\mathcal{W}^s(S_{\mathrm{S}}^2)) = 2 + 2 = 4$.[8] Similarly, $\Re(\lambda_{1,2}^4) > 0$ and $\Re(\lambda_3^4) < 0$ and, consequently, $\dim(\mathcal{W}^u(S_{\mathrm{S},\varepsilon}^4)) = \dim(\mathcal{W}^u(S_{\mathrm{S}}^4)) = 2 + 2 = 4$. Generically, two four-dimensional objects in a five-dimensional phase space intersect transversally. The transversality of the intersections is typically shown through a Melnikov integral [68, 86, 97, e.g.]. However, for this specific system, we take advantage of the additional structures of the problem. We define the so-called *take-off curve* as the unstable direction from which the singular orbit leaves Z^- on S_{S}^B, the *jump point* as the point on the take-off curve where a solution leaves the critical manifold to make the fast transition, and the *touchdown curve* as the union of points on S_{S}^A a solution could land on after the fast transition. Due to the fact that u, w, s are, to leading order, constant across the fast transition, the touchdown curve is the projection of the take-off curve onto S_{S}^A. The existence of an orbit relies on the fact that the touchdown curve intersects the stable direction of Z^+ and it is clear this intersection is transversal, see Fig. 3.5.3. The fact that this stable direction intersects the touchdown curve transversally is an indicator that the intersection $\mathcal{W}^u(S_{\mathrm{S}}^4) \cap \mathcal{W}^s(S_{\mathrm{S}}^2)$ is also transversal. Furthermore, during the fast transition, i.e. in the intersection $\mathcal{W}^s(S_{\mathrm{S}}^4) \cap \mathcal{W}^u(S_{\mathrm{S}}^4)$, u is constant and the dynamics during this transition are controlled by a Fisher-KPP-type

[8] The first "2" originates from the number of eigenvalues (3.18) on S_{S}^2 with negative real part (i.e the number of fast stable eigenvalues), while the second "2" comes from the number of slow variables.

equation (3.25) whose end state (in the two-dimensional state space (v, r)) has no unstable directions and supports a continuous family of TWs in c, implying the persistence of solutions under an ε perturbation. We exploit these structures in order to prove the transversality of the intersection $\mathcal{W}^u(S^4_{\mathrm{S}}) \cap \mathcal{W}^s(S^2_{\mathrm{S}})$.

We first analyse the behaviour of the 4−dimensional stable subspace $\mathcal{W}^s(S^2_{\mathrm{S}})$ and observe that the tangent space $T\mathcal{W}^s(S^2_{\mathrm{S}})$ at points in S^2_{S} is spanned by the four vectors $(0, \lambda^2_{2,3}, -\beta, 0, 0)^T$, $((1-\alpha)_+, 0, 0, 1, 0)^T$, $(0, 0, 0, 0, 1)^T$. The first three elements of the vectors $(0, \lambda^2_{2,3}, -\beta, 0, 0)^T$ are the stable eigenvectors $\vec{v}_{2,3}$ respectively, see (3.17), of the Jacobian evaluated on S^2_{S} appended with two 0 components representing w, s – components which remain constant across the fast transition. The latter vectors $((1-\alpha)_+, 0, 0, 1, 0)^T$, $(0, 0, 0, 0, 1)^T$ span the manifold S^2_{S}. Of the vectors that span $T\mathcal{W}^s(S^2_{\mathrm{S}})$ only $(0, \lambda^2_{2,3}, -\beta, 0, 0)^T$ will change under the evolution along the layer fibre. This is because the layer transition is governed by a Fisher-KPP-type equation in v, r, and the other components are to leading order constant. Additionally, as the end state of the Fisher-KPP equation has no unstable directions the space spanned by these two vectors will always contain the space spanned by $(0, 1, 0, 0, 0)^T$ and $(0, 0, 1, 0, 0)^T$, i.e. the basis vectors of the (v, r) phase space. Furthermore, $\vec{v}_1 \in \mathcal{W}^u(S^4_{\mathrm{S}})$ and $\vec{v}_1 \to (f(1-\alpha, 1, c, \alpha, c, 1/2), 0, 0)$ as the orbit approaches S^4_{S} in backwards z. Thus, $\vec{v}_1$, appended with zeros for w, s, is in the tangent space $T\mathcal{W}^u(S^4_{\mathrm{s}})$ and is proportional to $(1, 0, 0, 0, 0)^T$. This vector is linearly independent to the four vectors that span $T\mathcal{W}^s(S^2_{\mathrm{S}})$. At any point along the layer fibre, the combined tangent spaces of $\mathcal{W}^s(S^2_{\mathrm{S}})$ and $\mathcal{W}^u(S^4_{\mathrm{S}})$ contain the full tangent space to $\mathbb{R}^5$. From this, it follows directly that the intersection is transversal and the heteroclinic connection persists for $0 < \varepsilon \ll 1$ [39, 51, 53, 97, e.g.]. Consequently, (3.1) supports slow TW solutions for $0 < \alpha < 1$ and for sufficiently small ε.

3.5.3 $\alpha > 1$

For $\alpha > 1$ the situation is more involved since a dynamical transcritical bifurcation of critical manifolds is involved (when $\alpha w = 1$), see Fig. 3.5.2. This critical bifurcation occurs to the left (with respect to z) of the layer transition (at $z = 0$) for $1 < \alpha < 2$, while it occurs to the right of the layer transition for $\alpha > 2$. The latter case results in an interstitial gap only because part of the heteroclinic orbit is on S^1_{S} where both u, representing the normal cell density, and v, representing the tumour cell density, are zero to leading order. However, in both cases we can still use the same slow-fast splitting of the spatial domain (3.21) in the singular limit $\varepsilon \to 0$. Furthermore, the layer problem still exhibits Fisher–KPP type behaviour.

In more detail, since $\alpha > 1$ the heteroclinic orbit associated to the slow TW solution should approach $Z^- \in S^3_{\mathrm{S}}$, see (3.8) and (3.15), as $z \to -\infty$. Hence, the critical manifold of interest is S^3_{S} (3.15) for $-z \gg 1$. Consequently, the slow w and s components are

given by (3.20) and – to ensure that the solution has the correct asymptotic behaviour – $C_2^3 = 0$. That is,

$$w(z) = 1 + C_1^3 e^{\sqrt{\gamma}z}\,,\ s(z) = C_1^3\sqrt{\gamma}e^{\sqrt{\gamma}z}\,,\ \text{for } -z \gg 1. \tag{3.26}$$

Similarly, for $z \in I_{\rm s}^+$ the critical manifold of interest is $S_{\rm S}^2$ (since $Z^+ \in S_{\rm S}^2$) and the slow w and s components are given by (3.19) with $C_1^2 = 0$:

$$w(z) = C_2^2 e^{-\sqrt{\gamma}z}\,,\ s(z) = -C_2^2\sqrt{\gamma}e^{-\sqrt{\gamma}z}\,,\ \text{for } z \in I_{\rm s}^+. \tag{3.27}$$

The two critical manifolds $S_{\rm S}^{2,3}$ both undergo a (different) dynamical transcritical bifurcation at $\alpha w = 1$. If this bifurcation occurs at $z = \check{z} < 0$ (to the left of the layer transition at $z = 0$) then the heteroclinic orbit passes from $S_{\rm S}^3$ onto $S_{\rm S}^4$. In contrast, if this bifurcation occurs at $z = \hat{z} > 0$ (to the right of the layer transition) then the heteroclinic orbit transitions from $S_{\rm S}^1$ onto $S_{\rm S}^2$.

In the former case where the transition occurs at $z = \check{z} < 0$, we get that the slow w and s components after the transition are given by

$$w(z) = 1 + C_1^4 e^{\sqrt{\gamma}z} + C_2^4 e^{-\sqrt{\gamma}z}\,,\ s(z) = C_1^4\sqrt{\gamma}e^{\sqrt{\gamma}z} - C_2^4\sqrt{\gamma}e^{-\sqrt{\gamma}z}\,,\quad \text{for } z \in I_{\rm s}^- \text{ and } z > \check{z}, \tag{3.28}$$

see (3.20). However, by construction, the slow components should match as z approaches $\check{z}$. So, from combining (3.26) and (3.28), we get

$$w(z) = 1 + C_1^3 e^{\sqrt{\gamma}z}\,,\ s(z) = C_1^3\sqrt{\gamma}e^{\sqrt{\gamma}z}\,,\ \text{for } z \in I_{\rm s}^-, \tag{3.29}$$

see Fig. 3.5.3. Since the change of both w and s are, to leading order, constant during the transition through the fast field $I_{\rm f}$, see (3.22), if follows that (3.27) and (3.29) should match as z approaches zero. Furthermore, for $\alpha < 1$, the slow components are given by (3.23). Hence, $\check{z} \in I_{\rm s}^-$ such that $\alpha w(\check{z}) = 1$ is given by $\check{z} = \gamma^{-1/2}\log(2(\alpha-1)/\alpha) =: z_-$ (3.5), and $\check{z}$ is negative only for $1 < \alpha < 2$. That is, the dynamical transcritical bifurcation occurs only to the left of the layer transition, and the heteroclinic orbit transitions from $S_{\rm S}^3$ to $S_{\rm S}^4$, if $1 < \alpha < 2$. See also Fig. 3.5.2 and Fig. 3.5.3. As before, the leading order profiles in the slow fields are now known for all the components, and, in particular,

$$u(z) = \begin{cases} 0\,, & z < z_-\,, \\ (1-\alpha) + \dfrac{\alpha}{2}e^{\sqrt{\gamma}z}\,, & z > z_- \text{ and } z \in I_{\rm s}^-\,, \\ 1 - \dfrac{\alpha}{2}e^{-\sqrt{\gamma}z}\,, & z \in I_{\rm s}^+\,. \end{cases} \tag{3.30}$$

We proceed in a similarly fashion in the case where the bifurcation occurs to the right of the layer transition at $z = \hat{z} > 0$. Again, we obtain that the slow components in the

slow fields are given by (3.23). Consequently, $\hat{z} \in I_{\mathrm{s}}^{+}$ such that $\alpha w(\hat{z}) = 1$ is given by $\hat{z} = \gamma^{-1/2}\log(\alpha/2) =: z_{+}$ (3.2), and $\hat{z}$ is positive only for $\alpha > 2$. That is, the dynamical transcritical bifurcation only occurs to the right of the layer transition and the heteroclinic orbit transitions from S_{S}^{1} to S_{S}^{2}, if $\alpha > 2$, see Fig. 3.5.2 and Fig. 3.5.3. The leading order profiles in the slow fields are now known and the u-component is given by

$$u(z) = \begin{cases} 0\,, & z \in I_{\mathrm{s}}^{-}\,, \\ 0\,, & z < z_{+} \text{ and } z \in I_{\mathrm{s}}^{-}\,, \\ 1 - \dfrac{\alpha}{2}e^{-\sqrt{\gamma}z}\,, & z > z_{+}. \end{cases} \tag{3.31}$$

For both $1 < \alpha < 2$ and $\alpha > 2$, the layer dynamics in the fast field I_{f} is the same as for $0 < \alpha < 1$ in §3.5.2. That is, due to the logistic nature of the u-component in (3.14) and the particulars of the critical manifolds involved, the fast u-component actually does not change during the transition through the fast field I_{f}. Consequently, the layer transition is associated to a Fisher–KPP equation. In particular, for $1 < \alpha < 2$ the associated TW ODE is still given by (3.25) (since u is still $1 - \alpha/2$ during the transition, see (3.30)). For $\alpha > 2$ the associated TW ODE is

$$\frac{\mathrm{d}^2 v}{\mathrm{d}y^2} + c\frac{\mathrm{d}v}{\mathrm{d}y} + \beta v(1-v) = 0\,,$$

since $u = 0$ during the transition, see (3.31). Hence, in both cases there exists a heteroclinic connection between $(v, r) = (1, 0)$ and $(v, r) = (0, 0)$ in the fast field. The (v, r)-components are nonnegative for $1 < \alpha < 2$ if, and only if, $c \geq c_{min} := \sqrt{2\alpha\beta}$ (*i.e.* $\lambda_{2,3}^{2}$ (3.18) are real-valued). In contrast, the (v, r)-components are nonnegative for $\alpha > 2$ if, and only if, $c \geq \bar{c}_{min} := 2\sqrt{\beta}$ (*i.e.* $\lambda_{2,3}^{1}$ (3.18) are real-valued). This completes the analysis of the layer problem, and hence the analysis of the heteroclinic orbits in the singular limit $\varepsilon \to 0$, for $\alpha > 1$.

Persistence for $0 < \varepsilon \ll 1$

For $\alpha > 1$, we show the persistence of the singular heteroclinic orbits for sufficiently small ε in (3.7)-(3.9) (with $p = 1/2$) and thus the existence of slow TW solutions in (3.1). The added complexity – compared to the $0 < \alpha < 1$ case discussed in §3.5.2 – is related to showing the persistence of the transcritical dynamical bifurcation structure around $\alpha w = 1$ since the critical manifold S_{S}^{0} loses normal hyperbolicity here. In addition, as in the $0 < \alpha < 1$ case, the persistence of solutions across the fast transition will be shown.

The transcritical singularity results from the self-intersection of the critical manifold along the line $\alpha w = 1$. The persistence of the transcritical dynamical bifurcation structure around $\alpha w = 1$ follows from the observation that $u = 0$ is invariant for the full ε-dependent system ((3.7) with $p = 1/2$). Hence, we have $u = 0$ on the perturbed manifolds

$S^{1,3}_{\mathrm{S},\varepsilon}$. Furthermore, away from $\alpha w = 1$ the perturbed manifolds $S^{2,4}_{\mathrm{S},\varepsilon}$ are, to leading order, given by $S^{2,4}_{\mathrm{S}}$. Therefore, the intersection between S^4_{S} and S^3_{S} and the intersection between S^2_{S} and S^1_{S} must persist in the full ε-dependent system.

The persistence of singular orbits across the fast transition for $0 < \varepsilon \ll 1$ is shown by proving the transversality of the intersection $\mathcal{W}^u(S^4_{\mathrm{S}}) \cap \mathcal{W}^s(S^2_{\mathrm{S}})$ for $1 < \alpha < 2$, and the transversality of the intersection $\mathcal{W}^u(S^3_{\mathrm{S}}) \cap \mathcal{W}^s(S^1_{\mathrm{S}})$ for $\alpha > 2$. The argument follows similarly to the $0 < \alpha < 1$ case. The fast transition is governed by a Fisher-KPP-type equation (3.25) in each case and one can explicitly calculate the spanning vectors of the relevant tangent spaces in order to prove that the combined tangent spaces (of $\mathcal{W}^u(S^4_{\mathrm{S}})$ and $\mathcal{W}^s(S^2_{\mathrm{S}})$ for $1 < \alpha < 2$ and of $\mathcal{W}^u(S^3_{\mathrm{S}})$ and $\mathcal{W}^s(S^1_{\mathrm{S}})$ for $\alpha > 2$) contain the full tangent space to $\mathbb{R}^5$. Hence, the intersection is transversal in each case and the heteroclinic connections persists for $1 < \alpha < 2$ and $\alpha > 2$ [39, 51, 53, 97, e.g.]. Consequently, (3.1) supports slow TW solutions for $1 < \alpha < 2$ and $\alpha > 2$ for sufficiently small ε.

3.6 Summary and outlook

In this chapter, we analysed TW solutions supported by the nondimensionalised Gatenby–Gawlinski model (3.1). This model was originally proposed by Gatenby and Gawlinski in [32] to investigate the acid-mediation hypothesis of the Warburg effect, also known as aerobic glycolysis [104]. This hypothesis postulates that this Warburg effect is caused by the fact that the progression of certain tumours is facilitated by the acidification of the region around the tumour-host TW interface and this leads to an advantage of the tumour cells [33]. In the model, the acid-mediation hypothesis is characterised by an interstitial gap, a region in front of the invading TW interface devoid of cells, see also Fig. 3.2.1. The TW solutions of (3.1) have been analysed numerically in [32] and by using formal matched asymptotics in [27]. In particular, in [27] it was shown that the Gatenby–Gawlinski model (3.1) supports slow and fast TW solutions. Here, "slow" and "fast" refer to the asymptotic scaling of the speed c of a TW solution with respect to the small parameter ε (that measures the strength of the nonlinear diffusion of the tumour).

In this chapter, we embedded the TW problem associated to (3.1) into a slow-fast[9] structure and use geometric singular perturbation techniques to prove the formal results of [27] in the critical cases ($c \sim \mathcal{O}(1)$ and $c \sim \mathcal{O}(\sqrt{\varepsilon})$). In particular, we showed that the interstitial gap is present only if the destructive influence of the acid, modelled by the parameter α in (3.1), is strong enough. That is, the interstitial gap exists only for $\alpha > 2$, see also [27]. We showed that, from a geometric perspective, the interstitial gap can be understood as the distance between the TW interface – which has the characteristics of a Fisher–KPP wave – and a dynamical transcritical bifurcation of two parts of the critical manifold. For moderate strengths of the destructive influence of the acid, *i.e.* for

[9]Here, *slow-fast* refers to the difference in asymptotic scaling of the (nonlinear) diffusion coefficient of (3.1)

$1 < \alpha < 2$, parts of the critical manifold involved still undergo a dynamical transcritical bifurcation, however, this now occurs behind the TW interface and no region devoid of cells is thus created, see, for instance, the middle panel of Fig. 3.5.1.

3.6.1 Spectral stability of the Gatenby-Galenski model

The results of this chapter show that the Gatenby–Gawlinski model (3.1) supports, even for a fixed parameter set, a myriad of TW solutions with different speeds. A logical next question to answer is related to wave speed selection. That is, given a specific parameter set and initial condition, what is – if any – the speed of the TW solution the initial condition converge to? Because of the Fisher-KPP imprint of the V-component of the model, it can be expected that a dispersion relation relating the asymptotic behaviour of an initial condition around plus infinity and the linear spreading speed of the TW solution can be derived, see, for instance, [69,76,79]. However, a TW solution will not always travel with this linear spreading speed, see, for instance, [36]. It is also interesting to see if the observed wave speeds for the slow TW solutions equal the minimum wave speeds of the associated Fisher-KPP equations ($c_{min} := \sqrt{2\alpha\beta}$ for $0 < \alpha < 2$ and $\bar{c}_{min} := 2\sqrt{\beta}$ for $\alpha > 2$, see §3.5). That is, are the observed slow TW solutions *pushed* or *pulled fronts* [102]?

A first natural step to start tackling these questions is to study the stability properties of the slow and fast TW solutions, and a potential approach is to combine the analytic approach used in Chapter 2 with the Riccati Evans function approach developed in [35] to numerically compute eigenvalues.

3.6.2 Extensions and generalisations of the Gatenby-Galenski model

The Gatenby–Gawlinski model (3.1) is amendable for analysis because the nonlinear diffusion term in the equation for the tumour cells acts as a regular perturbation to the normal diffusion term (as U is constant to leading order during the fast transition), and the underlying equation has a Fisher-KPP imprint. A simplified model, obtained via a quasi-steady state reduction [62] of the full model, is given by

$$\begin{cases} \dfrac{\partial U}{\partial \tau} = U(1 - U - \alpha W), \\ \dfrac{\partial W}{\partial \tau} = \gamma(H(-x) - W) + \dfrac{\partial^2 W}{\partial x^2}, \end{cases}$$

where $H(\cdot)$ is the Heaviside step-function replacing the V-component of (3.1). This simplified model has similar characteristics to the full model (3.1), and, crucially, still supports TW solutions with an interstitial gap of length z_+ for $\alpha > 2$.

Finally, while we only establish the existence of slow and fast TW solutions to the original Gatenby–Gawlinski model (3.1), the methodology of embedding the problem into a slow-fast structure and subsequently studying the dynamics of the reduced and layer problems can also be used to prove the existence of TW solutions in generalizations of the Gatenby–Gawlinski model (such as models (3.3) and (3.4) studied in [42], respectively [75]). The argument for the persistence of solutions across the dynamical transcritical bifurcation for $0 < \varepsilon \ll 1$ follows from the invariance of $u = 0$ in the full ε-dependent system (3.7). A mathematically interesting question is whether this dynamical transcritical bifurcation also persists for similar systems where this invariance is broken, see [67, 72].

Chapter 4

Stability of defect solutions

Abstract

In this chapter we analyse the stability of *trivial defect solutions*. These solutions are, to leading order, constant solutions to a general $n-$dimensional system of RDEs with a small, spatially dependent, jump-type defect included. This work can be seen as a natural extension of [21] where the existence conditions for trivial and local defect solutions were established for a general system of ODEs with a small, spatially dependent, jump-type defect. We utilise these existence results as we analyse the stability of defect solutions to the RDE studied in this chapter. The analysis of trivial defect solutions in this chapter primarily concerns tracking potential point spectra that, upon the inclusion of the jump-type defect, emerge from the branch points of the absolute spectrum associated with the spatially homogeneous problem (see §1.3.4 for an introduction to the absolute spectrum). These potential point spectra are tracked as roots of an expansion of the Evans function (see §1.3.6 for an introduction to the Evans function) and emerge as $\mathcal{O}(\varepsilon)$ corrections to the temporal eigenvalue. The stability analysis of the trivial defect solutions can be seen as first step towards the stability analysis of local defect solutions.

4.1 Introduction

RDEs are relatively simple partial differential equations which exhibit a wide range of complex behaviours and patterns. The analysis of spatially localized stationary solutions and travelling waves, solutions that move with a constant speed and maintain their shape, are integral in the study of pattern formation. Much of the existing analysis on the existence and stability of stationary and travelling wave solutions has assumed spatially homogeneous background states. However, spatially dependent inhomogeneities can have a profound impact on the type of solutions, patterns formed and stability conditions. For example, travelling waves may be pinned, reflected, annihilated or split upon meeting an inhomogeneity [98, 100]. The analysis in this chapter focuses on step-function defects. Various approaches have been used for both the existence and stability analysis of RDEs with a step-function defect, such as [100] where pinned solutions are shown to exist for a three component FitzHugh-Nagumo type system using geometric singular perturbation theory. In [14] the stability of pinned solutions to the sine-Gordon equation with a step-function inhomogeneity are analysed using the underlying Hamiltonian structure. In [55] perturbations of near integrable problems are analysed utilising the structure of the leading order problem and in [13, 64] the stability of inhomogeneous waves with an

underlying Hamiltonian structure were studied. In [13] a finite length inhomogeneity was considered. A finite length inhomogeneity can be treated as two jump-type defects. As long as the inhomogeneity is sufficiently small it can be treated as weak defects and dealt with through the same methods outlined in this chapter. In [105] the authors analyse the front selection, existence and stability of travelling wave solutions to scalar equations in periodic media, slowly varying media and randomly varying media. The stability of stationary solutions to a perturbed RDE was considered in [54]. An expansion of the Evans function was formulated and a stability condition derived under the assumption that the perturbation is smooth, whilst the analysis of this chapter violates this smoothness assumption.

Here, we consider a generic RDE and add a step-function type perturbation. That is, we take the following $n-$dimensional RDE,

$$U_t = DU_{xx} + f(U), \tag{4.1}$$

with $(x,t) \in \mathbb{R}\times\mathbb{R}^+$, $f(U) : \mathbb{R}^n \to \mathbb{R}^n$ is a sufficiently smooth function and D is a diagonal matrix of diffusion coefficients which are assumed to be strictly positive, see Remark 4.1.1. We add a spatially dependent jump-type perturbation to obtain,

$$U_t = DU_{xx} + f(U) + \begin{cases} 0 & x \leq 0 \\ \varepsilon g(U) & x > 0, \end{cases} \tag{4.2}$$

where ε is a small parameter and $g(U) : \mathbb{R}^n \to \mathbb{R}^n$ is a sufficiently smooth function that is $\mathcal{O}(1)$ with respect to ε. We will refer to (4.1) as the *unperturbed PDE* and (4.2) as the *perturbed PDE*. The techniques outlined in [105] cannot be directly applied to (4.2) as the analysis of scalar solutions relies quite heavily on considering sub-solutions and super-solutions.

We analyse the impact of the jump-type defect on the stability of stable, stationary solutions to (4.1). However, we must first establish the existence of these stationary solutions as any assumptions, or conditions, that arise must be taken into account in the stability analysis. The existence equation associated with the unperturbed PDE (4.1), expressed as a system of first order ODEs, is the following $2n$-dimensional system,

$$\begin{pmatrix} u \\ v \end{pmatrix}' = \begin{pmatrix} v \\ -D^{-1}f(u) \end{pmatrix}. \tag{4.3}$$

Similarly, the existence equation associated with the perturbed PDE (4.2), expressed as a system of first order ODEs, is the following $2n$-dimensional system,

$$\begin{pmatrix} u \\ v \end{pmatrix}' = \begin{pmatrix} v \\ -D^{-1}f(u) \end{pmatrix} + \begin{cases} \begin{pmatrix} 0 \\ 0 \end{pmatrix} & x \leq 0, \\ \begin{pmatrix} 0 \\ -\varepsilon D^{-1}g(u) \end{pmatrix} & x > 0, \end{cases} \tag{4.4}$$

with $' = d/dx$, $v := u_x$ and $u, v \in \mathbb{R}^n$. We will refer to (4.3) as the *unperturbed existence equation* and to (4.4) as the *perturbed existence equation*. For the sake of clarity, throughout this chapter we will refer to the Jacobian matrices of the right-hand sides of (4.4) and (4.3) as the *Jacobian matrices* whereas we will refer to the Jacobian matrices associated with $f(u)$ and $g(u)$, denoted $J_f(u)$ and $J_g(u)$ respectively, as the *sub-Jacobian matrices*. Furthermore, we will refer to the eigenvalues of the Jacobian and sub-Jacobian matrices as *matrix eigenvalues*.

Following the definition of [21], a defect solution $\Gamma_\varepsilon(x)$ of (4.4) is defined as a solution to the perturbed existence equation (4.4) that approaches (in a graph sense) a solution $\Gamma(x)$ to the unperturbed existence equation (4.3) in the $\varepsilon \to 0$ limit, *i.e.* $\lim_{\varepsilon\to 0} \Gamma_\varepsilon(x) = \Gamma(x)$. There are three types of defect solutions identified in [21]; trivial defect solutions, local defect solutions and global defect solutions, see Figure 4.2.1 and Definition 4.2.1. This chapter will focus primarily on the analysis of the stability of trivial defect solutions.

In §4.2 we begin with a recap of the relevant existence analysis of [21] outlining how the hypotheses, assumptions and existence conditions of that paper apply to (4.4) in order to proceed with our stability analysis. We then set-up the perturbed stability problem. In §4.3 we formulate the Evans function for a trivial defect solution to a scalar bistable PDE as an illustrative example. We end the chapter by outlining how this method will be generalised for the stability analysis of the trivial defect solution to the n-dimensional problem.

Remark 4.1.1. *The assumption that the matrix of diffusion coefficients contains strictly positive entries is necessary as we frequently utilise the inverse of the diffusion matrix. If there is a zero entry in the diffusion matrix the existence problem associated with the perturbed problem* (4.2) *is a diffeo-algebraic problem which must be restricted to the manifold defined by the algebraic constraints before proceeding in a similar fashion.*

4.2 Set-up, definitions, and main results

We first outline the relevant existence results of the defect solutions as derived in [21] and set-up the stability problem. We begin with the formal definition of the different types of defect solutions, then we establish the existence and stability hypotheses of the

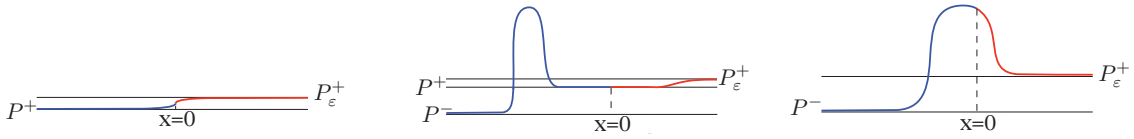

Figure 4.2.1: A depiction of three types of defect solutions. The defect occurs at the point $x = 0$. Left: a trivial defect solution. Centre: a local defect solution. The defect has occurred near P_ε^+. Right: a global defect solution. Image is from A. Doelman, P. van Heijster, and F. Xie. A geometric approach to stationary defect solutions in one space dimension. *SIAM Journal on Applied Dynamical Systems*, 15:655–712, 2016 copyright

equilibrium solutions to the unperturbed PDE. We summarise the existence conditions for trivial defect solutions that were established in [21] and formulate the stability problem by linearising about these defect solutions. We follow the definitions and notation of [21] where possible and adapt the analysis and results therein to the format of (4.2).

4.2.1 Types of defect solution

There are two key differences between our formulation of the unperturbed and perturbed existence equations compared to that of [21]. In [21] a general ODE of the form

$$\dot{u} = \begin{cases} h(u) & t \leq 0, \\ h(u) + \varepsilon j(u) & t > 0, \end{cases}$$

is considered, where $t \in \mathbb{R}$ and $h(u), j(u) : \mathbb{R}^k \to \mathbb{R}^k$ are sufficiently smooth functions. In contrast, our existence equation arises from an n-dimensional PDE. Thus, we have defined the first n entries of our $2n$-dimensional function by $u_x =: v$ in both the perturbed and unperturbed existence equations. As a result, our functions (compared to h) and our perturbations (compared to j) are special cases from the ones studied in [21]. Secondly, as our primary focus is on the analysis of the trivial defect solutions our assumptions on the unperturbed and perturbed existence equations are less restrictive and will be stated in terms of $f(u)$ and $g(u)$ rather than the full right hand side of the existence equations.

We label the roots of $f(u)$ for which the Jacobian of (4.3) is hyperbolic as ρ_i for $i = 1, 2, ..., N$ where N is a positive (possibly infinite) integer. These roots correspond to equilibrium solutions of the unperturbed existence equation (4.3) when $v = 0$, *i.e.* when $(u, v) = (\rho_i, 0)$ for $i = 1, 2, ..., N$ which we denote by $P_i := (\rho_i, 0)$ for $i = 1, 2, ..., N$. For the existence and stability analysis we require that the function $f(u)$ has at least one such isolated root that is hyperbolic, *i.e.* we require $N \geq 1$. However, we utilise the following lemma to simplify this requirement.

Lemma 4.2.1. *For $i = 1, 2, ..., N$ the equilibrium solution P_i are hyperbolic in the sense that the Jacobian of (4.3) has no purely imaginary matrix eigenvalues if and only if all of the matrix eigenvalues of $D^{-1}J_f(\rho_i)$ have negative real part.*

Proof. The Jacobian associated with the unperturbed existence equation (4.3) at the equilibrium solution $u = \rho_i$ is given by,

$$\begin{pmatrix} 0 & I_n \\ -D^{-1}J_f(\rho_i) & 0 \end{pmatrix},$$

for $i = 1, 2, ..., N$, where I_n is the n-dimensional identity matrix. The characteristic polynomial of this Jacobian matrix is given by

$$det(\mu^2 I_n + D^{-1}J_f(\rho_i)) = 0.$$

It is clear that the eigenvalues of the Jacobian are given by the square root of the eigenvalues of $-D^{-1}J_f(\rho_i)$. Therefore, the equilibrium solutions P_i are hyperbolic (in the sense that the Jacobian matrix has no purely imaginary matrix eigenvalues) if and only if the matrix $D^{-1}J_f(\rho_i)$ has only matrix eigenvalues with strictly negative real part. □

In other words, we only need to make the following assumption on $f(u)$.

Hypothesis 4.1. *The function $f(u)$ has at least one isolated root, denoted u_0. The matrix $D^{-1}J_f(u_0)$ associated with this solution has eigenvalues with strictly negative real part and these matrix eigenvalues are simple.*

Cases with purely imaginary eigenvalues are of interest in applications such as edge bifurcations [55]. However, these cases are marginally spectrally stable. We only consider equilibria with negative-definite sub-Jacobians as we focus on the impact of the inclusion of a jump-type defect on an otherwise spectrally stable solution.

A consequence of Hypothesis 4.1 is that the unperturbed existence equation (4.3) has at least one equilibrium solution $(u, v) \equiv (u_0, 0)$ and the Jacobian matrix associated with (4.3) is also hyperbolic at this equilibrium solution with $2n$ simple eigenvalues. For ε sufficiently small, the implicit function theorem implies that the *fully perturbed existence equation*,

$$\begin{pmatrix} u \\ v \end{pmatrix}' = \begin{pmatrix} v \\ -D^{-1}\left(f(u) + \varepsilon g(u)\right) \end{pmatrix}, \tag{4.5}$$

also has an isolated, hyperbolic equilibrium, see, for instance, [51]. More precisely, if (4.3) has N isolated hyperbolic equilibria then (4.5) has N isolated hyperbolic equilibria, P_i^ε, such that $\lim_{\varepsilon\to 0} P_i^\varepsilon = P_i$. The eigenvalues of the Jacobian associated with (4.5) evaluated at these equilibria P_i^ε are also $\mathcal{O}(1)$ with respect to ε. Furthermore, Hypothesis 4.1, together with the implicit function theorem, implies that there exists at least one

root of $f(u) + \varepsilon g(u)$, denoted u^ε, which is isolated such that $\lim_{\varepsilon\to 0} u^\varepsilon = u_0$. Thus, The Jacobian matrix associated with (4.5) is hyperbolic with simple matrix eigenvalues when $(u, v) \equiv (u^\varepsilon, 0)$. Defect solutions $\Gamma_\varepsilon(x)$ are solutions to (4.2) that approach (in a graph sense) a solution $\Gamma(x)$ to (4.1) in the limit $\varepsilon \to 0$ and we only consider $\Gamma(x)$ that connect hyperbolic equilibria. From Hypothesis 4.1 we know that there exists at least one such equilibria $(u_0, 0)$. We denote the end points of $\Gamma(x)$ as $P^\pm := \lim_{x\to\pm\infty} \Gamma(x)$ and $P^\pm_\varepsilon := \lim_{x\to\pm\infty} \Gamma_\varepsilon(x)$ respectively, with the observation that P^- can be equal to P^+. Furthermore, one end point of $\Gamma_\varepsilon(x)$ will be equal to the corresponding end point of $\Gamma(x)$, *i.e.* either $P^-_\varepsilon = P^-$ or $P^+_\varepsilon = P^+$, see Figure 4.2.1.

As in [21], (4.2) has been parametrised in such a way that the defect occurs at $x = 0$. We refer to $x = 0$ as the *defect point* in the remainder of this thesis. We may now distinguish between three types of defect solutions by the location of the defect point in the phase portrait of the solution.

Definition 4.2.1. *([21] Definition 1.4) A defect solution $\Gamma_\varepsilon(x)$ is called*

- *a trivial defect solution if $P^- = P^+$ and*

$$\lim_{\varepsilon\to 0} \left(\sup_{x\in\mathbb{R}} ||\Gamma_\varepsilon(x) - P^+|| \right) = 0;$$

- *a local defect solution if either*

$$\lim_{\varepsilon\to 0} \left(\sup_{x>0} ||\Gamma_\varepsilon(x) - P^+|| \right) = 0 \quad or \quad \lim_{\varepsilon\to 0} \left(\sup_{x\leq 0} ||\Gamma_\varepsilon(x) - P^-|| \right) = 0$$

- *a global defect solution if*

$$\lim_{\varepsilon\to 0} \left(\sup_{x>0} ||\Gamma_\varepsilon(x) - P^+|| \right) > 0 \quad and \quad \lim_{\varepsilon\to 0} \left(\sup_{x\leq 0} ||\Gamma_\varepsilon(x) - P^-|| \right) > 0.$$

As we are primarily interested in the trivial defect solution, we choose that the defect solution occurs near a single hyperbolic equilibrium $u = u_0$ described in Hypothesis 4.1, that is $P^- = P^+ = (u_0, 0)$. Hence, the trivial defect solution $\Gamma_\varepsilon(x)$ asymptotes to $\lim_{x\to-\infty} \Gamma_\varepsilon(x) = P^+$ and $\lim_{x\to\infty} \Gamma_\varepsilon(x) = P^+_\varepsilon = (u^\varepsilon, 0)$. Moreover, $\Gamma(x) \equiv P^+$.

4.2.2 The stability of equilibrium solutions to the unperturbed PDE

As we are motivated by the analysis of local defect solutions, we focus on the effect of the introduced defect on equilibrium solutions $P^+ = (u_0, 0)$ that are spectrally stable, see §5.4.1 for further discussion of local defect solutions. In this section we establish the spectral stability of the equilibrium solution P^+. We approach this problem in two ways in this chapter; in this section we locate the essential and absolute spectrum associated with the equilibrium solution and in §4.2.5 we formulate the Evans function associated with the equilibrium solution. Note, there is no point spectrum associated with constant solutions.

This can be seen through the calculation of the Evans function or by observing that for any given value $\lambda \in \mathbb{C}$, to the right of the essential and absolute spectrum, the Jacobian matrix associated with (4.3) is constant and invertible. Thus, locating the essential and absolute spectrum is sufficient to establish the spectral stability of an equilibrium solution to the unperturbed PDE. We formulate the Evans function in §4.2.5 as it is the basis for our analysis of the trivial defect solution and is thus necessary in this case.

We perturb about the equilibrium solution via the substitution $u(x,t) = u_0 + \varepsilon_1 p(x,t)$ where $0 < \varepsilon_1 \ll 1$ and $p(x,t)$ is the perturbation. We take the perturbation to be of the form $p(x,t) = e^{\lambda t}p(x)$. The linearised equation associated with (4.1) (*i.e.* to leading order in ε_1), referred to as the *unperturbed eigenvalue problem*, is,

$$\lambda p = D p_{xx} + J_f(u_0)p =: \mathcal{L}_0 p. \tag{4.6}$$

The natural domain for the linear operator $\mathcal{L}_0$ is $H^2(\mathbb{R}^n)$ as it is derived from a second order reaction diffusion equation. We seek the spectrum of $\mathcal{L}_0$ for which we have the following definition stated in Chapter 1 as Definition 1.3.1 and restated here for convenience;

Definition 4.2.2. *([88] Definition 3.2) We say $\lambda \in \mathbb{C}$ is in the spectrum of an operator $\mathcal{L}$, denoted $\sigma(\mathcal{L})$, if the operator $\mathcal{L} - \lambda I$, where I is the identity matrix, is not invertible, i.e. the inverse does not exist or is not bounded.*

The spectrum of an operator falls naturally into two parts; the *essential spectrum*, denoted $\sigma_{ess}(\mathcal{L})$ and the *point spectrum*, denoted $\sigma_{pt}(\mathcal{L})$ [41]. It is more straightforward to use a system of first order system of ODEs. Therefore, we transform (4.6) into such a system via the introduction of the variable $q := p_x$. This results in the equivalent eigenvalue problem,

$$\mathcal{T}_0(\lambda)\begin{pmatrix} p \\ q \end{pmatrix} := \underbrace{\begin{pmatrix} 0 & I_n \\ D^{-1}\left(\lambda I_n - J_f(u_0)\right) & 0 \end{pmatrix}}_{A_0(\lambda)}\begin{pmatrix} p \\ q \end{pmatrix} = 0. \tag{4.7}$$

As in Definition 1.3.3, we define the asymptotic operator associated with $\mathcal{T}_0$,

$$\mathcal{T}_{0,\infty}(\lambda) := \begin{cases} A_-(\lambda) := \lim\limits_{x\to-\infty} A_0(\lambda) & x \le 0, \\ A_+(\lambda) := \lim\limits_{x\to\infty} A_0(\lambda) & x > 0. \end{cases} \tag{4.8}$$

We have the following definition for the essential spectrum stated in Chapter 1 as Definition 1.3.4 and restated here for convenience;

Definition 4.2.3. *([54] Definition 3.1.11) . We say $\lambda \in \sigma_{ess}(\mathcal{T}_\infty)$, the essential spectrum of $\mathcal{T}_{0,\infty}$, if either*

i. $A_+(\lambda)$ *and* $A_-(\lambda)$ *are hyperbolic with a different number of unstable matrix eigenvalues, equivalently the Morse indices* $i_\pm(A)$ *as discussed in §1.3.2 differ, i.e.* $i_+ - i_- \neq 0$*; or*

ii. $A_+(\lambda)$ *or* $A_-(\lambda)$ *has at least one purely imaginary matrix eigenvalue.*

In our case, the operator $\mathcal{T}_0(\lambda)$ is spatially invariant and the associated asymptotic operator is thus simply given by $\mathcal{T}_{0,\infty}(\lambda) = \mathcal{T}_0(\lambda)$ and the so-called asymptotic matrices are equal, *i.e.* $A_-(\lambda) = A_+(\lambda) = A_0(\lambda)$. This simplifies the computation of the essential spectrum significantly. As the asymptotic matrices are equal, they always have the same number of unstable matrix eigenvalues for all $\lambda \in \mathbb{C}$. Thus, the essential spectrum consists only of values $\lambda \in \mathbb{C}$ such that $A_0(\lambda)$ has at least one purely imaginary matrix eigenvalue *i.e.* they are determined by the roots of the dispersion relations.

Another important concept in stability analysis is that of the absolute spectrum. This is not spectrum in the sense that is does not arise from Definition 4.2.2. However, the absolute spectrum is contained to the left (in the complex plane) of the borders of the essential spectrum. The essential spectrum can be shifted by weighting the function space, *i.e.* by only allowing perturbations with exponential decay (the rate of which is referred to as the weight) as $x \to -\infty$ and/or as $x \to \infty$ [54, 93], see also §1.3.3. However, the absolute spectrum is not shifted by weighting the space. Thus, the absolute spectrum marks the potential maximum for how far the essential spectrum can be shifted into the left half plane. The presence of absolute spectrum in the right half plane causes the solution to be spectrally unstable in all weighted spaces as it indicates the presence of essential spectrum in the right half plane. The absolute spectrum will also come into play in the use of the Evans function, see §4.2.5.

Definition 4.2.4. *([88] Definition 6.1) Take an N dimensional asymptotic operator,* $\mathcal{T}_\infty$*, in the form of* (4.8)*, that is well-posed in the sense that* $i_+ = i_- = j$ *for* $\Re(\lambda) \gg 1$*. For* $\lambda \in \mathbb{C}$ *we rank the N spatial eigenvalues* $\mu_i^\pm$ *of the asymptotic matrices* $M_\pm$ *by the magnitude of their real parts,* i.e.

$$\Re(\mu_1^\pm(\lambda)) \geq \Re(\mu_2^\pm(\lambda)) \geq \ldots \geq \Re(\mu_j^\pm(\lambda)) \geq \Re(\mu_{j+1}^\pm(\lambda)) \geq \ldots \geq \Re(\mu_N^\pm(\lambda)).$$

We define the sets

$$\sigma_{\text{abs}}^+ = \left\{ \lambda \in \mathbb{C} \,\middle|\, \Re(\mu_j^+) = \Re(\mu_{j+1}^+) \right\} \text{ and } \sigma_{\text{abs}}^- = \left\{ \lambda \in \mathbb{C} \,\middle|\, \Re(\mu_j^-) = \Re(\mu_{j+1}^-) \right\}, \tag{4.9}$$

and the absolute spectrum of $\mathcal{T}_\infty$ *(and of* $\mathcal{T}$*) is* $\sigma_{\text{abs}} := \sigma_{\text{abs}}^+ \cup \sigma_{\text{abs}}^-$.

In the case of trivial defect solutions we have, to leading order, $\sigma_{\text{abs}}^+ = \sigma_{\text{abs}}^-$ thus we will drop the superscript.

As the equation (4.6) is spatially independent, the essential spectrum can be calculated directly from the dispersion relations of $A_0(\lambda)$. The characteristic polynomial of $A_0(\lambda)$

is $det(A_0(\lambda) - \mu I_n) = 0$ where μ are the spatial eigenvalues. As $A_0(\lambda)$ consists of block matrices which commute this expression is given by

$$det\left(\mu^2 I_n - D^{-1}(\lambda I_n - J_f(u_0))\right) = 0.$$

This brings us to our most restrictive assumption. In order to make explicit calculations of the Evans function tractable we must assume that D^{-1} and $D^{-1}J_f(u_0)$ are simultaneously diagonalisable. This requires either that $J_f(u_0)$ is diagonal or that the diagonal entries of D are equal. The assumption that is less restrictive and more relevant to our interests is the latter.

Hypothesis 4.2. *The diffusion coefficient of every population is given by the constant δ, that is $D = \delta I_n$.*

The matrix eigenvalues of the Jacobian of (4.3) are $\pm\sqrt{-\frac{\nu_i}{\delta}}$ for $i = 1, 2, ..., n$. Though Hypothesis 4.2 is restrictive, it is necessary as the stability analysis for general functions $f(u), g(u)$ is computationally prohibitive without explicit knowledge of the form of $f(u), g(u)$ and of the entries of the matrix D. However, if the explicit form of the model is known one may invert the matrix D and continue the calculation as presented here. In other words, systems that do not satisfy Hypothesis 4.2 will follow the methodology presented within this chapter. Moreover, Hypothesis 4.2 is always true for scalar equations. We denote the matrix eigenvalues of $J_f(u_0)$ as ν_i for $i = 1, 2, ..., n$. In this case Hypotheses 4.1 and 4.2 imply $\Re(\nu_i) < 0$ and $\nu_i \neq \nu_j$ for $i, j = 1, 2, ..., n$, $i \neq j$.

As we assumed that $D^{-1}J_f(u_0)$ has simple eigenvalues with non-zero real part we know $\frac{1}{\delta}J_f(u_0)$ is diagonalisable and thus we set $\frac{1}{\delta}J_f(u_0) = \frac{1}{\delta}P\Lambda P^{-1}$ where P is an invertible matrix and $\Lambda = diag(\nu_1, \nu_2, ..., \nu_n)$ is the diagonal matrix of eigenvalues of $J_f(u_0)$. Then, from the characteristic polynomial of $A_0(\lambda)$,

$$\begin{aligned}
0 &= det\left(P\mu^2 I_n P^{-1} - P\frac{\lambda}{\delta}I_n P^{-1} - \frac{1}{\delta}P\Lambda P^{-1}\right) \\
&= det\left(P\left(\mu^2 I_n - \frac{1}{\delta}(\lambda I_n - \Lambda)\right)P^{-1}\right) \\
&= |P| det\left(\mu^2 I_n - \frac{1}{\delta}(\lambda I_n - \Lambda)\right)|P^{-1}| \\
&= det\left(\mu^2 I_n - \frac{1}{\delta}(\lambda I_n - \Lambda)\right) \\
&= \prod_{i=1}^{n}\left(\mu^2 - \frac{1}{\delta}(\lambda - \nu_i)\right).
\end{aligned}$$

So, the $2n$ spatial eigenvalues associated with $A_0(\lambda)$ are $\mu_i^{\pm} = \pm\sqrt{\frac{1}{\delta}(\lambda - \nu_i)}$ for $i = 1, 2, ..., n$. Recall that, as the $A_0(\lambda)$ is spatially independent, the asymptotic matrices at the two end states $x \to \pm\infty$ are both given by $A_0(\lambda)$. Setting $\mu = ik$ gives the n dispersion

relations associated with $A_0(\lambda)$ at each end state $x \to \pm\infty$ as $\lambda = -\delta k^2 + \nu_i$. We denote the spatial eigenvalue with the largest real part as ν^*. We can see from the spatial eigenvalues μ_i that the Morse indices $i_+(\lambda)$ and $i_-(\lambda)$ are equal when $\Re(\lambda) > \Re(\nu^*)$. That is, if $\Re(\lambda) > \Re(\nu^*)$ then λ is in the resolvent of the essential spectrum. Thus, in an unweighted space, we can see that the essential spectrum consists of horizontal lines in the complex plane consisting of values of λ with $\Re(\lambda) \leq \Re(\nu_i)$, recalling that, by assumption, $\Re(\nu_i) < 0$ for all i. Furthermore, we can conclude that all values λ such that $\lambda = \nu_i$ are branch points of the absolute spectrum as at these points the pair of spatial eigenvalues $\mu_i^{\pm} = \pm\sqrt{\frac{1}{\delta}(\lambda - \nu_i)}$ for a given i have $\Re(\mu_i^{\pm}) = 0$ and thus, by Definition 4.2.4, $\lambda = \nu_i$ for $i = 1, 2, ..., n$ are contained in the absolute spectrum. We denote the leading branch point, that is $\lambda = \nu^*$, as λ_{br}^*.

Remark 4.2.2. *The assumption in Hypothesis 4.1 that the sub-Jacobian associated with $f(u)$ at $u = u_0$ has only simple eigenvalues can be relaxed. Under the assumption the n matrix eigenvalues of $J_f(u_0)$ each have algebraic and geometric multiplicity of 1. As a result, the $2n$ spatial eigenvalues of the unperturbed eigenvalue problem are simple for $\Re(\lambda) > \Re(\lambda_{\text{br}}^*)$. If we relax this assumption, i.e. we allow the algebraic and/or geometric multiplicity of the matrix eigenvalues of $J_f(u_0)$ to be greater than 1 we can use the Jordan normal form rather than the diagonal matrix Λ to calculate the spatial eigenvalues. This is algebraically more intensive but the stability analysis follows similarly. The main issue is the branch point of the absolute spectrum. If the leading matrix eigenvalue, ν_i^*, of $J_f(u_0)$ has multiplicity greater than 1 then the leading branch point λ_{br}^* will be of higher order. This will increase the complexity of calculations greatly. If any matrix eigenvalue other than the leading matrix eigenvalue has algebraic or geometric multiplicity greater than 1 then the spatial eigenvalues will have corresponding increased multiplicity but will only contribute to the generalised absolute spectrum and furthermore, will be to the left of the branch point, which we do not consider as part of the domain of the Evans function.*

4.2.3 The existence trivial defect solutions to the perturbed PDE

In order to establish the groundwork for the analysis of local defect solutions, we require the following assumption regarding the $2n$-length perturbation with n zero entries, $(0, \varepsilon D^{-1} g(u))^T$. This assumption is adapted from Hypothesis 3 of [21].

Hypothesis 4.3. *The term $D^{-1}g(u)$ is asymptotically strictly order 1. In other words, $\lim_{x\to\pm\infty} D^{-1}g(u)$ is $\Theta(1)$ with respect to ε.*

This assumption is decidedly weaker than Hypothesis 3 of [21] though strong enough for our analysis of the trivial defect solution.

We now state the primary result of [21] utilised in this chapter.

Lemma 4.2.3. *([21] Lemma 1.7) Assume that Hypotheses 4.1 and 4.3 hold. Then, for $\varepsilon > 0$ small enough, system (4.4) has a unique trivial defect solution $\Gamma_\varepsilon(x)$ connecting P^+ and P_ε^+, where $P^+ = \lim_{\varepsilon\to 0} P_\varepsilon^+$.*

Remark 4.2.4. *There are several assumptions made on the perturbed and unperturbed equations by [21] that we have not included here. These assumptions were omitted as they are not necessary for the existence or stability analysis of the trivial defect solution. These assumptions are, however, necessary for the analysis of the local defect solutions, see §5.4.1.*

4.2.4 The perturbed spectral problem

To determine the spectral stability of $\Gamma_\varepsilon(x)$ we must linearise the perturbed PDE (4.2) about the trivial defect solution. Let $U(x,t) = \Gamma_\varepsilon(x) + \varepsilon_2 p(x,t)$ with $0 < \varepsilon_2 \ll 1$ where $p(x,t)$ is a perturbation in an appropriately chosen Banach space. As in the unperturbed case we take $p(x,t) = e^{\lambda t}p(x)$. The linearised eigenvalue problem associated with the perturbed PDE (4.2), referred to as the *perturbed eigenvalue problem* is thus,

$$\begin{aligned}\lambda p =& Dp_{xx} + J_f(\Gamma_\varepsilon)p + \begin{cases} 0 & x \le 0 \\ \varepsilon J_g(\Gamma_\varepsilon)p & x > 0, \end{cases} \\ =:& \mathcal{L}_\varepsilon p,\end{aligned} \tag{4.10}$$

where we have omitted the argument of the trivial defect solution. The natural domain for a second order reaction diffusion equation is $H^2(\mathbb{R}^n)$. However, due to the loss of continuity, caused by the defect, the domain of $\mathcal{L}_\varepsilon$ is reduced to $H^1(\mathbb{R}^n)$. As for the unperturbed problem we set $q := p_x$ to obtain the equivalent operator,

$$\mathcal{T}_\varepsilon(\lambda)\begin{pmatrix} p \\ q \end{pmatrix} := \begin{pmatrix} 0 & I_n \\ D^{-1}\left(\lambda I_n - J_f(\Gamma_\varepsilon)\right) & 0 \end{pmatrix}\begin{pmatrix} p \\ q \end{pmatrix} - \begin{cases} \begin{pmatrix} 0 \\ 0 \end{pmatrix} & x \le 0 \\ \begin{pmatrix} 0 \\ D^{-1}\varepsilon J_g(\Gamma_\varepsilon)p \end{pmatrix} & x > 0 \end{cases} \tag{4.11}$$

4.2.5 The Evans function

The primary tool we will be using for our analysis in this chapter is the Evans function which was introduced in §1.3.6. The Evans function is an analytic tool for locating the point spectrum associated with an operator. Though our solution to the unperturbed existence equation (and leading order solution to the perturbed existence equation) is an equilibrium solution, and thus, has no associated point spectrum, the Evans function proves useful for tracking any potential spectra that emerge from the branch points of the absolute spectrum upon the introduction of the jump-type defect.

Recalling that, for (4.7) the asymptotic matrices are equal, *i.e.* $A_-(\lambda) = A_+(\lambda) = A_0(\lambda)$, we denote the unstable eigenspace associated with $A_0(\lambda)$ as $\mathbb{E}^u_-$ and similarly the stable subspace of $A_0(\lambda)$ as $\mathbb{E}^s_+$. The natural domain of the Evans function is the region denoted Ω_1 which consists of the values $\lambda \in \mathbb{C}$ to the right of the rightmost boundary of the essential spectrum, *i.e.* the region containing λ with $\Re(\lambda) \gg 1$. On this domain $A_0(\lambda)$ is hyperbolic as it is outside of the essential spectrum as established in §4.2.2. Furthermore, as our solution is hyperbolic (in the sense that the Jacobian of (4.4) is hyperbolic) and by our explicit calculation of the spatial eigenvalues in §4.2.2 we have $\dim(\mathbb{E}^u_-) = \dim(\mathbb{E}^s_+) = n$.

The natural domain Ω_1 of the Evans function does not include the essential spectrum nor the absolute spectrum, [54]. However, the Evans function can be extended analytically into the essential spectrum and the absolute spectrum acts as a branch cut for the Evans function. The branch points of the absolute spectrum are also roots of the Evans function though they are not in Ω_1.

The Evans function $E(\lambda)$ is independent of the choice of x and is analytic on Ω_1 [88]. For $\lambda \in \Omega_1$ the Evans function has the following properties. This theorem was stated previously as 1.3.3 and is restated here for convenience.

Theorem 4.2.5. *([88] Theorem 4.1):*

- *$E(\lambda)$ is real if λ is real.*
- *$E(\lambda) = 0$ if and only if λ is a point eigenvalue of the associated linear operator.*
- *The order of λ as a root of the Evans function corresponds to the algebraic multiplicity of λ as an eigenvalue.*

We consider a regular expansion of $\lambda \in \Omega_1$, *i.e.* $\lambda = \lambda_0 + \varepsilon\lambda_1 + \varepsilon^2\lambda_2 + \mathcal{O}(\varepsilon^3)$, and, as the Evans function is analytic in λ, we obtain the expansion of the Evans function,

$$\begin{aligned} E(\lambda(\varepsilon), \varepsilon, x) = E(\lambda_0, 0, x) &+ \varepsilon \left(\frac{\partial E}{\partial \varepsilon}(\lambda_0, 0, x) + \lambda_1 \frac{\partial E}{\partial \lambda}(\lambda_0, 0, x) \right) \\ &+ \frac{1}{2}\varepsilon^2 \left(\frac{\partial^2 E}{\partial \varepsilon^2}(\lambda_0, 0, x) + 2\lambda_2 \frac{\partial E}{\partial \lambda}(\lambda_0, 0, x) + 2\lambda_1 \frac{\partial^2 E}{\partial \lambda \varepsilon} + \lambda_1^2 \frac{\partial^2 E}{\partial \lambda^2} \right) \\ &+ \mathcal{O}(\varepsilon^3). \end{aligned} \tag{4.12}$$

By Abel's formula the Evans function $E(\lambda(\varepsilon), \varepsilon, x)$ is independent of the spatial variable x since $\mathrm{Tr}(A_0(\lambda) = 0$ and the coefficient matrix of $T_\varepsilon(\lambda)$ has trace of 0. We have deliberately included x above for clarity as we later equate at $x = 0$. The Evans function for the defect solution is defined as

$$E(\lambda(\varepsilon), \varepsilon, x) := \det\left(p^1_L(x), \dots p^n_L(x), p^1_R(x), \dots, p^{2n}_R(x) \right) \tag{4.13}$$

where p_L^i for $i = 1, \ldots, n$ are linearly independent solutions to (4.10) that decay to $\mathbb{E}_-^u$ as $x \to -\infty$ and p_R^i for $i = 1, \ldots, n$ are linearly independent solutions to (4.10) that decay to $\mathbb{E}_+^s$ as $x \to \infty$. In order to simplify calculations, we will be evaluating the Evans function at $x = 0$.

The roots of the Evans function of a trivial defect solution are, to leading order, given by those of the constant solution to the homogeneous case. The spectrum of the constant solution consists only of the essential spectrum (which coincides with the absolute spectrum). The inclusion of a small, spatially dependent, jump-type defect causes the branch point of the absolute spectrum associated with an equilibrium solution of the unperturbed PDE (4.1) to split into two branch points of the absolute spectrum associated with the trivial defect solution to the perturbed PDE (4.2). These two perturbed branch points are $\mathcal{O}(\varepsilon)$ perturbations of the unperturbed branch point. Any point spectra that emerge as a result of the inclusion of the jump-type defect will be given, to leading order, by the two branch points of the perturbed system. Note that, in order to obtain the $\mathcal{O}(\varepsilon^k)$ term of the eigenvalue expansion one must calculate the $\mathcal{O}(\varepsilon^{k+1})$ term of the Evans function expansion.

4.3 A scalar example: The bistable equation with a generic defect

In this section, we will derive the profile of a trivial defect solution for a perturbed scalar example and perform the stability analysis of this trivial defect solution as an illustrative example with explicit functions.

Consider the scalar bistable equation,

$$u_t = u_{xx} + u - u^3, \tag{4.14}$$

with $(x, t) \in \mathbb{R} \times \mathbb{R}^+$, $u \in \mathbb{R}$. The bistable equation has three equilibrium solutions; $u = \pm 1$, which are spectrally stable solutions, and $u = 0$ which is spectrally unstable. We analyse the stability of the trivial defect solution about the homogeneous steady state $u = -1$ for the scalar bistable equation with an added linear jump defect. That is, (4.2) with $n = 1$, $f(u) = u - u^3$ and $g(u) = u$, *i.e.*

$$u_t = u_{xx} + u - u^3 + \begin{cases} 0 & x \leq 0, \\ \varepsilon u & x > 0. \end{cases} \tag{4.15}$$

The choice $g(u) = u$ is a generic perturbation for the steady state $u = -1$ as outlined above, however this function is *not* a generic defect for the steady state $u = 0$.

We consider the trivial defect solution $\hat{u}$ near the equilibrium $u = -1$ with $\lim_{x \to -\infty} \hat{u} = -1 =: P^-$ and $\lim_{x \to +\infty} \hat{u} = -\sqrt{1+\varepsilon} = -1 - \frac{\varepsilon}{2} + \frac{\varepsilon^2}{8} + \mathcal{O}\left(\varepsilon^3\right) =: P_\varepsilon^+$. The Jacobian associated with $f(u)$ in this example is $J_f(u) = 1 - 3u^2$. The isolated equilibrium solution

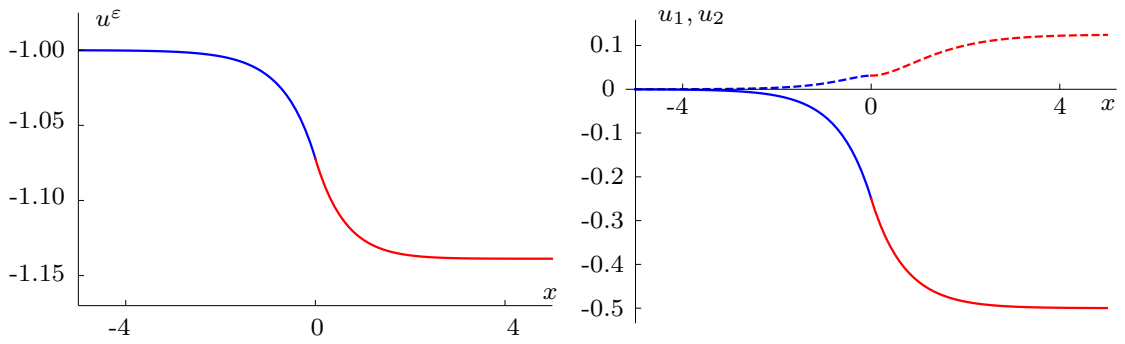

Figure 4.3.1: Trivial defect solution profile to the scalar bistable equation. In both images blue represents solutions to (4.3) for $x < 0$ and red represents solutions to (4.3) for $x \geq 0$. Left panel: The trivial defect solution to the scalar bistable equation. Solution profile is calculated to $\Theta(\varepsilon^2)$. Right panel: The $\Theta(\varepsilon)$ solution profile $u_1(x)$ (dashed) and the $\Theta(\varepsilon^2)$ solution profile $u_2(x)$ (solid).

$u = -1$ thus has $J_f(-1) = -2$, satisfying Hypothesis 4.1 and as $g(u) = u$ is generic for $u = -1$ Hypothesis 4.3 is also satisfied. Thus Lemma 4.2.3 guarantees the existence of a unique trivial defect solution.

4.3.1 The essential and absolute spectrum of the unperturbed bistable equation

We now compute the essential and absolute spectrum of the unperturbed bistable equation. The results of this section are well-known, see for example [54], but are included here for completeness. As in Example 1 of Chapter 1, we make the substitution $u(x,t) = u_0 + p(x,t) = -1 + e^{\lambda t}p(x)$ into (4.15) where $p(x)$ is a small perturbation. By considering only leading order perturbation terms, we obtain the linearised operator

$$\lambda p = p_{xx} + (1 - 3u_0^2)p = p_{xx} - 2p =: \mathcal{L}_0 p,$$

with $\mathcal{L}_0 : H^1(\mathbb{R}) \to H^1(\mathbb{R})$. We set $q := p_x$ and define the operator $\mathcal{T}(\lambda) : H^1(\mathbb{R}) \times L^2(\mathbb{R}) \to H^1(\mathbb{R}) \times L^2(\mathbb{R})$ by

$$\mathcal{T}(\lambda)\begin{pmatrix} p \\ q \end{pmatrix} := \left(\frac{d}{dx} - A(\lambda)\right)\begin{pmatrix} p \\ q \end{pmatrix} = 0, \text{ with } A(\lambda) := \begin{pmatrix} 0 & 1 \\ \lambda + 2 & 0 \end{pmatrix}.$$

As $A(\lambda)$ is spatially homogeneous, the asymptotic operators are simply $A_\pm(\lambda) = A(\lambda)$. Thus, to calculate the dispersion relation we take $\mu = ik$ as the matrix eigenvalue of $A(\lambda)$ where $k \in \mathbb{R}$ is a parameter and evaluate the characteristic polynomial of $A(\lambda)$. The boundary of the essential spectrum (Part ii of Definition 2.4.) is

$$\lambda = -k^2 - 2.$$

The essential spectrum consists only of this dispersion relation as for $\lambda \neq -k^2 - 2$, $k \in \mathbb{R}$ the number of unstable eigenvalues of $A_-(\lambda)$ and $A_+(\lambda)$ are equal.

The matrix eigenvalues of $A(\lambda)$ are given by

$$\mu_{1,2} = \pm\sqrt{\lambda + 2},$$

where, as $A_+(\lambda) = A_-(\lambda)$, we have dropped the superscript. The absolute spectrum of the operator $\mathcal{L}_0$ consists of the values of λ for which the real part of these two matrix eigenvalues are equal, *i.e.*

$$\sigma_{\text{abs}} = \{\lambda : Im(\lambda) = 0 \text{ and } \lambda \leq -2\}.$$

As the solution is constant, the essential spectrum and the absolute spectrum coincide in this case.

4.3.2 The solution profile of the trivial defect solution

We now derive the solution profile for the trivial defect solution to (4.15) about $u = -1$ to $\Theta(\varepsilon^2)$. We use a regular expansion, $u = u_0 + \varepsilon u_1 + \varepsilon^2 u_2 + \mathcal{O}(\varepsilon^3)$, with $u_0 = -1$ and find u_1 and u_2. Solutions to the unperturbed PDE (4.15) can be taken as $u \in C^2$ but the introduction of the discontinuous spatial defect implies $u \in C^1$. The leading order existence equation is $0 = (u_0)_{xx} + u_0 - u_0^3$, $\forall x \in \mathbb{R}$. The $\Theta(\varepsilon)$ existence equation is

$$0 = (u_1)_{xx} + (1 - 3u_0^2)u_1 + \begin{cases} 0 & x \leq 0, \\ u_0 & x > 0. \end{cases}$$

As $u_0 = -1$ this ODE is linear and homogeneous for $x < 0$ and is linear and non-homogeneous for $x \geq 0$. We use variation of parameters to obtain the solution,

$$u_1 = \begin{cases} -\frac{e^{\sqrt{2}x}}{4} =: u_{1,L} & x \leq 0, \\ -\frac{1}{2} + \frac{1}{4}e^{-\sqrt{2}x} =: u_{1,R} & x > 0. \end{cases}$$

Where the subscripts L and R to denote solutions defined on the 'left' domain ($x < 0$) and 'right' domain ($x \geq 0$) respectively. The $\Theta(\varepsilon^2)$ existence equation is

$$0 = (u_2)_{xx} + \left(1 - 3u_0^2\right) u_2 - 3u_0 u_1^2 + \begin{cases} 0 & x \leq 0, \\ u_1 & x > 0. \end{cases}$$

For all x this ODE is non-homogeneous and the associated homogeneous ODE is

$$0 = (u_2)_{xx} + \left(1 - 3u_0^2\right) u_2.$$

We again use variation of constant to obtain the solution,

$$u_2 = \begin{cases} \frac{1}{16}e^{\sqrt{2}x} - \frac{1}{32}e^{2\sqrt{2}x} =: u_{2,L} & x \leq 0, \\ \frac{1}{8} - \frac{1}{16}\left(1 + 2\sqrt{2}x\right)e^{-\sqrt{2}x} - \frac{1}{32}e^{-2\sqrt{2}x} =: u_{2,R} & x > 0. \end{cases}$$

Calculating the solution profile to $\Theta(\varepsilon^2)$ is sufficient to track the $\Theta(\varepsilon)$ corrections of the temporal eigenvalues and thus we move on to the stability analysis of the trivial defect solution.

4.3.3 The eigenvalue problem and the Evans function

To determine the stability of the trivial defect solution $u = u_0 + \varepsilon u_1 + \varepsilon^2 u_2 + \mathcal{O}(\varepsilon^3)$ of (4.15), we consider $U(x,t) = u(x) + \varepsilon_1 p(x,t)$ with $0 < \varepsilon_1 \ll 1$ and where p is a perturbation in some appropriately chosen Banach space with $p(x,t) = e^{\lambda t}p(x)$. In this case we take $p(x) \in H^1(\mathbb{R})$. Substituting U into (4.15) and by considering only leading order terms of $p(x)$ we obtain the eigenvalue problem for the linearised system, *i.e.*

$$\lambda p = p_{xx} + (1 - 3u^2)p + \begin{cases} 0 & x \leq 0, \\ \varepsilon p & x > 0. \end{cases} \tag{4.16}$$

In order to obtain and explicit expression for the $\Theta(\varepsilon^2)$ correction term of the Evans function, which provides the $\Theta(\varepsilon)$ correction term of λ, we must calculate the explicit solutions to (4.16) up to $\Theta(\varepsilon^2)$. Specifically, we seek solutions (4.16), calculated on $x < 0$, with $\lim_{x\to-\infty} p(x) = 0$, which we denote with the subscript L and solutions calculated on $x \geq 0$ with $\lim_{x\to\infty} p(x) = 0$, which we denote with a subscript R. We take $\lambda = \lambda_0 + \varepsilon\lambda_1 + \varepsilon^2\lambda_2 + \mathcal{O}(\varepsilon^3)$ with $\Re(\lambda_0) > -2$ (*i.e.* to the right of σ_{abs}) and $p(x,\lambda) = p_0(x,\lambda) + \varepsilon p_1(x,\lambda) + \varepsilon^2 p_2(x,\lambda) + \mathcal{O}(\varepsilon^3)$ and solve each order of the eigenvalue problem. The leading order eigenvalue problem is,

$$\lambda_0 p_0 = (p_0)_{xx} + (1 - 3u_0^2)p_0,$$

which is linear in p_0 leading to the solution,

$$p_{0,L}(x) = A_0 e^{\sqrt{\lambda_0+2}\,x}, \qquad p_{0,R}(x) = B_0 e^{-\sqrt{\lambda_0+2}\,x},$$

where A_0, B_0 are arbitrary integration constants. The $\Theta(\varepsilon)$ term of the eigenvalue problem is given by,

$$\lambda_0 p_1 + \lambda_1 p_0 = (p_1)_{xx} + (1 - 3u_0^2)p_1 - 6(u_0 u_1)p_0 + \begin{cases} 0 & x \leq 0, \\ p_0 & x > 0. \end{cases}$$

which, by variation of parameters, has the solution,

$$\begin{aligned} p_{1,L}(x) = e^{\sqrt{\lambda_0+2}x} &\left(A_1 + A_0\lambda_1 \left(\frac{x}{2\sqrt{\lambda_0+2}} - \frac{1}{4(\lambda_0+2)} \right) \right) \\ &+ \frac{3A_0 e^{\left(\sqrt{2}+\sqrt{\lambda_0+2}\right)x}}{4(1+\sqrt{2}\sqrt{\lambda_0+2})}, \\ p_{1,R}(x) = e^{-\sqrt{\lambda_0+2}\,x} &\left(B_1 - B_0(\lambda_1+2) \left(\frac{x}{2\sqrt{\lambda_0+2}} + \frac{1}{8+4\lambda_0} \right) \right) \\ &- \frac{3B_0 e^{-\left(\sqrt{2}+\sqrt{\lambda_0+2}\right)x}}{4\sqrt{2}\sqrt{\lambda_0+2}+4}, \end{aligned}$$

where A_1, B_1 are arbitrary integration constants. The $\Theta(\varepsilon^2)$ term of the eigenvalue problem is given by,

$$\begin{aligned} \lambda_0 p_2 + \lambda_1 p_1 + \lambda_2 p_0 = (p_2)_{xx} + (1 - 3u_0^2)p_2 - 6(u_0 u_1)p_1 \\ - (3u_1^2 + 6u_0 u_2)p_0 + \begin{cases} 0 & x \leq 0, \\ p_1 & x > 0. \end{cases} \end{aligned}$$

which, by variation of parameters, has the solution,

$$
\begin{aligned}
p_{2,L}(x) = e^{\sqrt{\lambda_0+2}x}&\left(A_2 + \lambda_1^2\frac{A_0\left(1+\sqrt{\lambda_0+2}x\left(\sqrt{\lambda_0+2}x-2\right)\right)}{8\left(\lambda_0+2\right)^2}\right.\\
&\left.+\frac{1}{4}(A_0\lambda_2+A_1\lambda_1)\left(\frac{2x}{\sqrt{\lambda_0+2}}-\frac{1}{\lambda_0+2}\right)\right)\\
&+e^{\left(\sqrt{2}+\sqrt{\lambda_0+2}\right)x}\left(-\frac{3\left(\sqrt{2}\sqrt{\lambda_0+2}-1\right)(A_0-4A_1)}{32\lambda_0+48}\right.\\
&+3A_0\lambda_1\left(\frac{-7\left(\sqrt{2}\sqrt{\lambda_0+2}+2\right)-\lambda_0\left(3\sqrt{2}\sqrt{\lambda_0+2}+7\right)}{8(\lambda_0+2)^{3/2}\left(\sqrt{\lambda_0+2}+\sqrt{2}\right)\left(2\sqrt{\lambda_0+2}+\sqrt{2}\right)^2}\right.\\
&\left.\left.+\frac{\left(\sqrt{2}\lambda_0+3\left(\sqrt{\lambda_0+2}+\sqrt{2}\right)\right)x}{4\sqrt{\lambda_0+2}\left(\sqrt{\lambda_0+2}+\sqrt{2}\right)\left(2\sqrt{\lambda_0+2}+\sqrt{2}\right)^2}\right)\right)\\
&+e^{\left(\sqrt{\lambda_0+2}+2\sqrt{2}\right)x}\frac{3A_0\left(\sqrt{2}\sqrt{\lambda_0+2}(\lambda_0-3)+\lambda_0+6\right)}{32\lambda_0(2\lambda_0+3)}\\
p_{2,R}(x) = e^{-\sqrt{\lambda_0+2}x}&\left(B_2+\lambda_1^2\frac{B_0\left(1+\sqrt{\lambda_0+2}x\left(\sqrt{\lambda_0+2}x+2\right)\right)}{8\left(\lambda_0+2\right)^2}\right.\\
&+B_0\left(\frac{1}{2\left(\lambda_0+2\right)^2}+\frac{x^2(\lambda_1+1)}{2(\lambda_0+2)}+\frac{x}{(\lambda_0+2)^{3/2}}\right)\\
&\left.-\left(B_1+\frac{1}{2}\left(B_1\lambda_1+B_0\lambda_2\right)-\frac{B_0\lambda_1}{\lambda_0+2}\right)\left(\frac{1}{2\left(\lambda_0+2\right)}+\frac{x}{\sqrt{\lambda_0+2}}\right)\right)\\
&+e^{-\left(\sqrt{2}+\sqrt{\lambda_0+2}\right)x}\left(\frac{3B_1}{4\left(\sqrt{2}\sqrt{\lambda_0+2}+1\right)}+\frac{3\left(\lambda_0\left(2\lambda_0-9\right)-24\right)}{16\left(\lambda_0+2\right)\left(2\lambda_0+3\right)^2}\right.\\
&+\frac{3\left(\lambda_0\left(2\lambda_0+15\right)+24\right)}{8\sqrt{2}\sqrt{\lambda_0+2}\left(2\lambda_0+3\right)^2}+\left(\frac{3\left(\lambda_0+1\right)}{4\sqrt{\lambda_0+2}\left(2\lambda_0+3\right)}+\frac{3}{\sqrt{2}\left(8\lambda_0+12\right)}\right)x\\
&\left.+\frac{3\lambda_1B_0}{4\sqrt{2}\sqrt{\lambda_0+2}\left(2\sqrt{\lambda_0+2}+\sqrt{2}\right)^2}\left(\frac{(2\lambda_0+3)x}{\left(\sqrt{\lambda_0+2}+\sqrt{2}\right)}+\frac{\sqrt{2}}{2\sqrt{\lambda_0+2}}+3\right)\right)\\
&+e^{-\left(2\sqrt{2}+\sqrt{\lambda_0+2}\right)x}B_0\left(\frac{3\sqrt{\lambda_0+2}\left(\lambda_0-3\right)}{16\sqrt{2}\lambda_0\left(2\lambda_0+3\right)}+\frac{3\left(\lambda_0+6\right)}{32\lambda_0\left(2\lambda_0+3\right)}\right)
\end{aligned}
$$

where A_2, B_2 are arbitrary constants.

We are now equipped to calculate the Evans function to $\Theta(\varepsilon^2)$. We formulate the Evans function for the trivial defect solution

$$
E(\lambda(\varepsilon),\varepsilon,x) = \begin{vmatrix} p_L(x) & p_R(x) \\ p_L'(x) & p_R'(x) \end{vmatrix},
$$

where $p_L = p_{0,L}+\varepsilon p_{1,L}+\varepsilon^2 p_{2,L}+\mathcal{O}(\varepsilon^3)$ and similar for p_R. As we calculated p_L on $x<0$ and p_R on $x\geq 0$ it is natural to evaluate the Evans function at $x=0$. Thus, we have the expansion of the Evans function,

$$
\begin{aligned}
E(\lambda(\varepsilon),\varepsilon,0) &= E_0 + \varepsilon E_1 + \varepsilon^2 E_2 + \mathcal{O}(\varepsilon^3) \\
&= \begin{vmatrix} p_{0,L}(0) & p_{0,R}(0) \\ p'_{0,L}(0) & p'_{0,R}(0) \end{vmatrix} + \varepsilon \left(\begin{vmatrix} p_{0,L}(0) & p_{1,R}(0) \\ p'_{0,L}(0) & p'_{1,R}(0) \end{vmatrix} + \begin{vmatrix} p_{1,L}(0) & p_{0,R}(0) \\ p'_{1,L}(0) & p'_{0,R}(0) \end{vmatrix} \right) \\
&+ \varepsilon^2 \left(\begin{vmatrix} p_{0,L}(0) & p_{2,R}(0) \\ p'_{0,L}(0) & p'_{2,R}(0) \end{vmatrix} + \begin{vmatrix} p_{1,L}(0) & p_{1,R}(0) \\ p'_{1,L}(0) & p'_{1,R}(0) \end{vmatrix} + \begin{vmatrix} p_{2,L}(0) & p_{0,R}(0) \\ p'_{2,L}(0) & p'_{0,R}(0) \end{vmatrix} \right) + \mathcal{O}(\varepsilon^3)
\end{aligned}
$$

The $\Theta(1)$ term of this expansion gives,

$$E_0 = -2A_0B_0\sqrt{\lambda_0+2},$$

which has no roots in the natural domain of the Evans function, $\Re(\lambda) > -2$. Obviously, restricting λ to the real line and in the limit $\lim_{\lambda_0\to-2} E_0 = 0$, *i.e.* the function has a root on the boundary of the natural domain Ω_1. This root is the branch point of the absolute spectrum.

The $\Theta(\varepsilon)$ term of the Evans function expansion is

$$E_1 = -2(A_0B_1 + A_1B_0)\sqrt{\lambda_0+2}.$$

Again, this term has no roots other than in the limit $\lambda_0 \to -2$ (with λ_0 restricted to the real line) and this root is the branch point of the absolute spectrum. The $\Theta(\varepsilon^2)$ term of the Evans function expansion is

$$
\begin{aligned}
E_2(\lambda) = -2(A_0B_2 + A_1B_1 + A_2B_0)\sqrt{\lambda_0+2} + \frac{A_0B_0\lambda_1^2}{8(\lambda_0+2)^{3/2}} + \frac{A_0B_0\lambda_1}{4(\lambda_0+2)^{3/2}} \\
\frac{3A_0B_0\lambda_0}{4\sqrt{\lambda_0+2}\,(2\lambda_0+3)^{\,2}} - \frac{3A_0B_0\,(\lambda_0+1)\,(2\lambda_0+9)}{4\sqrt{2}\,(2\lambda_0+3)^{\,2}},
\end{aligned}
$$

which is quadratic in λ_1. The limit $\lim_{\lambda_0\to-2} E_2$ does not exist. However, in equating each term in the expansion of the Evans function to zero we obtain the following expression for λ_1

$$
\begin{aligned}
\lambda_1^{\pm} = -1 \pm \frac{(\lambda_0+2)}{A_0B_0} \Bigg(& \frac{3\sqrt{2}A_0^2B_0^2\,(\lambda_0+1)\,(2\lambda_0+9)}{\sqrt{\lambda_0+2}\,(2\lambda_0+3)^{\,2}} \\
& + A_0B_0 \left(\frac{A_0B_0\left(9-2\lambda_0^2\right)}{(\lambda_0+2)^{\,2}\,(2\lambda_0+3)^{\,2}} + 16(A_2B_0 + A_1B_1 + A_0B_2) \right) \Bigg)^{\frac{1}{2}}
\end{aligned}
$$

which is the $\mathcal{O}(\varepsilon)$ correction to the temporal eigenvalue resulting from the inclusion of the jump-type defect. In the limit $\lambda_0 \to -2$ we have

$$\lim_{\lambda_0 \to -2} \lambda_1^+ = 0 \quad \text{and} \quad \lim_{\lambda_0 \to -2} \lambda_1^- = -2.$$

Hence, the 'roots' of the Evans function about the trivial defect solution are $\lambda = -2 - 2\varepsilon + \mathcal{O}(\varepsilon^2)$ and $\lambda = -2 + \mathcal{O}(\varepsilon^2)$. These values are both outside of the natural domain of the Evans function to $\Theta(\varepsilon)$ and could potentially emerge into the natural domain of the Evans function at higher order correction terms through complex terms. However, they will not destabilise the trivial defect solution.

4.4 Summary and outlook

In this chapter we demonstrated the expansion of the Evans function for the trivial defect solution to a 2nd order scalar PDE, the bistable equation. Here we outline the procedure for the full problem; the stability of the trivial defect solution to the n-dimensional problem (4.2). As per Hypothesis 4.1 we assume there exists an isolated, hyperbolic equilibrium point $u = u_0$ to (4.1), by Hypothesis 4.2 we assume all diffusion coefficients are given by δ. Therefore, by Lemma (4.2.3), a trivial defect solution exists. Furthermore, we take the equilibrium point to be a spectrally stable solution to (4.1) as we are interested in the effect the defect has on a spectrally stable solution. We must first derive the trivial defect solution profile to $\Theta(\varepsilon^2)$, then we formulate the Evans function to $\Theta(\varepsilon^2)$ in order to track the potential point spectra that emerge from the branch points to $\Theta(\varepsilon)$.

As in the scalar case we use a regular expansion, $u = u_0 + \varepsilon u_1 + \varepsilon^2 u_2 + \mathcal{O}(\varepsilon^3)$, and take $u \in C^1$ and solve each order of the existence equation to obtain u_0, u_1 and u_2. We will derive explicit expression for the $\Theta(\varepsilon^2)$ correction term of the Evans function, which provides the $\Theta(\varepsilon)$ correction term of λ. We take $\lambda = \lambda_0 + \varepsilon\lambda_1 + \varepsilon^2\lambda_2 + \mathcal{O}(\varepsilon^3)$ with $\Re(\lambda_0) > \Re(\nu^*)$, *i.e.* to the right of the leading edge of the absolute spectrum, and $p(x, \lambda) = p_0(x, \lambda) + \varepsilon p_1(x, \lambda) + \varepsilon^2 p_2(x, \lambda) + \mathcal{O}(\varepsilon^3)$.

As the roots of the Evans function are, to leading order, in the left half plane the solution will remain spectrally stable. We can obtain an explicit expression for the $\Theta(\varepsilon)$ correction term to λ for the trivial defect solution. This calculation will inform our analysis of local defect solutions which can be interpreted as a concatenation of a trivial defect solution and a stationary solution, see Figure 4.2.1.

Chapter 5

Summary and outlook

5.1 Summary

Throughout this thesis we have analysed the existence and/or spectral stability of three dynamical systems that are each non–standard in different ways. First, a Keller-Segel model for bacterial chemotaxis for which we have proved the previously unknown result that there exists a range of parameters such that the travelling wave solutions are transiently unstable, *i.e.* spectrally stable in an appropriately weighted function space. The motion of travelling wave solutions is driven by the chemotactic function with the wave speed determined by the size of the bacterial population rather than an inherent wave speed that arises from changing to a moving frame of reference as is the case in most well known travelling wave problems (such as the Fisher-Kolmogorov-Petrovsky-Piscounov equation). This structure resulted in an atypical spectral structure with the leading edge of the absolute spectrum crossing into the right half plane away from the real axis as the chemotactic parameter β increases. Furthermore, we showed a connection from the sublinear and constant consumption cases ($0 \leq m < 1$) to the more well studied linear consumption case ($m = 1$) which has been shown to be nonlinearly stable under certain conditions [77]. The relationship is seen through the absolute spectrum which deforms with increasing m until we have the marginal case $m = 1$, where the absolute spectrum does not enter into the right half plane but tangentially contains the origin. We also showed that the eigenvalue $\lambda = 0$ is of multiplicity two in the sublinear and constant consumption cases and is embedded in the absolute spectrum in the linear consumption case.

This work has opened several new questions and provided a foundation for future work to address these open questions. Though there exists results pertaining to the nonlinear stability of the linear consumption case, the nonlinear stability of the sublinear and constant consumption cases remains open. The quasilinear nature of the linearised operator associated with the travelling waves prevents us from immediately concluding nonlinear stability in the parameter regimes that are transiently unstable and more analysis is required. There is also the question of the dynamical implications of the onset of absolute instability with the increase of the chemotactic parameter β. Specifically one expects oscillatory behaviour due to the complex valued leading edge of the absolute spectrum. There is potential for more numerical and theoretical analysis of this bifurcation.

In Chapter 3 we examined the existence of travelling wave solutions in the Gatenby-Galenski model for tumour invasion with the acid-mediation hypothesis. We rigorously

proved the existence of these travelling wave solutions and we provide a mathematical explanation for the existence of an interstitial gap. This interstitial gap has previously been observed both numerically and experimentally [27, 32]. The width of the gap is determined by the distance between a layer transition of the tumour and a dynamical transcritical bifurcation of two components of the critical manifold. This transcritical bifurcation prevented us from using GSPT directly as Fenichel theory does not apply at the transcritical bifurcation where normal hyperbolicity is lost. We proved the persistence of the singular solutions across the fast transition (which is standard in the application of GSPT) and across this dynamical transcritical bifurcation. The logical next step for the analysis of the Gatenby-Gawlenski model is to analyse the spectral stability of the travelling wave solutions. The complication arises in that the fast-slow structure of the problem results in a non-local eigenvalue problem, see §3.6.1.

In Chapter 4 we studied the spectral stability of a trivial defect solution for a second order scalar PDE. The existence of both trivial and local defect solutions was established in [21] for general n-dimensional reaction diffusion models with a jump-type defect. Through the use of an Evans function expansion we show that for a sufficiently small defect a stable constant solution in the associated homogeneous problem remains stable with the inclusion of a jump-type defect. Moreover, we show that the correction term for the roots of the Evans function are, to leading order, given by the branch point of the absolute spectrum associated with the constant solution. These roots may be either perturbed branch points or point spectra that emerge from the absolute spectrum under the inclusion of the defect. There are many open questions in the area of stability of defect solutions, with the overall goal of a unified and general theory for spectral analysis of defect solutions. Local defect solutions are, in general, not explicitly solvable in terms of their profiles and, in turn, the eigenvalue problem is not explicitly solvable. The suggested path forward is the analysis of specific models for which the existence of local defect solutions has been proved such as the Fitzhugh-Nagumo (FHN) model or the Extended Fisher-Kolmogorov (EFK) equation.

5.2 Future work for the Keller-Segel model with logarithmic chemosensitivity

The future work for the Keller-Segel model with logarithmic chemosensitivity was discussed in detail in §2.8. We refer to §2.8 for a discussion of the nonlinear (in)stability of the Keller-Segel model, the quasilinear nature of the linearised operator, and the dynamical implications of the spectral structure and the bifurcation from a transiently unstable state to an absolutely unstable state as the chemotactic parameter increases.

5.3 Future work for the Gatenby-Gawlinski model with the acid-mediation hypothesis

The future work for the Gatenby-Gawlinski model with the acid-mediation hypothesis was discussed in detail in §3.6. We refer to §3.6 for a discussion of the generalisations of the model as well as a discussion of numerical stability analysis. Here we discuss a potential approach for the theoretical stability analysis.

5.3.1 Stability of solutions to the Gatenby-Gawlinski model

As stated in Chapter 1, it is often difficult to calculate the Evans function explicitly. The Non Local Eigenvalue Problem (NLEP) approach offers an alternative method for calculating the Evans function explicitly by utilising the additional structure in singularly perturbed equations [17–19]. Consider the *fast* system

$$\begin{aligned} \dot{u} &= f(u, v, \varepsilon, p), \\ \dot{v} &= \varepsilon g(u, v, \varepsilon, p), \end{aligned} \tag{5.1}$$

where $\dot{} = d/dx$, $0 < \varepsilon \ll 1$ and p represents the system parameters. We can make the change of variable $z = \varepsilon x$ to obtain the *slow* system

$$\begin{aligned} \varepsilon u' &= f(u, v, \varepsilon, p), \\ v' &= g(u, v, \varepsilon, p), \end{aligned} \tag{5.2}$$

where $' = d/dz$. We describe u as the fast variable and v as the slow variable as in (5.1) v is approximately constant while u varies. The two systems are equivalent as long as $\varepsilon \neq 0$ but no longer agree in the $\varepsilon \to 0$ limit. This is what makes the problem singularly perturbed and gives it a fast-slow structure. If $\mathcal{T}(\lambda)$ (1.9) is a singularly perturbed system we can decompose the Evans function to the product of the analytic Evans function for the fast system and the meromorphic Evans function for the slow system for $\varepsilon \to 0$. That is, the Evans function $E(\lambda)$ is, to leading order, given by

$$E(\lambda) = E_{fast}(\lambda) E_{slow}(\lambda).$$

The fast and slow systems are lower dimensional than the full problem. If they are explicitly solvable we may obtain the explicit Evans function (to leading order in ε) using this decomposition. The NLEP approach was developed in [17] to analyse the stability of the 1D Gray-Scott model. This model has one fast variable and one slow variable resulting in a four dimensional eigenvalue problem. Using the NLEP approach the Evans function is decomposed to a 2D eigenvalue problem in the fast dynamics and a 2D non-local eigenvalue problem in the slow dynamics. In [99] the authors extend the NLEP method for N-dimensional eigenvalue problems with one fast variable and $N - 1$ slow

variables. The NLEP approach requires careful analysis as it introduces extraneous poles and zeroes to the Evans function which cancel with each other. This is referred to as the *NLEP paradox* [17]. Part of future work is the utilisation of the NLEP approach for the stability analysis of the travelling wave solutions to the Gatenby-Gawlenski model.

5.4 Future work on the stability of defect solutions

The future work for trivial defect solutions to $n-$dimensional RDEs is discussed in §4.4. Here we discuss the setup and a potential approach for the analysis of local defect solutions to $n-$dimensional RDEs.

5.4.1 Local defect solutions to n−dimensional RDEs

In ongoing and future work, we return to (4.2) and consider a local defect solution as defined in Definition 4.2.1. A local defect solution is, to leading order, a non-constant, solution to the homogeneous problem. The leading order solution is translation invariant in the homogeneous system. We assume there exists such a stationary solution that persists in (4.2). Furthermore, we assume that the solution to the homogeneous problem is spectrally stable; the eigenvalue $\lambda = 0$ is simple and the essential spectrum and all non-zero point spectrum are contained in the open left half plane.

The added complexity for the analysis of local defect solutions is the leading order profile u_0 is nonlinear and thus the linearised eigenvalue problem is not, in general, explicitly solvable. There is some added information in the case of a local defect solution in that the leading order eigenfunction associated with $\lambda = 0$ is known to be the spatial derivative of the solution to the homogeneous problem, see (1.18). In general, the Evans function cannot be computed explicitly, however we aim to use the structure and approach used for the Evans function of the trivial defect solution to analogously approach local defect solutions for specific models.

5.4.2 The Fitzhugh-Nagumo model with a jump-type spatial defect

The Fitzhugh-Nagumo (FHN) model is an example of a relaxation oscillator and is often used to model excitable media. Due to the oscillatory and/or spiking behaviour of this model it is receptive to GSPT analysis. The FHN model is a higher dimensional model in terms of populations. The model has the potential to support local defect structures. In particular, we consider the modified FHN equation with a jump-type defect;

$$\begin{aligned} u_t &= \varepsilon^2 u_{xx} + u - u^3 - \varepsilon(\alpha v + \beta w + \gamma(x)) \\ \tau v_t &= v_{xx} + u - v \\ \theta w_t &= D^2 w_{xx} + u - w. \end{aligned} \tag{5.3}$$

where

$$\gamma(x) = \begin{cases} \varepsilon\gamma_1, & x \leq 0, \\ \gamma_2, & x > 0. \end{cases}$$

The equation (5.3) has been studied in terms of both existence and stability in [21,98,100] where it was shown that the model supports stationary solution in the form of pinned fronts and pulses. The existence conditions, stability conditions and the relationship between the stability condition and the pinning distance were shown in [21,98,100]. Thus, (5.3) acts as a testbed for the extension of the theory developed in Chapter 4 to higher dimensional systems. We aim to compare our Evans function approach to the stability conditions derived in the literature to confirm the accuracy of our method.

There are added complexities to the modified FHN defect model that will also help us expand and generalise our Evans function approach. The equation (5.3) has a clear slow fast structure and thus GSPT will be necessary for the existence analysis. The slow-fast structure also adds an extra level of complexity to the stability analysis. It is not yet clear if the Evans function for defect solutions outlined in Chapter 4 will capture the eigenvalues of the system correctly and it is possible a modified version of the NLEP approach, discussed in §5.3.1, may be needed.

5.4.3 The extended Fisher-Kolmogorov equation with a jump-type spatial defect

As part of the ongoing and future work we will also consider the Extended Fisher-Kolmogorov (EFK) equation.

$$u_t = -hu_{xxxx} + u_{xx} + u - u^3 + \begin{cases} 0, & x \leq 0, \\ \varepsilon g(u, u_x, u_{xx}, u_{xxx}), & x > 0. \end{cases}$$

The associated homogeneous problem (*i.e.* when $\varepsilon = 0$) has been studied in terms of existence and stability, see [83,102] and references therein. Furthermore, the EFK equation with a defect was shown in [21] to support countably many local defect kink solutions (under a condition on h). The existence analysis for the EFK model and EFK defect model facilitate our use of this example to test our Evans function approach for the stability of defect solutions. The EFK also provides a contrasting example to the FHN model. Whilst the FHN has pinned solutions with stability dependent on the pinning distance, the EFK has countably many local defect solutions [21]. There is no explicit expression known for the solution profiles and we would have to rely on numerical methods. This provides a good opportunity to explore how the Evans function for defect models can be implemented numerically.

References

[1] J. Adler. Chemotaxis in bacteria. *Science*, 153(3737):708–716, 1966.

[2] J. Alexander, R. Gardner, and C.K.R.T. Jones. A topological invariant arising in the stability analysis of travelling waves. *J. reine angew. Math*, 410:167–212, 1990.

[3] S. Balasuriya, K. Harley, P. van Heijster, and L. Sewalt. Influences of Allee effects in the spreading of malignant tumours. *J. Theoret. Biol.*, 394:77–92, 2016.

[4] B. Barker. Evans function computation. *Brigham Young U. All Theses and Dissertations*, 2009.

[5] B. Barker, J. Humpherys, and K. Zumbrun. STABLAB: A MATLAB-based numerical library for Evans function computation, 2009.

[6] C.M. Bender and S.A. Orszag. *Advanced mathematical methods for scientists and engineers I: Asymptotic methods and perturbation theory*. Springer Science & Business Media, 2013.

[7] D.L. Benson, P.K. Maini, and J.A. Sherratt. Diffusion driven instability in an inhomogeneous domain. *Bull. Math. Biol.*, 55:365–384, 1993.

[8] Koushiki Bose, Tyler Cox, Stefano Silvestri, and Patrick Varin. Invasion fronts and pattern formation in a model of chemotaxis in one and two dimensions. *SIAM Undergrad. Res. Online*, 6:228–245, 2013.

[9] H. Brezis. *Functional analysis, Sobolev spaces and partial differential equations*. Springer Science & Business Media, 2010.

[10] P.N. Davis, P. van Heijster, and R. Marangell. Absolute instabilities of travelling wave solutions in a Keller–Segel model. *Nonlinearity*, 30:4029–4061, 2017.

[11] P.N. Davis, P. van Heijster, and R. Marangell. Spectral stability of travelling wave solutions in a Keller–Segel model. *Appl. Numer. Math.*, 141:54–61, 2018.

[12] P.N. Davis, P. van Heijster, R. Marangell, and M.R. Rodrigo. Traveling wave solutions in a model for tumor invasion with the acid-mediation hypothesis. *Submitted*, 2018.

[13] G. Derks. Stability of fronts in inhomogeneous wave equations. *Acta Applicandae Mathematicae*, 137:1–18, 2014.

[14] G. Derks, A. Doelman, C.J.K. Knight, and H. Susanto. Pinned fluxons in a Josephson junction with a finite-length inhomogeneity. *European Journal of Applied Mathematics*, 23:201–244, 2012.

[15] G. Derks, A. Doelman, S.A. van Gils, and H. Susanto. Stability analysis of π-kinks in a $0-\pi$ Josephson junction. *SIAM journal on applied dynamical systems*, 6:99–141, 2007.

[16] E.J. Doedel and B.E. Oldeman. *Auto-07p: Continuation and bifurcation software*, 2012.

[17] A. Doelman, R.A. Gardner, and T.J. Kaper. Stability analysis of singular patterns in the 1D Gray-Scott model: a matched asymptotics approach. *Physica D: Nonlinear Phenomena*, 122:1–36, 1998.

[18] A. Doelman, R.A. Gardner, and T.J. Kaper. Large stable pulse solutions in reaction-diffusion equations. *Indiana U. Math. J.*, 50:443–507, 2001.

[19] A. Doelman, R.A. Gardner, and T.J. Kaper. *A stability index analysis of 1-D patterns of the Gray-Scott model*. American Mathematical Soc., 2002.

[20] A. Doelman, P. van Heijster, and T.J. Kaper. Pulse dynamics in a three-component system: existence analysis. *Journal of Dynamics and Differential Equations*, 21(1):73–115, 2009.

[21] A. Doelman, P. van Heijster, and F. Xie. A geometric approach to stationary defect solutions in one space dimension. *SIAM Journal on Applied Dynamical Systems*, 15:655–712, 2016.

[22] Y. Ebihara, Y. Furusho, and T. Nagai. Singular solutions of traveling waves in a chemotactic model. *Bull. Kyushu Inst. Tech. Math. Natur. Sci.*, 39:29–38, 1992.

[23] J. Evans. Nerve axon equations. I. Linear approximations. *Indiana Univ. Math. J.*, 21:877–885, 1972.

[24] J. Evans. Nerve axon equations. II. Stability at rest. *Indiana Univ. Math. J.*, 22:75–90, 1972.

[25] J. Evans. Nerve axon equations. III. Stability of the nerve impulse. *Indiana Univ. Math. J.*, 22:73, 1972.

[26] J. Evans. Nerve axon equations. IV. The stable and unstable impulse. *Indiana Univ. Math. J.*, 24:123–124, 1975.

[27] J. Fasano, M.A. Herrero, and M.R. Rodrigo. Slow and fast invasion waves in a model of acid-mediated tumour growth. *Math. Biosci.,*, 220:45–56, 2009.

[28] D.L. Feltham and M.A.J. Chaplain. Travelling waves in a model of species migration. *Appl. Math. Lett.*, 13:67–73, 2000.

[29] N. Fenichel. Persistence and smoothness of invariant manifolds for flows. *Indiana Univ. Math. J*, 21, 1971.

[30] N. Fenichel. Geometric singular perturbation theory for ordinary differential equations. *Journal of Differential Equations*, 31:53–98, 1979.

[31] R.A. Fisher. The wave of advance of advantageous genes. *Ann. Eugen.*, 7:355–369, 1937.

[32] R. A. Gatenby and E. T. Gawlinski. A reaction-diffusion model for cancer invasion. *Cancer Res.*, 56:5745–5753, 1996.

[33] R. A. Gatenby and R. J. Gillies. Why do cancers have high aerobic glycolysis? *Nat. Rev. Cancer*, 4:891–899, 2004.

[34] D. Hanahan and R. A. Weinberg. Hallmarks of cancer: the next generation, cell. *Cell*, 144:646–674, 2011.

[35] K. Harley, P. van Heijster, R. Marangell, G.J. Pettet, and M. Wechselberger. Numerical computation of an Evans function for travelling waves. *Math. Biosci.*, 266:36–51, 2015.

[36] K. Harley, P. van Heijster, G. J. Pettet, R. Marangell, and M. Wechselberger. Existence of traveling wave solutions for a model of tumor invasion. *SIAM J. Appl. Dyn. Syst.*, 13:366–396, 2014.

[37] K. Harley, P. van Heijster, G. J. Pettet, R. Marangell, and M. Wechselberger. Novel solutions for a model of wound healing angiogenesis. *Nonlinearity*, 27:2975–3003, 2014.

[38] K. Harley, P. van Heijster, and G.J. Pettet. A geometric construction of travelling wave solutions to the Keller-Segel model. *ANZIAM J.*, 55:C399–C415, 2014.

[39] G. Hek. Geometric singular perturbation theory in biological practice. *J. Math. Biol.*, 60:347–386, 2010.

[40] P. Henrici. *Applied and Computational Complex Analysis Volume 1.* John Wiley, New York, 1988.

[41] D. Henry. *Geometric Theory of Semilinear Parabolic Equations.* Springer-Verlag, New York, 1981.

[42] A. B. Holder, M. R. Rodrigo, and M.A. Herrero. A model for acid-mediated tumour growth with a nonlinear acid production term. *Appl. Math. Comp.*, 227:176–198, 2014.

[43] M. Holz and S.H. Chen. Quasi-elastic light scattering from migrating chemotactic bands of Escherichia Coli. *Biophys. J,*, 23:15–31, 1978.

[44] D. Horstmann. From 1970 until present: the Keller-Segel model in chemotaxis and its consequences. *Jahresber. Dtsch. Math.-Ver.*, 105:103–165, 2003.

[45] D. Horstmann and M. Winkler. Boundedness vs. blow-up in a chemotaxis system. *J. Differ. Equ.*, 215:52–107, 2005.

[46] H. Ikeda. Front dynamics in heterogeneous diffusive media. *Physica D: Nonlinear Phenomena*, 239:1637–1649, 2010.

[47] R.K. Jackson, R. Marangell, and H. Susanto. An instability criterion for nonlinear standing waves on nonzero backgrounds. *J. Nonlinear Science*, 24:1177–1196, 2014.

[48] N. Jacobson. *Basic Algebra I.* Freeman and Co., 1974.

[49] H.Y. Jin, J. Li, and Z.A. Wang. Asymptotic stability of traveling waves of a chemotaxis model with singular sensitivity. *J. Differ. Equ.*, 255:193–219, 2013.

[50] C.K.R.T. Jones. Stability of the travelling wave solution of the fitzhugh-nagumo system. *Transactions of the American Mathematical Society*, 286(2):431–469, 1984.

[51] C.K.R.T. Jones. *Geometric singular perturbation theory.* Springer, 1995.

[52] K. Kang, T. Kolokolnikov, and M.J. Ward. The stability and dynamics of a spike in the 1D Keller-Segel model. *IMA J. Appl. Math.*, 72:140–162, 2007.

[53] T.J. Kaper. *An introduction to geometric methods and dynamical systems theory for singular perturbation problems*, volume 56. American Mathematical Soc., 1999.

[54] T. Kapitula and K. Promislow. *Spectral and dynamical stability of nonlinear waves.* Springer, New York, 2013.

[55] T. Kapitula and B. Sandstede. Edge bifurcations for near integrable systems via Evans function techniques. *SIAM journal on mathematical analysis*, 33:1117–1143, 2002.

[56] T. Kapitula and B. Sandstede. Eigenvalues and resonances using the Evans function. *Discrete and continuous dynamical systems*, 2004.

[57] T. Kato. *Perturbation Theory for Linear Operators.* Springer-Verlag, Berlin, Germany, 1995.

[58] J. Keener and J. Sneyd. *Mathematical physiology: I: cellular physiology*, volume 1. Springer Science & Business Media, 2010.

[59] E.F. Keller and G.M. Odell. Necessary and sufficient conditions for chemotactic bands. *Math. Biosci.*, 27:309–317, 1975.

[60] E.F. Keller and L.A. Segel. Model for chemotaxis. *J. Theoret. Biol.*, 30:225–234, 1971.

[61] E.F. Keller and L.A. Segel. Traveling bands of chemotactic bacteria: a theoretical analysis. *J. Theoret. Biol.*, 30:235–248, 1971.

[62] V. Kirk, J. Sneyd, M. Wechselberger, and W. Zhang. Changes in the criticality of hopf bifurcations due to certain model reduction techniques in systems with multiple timescales. *J. Math. Neurosci.*, 1, 2011.

[63] C.J.K. Knight and G. Derks. A stability criterion for the non-linear wave equation with spatial inhomogeneity. *Journal of Differential Equations*, 259:4745–4762, 2014.

[64] C.J.K. Knight, G. Derks, A. Doelman, and H. Susanto. Stability of stationary fronts in a non-linear wave equation with spatial inhomogeneity. *Journal of Differential Equations*, 254:408–468, 2013.

[65] A.N. Kolmogorov, I. Petrovskii, and N. Piskunov. A study of the diffusion equation with increase in the amount of substance, and its application to a biological problem. *Bjull. Moskovskovo Gos. Univ.,*, 17:1–72, 1937.

[66] T. Kolokolnikov, J. Wei, and A. Alcolado. Basic mechanisms driving complex spike dynamics in a chemotaxis model with logistic growth. *SIAM J. Appl. Math.*, 74:1375–1396, 2014.

[67] M. Krupa and P. Szmolyan. Extending slow manifolds near transcritical and pitchfork singularities. *Nonlinearity*, 14:1473–1491, 2001.

[68] C. Kuehn. *Multiple time scale dynamics*, volume 191. Berlin: Springer, 2015.

[69] D. A. Larson. Transient bounds and time-asymptotic behavior of solutions to nonlinear equations of fisher type. *SIAM J. Appl. Math.*, 34:93–103, 1978.

[70] J. Li, T. Li, and Z.A. Wang. Stability of traveling waves of the Keller–Segel system with logarithmic sensitivity. *Math. Models Methods Appl. Sci.*, 24:2819–2849, 2014.

[71] T. Li and Z.A. Wang. Steadily propagating waves of a chemotaxis model. *Math. Biosci.*, 240:161–168, 2012.

[72] W. Liu, D. Xiao, and Y. Yi. Relaxation oscillations in a class of predator–prey systems. *J. Differ. Equations*, 188:306–331, 2003.

[73] R. Marangell, C.K.R.T. Jones, and H. Susanto. Localized standing waves in inhomogeneous schrödinger equations. *Nonlinearity*, 23:2059, 2010.

[74] R. Marangell, H. Susanto, and C.K.R.T. Jones. Unstable gap solitons in inhomogeneous nonlinear schrödinger equations. *Journal of Differential Equations*, 253:1191–1205, 2012.

[75] J.B. McGillen, E.A. Gaffney, N.K. Martin, and P.K. Maini. A general reaction-diffusion model of acidity in cancer invasion. *J. Math. Biol.*, 68:1199–1224, 2014.

[76] H.P. McKean. Application of Brownian motion to the equation of Kolmogorov–Petrovskii–Piskunov. *Comm. Pure Appl. Math.*, 28:323–331, 1975.

[77] M. Meyries. Local well posedness and instability of travelling waves in a chemotaxis model. *Adv. Differ. Equ.*, 16:31–60, 2011.

[78] M. Meyries, J.D.M. Rademacher, and E. Siero. Quasi-Linear Parabolic Reaction-Diffusion Systems: A User's Guide to Well-Posedness, Spectra, and Stability of Travelling Waves. *SIAM J. Appl. Dyn. Syst.*, 13:249–275, 2014.

[79] J.D. Murray. *Mathematical biology I: an introduction*. Springer, New York, 2002.

[80] T. Nagai and T. Ikeda. Traveling waves in a chemotactic model. *J. Math. Biol.*, 30:169–184, 1991.

[81] R. Nossal. Boundary movement of chemotactic bacterial populations. *Math. Biosci.*, 13:397–406, 1972.

[82] A. Novick-Cohen and L.A. Segel. A gradually slowing travelling band of chemotactic bacteria. *J. Math. Biol.*, 19:125–132, 1984.

[83] L.A. Peletier and W.C. Troy. *Spatial patterns: higher order models in physics and mechanics*, volume 45. Springer Science & Business Media, 2012.

[84] G.J. Pettet and M. Wechselberger. Folds, canards and shocks in advection-reaction-diffusion models. *Nonlinearity*, 23:1949–1969, 2010.

[85] J.D.M. Rademacher, B. Sandstede, and A. Scheel. Computing absolute and essential spectra using continuation. *Phys. D*, 229:166–183, 2007.

[86] C. Robinson. Sustained resonance for a nonlinear system with slowly varying coefficients. *SIAM J. Math. Anal.*, 5:847–860, 1983.

[87] G. Rosen and S. Baloga. On the stability of steadily propagating bands of chemotactic bacteria. *Math. Biosci.*, 24:273–279, 1975.

[88] B. Sandstede. Stability of travelling waves. *Handb. Dyn. Syst.*, 2:983–1055, 2002.

[89] B. Sandstede and A. Scheel. Essential instability of pulses and bifurcations to modulated travelling waves. *Proc. Roy. Soc. Edinburgh Sect. A*, 129:1263–1290, 1999.

[90] B. Sandstede and A. Scheel. Absolute and convective instabilities of waves on unbounded and large bounded domains. *Phys. D*, 145:233–277, 2000.

[91] B. Sandstede and A. Scheel. Spectral stability of modulated travelling waves bifurcating near essential instabilities. *Proc. Roy. Soc. Edinburgh Sect. A*, 130:419–448, 2000.

[92] B. Sandstede and A. Scheel. On the structure of spectra of modulated travelling waves. *Math. Nachr.*, 232:39–93, 2001.

[93] D.H. Sattinger. Weighted norms for the stability of traveling waves. *J. Differ. Equ.*, 25:130–144, 1977.

[94] H. Schwetlick. Traveling waves for chemotaxis–systems. *Proc. Appl. Math. Mech.*, 3:476–478, 2003.

[95] T.L. Scribner, L.A. Segel, and E.H. Rogers. A numerical study of the formation and propagation of traveling bands of chemotactic bacteria. *J. Theoret. Biol.*, 46:189–219, 1974.

[96] J.A. Sherratt, A.S. Dagbovie, and F.M. Hilker. A mathematical biologist's guide to absolute and convective instability. *Bull. Math. Biol.*, 76:1–26, 2014.

[97] P. Szmolyan. Transversal heteroclinic and homoclinic orbits in singular perturbation problems. *J. Differ. Equations*, 92:252–281, 1991.

[98] P. van Heijster, C.-N. Chen, Y. Nishiura, and T. Teramoto. Pinned solutions in a heterogeneous three-component fitzhugh–nagumo model. *Journal of Dynamics and Differential Equations*, 31:153–203, 2019.

[99] P. van Heijster, A. Doelman, and T.J. Kaper. Pulse dynamics in a three-component system: stability and bifurcations. *Physica D: Nonlinear Phenomena*, 237:3335–3368, 2008.

[100] P. van Heijster, A. Doelman, T.J. Kaper, Y. Nishiura, and K.I. Ueda. Pinned fronts in heterogeneous media of jump type. *Nonlinearity*, 24:127, 2011.

[101] P. van Heijster, A. Doelman, T.J. Kaper, and K. Promislow. Front interactions in a three-component system. *SIAM Journal on Applied Dynamical Systems*, 9:292–332, 2010.

[102] W. van Saarloos. Front propagation into unstable states. *Phys. Rep.*, 386:29–222, 2003.

[103] Z.A. Wang. Mathematics of traveling waves in chemotaxis. *Discrete Contin. Dyn. Syst. B*, 13:601–641, 2013.

[104] O. Warburg. *The Metabolism of Tumors*. The Rockefeller University Press, London, 1930.

[105] J. Xin. Front propagation in heterogeneous media. *SIAM review*, 42:161–230, 2000.

[106] Xiaohui Yuan, Takashi Teramoto, and Yasumasa Nishiura. Heterogeneity-induced defect bifurcation and pulse dynamics for a three-component reaction-diffusion system. *Physical Review E*, 75(3):036220, 2007.

Appendix A

Proof of Lemma 2.3.4

Lemma. ***2.3.4*** *The polynomial*

$$f(\beta) = 310\beta^{10} - 3234\beta^9 + 17112\beta^8 - 49101\beta^7 + 76180\beta^6 - 58398\beta^5 + 10056\beta^4 + 15040\beta^3 - 9680\beta^2 + 1716\beta - 4.$$

has only one real root for $\beta \in [1, \infty)$. Moreover, this root is irrational.

Proof. The second part of the lemma is straightforward to prove and follows immediately from the rational root theorem.

To prove the first part of the lemma, we use Sturm's theorem, see, for example [48]. Therefore, we form the Sturm chain or Sturm sequence of $f(\beta)$. The Sturm chain or Sturm sequence $S(\beta) = \{f_0(\beta), f_1, \cdots, f_m\}$ is defined as follows

$$\begin{aligned} f_0(\beta) &:= f(\beta)\,, \\ f_1(\beta) &:= f'(\beta) \\ f_2(\beta) &:= -rem(f_0, f_1) = f_1(\beta)q_1(\beta) - f_0(\beta)\,, \\ f_3(\beta) &:= -rem(f_1, f_2) = f_2(\beta)q_2(\beta) - f_1(\beta)\,, \\ &\vdots \\ 0 &:= -rem(f_{m-1}, f_m)\,, \end{aligned}$$

with $rem(f_i, f_{i+1})$ and q_i are the remainder and the quotient of the polynomial long division of f_i by f_{i+1}, and where m is the minimal number of polynomial divisions (never greater than $deg(f)$) needed to obtain a zero remainder. Next, define $\sigma(x)$ as the number of sign changes in the sequence $S(x)$. Then, Sturm's theorem says that the number of zeros of $f(\beta)$ in $(a, b]$ is determined by $\sigma(a) - \sigma(b)$.

In our case we have

$$
\begin{aligned}
f_0(\beta) &= f(\beta) \\
f_1(\beta) &= 1716 - 19360\beta + 45120\beta^2 + 40224\beta^3 - 291990\beta^4 + 457080\beta^5 - 343707\beta^6 + 136896\beta^7 \\
&\quad -29106\beta^8 + 3100\beta^9 \\
f_2(\beta) &= -(678193/3875) + (368346\beta)/775 + (2353648\beta^2)/775 - (57056552\beta^3)/3875 \\
&\quad +(37862703\beta^4)/1550 - (14325693\beta^5)/775 + (83458219\beta^6)/15500 \\
&\quad +(112239\beta^7)/250 - (2991399\beta^8)/7750 \\
f_3(\beta) &= -(\beta 13202524226091000/994274219689) + (155600128891066000\beta)/2982822659067 \\
&\quad +(150831661766230000\beta^2)/994274219689 \\
&\quad -(3094307548371224000\beta^3)/2982822659067 \\
&\quad +(6037396562666682500\beta^4)/2982822659067 \\
&\quad -(1863731780029233000\beta^5)/994274219689 \\
&\quad +(843031062821452750\beta^6)/994274219689 - (448854351815897500\beta^7)/2982822659067 \\
f_4(\beta) &= 14766404406834610812581283621584 9/64990396498086931405075396937 50 \\
&\quad +(28907401679797358926550209307 4606\beta)/32495198249043465702537698468 75 \\
&\quad -(75600227651143669138237763517 1201\beta^2)/64990396498086931405075396937 5 \\
&\quad + (10448326275315050230926591637980806\beta^3)/32495198249043465702537698468 75 \\
&\quad -(40281887198192683098950204567078 1\beta^4)/10398463439693909024812063510 0 \\
&\quad +(70762388380933297341824453389660 56\beta^5)/32495198249043465702537698468 75 \\
&\quad -(12160141588823059777538357270448989\beta^6)/25996158599234772562030158775000 \\
f_5(\beta) &= 91038087087060537279105670551109343624571301184591232650 0000/ \\
&\quad 14872058485683789578257638622568387161673640072442108828 9 - \\
&\quad (10838520128580040986986933988664109542082221078104692489800000\beta)/ \\
&\quad 14872058485683789578257638622568387161673640072442108828 9 + \\
&\quad (36190383628040042980417879995753984274979401140531887144600000\ \beta^2)/ \\
&\quad 14872058485683789578257638622568387161673640072442108828 9 - \\
&\quad (52004824040349424279680794372886495070307424566774046048400000\beta^3)/ \\
&\quad 14872058485683789578257638622568387161673640072442108828 9 + \\
&\quad (34292164307308671014701162854870465140219078147059489624200000\ \beta^4)/ \\
&\quad 14872058485683789578257638622568387161673640072442108828 9 - \\
&\quad (85806983146033916471118567480768681790297102916895366395000 00\ \beta^5)/ \\
&\quad 14872058485683789578257638622568387161673640072442108828 9
\end{aligned}
$$

$$
\begin{aligned}
f_6(\beta) \;=\; & -(9810802742250840808302321760434585250370511405569317254320472465089\cdots \\
& 1042915390122319460073/ \\
& 1770174603037427803286565297877273021934571601798537750400552469301\cdots \\
& 9790557034762618693750 0) + \\
& (619563023803823243811857208813244103721010429950791043830027191308423\cdots \\
& 74392827893549019414731\beta)/ \\
& 1770174603037427803286565297877273021934571601798537750400552469309 7\cdots \\
& 9055703476261869375000 - \\
& (5854418038389406386811310331954096162989240664784816181197614193433 61\cdots \\
& 1070527800066533467191\beta^2)/ \\
& 8046248195624671833120751353987604645157143644538807956366147587771 7\cdots \\
& 75259248920994062500 + \\
& (5537137175143265623469685435312395840256306285849677402476219717944 88\cdots \\
& 58538196680136104333689\beta^3)/ \\
& 8850873015187139016432826489386365109672858008992688752002762346548 9\cdots \\
& 527851738130934687500 - \\
& (1707908328418014596982098044275575075874679622773798715928710020859 77\cdots \\
& 64088867929139865667747\beta^4)/ \\
& 8850873015187139016432826489386365109672858008992688752002762346548 9\cdots \\
& 527851738130934687500
\end{aligned}
$$

$$
\begin{aligned}
f_7(\beta) \;=\; & 1251283856820957258191318829739316639308756723880152636374607691728303\cdots \\
& 7942891563169843757272776908779474315395278673493466555000000/ \\
& 1961363224255435567435470167679350323340493604637205259027591991834 4\cdots \\
& 7433409582710992901902440945413289863453291971647605870148 1 - \\
& (4440289135575671165896895129708488897085771490200191703252364385906 76\cdots \\
& 109541627480077589912851497553392395354738098493881444387500 00\beta)/ \\
& 1961363224255435567435470167679350323340493604637205259027591991834 4\cdots \\
& 7433409582710992901902440945413289863453291971647605870148 1 + \\
& (4986063747389638104062336501448492023832875933877693594622705807041 27\cdots \\
& 57659121858541242649980136393768988580766478204138667526250000\beta^2)/ \\
& 1961363224255435567435470167679350323340493604637205259027591 9\cdots \\
& 9183447433409582710992901902440945413289863453291971647605870148 1 - \\
& (1761486910995452696789839565587668622993352032586346799484298025467 3\cdots \\
& 64105352113283178148604660702698220469811371323298848970000000\beta^3)/ \\
& 1961363224255435567435470167679350323340493604637205259027591 9\cdots \\
& 9183447433409582710992901902440945413289863453291971647605870148 1
\end{aligned}
$$

$$
\begin{aligned}
f_8(\beta) \;=\; & -(17846112922078425485045612709308038793270467820684368730326071705764\cdots \\
& 04658873533977139247843510001482855636031491708413102844639807810990830\cdots \\
& 01270241561373454298319074182909/ \\
& 18258769339077315340438955052554706841655785474504127563358626310 4\cdots \\
& 80364418875697345865551671689093279532649119793353881341782595672097440\cdots \\
& 59360828682636962527417926650000000) - \\
& (28015162981766508413107485011091618694842618250218940064641096339558 2\cdots \\
& 23818260411168098297564191821091907090530633042768426716594059863261150\cdots \\
& 60450327947180799498673493387119 3\beta)/ \\
& 21910523206892778408526746063065648209986942569404953076030351572576\cdots \\
& 43730265083681503866200602691193543917894375202465761013911480651693510\cdots \\
& 23299441916435503290151198000000 0 + \\
& (36012437184032849449947571967184749705100705487034479421176434803555 6\cdots \\
& 50652894807338633826739183200151764715416123004659979666018675216440100\cdots \\
& 37498114756154693465981073131122 7\beta^2)/ \\
& 21910523206892778408526746063065648209986942569404953076030351572576\cdots \\
& 43730265083681503866200602691193543917894375202465761013911480651693510\cdots \\
& 23299441916435503290151198000000 0
\end{aligned}
$$

$$
\begin{aligned}
f_9(\beta) \;=\; & -(49432407126386176344097831763209942578480422043519856589011831246073\cdots \\
& 55376560885792355948206605950583088831852269497451317017270565549707260\cdots \\
& 72254587581484612842398279075691314999554121804589369037217069446695680\cdots \\
& 9377360000000/ \\
& 66122155034605274389927460267159037186336315135569175758836544775 0\cdots \\
& 94331770575097552021559832171013331421971024634137575957053025962363950\cdots \\
& 55895539223847794273004835342533847569131094231348708569359327434963230\cdots \\
& 20308756209) + \\
& (58397790528876079263459126305799896941194607872605798212097255593708 1\cdots \\
& 15108559685020712967073677431990875666224009552804241153632200033664310\cdots \\
& 00065183922920624090542192025642937349880405393062448063006165088644930\cdots \\
& 114760000000\beta)/ \\
& 66122155034605274389927460267159037186336315135569175758836544775 0\cdots \\
& 33177057509755202155983217101333142197102463413757595705302596236395 5\cdots \\
& 89553922384779427300483534253384756913109423134870856935932743496323 2\cdots \\
& 308756209
\end{aligned}
$$

$$
\begin{aligned}
f_{10}(\beta) \;=\; & 153802873056109831544489532832247119662876270880119403195739273890831 5\cdots \\
& 26310627368936631781082374860116499403448930524704297909951488663702 95\cdots \\
& 22932902714345739869607452217395706987886322336051522458867672978987 20\cdots \\
& 83258302282525017558495099901619129980010947051355960270559/ \\
& 64852816506865562536520901113278376616298656315039988694425187908656 76\cdots \\
& 70056856134683412695278212516425557914819501570982805704750320957398 59\cdots \\
& 00198496907954088021342759601915010473500253780426558528503006902066 81\cdots \\
& 29155620914236841242909634443650219589271236252062413000000 0 .
\end{aligned}
$$

Since $f_{10}(\beta) \neq 0$ our polynomial is square free [48]. So,

$$sgn(S(1)) = \{-1, -1, 1, 1, -1, -1, -1, 1, 1, 1, 1\}$$

and we get $\sigma(1) = 3$. Similarly, by looking at the signs of the leading terms of the polynomials we have

$$sgn(S(\infty)) = \{1, 1, -1, -1, -1, -1, -1, -1, 1, 1, 1\},$$

so $\sigma(\infty) = 3$. Hence, $f(\beta)$ has only root in $(1, \infty)$. Moreover, $f(1) \neq 0$, so $f(\beta)$ has only root in $[1, \infty)$. Finally, $f(1) < 0$ while $f(2) > 0$ which shows that the root is inside $(1, 2)$.

□